



Corrosion and Emission Reduction of Utility Boilers Through Intelligent Systems (CERUBIS)

A large, abstract graphic at the bottom of the page features flowing, wavy lines in shades of blue and white, resembling water or steam. In the center, there is a faint watermark-like image of a globe with a grid pattern.

EUR 30540 EN

Corrosion and Emission Reduction of Utility Boilers Through Intelligent Systems (CERUBIS)
European Commission

Directorate-General for Research and Innovation
Directorate D – Clean Planet
Unit D.3 — Low Emission Future Industries
Contact Andrea Gentili
E-mail RTD-STEEL-COAL@ec.europa.eu
RTD-PUBLICATIONS@ec.europa.eu

European Commission
B-1049 Brussels

Manuscript completed in 2020.

This document has been prepared for the European Commission however it reflects the views only of the authors, and the Commission cannot be held responsible for any use which may be made of the information contained therein.

More information on the European Union is available on the internet (<http://europa.eu>).

Luxembourg: Publications Office of the European Union, 2020

PDF ISBN 978-92-76-27849-8 ISSN 1831-9424 doi: 10.2777/785362 KI-NA-30-540-EN-N

© European Union, 2021.

Reuse is authorised provided the source is acknowledged. The reuse policy of European Commission documents is regulated by Decision 2011/833/EU (OJ L 330, 14.12.2011, p. 39).

For any use or reproduction of photos or other material that is not under the EU copyright, permission must be sought directly from the copyright holders.

All pictures, figures and graphs © Instytut Energetyki (IEn), RFCR-CT-2014-00008 (CERUBIS)

Research Fund for Coal and Steel

Corrosion and Emission Reduction of Utility Boilers Through Intelligent Systems

(CERUBIS)

Tomasz Golec, Sławomir Kakietek, Krzysztof Jagiełło

Instytut Energetyki (I En)
Mory 8 Street, PL-01-330 Warszawa, POLAND

Joerg Mayer, Eva Miller, Patricia Winter

Universitaet Stuttgart (USTUTT)
Keplerstrasse 7, DE-70174 Stuttgart, GERMANY

Tomasz Hardy

Politechnika Wrocławskiego (PWr)
Wybrzeże Wyspiańskiego 27, PL-50-370 Wrocław, POLAND

Mariusz Cieplik, Simon Leiser

Nederlandse Organisatie voor toegepast-natuurwetenschappelijk onderzoek (TNO)
Anna van Buerenplein 1, 2595 DA Den Haag, NETHERLANDS

Ruud Hartveld, Jorgen Konings

Hukseflux Thermal Sensors (HF)
Delftsempark 31, NL-2628 XJ Delft, NETHERLANDS

Jerzy Antczak, Jerzy Sawicki

PGE Górnictwo i Energetyka Konwencjonalna (PGEGI EK)
Węglowa 5 Street, PL-97-400 Bełchatów, POLAND

Grant Agreement RFCR-CT-2014-00008

1 July 2012 to 31 December 2015

Final Report

Table of contents

1	<u>Final summary</u>	5
1.1	<i>Project objectives</i>	5
1.2	<i>Project novelties and main results</i>	6
1.3	<i>Conclusions and possible applications</i>	13
2	<u>Scientific and technical description of results</u>	15
2.1	<i>Background of the project in relation to its scientific and technical objectives</i>	15
2.2	<i>The research approach</i>	17
2.3	<i>Description of activities and discussion</i>	19
2.3.1	Identification of corrosion and slagging boundary conditions under different emissions demands – WP1	19
2.3.2	Development, intra-validation and integration of different corrosion and flow sensors - WP2	25
2.3.3	Development of intelligent software tools for visualisation, monitoring, control and optimisation and its integration with different sensing systems - WP3	35
2.3.4	Full-scale tests of the developed monitoring and optimisation systems at two locations - WP4	43
2.3.5	Project management - WP5	57
2.4	<i>Conclusions</i>	59
2.5	<i>Exploitation and impact of the research results</i>	67
3	<u>List of figures</u>	69
4	<u>List of tables</u>	70
5	<u>List of acronyms and abbreviations</u>	70
6	<u>List of references</u>	71
7	<u>Appendices</u>	73
A1	<i>Research stands used in the project</i>	73
A2	<i>Development of the gas analysers</i>	77
A3	<i>Development of the corrosion probe</i>	87
A4	<i>Development of the resistance method</i>	93
A5	<i>Development of the steam flow meter</i>	100
A6	<i>Development of the intelligent software</i>	107
A7	<i>Results of CIBOP optimisation of boiler no. 5 in BPP</i>	127
A8	<i>Techno-economic evaluation – structure of CIBOP operating costs</i>	131

1 Final summary

1.1 Project objectives

The overall project objective was to reduce the risk of corrosion and to optimise the efficiency of utility boilers in the light of new gaseous emission regulations and new regulations for efficient energy production. Tube failure is the leading cause of forced boiler shutdowns and constitutes a major cost for electricity utilities. With the increasing application of staged combustion – introduced to limit NO_x emissions through primary reduction measures – the problem of more pronounced reducing zones in the boiler became a significant issue. In the reducing zones, corrosion proceeds quickly and waterwall lifetime can be shortened to just one year or less in some cases.

The final practical goal of the CERUBIS project was to develop and demonstrate a reliable and not very expensive tool, i.e. a combined online corrosion/sludging monitoring system, to determine corrosion and sludging rates in utility boilers, enabling the prediction of possible faults in membrane walls and supporting boiler maintenance.

In consequence, the CERUBIS project sought to enhance the flexibility, operability and environmental performance of coal-fired power stations, reduce the risk of incurring great expenses triggered by unexpected boiler breakdown.

To this end, new sensors and measurement devices, sensing systems and intelligent (smart) software systems were to be developed, investigated, tested and validated on laboratory and pilot scale test facilities (up to 0.5 MW_{th}). Finally, the developed systems were to be installed at two real scale utility 380 MW_e hard coal and lignite coal fired boilers in Opole and in **Bełchatów Power Plants** in order to be tested, investigated and validated through one year of operation.

The project in particular focused on the following scientific objectives:

- Determination of corrosion and sludging behaviour under different emission regimes (NO_x, CO₂) for different types of tube materials with multi fuel criteria. Fuel quality can increase or decrease corrosion/sludging and emission phenomena. Thus, using fuel mixtures in utility boilers is very important not only for boiler efficiency but also for maintenance or unexpected malfunction by corrosion and gaseous emissions.
- Determination of potential measuring techniques to identify corrosion and sludging in the combustion chamber of the utility boilers.
- Development, manufacture, testing and validation of sensors and sensing systems for **corrosion/sludging “detection”**.
- Ideation, development, investigation and validation of intelligent software based on artificial intelligence approach (e.g. neural networks, genetic algorithms, immune systems) and expert systems.
- Development, testing and validation of supportive numeric models (CFD).

Technological objectives were:

- Optimisation of boilers performance using two different low NO_x emission techniques (by primary – **Bełchatów Power Plant** and primary connected with SNCR methods – Opole Power Plant) keeping corrosion and sludging at acceptable levels.
- Developing standard practices for operating the boilers with minimum emissions and at a low maintenance cost.
- Development of a maintenance software package for predicting the faults in utility boiler evaporators and heat exchangers.
- Ideation, development and validation of a Common Intelligent Boiler Operation Platform – CIBOP

To better understand the scope of the project, the following definitions are useful:

- Sensor – a measuring element, developed by the project partners specifically for the project or commercially available.
- Measurement device – a device which can be directly mounted in the power plant, consisting of one or more sensors and equipped with all requisite elements for long-term, reliable operation including local control system developed by the project partner responsible for the development of the specific sensing and monitoring technique.
- Sensors platform – combination of at least two different type of measurement devices, based on direct and indirect sensors. A sensors platform consists of more than one measurement devices of each type.
- Sensing system – system integrating one or more sensor platforms with an existing boiler measurement and control system.
- Common Intelligent Boiler Operation Platform (CIBOP) – a boiler diagnostic system consisting of a sensing system and intelligent software to process data garnered from the sensing system and equipped with an interface for handling purposes.
- Artificial neural networks (ANN) are computing systems that are inspired by, but not identical to, biological neural networks that constitute animal brains. Such systems "learn" to perform tasks by considering examples (training data), generally without being programmed with task-specific rules.

1.2 Project novelties and main results

Low O₂ corrosion and slagging are complicated phenomena. Most corrosion studies conducted worldwide focus on corrosion behaviour of various alloys in various environments. A great variety of projects address corrosion issues during the co-firing of biomass and RDF as well as corrosion witnessed in thermal waste treatment plants. Laboratory tests are particularly popular, due to their low cost and the relatively limited complexity of the used setups. In only a few cases were corrosion probes exposed in combustion chambers to complement the corrosion profile (e.g. OxyCorr, CORROSION projects). Such studies produced a raft of various and valuable information which should be considered during boiler construction, retrofit and operation. However, they seldom provide supporting information for the planning of plant revision and regular minor maintenance activities. Furthermore, the limited timespan of such tests (up to 2-3 weeks) does not give an appropriate picture of the long-term process of corrosion.

There are also no simple models or formulas that directly determine the corrosion or slagging rate in a specific area of an evaporator or on superheaters. Existing solutions rely on various measurement techniques, which do give some information about the rates and affected areas. However, such sensors/probes are seldom installed in power plants.

Even if some sensors are installed, in order to diagnose corrosion or slagging phenomena, measurements last at most several days or weeks, no longer. The reason for this is the high cost of such measurements.

With the development of sensors, it has become possible to track a number of relevant processes in the flue gas environment, offering a possibility to monitor boundary layer conditions inside the boiler continuously, as outlined in the CORRLOG project deliverables.

However, there has as yet been no attempt to integrate the various techniques simultaneously. Hence, the most important added value of the CERUBIS project is the incorporation of the selected (different) sensors into an integrated complex online corrosion monitoring system via the generation of an intelligent diagnostic tool - Common Intelligent Boiler Operation Platform – CIBOP.

The main and novel idea of the CERUBIS project was to develop, test and verify a diagnostic platform for corrosion and slagging monitoring based on:

- parallel application of different type of inexpensive sensors and sensing systems,
- artificial intelligence (AI) techniques for data processing and interpretation which do not require additional sophisticated theoretical models and reduce the number of measurement devices required.

New sensors, measuring devices, sensing systems and intelligent software systems were developed, investigated, tested and validated on laboratory and pilot scale test facilities (up to 0.5 MW_{th}).

Since long-term operation is essential for reliable corrosion prediction in quantitative terms, the systems finally were installed in two 380 MW_e utility hard coal and lignite fired boilers at Opole and **Bełchatów Power Plants and** were tested, investigated and validated through a half year of operation.

The project application was in 2013 and execution lasted until the end of June 2018. Development and commercialization of corrosion sensors was ongoing during this time. The diagnostic system developed as part of the project is unique and very innovative, owing to the application of at least four different sensor types and relevant sensing systems in two boilers and their proven long-term operation in the extreme conditions that are present in a coal fired boiler. The sensors and measurement systems are used in an ingenious way in the comprehensive CIBOP diagnostic system, which monitors corrosion across the entirety of the surface of the combustion chamber. The system goes beyond predicting the corrosion rate locally in the places where the sensors themselves are mounted to estimating the corrosion rates to the whole area of membrane walls of the combustion chamber of the boiler.

The standout achievements were (i) determining the correlation between indirect and direct sensor indications (short and long term) and (ii) developing a model of loss of wall thickness over time.

Since the sensors have to work in the extreme conditions of a coal fired boiler, one of the key features of the measuring system has its self-diagnostics during normal operation. Historical data is used to inform the system that the reliability of its own current measurements is ensured.

Next to the novelties described a diagnostic system design philosophy was developed to underpin this innovative new system, cutting the costs of introducing this innovative monitoring approach. The costs of setting up the sensors can be reduced through smart system design, achieved by shared connection points and shared wiring for corrosion, fouling (heat flux), steam flow and flue gas sampling.

The main features and advantages of the diagnostic system are described next. The O₂ and CO concentrations in flue gases at the membrane wall boundary layer of the combustion chamber are a good indication of corrosion risk. Data on H₂S concentrations is important too, as Hs2 is responsible for sulphur corrosion, which was confirmed to be the prevailing mechanism in the boilers investigated in the project.

O₂ concentrations can be measured with relatively inexpensive zirconia sensors, with a suitable gas sampling system for analysis. With regard to measuring CO and H₂S concentrations, the project investigated the use of electrochemical and infrared sensors.

To keep costs to a minimum without impacting quality of outcome, the method that was developed uses measurements by several few sensors (4 to 6) on each wall of the combustion chamber.

The system works on the basis of continuous measurement of O₂ concentration at selected locations in the wall boundary layer of the combustion chamber and applies artificial neural networks (ANN) to extrapolate the concentration of O₂ and CO across the whole surface area of the combustion chamber. ANN is a black box model: no knowledge about the physical and chemical processes is needed, provided sufficient training data is used.

Continuous measurement of O₂ concentration is carried out by special probes placed on the walls of the combustion chamber and connected to gas analysers developed as part of the project. The gas analysers can be equipped with different gas sensors and are an element of different gas sensing systems, which are equipped also with electrical power and pressurized air supply and a data processing unit.

ANNs are trained to predict the concentration of the gas components on the basis of previous multivariant measurements of O₂ and CO concentrations in the wall boundary layer.

These measurements are carried out at several dozen points located on each of the walls of the combustion chamber.

Based on the training, the ANN predicts the concentrations of O₂ and CO at all points where multivariant measurements were carried out previously.

A given ANN has only one output – concentration of O₂ or CO at one point on the wall of the combustion chamber. The network inputs are O₂ values from the probes installed on this wall.

Then, based on the measured and predicted O₂ values, the system generates O₂ concentration maps for the whole furnace wall. The evaporator pipe corrosion hazard maps can be plotted in a six-step scale on the basis of the values of O₂ and CO concentrations.

As the corrosion hazard is determined on the basis of gas component concentrations, which are only corrosion indicators, gas sensors are called indirect sensors.

Measurements using additional direct corrosion rate sensors were used to assessing the risk indicator to gauging the direct corrosion rate in mm/year – the main objective of the project.

Two types of corrosion rate measurement were used in the project (direct sensors):

- Measurement of electrical resistance of a selected part of the evaporator walls.
- A corrosion probe located in the boiler combustion chamber (in the wall boundary layer) measuring the change in resistance of a metal component.

The measurement results were then used to produce calibration models for converting of corrosion risk to direct wall thickness loss. Determining correlations between findings from indirect and direct sensors (short and long term) and finally developing a model of wall thickness loss in mm/year is a central and very important achievement of the CERUBIS project.

The diagnostic system that was developed is equipped with an optimiser to provide data on optimal distributions of primary and secondary air to the boiler, ensuring best protection of the evaporator walls while maintaining acceptable values for NO_x and CO emissions and unburned carbon in ash.

A module that diagnoses the risk of combustion chamber slagging forms an integral part of the system. It is based on burned fuel data, geometrical data of the boiler and current operating parameters. The module consists of:

- ANN to estimate the slagging behaviour of fuels or blends without laboratory experiments (except for ANN training).
- The expert system (ES) to estimate large boiler combustion behaviour, in particular slagging influenced furnace exit temperature changes.

The module is based on the indirect methods, so the application of the direct method for diagnosing combustion chamber slagging and superheater fouling was also investigated as a supporting method by quantitatively accessing the steam flow in individual steam pipes.

The method is based on measuring the heat flux between the boiler steam pipe and the sensor. The heat flux is proportional to the overall heat transfer coefficient and the temperature difference between the medium and the sensor. If the properties of the working medium are known, the steam flow can be monitored quantitatively. When the steam flow changes, the convective heat transfer coefficient will change and hence a change in heat flux can be detected. In combination with a heat flux measurement mounted directly on the steam pipe in the boiler, deposit build-up and fouling phenomena can be detected when inlet and outlet steam properties are known.

The general characteristics of the desired diagnostic system described above directed the scope and nature of the project tasks, as set out in the Technical Annex (TA).

In order to reach project goals, it was necessary to develop and refine measurement systems, and to gather sufficient data (laboratory and industrial) to create models and train ANNs.

Project tasks results were obtained at laboratory, pilot and industrial scale and, finally, the new CIBOP diagnostic system was implemented and tested on two boilers under operational conditions. This comprehensive approach was designed to confirm the usefulness of the chosen methodology in future applications.

In the following sections, the project results are summarized per work package.

WP1 - Identification of corrosion and slagging boundary conditions under different emissions demands

Three main results have been obtained in this WP.

1. Gathering slagging data for different fuels from the IEN 20 kW slagging reactor, which is optimized to investigating pulverised solid fuel combustion (Task 1.1). After the CERUBIS investigation the fuels in the slagging database was increased to 64. All data was used to train the ANN in the CIBOP system in WP3.
2. Determination of corrosion, slagging and fouling behaviour under different emission regimes (NO_x , CO_2) for different types of tube materials and different fuels (Tasks. 1.1, 1.2 and 1.3). This activity was carried out by collection and subsequent chemical/physical analyses of fly ash deposits in a 0.5 MW pilot facility at USTUTT and in both investigated boilers during measurement campaigns. Cooled and uncooled probes with deposition rings made from different steels were used. In addition, deposition probes were used to determine the rate of deposit growth. Samples from the deposition probe taken by TNO during boiler measurements were also subject to chemical/physical analyses. Selected steel materials were examined in the USTUTT laboratory corrosion test rig. In general, the results obtained broadened knowledge about corrosion mechanisms, in particular those occurring in the investigated boilers. Among others, sulphur corrosion was confirmed to be a prevailing mechanism in the investigated boilers. One very important output from the deposition tests in the 0.5 MW pilot facility was that the deposit growths in the pilot facility was very similar to the ones observed in the IEN 20 kW slagging reactor. The latter was then used to generate data for ANN training for the CIBOP slagging module. It was confirmed that IEN small scale results are applicable for large scale slagging predictions.
3. Acquiring high volume large data sets from the two utility boilers where the CIBOP was eventually installed and tested (Task 1.3). Several measuring campaigns were held: three in **Bełchatów** Power Plant (BPP) boiler no. 5 and two in Opole Power Plant (OPP) boiler no. 3. The campaigns were prepared by PGEGIEK and IEN and executed by all project partners. There were three main objectives of the campaigns: determination of the slagging and corrosion risks in both boilers, obtain data for ANN training and validation in WP3 and gather data for CFD calculations in WP3. The campaigns included:
 - measurement of O_2 , CO , CO_2 , H_2S and temperature in the boundary layers of four boiler walls,
 - fly ash sampling from the boundary layers of three boiler walls,
 - measurement of SO_2 , NO , NH_3 , HCN , H_2O , HCl , HF at several points in the boundary layer of one boiler wall,
 - measurement of O_2 and CO and temperature at two locations in the combustion chamber
 - measurement of air-dust flows from two mills and determination of temperature and O_2 concentration in selected ducts/dryers,
 - long term collection of deposits and fly ashes by cooled and uncooled probes at several points,
 - gathering of process parameters of the units
 - taking samples of fuels and bottom and fly ashes.

Work results of package WP1 were very informative and formed the necessary background and reference data for planning and conduction of measurements and led to design choices for various online corrosion detection systems, which were developed in the project in WP2. Furthermore, the results supported the development of the full-scale comprehensive concept of online corrosion detection systems in WP3.

WP 2 - Development, intra-validation and integration of different corrosion slagging sensors

A broad range of sensors and sensing methods to monitor either the corrosion rate directly or the relative corrosion risk of evaporator walls in thermal power plants were evaluated as part of Task 2.1. Those selected and investigated in the project are listed in Tab. 1.1.

After an evaluation of technically and economically feasible sensing systems, a set of sensor types was selected for further evaluation within the project. Tab. 1.1 lists the applied methods and/or sensor types.

Development of measurement devices based on the methods listed in the Table and sensor types was done in three sub-tasks:

- Task 2.2 - indirect corrosion/slaggering techniques using O_2 , CO and H_2S sensors,
- Task 2.3 - direct corrosion rate measurement techniques using electrical resistance measurement of evaporator wall segments and electrical resistance of a steel element on a corrosion probe,
- Task 2.4 - steam flow metering technique.

All sensors and measurement devices were developed and tested under laboratory conditions and finally integrated into several sensing platforms (Task 2.5). A sensor platform denotes the combination of least two of the above-mentioned sensors, from which the rate of corrosion can be estimated for a wider area of the evaporator wall (not only locally). Direct corrosion/sludging sensors (wall resistance measurement, corrosion probe) determine the corrosion rate locally and long exposure time is needed to estimate the corrosion rate.

Tab 1.1 Overview of methods and sensors investigated in WP2

Method/sensor type	Measured variables	Derived quantities	Beneficiary
Electrical resistance of boiler wall – own sensors	Resistance, temperature	Corrosion rate	HF
Corrosion probe - electrical resistance of sensor from boiler strelle – own sensor	Resistance, temperature	Corrosion rate	PWR
Ultrasonic wall thickness measurement – commercial sensor	Wall thickness	Corrosion rate	IEN
Reduction conditions at boiler wall - different types of commercial sensors (zirconia and electrochemical)	O ₂ , CO, H ₂ S concentration	Corrosion risk	IEN, PWR
Steam flow – own sensor	Heat flux, temperature	Steam mass flow, (deposit built-up)	TNO

On other hand, indirect methods (O₂, CO, H₂S measurements) can determine the corrosion risk almost instantaneously for a wider area, up to entire evaporator walls. Thus, the combination of direct and indirect methods was required for good and economically reasonable system operation. From eleven sensor platforms specified in Task 2.5, three were chosen as the most promising for pilot scale experiments. Pilot scale measurements (Task 2.6) were carried out at two 0.5 MW test facilities at IEN and USTUTT. IEN conducted measurements mainly with combustion of lignite (with different levels of moisture) and biomasses, also including some oxy-fuel combustion tests, while USTUTT carried out investigations with hard coal with different amounts of ash for air mode only. In total, 18 cases were investigated: 12 at IEN and six at USTUTT.

Initially, it was planned that the measurement devices would be tested and verified only at pilot scale. However, it was decided to better carry out such tests on real scale conditions in parallel since more useful conclusions/indications could be achieved on basis of both approaches. In fact, in Task 3.3 all of the measurement devices developed were tested both in **Bełchatów** and Opole Power Plants. The pilot scale was retained in a sense and taken into context, since particular measurement devices were tested as standalone systems, neither integrated with others nor with the boiler measurement system.

It should be underlined that the most important and at the same time most challenging element of WP2 was developing and constructing of measuring equipment, and to a lesser extent the testing of sensors at laboratory level, due to the stringent requirements for these devices.

There was a play-off between the desire to keep costs down and the need to ensure long-term stability and reliability when operated under harsh conditions in a coal fired boiler. Hence, it was vital to carry out the abovementioned tests in power plants even before constructing and testing of the integrated diagnostic system.

Tab. 1.2 lists the measurement devices manufactured in the project under WP2 and their application in the test boilers. These were the optimized versions of the measurement devices developed, ignoring the many prototype and intermediate versions constructed and tested. Furthermore, 24 measurement devices for O₂ concentration measurement originating from previous IEN activity were used in the project and incorporated into the sensing platforms at the **Bełchatów** power plant.

Tab. 1.2 Measurement devices installed in the boilers

Method/sensor type	Bełchatów Power Plant	Opole Power Plant
O ₂ concentration (old type)	24	
O ₂ concentration (type 1)		4
O ₂ concentration (type 2)		4
O ₂ , CO concentration		4
O ₂ , CO, H ₂ S concentration		4
Corrosion probe	1	2
Wall resistance	1	2
Steam flowmeters	2	4

After pilot scale tests five sensor platforms were selected to be mounted and tested during long term operation in real scale boilers: three platforms in **Opole Power Plant** and two in **Bełchatów Power Plant** (Task 3.1 and Task 3.2). Opole Power Plant was equipped with more platforms than Bełchatów due to the higher corrosion risks observed. Locations of particular measurement devices of these platforms at Bełchatów Power Plant are shown in Fig. 1.1 while Fig. 1.2 presents similar picture for Opole Power Plant.

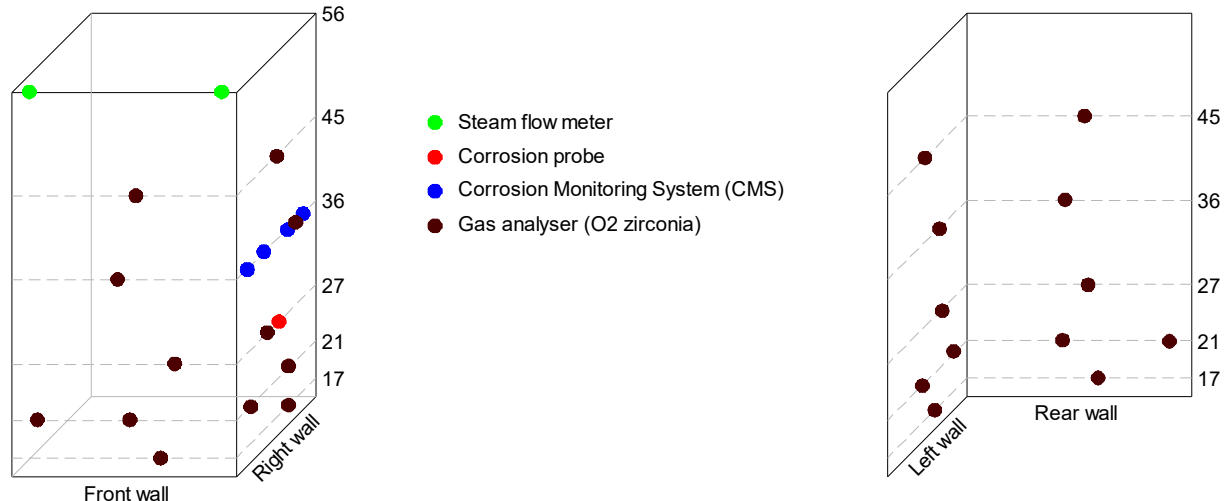


Fig. 1.1 Sensor platforms deployment in boiler no. 5 in BPP

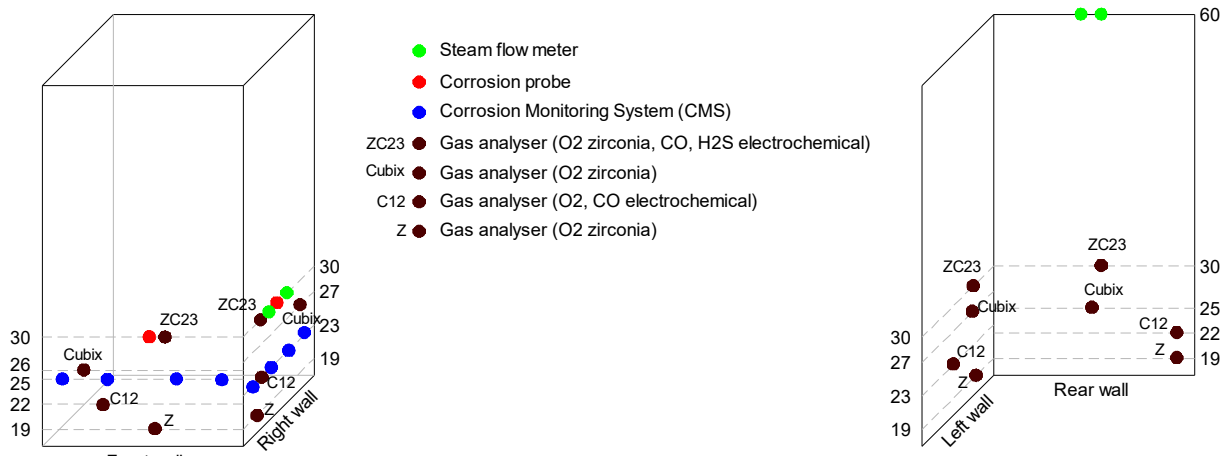


Fig. 1.2. Sensor platforms deployment in boiler no. 3 in OPP

Each of the measurement device had its own hardware like pumps, solenoid valves, various mechanical parts for assembly, cooling systems etc. as well as local control system. These control systems were developed and manufactured for pilot scale conditions and under WP3 they were adapted to meet tougher real scale conditions and power plant demands. The control systems of measurement devices were connected with the main CIBOP server, which handled the data. The CIBOP server was connected to the boiler/power plant data handling system and was the heart of the boiler diagnostic system, as it hosted intelligent software for data processing and interpretation. This way, two sensing systems were created, one at each power plant, as is shown in Fig. 1.3. One key aspect of the project was developing software based on artificial intelligence and creating an intelligent system for data processing and interpretation, which together with the abovementioned sensing system creates an integrated boiler diagnostic system called: Common Intelligent Boiler Operation Platform – CIBOP.

The software was developed under Task 3.4 and partially based earlier developed software like Slagann (model of slagging), Dawid (model of high temperature corrosion determination) and Rachel (model of utility boiler optimisation). All of this software was enhanced during the project and new components added, like diagnostic of the sensing system and models of wall thickness loss. This last one was a very important part, elaborated on the basis of investigating correlations between indirect and direct sensor indications (short and long term) collected among others in Task 3.3.

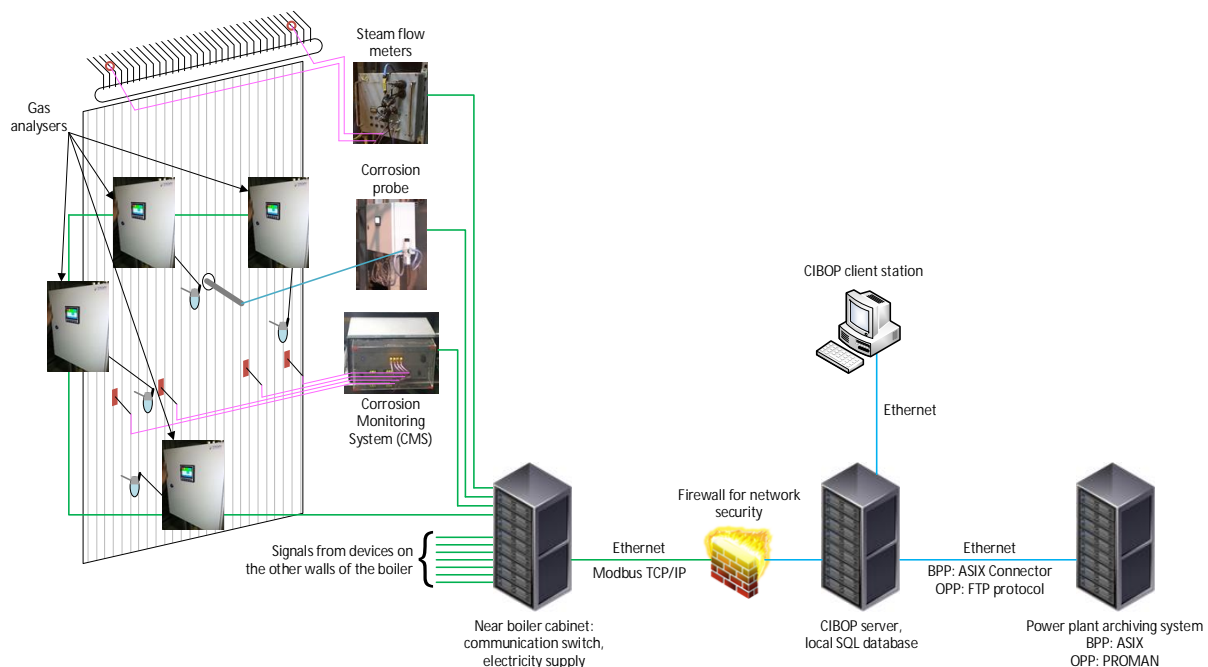


Fig. 1.3 Sensing systems in BPP and OPP – overview chart does not include real numbers of sensors or their location

In the former version of the software only O₂ concentrations and corrosion risk were determined. Work on the CERUBIS project enabled the transition to assessing current and predicted rate of wall thickness loss in mm/year. It is also possible to assess the total loss of wall thickness over a given period of time. One of the models (O₂ model) was calibrated based on standard wall thickness measurements carried out by power plants every 2-3 years. These measurements may be used for verification during operation of this and other models and for making possible corrections.

The boiler optimiser is a novel achievement in itself, showing recommended air distribution to minimise this corrosion rate.

One of the main features of the new CIBOP software is the integration on a single platform of all improved and newly developed computer programs as well as their integration with data handling of the sensing system.

Summarising, CIBOP is a sophisticated diagnostic system enabling continuous and long-term monitoring of boiler corrosion and slagging risk. CIBOP consists of:

- Measurement devices of different types installed in the boiler, i.e. different types of sensors with all necessary auxiliary equipment,
- Data acquisition system for all measurement devices,
- Data acquisition system collecting selected data from the power plant DCS system,
- Software for analysis of the gathered data and transfer as useful information displayed at the dedicated Graphical User Interface (GUI).

The software and GUI are divided into four modules:

1) Corrosion risk module (name: Rachela)

This module shows all current measurements carried out by the sensors, the most important data from the boiler DCS, and maps of the concentration of O₂ at the wall boundary layer, the risk of corrosion and the dynamics of the evaporator wall thickness loss determined based on the O₂ model.

The above maps can be plotted for different periods of time, as averages e.g. daily, monthly or yearly. The program also displays suggested values of new air distribution to the combustion chamber proposed by the optimiser for current boiler operation parameters (power, configuration of working mills and fuel feeders), for the purpose of reducing NO_x emissions and enhancing protection of the evaporator walls against corrosion. All reported values can also be generated in the form of reports in an Excel file.

2) Slagging risk module (name: Slagann)

This module shows some current data from the boiler DCS and predicts the risk of slagging for the given fuel: temperature of beginning of slagging, slagging intensity and flue gas temperature at outlet of the combustion chamber. The final result — the risk of slagging — is shown in four colour coded hazard classes and can be calculated by three different models. Users can also check how changes of some parameters may affect the risk of slagging.

3) Measurement accuracy module (name: Accuracy)

This module displays the level of reliability of all measurements from the installed sensors in the in four colour-coded classes. The classification into the relevant group (scale) is done by

comparing the measured value against the historical values obtained for similar boiler operation parameters.

In addition, the program determines the accumulated average reliability for each of the walls of the furnace chamber and it is possible to plot a map of reliability of measurements, but exclusively for O₂ concentrations, because maps can only be created on the basis of more measurements.

- 4) Module integrating data from all implemented measurements systems (name: Integration)
This module displays all measurement values and boiler operating parameters, similar to that in the Rachel module together with the optimisation part and maps.
The module was extended to predict evaporator wall thickness loss, determined on the basis of four models: O₂, O₂ + CO, CMS, corrosion probe (the O₂+CO model is not currently active).
Based on each of the three models, one can plot a map of the rate of loss of evaporator wall thickness in the current state or as a mean loss from the last specified period, optionally from a few hours to one year.
Loss in future periods can be predicted in two options: when the boiler is running according to DCS settings or the boiler is running according to the settings of the genetic optimiser, but the program predicts such dynamics only for the given power of the boiler and configuration of working mills. If the user wishes to specify the future rate of corrosion for a variable boiler operation, this must be done separately for each power range and configuration of working mills and then summed up.

As can be seen, use of ANN is a crucial part of the diagnostic system that was developed. Its prediction quality depends very much on having a sufficient volume of data for training. Since power plant measurement campaigns are expensive and time-consuming, CFD analysis was introduced in order to supply more training data with regard to O₂ and CO in boundary layers, outlet temperature from combustion chamber as well as NO_x and CO emissions.

In Task 3.5 CFD modelling of the two boilers – hard and brown coal fired – used in the project was carried out. The results were used as additional data to develop, train and validate intelligent software to predict corrosion and slagging.

WP 4 -Full-scale tests of the developed monitoring and optimisation systems at two locations

In WP4 all of the sensors, approaches, techniques and software developed to that point were tested and verified in real scale conditions in boiler no. **5 in Bełchatów Power Plant** (brown coal) and in boiler no. 3 in Opole Power Plant.

In the first place, in Task 4.1., the boilers were adapted for future installation of sensors and systems. This task was also designated for several campaigns of measurement of corrosion rates by ultrasonic wall thickness measurement (input to Task 3.4). These measurements showed that there is a very low corrosion rate at **Bełchatów Power Plant**, not more than 0.03 mm/year. However, in the case of Opole Power Plant high rates of corrosion occur for each wall, even in excess of 1 mm/year.

In the first two years of the project particular measurement devices were preliminarily mounted in both boilers to check their usability in extreme boiler conditions (Task 4.2). Finally, the whole CIBOP was mounted in both boilers and fully connected to power plant infrastructure except for online access to DCS of the boilers (Task 4.3).

For various reasons, the system had not run in full mode for one year starting from July 2017, as was planned, although parts of the system worked even earlier. All circumstances were reported to the EU Project Officer and finally 0.5 year of operation of the whole system was accepted. The system was run in January 2018 and was in operation after 30.06.2018 too (Task 4.4), but mainly data from the first half of the year were analysed.

In this period boiler no. 5 in **Bełchatów Power Plant** worked in total almost 4100 h while boiler no. 3 in Opole Power Plant less than 3900 h. Boiler shutdowns were forced by the operator of the Polish energy system. During operation of the CIBOP systems several failures occurred with the installed sensor platforms and other devices. Overheating was the main reason for failure. In spite of that, the gathered data enabled analysis of more than 2500 hours of CIBOP operation and its performance at each boiler. The two main products obtained from the long-term operation of CIBOP are:

- 1) Experience with long-term operation of all system components. A great deal of practical information was obtained, which is very useful for further improvement of the diagnostic system and its future applications. These tests provided information for assessing the real cost of the system, which was used in Task 4.5 for techno-economical evaluation of the system.
- 2) Data for improvement and calibration of CIBOP software. Especially valuable were data from resistance and corrosion sensors, which requires long term operation for the purpose of obtaining quantitative data. These data were used to improve and calibrate two models correlating material loss rate with O₂ concentration measurements, i.e. the O₂-electrical resistance model and the O₂-corrosion probe model.

1.3 Conclusions and possible applications

Investigation in the power plants carried out by various types of short-term deposition probes and SEM analysis has shown that such diagnostic methods may not reflect the actual corrosion process and may not be used directly for assessment of the corrosion rate. This is caused by the short exposition time of the probe in the boiler and furthermore by the fact that local conditions (temperatures and properties of gas phase and fly ash) can vary greatly during long-term boiler operation.

A much more reliable approach than the above mentioned is the estimation of corrosion rate based on long-term resistance-based methods, i.e. resistance corrosion probes or the method of measuring the resistance of the membrane walls of the boiler (CMS).

These methods allow to directly determine the rate of the thickness loss of the evaporator material in mm/y without having to identify exactly the degradation process itself. This is done solely on the basis of the change in the electric resistance of the boiler wall itself, or a simulation thereof, in the form of a corrosion probe introduced into the boiler.

Both methods were developed within the project and successfully tested and applied in CIBOP during full-scale campaigns.

The project confirmed previous observations reported in the literature, that the concentrations of O₂ and CO in the evaporator wall boundary gas layer are a valuable indicator for assessing the risk of high-temperature corrosion phenomena. It was also found that H₂S measurement is not indispensable in assessing the rate of corrosion due to coinciding character of H₂S concentrations with CO concentrations. Hence CO is a sufficiently good H₂S indicator.

The measurement of O₂ and CO is a short-term method, and the results are obtained practically online for each sensor location. In addition, using intelligent ANN-based software one can get results of O₂ and CO concentrations for the entire surface of walls of the combustion chamber.

Moreover, it was confirmed that these concentrations can be used to determine the rate of corrosion using dedicated developed sub-models, based on the resistance measurements.

A great achievement of the project is the development of a method for determining the corrosion rate on the entire surface of the walls of the boiler's combustion chamber based on measurements of O₂ concentrations only at several measuring points per wall. The method requires simultaneous, longer (several months) measurement of the corrosion rate and O₂ concentration in the combustion chamber in at least two locations with different oxygen concentrations.

Based on the results of this measurements, the corrosion model is developed in the form of mathematical dependencies of corrosion rate in the function of the O₂ concentration averaged for the entire measurement time. This allows for the determination of the corrosion rate anywhere in the boiler wall as long as the actual oxygen concentration is known there.

This method is applied on the CIBOP platform, which uses the idea of coupling quick indirect gas analysis with the slow, long-term, resistance-based direct measurement of the corrosion rate.

The calculation of the corrosion rate for the entire walls of the boiler was done by CIBOP using O₂ concentration data gathered by CIBOP during a half a year campaign. The CMS model and the corrosion probe models were calibrated according to above mentioned method during this campaign. Another method for the determination of the corrosion rate depending on the local O₂ concentration was the use of results of periodic measurements of pipe thickness in the boiler and linking them with the O₂ concentration calculated and averaged by CIBOP for the period of the half year measuring campaign. This was also implemented into CIBOP as an O₂ model

Another central aspect of the CERUBIS project was the development of software based on Artificial Intelligence (AI) algorithms and creating an intelligent system for data processing and interpretation. This software interface together with the earlier described sensing systems, forms the main deliverable of this project, namely the integrated boiler diagnostic system called Common Intelligent Boiler Operation Platform – CIBOP. The overall operating strategy of CIBOP is as follows:

- Initially, CIBOP collects signals from all different implemented sensors, subsequently checks their credibility (measurement accuracy module is a part of the intelligent diagnostic system) and archives them for further use. This data relates to the current state and place in the combustion chamber where the individual sensors are located.
- CIBOP also collects the boiler's operational data at the same time, on the one hand to monitor its operation, but also to provide additional data for use by smart software included in the system.

Thanks to the use of Artificial Intelligence (ANN and GA – hence the name CIBOP - Common Intelligent Boiler Operation Platform), the diagnostic platform software processes data from the sensors and the boiler into useful information for the visualization of the current and predicted status of the boiler combustion chamber.

Admittedly, not all integrations were fully realized within the project duration. Such was the case with the NISTFLOM system as the steam flow meters signals, were recorded diagnosed, and displayed, but not further integrated into predictive and decisive CIBOP routines. This mostly in view of the signal drift issues and lack of quantitative translation of the signal into the actual stem flow at the time. Nevertheless, it was demonstrated that normalized steam flows can be monitored

reliably. The latter are sufficient for the implementation of a smart soot blowing strategy in future applications.

Within the project duration, there was no possibility of a direct (on-line) interpretation of resistance measurement signals (CMS and the resistivity-based corrosion probe) in the form of the rate of loss of pipe thickness. This proved impossible due to the nature of the signal, i.e. very slow change over time. These signals are diagnosed, displayed and recorded for subsequent processing and development or updating corrosion models.

Although CIBOP operation were limited to half a year as was the calibration of its corrosion models was not complete, the studies carried out made it possible to compare the corrosion rate determined by CIBOP according to the developed sub-routines (based on different inputs) with the actual rate determined on the basis of the aforementioned measurements of the thickness of the evaporator pipes.

These obtained results confirm in general a good alignment of the prediction of corrosion rate using long-term results from CMS and corrosion probe combined with the CIBOP software.

CIBOP allows also to predict the impact of the change in boiler operating parameters on the future corrosion rate in different time horizons as well as to optimize boiler operation for limitation of the corrosion rate as well the flue gas emissions.

Another important feature of CIBOP is the potential to reduce the corrosion rate in the boiler by optimizing boiler operating parameters. Setting the boiler parameters according to CIBOP indications substantially decreases the averaged corrosion rates compared to the operation of the boiler according to default boiler DCS settings.

The integral CIBOP system and each part of it separately, can readily be installed at utility boilers on a commercial basis, however the full economic evaluation could not be provided, within the limited time span and the extend of the integration of the CIBOP in the two power plants. Nevertheless, the evidence was generated that CIBOP is capable of reducing potential corrosion and better predict its course, making it possible to plan maintenance shutdowns, before emergency situations arise.

Besides the whole system, the specific individual measurement devices and integrated measurement platforms were developed in the project to a level enabling them to be offered on the market.

The undoubted achievement of the project is the development of low cost gas analyzers for measuring O₂ and CO (optionally H₂S) in the combustion chamber of pulverized coal boiler.

It should be strongly emphasized that such analyzer is well-adapted to the extremely difficult conditions for measuring these gases concentrations in the combustion chamber, i.e. temperatures above 1200 °C, dusty environment, slag and flame presence, active chemical reaction zone.

Another impressive step forward was also made in the direct measurement of the corrosion rate, i.e. electric resistance measurement on live, full-scale evaporator walls as well as the compact, local corrosion probe. Through the four years of the project the professional systems were developed, tested in extreme boiler conditions for months or even years in some cases.

A by-product of the CMS system development is a dedicated temperature measurement system for steel (boiler) tubes, which was necessary for the developed resistance measurement system itself. The product is called the Tube Temperature Measuring System or TTMSYS and is ready for commercial deployment.

Also the NISTFLOM steam flow meters developed and tested in the CERUBIS project can be used individually as water/steam distribution imbalance diagnostics or as fouling indicators for boilers soot blowing systems.

Such devices, ready for installation on the boiler and having unique features dedicated to and integrated in CIBOP, were not available on the market at the starting point of the project.

2 Scientific and technical description of results

2.1 Background of the project in relation to its scientific and technical objectives

The ever more stringent NO_x emission regulations, the volatility of the prices in the EU-ETS (EU Emission Trading Scheme) are forcing fossil fuel-fired power plants to implement new technologies and increase flexibility. Amongst other technical solutions, this implies the use of deep-air-staged combustion techniques, which introduce a reducing atmosphere in the combustion chamber of the boilers. Amplified further by the high(er) load variability due to the market constraints and the prioritized position of the renewable electricity, this leads to worse control of the oxygen distribution in the combustion chamber [1,2,3] and results in increased risk of slagging, fouling- and -induced corrosion. In turn, these degradation phenomena lead to increased wear and tear of the evaporator walls and other steam-rising infrastructure, leading overall to lower availability and higher cost of operation.

To mitigate the impact on the availability, the current maintenance practice dictates frequent shut downs and inspection of the state and particularly the thickness of the material of the steam-rising infrastructure. This solution is nonetheless inefficient, as it needs the boiler to shut down completely. It is also often insufficient in tracking down the wear fast enough to avoid unplanned shut downs altogether, when facing exponential increase of the wear under specific circumstances.

Hence, there is a clear need to monitor and control in real time the corrosion risks and the actual rate of the degradation process, in order to minimize the chance for an unexpected shut-down of the boiler.

As there are many factors contributing to the risk of corrosion, (i.e. the reducing environment inside the furnace [4], mineral ash components containing sulphur, chlorine, and potassium [5] leading to high corrosion rates and the overall Red/Ox conditions in the vicinity of the steam-rising surface as well as its actual surface temperature), it is not easy to select a single process parameter for such an on-line monitoring. It was shown [6] nonetheless that the corrosion rate is corelates closely with the temperature of the external tube surface and with the distribution of the local CO concentration in the boundary layer at the furnace walls. Recent studies have shown that O₂ and/or CO concentrations in flue gases in the wall boundary layer can be a good indicator for corrosion risk, as it allows to detect the presence of the reducing zones were found [6,7]. However, to date very limited real boiler live data are at hand as these systems typically only monitor the O₂ and/or CO concentrations at a very limited number of points in the system. Economic analyses indicate there are real benefits arising from the use of simple methods of corrosion protection such as protective air curtains in conjunction with continuous monitoring of the furnace wall boundary layer [8]. In practice, the areas of the boiler walls at high corrosion risk can be determined by monitoring the composition of the flue gas in the boundary layer of the walls on either a continuous or a periodic basis [9,10,11,12]. Hence within this project one of the objectives was to extend that capability, by installing and monitoring the boiler-wall O₂ and/or CO concentrations by a broad array of wall-mounted sensors. Deposited in a number of patents (PL202007, PL208085, PL208320, PL206421, PL383029) these monitoring systems involve probes/gas sensors sampling flue gas from the boundary layer through specially manufactured adapters/openings in membrane walls between pipes. The flue gas from these points is sampled, conditioned and sent for O₂ analysis [30] or measured directly on the spot by a zirconium probe [12,13].

The first continuous measuring system, which was limited to the measurement of only O₂ concentration in the boundary layer of the walls, was tested in Opole Power Plant in 2006 [12,14].

A similar **monitoring system was tested in the Belchatów Power Plant** with a diagnostic subsystem to determine its failures [10], and a boiler optimisation system was introduced as well. The system thus was more advanced than the one tested in the Opole Power Plant.

The experience gained thus far was used to define the critical system elements that impact reliability. These included technical failures, unreliable measurements of O₂, clogging of the measurement path by fly ash and condensing water, durability of electronic devices and pumps, reliability of sensors and their life span, etc.

Moreover, additional features required for an ideal boiler diagnostic system were then formulated – most importantly, reliable online determination of corrosion rates as well as corrosion affected areas of the membrane walls. Its importance stems from the fact that it enables power plants to avoid failures of tubes (and resulting boiler shutdowns) and to better plan maintenance campaigns. Other features are: the need to measure gaseous components other than O₂, need for a diagnostic subsystem of the main system, boiler optimisation module dedicated to minimising the corrosion risk.

The CERUBIS project was planned to move beyond existing knowledge and practice and towards developing an ideal diagnostic system to overcome existing technical problems and fulfil expectations for such a system.

The project focused in particular on the following scientific objectives:

- Determination of corrosion and slagging behaviour under different emission regimes (NO_x , CO_2) for different types of tube materials with multi-fuel criteria. Fuel quality can increase or decrease corrosion/sludging and emission phenomena. Thus, the use of fuel blends in utility boilers is very important not only for boiler efficiency but also for maintenance or unexpected malfunction by corrosion and gaseous emissions. This aspect is tackled in the project, by sampling and exhaustive analyses of fuel blends chemical composition and physical properties. Furthermore this is aided by in-boiler sampling of (partly converted) ashes and deposits, in broadly scoped measurement campaigns by partners IEN, USTUTT, TNO in co-operation with PGEGIEK. Also, IEN, USTUTT and ECN performed lab- and pilot-scale combustion investigations using the real-life sampled fuels, whereby the designated monitoring techniques of USTUTT, TNO and HF were tested, while generating in-depth knowledge of the behaviour of the specific corrosion-related elements.
- Determination of measuring techniques to identify corrosion and slagging in the combustion chamber of utility boilers. Next to the preparation of the inventory of the potential techniques, this was done by looking specifically at the unification of the measurement and data logging/handling interfaces, for the ease of simultaneous use of various techniques, involving partners HF, TNO and IEN.
- Development, manufacture, testing and validation of sensors and sensing systems to detect corrosion/sludging. This included manufacture of two novel measurement systems based on the indirect steam flow measurement (NISTFLOM of partner TNO) and a electrical resistance based wall-thickness monitoring system (CMS of partner HF).
- Ideation, development, investigation and validation of intelligent software based on an artificial intelligence approach (e.g. neural networks, genetic algorithms, immune systems) and expert systems. Paramount in achieving this goal was the to deliver the relevant data (or model parameter derived there from) in a consistent and appropriately structured way.
- Development, testing and validation of supportive numeric models (CFD).

Technological objectives were based on the application of the above mentioned scientific objectives in real-life:

- Optimisation of boiler performance using two different low NO_x emission techniques (by primary – **Bełchatów Power Plant** and primary connected with SNCR methods – Opole Power Plant) keeping corrosion and slagging at acceptable levels.
- Developing standard practices for operating boilers at minimum emissions and low maintenance cost.
- Development of a maintenance software package to predict faults in utility boiler evaporators and heat exchangers.
- Ideation, development and validation of Common Intelligent Boiler Operation Platform – CI BOP

2.2 The research approach

The main idea of the CERUBIS project was to develop, test and verify a diagnostic platform for corrosion and slagging monitoring on two utility boilers based on inexpensive sensors and artificial intelligence techniques that do not require additional sophisticated models.

The O₂ and CO concentrations in flue gases at the near wall layer of the boiler furnace chamber are a good indication of the corrosion risk. Information about H₂S concentrations could also be important due to fact that this component is responsible for sulphur corrosion, which was confirmed as the prevailing mechanism for corrosion in the boilers investigated in the project

It is possible to measure O₂ concentrations with relatively inexpensive zircon sensors with a suitable gas sampling system for analysis. The use of electrochemical and infrared sensors was investigated in the project with a view to measuring CO and H₂S concentrations.

Aiming at cost reduction, the method developed uses measurement only with several sensors (4 to 6) on each wall of the combustion chamber.

The system works on the basis of continuous measurement of O₂ concentration at selected locations of the wall layer of the boiler combustion chamber and using artificial neural networks (ANNs) to determine the concentration of O₂ and CO in the whole wall layer of the combustion chamber. ANN is a black box model - no knowledge about the process is needed, provided sufficient training data is used.

Continuous measurement of O₂ concentration is carried out by special probes placed on the walls of the combustion chamber and connected to gas analysers developed as part of the project.

The gas analysers can be equipped with different gas sensors and are an element of different gas sensing systems, which are equipped also with electrical power and pressurized air supply and a data processing unit

ANNs are trained to predict the gas components concentration on basis of previous multivariant measurements of O₂ and CO concentrations in the wall layer. These measurements are carried out at several dozen points located on each of the walls of the combustion chamber. Based on the training, ANN determine the concentration of O₂ and CO at all points where multivariant measurements were carried out.

A given neural network has only one output – a concentration of O₂ or CO at one point at the wall of the combustion chamber. The network inputs are O₂ values from the probes installed on this wall. Then, based on the measured and predicted O₂ values, the system generates O₂ concentration maps. The evaporator pipe corrosion hazard maps can be plotted in a six-step scale on the basis of the values of O₂ and CO concentrations.

As the corrosion hazard is determined on the basis of gas component concentrations, which are only corrosion indicators, gas sensors are called indirect sensors.

Measurements using additional direct corrosion rate sensors were used for transition from the assessment of the risk indicator to the direct corrosion rate in mm/year, what in fact was the main objective of the project,

Two types of corrosion rate measurement were used in the project (direct sensors):

- Measurement of electrical resistance of selected parts of evaporator walls.
- A corrosion probe located in the boiler combustion chamber (at the wall layer) measuring the change in resistance in a metal component.

The measurement results were then used to produce models for converting corrosion risk to direct wall thickness loss. Determining correlations between findings from indirect and direct sensors (short and long term) and finally developing a model of wall thickness loss in mm/year is a central and very important achievement of the CERUBIS project.

The diagnostic system that was developed is equipped with a genetic optimiser to provide data on the distribution of primary and secondary air in the boiler, to inform best protection of the evaporator walls while maintaining acceptable values for NO_x, CO emission and unburned carbon in ash.

A module that diagnoses the risk of combustion chamber slagging forms an integral part of the system. It is based on burned fuel data, geometrical data of the boiler and current operating parameters. The module consists of:

- ANN to estimate the slagging behaviour of fuels or blends without laboratory experiments (except for ANN training),
- expert system (ES) to estimate large boiler combustion behaviour, in particular slagging influenced temperature at the outlet of the combustion chamber.

The module is based on the indirect method, so application of the direct method for diagnosing combustion chamber slagging and superheater fouling was also investigated as a supporting method. The method is based on measuring the heat flux between the boiler steam pipe and the sensor. The heat flux is proportional to the overall heat transfer coefficient and the temperature difference between the medium and the sensor. If the properties of the working medium are known, the steam flow can be monitored quantitatively. When the steam flow changes, the convective heat transfer coefficient will change and hence a change in heat flux can be detected. In combination with a heat flux measurement mounted directly on the steam pipe in the boiler, deposit build-up and fouling phenomena can be detected.

The general characteristics of the desired diagnostic system described above directed the scope and nature of the project tasks, as set out in the Technical Annex (TA).

It was necessary to develop and refine measurement systems, and to gather sufficient data (laboratory and industrial) to create models and train ANNs.

Project task results were obtained at laboratory, pilot and industrial levels and, finally, the new CIBOP diagnostic system was implemented and tested on two boilers under operational conditions. This comprehensive approach was designed to confirm the usefulness of the chosen methodology in future applications.

Two different large-scale ($>1000 \text{ MW}_{\text{th}}$) utility boilers were chosen for industrial scale investigations as well as for installation and long-term testing of the CIBOP. These were lignite fired boiler no. 5 in **Bełchatów Power Plant** (BPP) and hard coal fired boiler no. 3 in Opole Power Plant (OPP). This allowed the project to take into account various issues arising in both types of power plants.

To better understand the scope of the project, the following definitions are useful:

- Sensor – a measuring element, developed by the project partners specifically for the project or commercially available.
- Measurement device – a device which can be directly mounted in the power plant, consisting of one or more sensors and equipped with all requisite elements for long-term, reliable operation including local control system developed by the project partner responsible for the development of the specific sensing and monitoring technique.
- Sensors platform – combination of at least two different type of measurement devices, based on direct and indirect sensors. A sensors platform consists of more than one measurement devices of each type.
- Sensing system – system integrating one or more sensor platforms with an existing boiler measurement and control system.
- Common Intelligent Boiler Operation Platform (CIBOP) – a boiler diagnostic system consisting of a sensing system and intelligent software to process data garnered from the sensing system and equipped with an interface for handling purposes.
- Artificial neural networks (ANN) are computing systems that are inspired by, but not identical to, biological neural networks that constitute animal brains. Such systems "learn" to perform tasks by considering examples (training data), generally without being programmed with task-specific rules.

2.3 Description of activities and discussion

2.3.1 Identification of corrosion and slagging boundary conditions under different emissions demands – WP1

This first WP was focused on laboratory, pilot scale and full-scale investigations of corrosion and slagging phenomena. The main objective of WP1 was collecting various information to give background and reference for the planned and then conducted measurements with various online corrosion detection systems which were developed in the project in WP2. The information gathered also supported the development of the whole concept of online corrosion detection systems in WP3.

Task 1.1- Corrosion and slagging tests in laboratory test rigs.

Corrosion laboratory investigation of two alloys (grade 1.7335 (13CrMo4-5) and 1.4903 (X10CrMoVNb9-1 also known as T91) were carried out in USTUTT on a test rig shown in Appendix 1 in order to support the evaluation of corrosion mechanism observed in the utility boilers and to obtain data which could be used in WP3 for training ANN. Tests were run in an atmosphere simulating combustion. The specimen alloy rings were exposed to adjustable temperatures (550-650 °C). The time steps used as an internal standard were 24h, 350h and 1000h. The metal rings were positioned in ceramic cups together with or without ash deposit (several Cl-rich deposits). Three different gaseous atmospheres were introduced: inert/reducing (100% N₂), oxidising (97% N₂, 3% O₂) and oxidising and sulphatic (3% O₂, 500 mg/cm³ SO₂, N₂ rest).

Three fuel ashes from combustion of straw, wood and coal at 0.5 MW test facility were used as deposit. In addition, two synthetic deposits (KCl and KCl mixed with K₂SO₄) were also used. One investigation was carried out without any deposit. The results and discussion were given in [15,16]. The data obtained were not finally used in WP3 for ANN training due to difficulties with finding correlations between these data and the data obtained from pilot scale testing and from the power plants.

Simulations of thermodynamic equilibrium using FactSage software were carried out in order to find relations between particular fuel/ash components and their influence on slagging/fouling behaviour. The simulations were done for two coals: bituminous hard coal (acid components) and lignite (more base components like Ca) and for (biomass Cl-rich). More information about FactSage calculations was placed in [15,16].

The results of these simulations were used for planning purposes as regards the fuels and fuel mixtures to be investigated at IEN in the 20 kW slagging reactor. This experiment was aimed to gather slagging data to be used to train the ANN in the CIBOP system in WP3.

IEN's slagging facility described in A2 is oriented for investigations of combustion of pulverised solid fuels. It is used to obtain slagging properties of solid fuel for various temperatures of combustion. On the basis of experimental results, the beginning temperature of slagging (T_{beg}) and an indicator of slagging intensity (k_z) are obtained from equations shown in A2.

30 solid fuels and its mixtures were investigated and relevant slagging indexes were determined. Seven hard coals (5 from Poland, 2 from abroad), two Polish lignites and three kinds of biomass (pine, beech, straw) – raw and torrefied were chosen.

Detailed data for technical and ash mineral analysis of investigated fuels as well as determined values of k_z , T_{beg} B_z for four temperatures (800, 1000, 1200 and 1400 K) were placed in [15,16]. After the CERUBIS investigation the number of fuels in the IEN slagging database was increased to 64. All data were used to train the ANN in the CIBOP system in WP3.

Task 1.2 - Pilot scale investigations in USTUTT.

After the broadened investigations at the 20 kW IEN slagging reactor it was decided that the initially planned experiments at USTUTT 20 kW reactor were unnecessary and would not be carried out. More attention was focused on investigations at the USTUTT 0.5 MW test facility (Appendix 1), especially due to scale concerns (20 times bigger than a small reactor). Instead of the two fuels initially planned to be investigated (one hard coal + one biomass), six fuels were investigated (four hard coals, one biomass and one co-firing tests) as shown in Tab.2.1.

Moreover, one fuel, i.e. hard coal from Opole Power Plant (OPP) was investigated in several scales (20 kW IEN slagging reactor, 500 kW USTUTT reactor and 1000 MW real scale utility boiler) in order to test the scale effect. Hard coal from Opole power plant was chosen due to fact that boiler no. 3 has a high corrosion rate.

Due to the wide scope and long duration of the tests, experiments were carried out under two projects: CERUBIS (3 fuels, deposition probes, uncooled probes) and SECTOR (two fuels, cooled deposition probes). Table 2.1 includes tests with a cooled probe and two types (USTUTT and TNO) of deposition probes carried out in the power plants in Task 1.3.

Tab. 2.1 Overall matrix of pilot scale investigations and fuel/ash data of investigated fuels; (✓ - carried out, X - not carried out)

Activities/ Fuel-Ash analysis	Fuel type (HC – hard coal, BC – lignite)						
	EI Cerrejon HC	Opole HC	US HC	Sebuku HC	Bełchatów BC	Torr. Spruce	50% Torr.Spr. + 50% EI HC
Collect. of fly ashes	✓	X	X	X	X	✓	X
Uncooled probe	✓	X	X	X	X	✓	✓
Cooled probe	✓	Carried out in Task 1.3	X	X	Carried out in Task 1.3	✓	✓
Deposition probe	X	✓ (USTUTT) + Task 1.3(TNO)	✓	✓	✓ (TNO in Task 1.3)	X	X
Fuel analysis as investigated (%)							
Ash	14.3	22.8	8.4	12.2	17.8	0.4	as result of mixture
Volatiles	34.4	29.4	35.1	39.4	37	74.3	
C	79	60	70	60	43.3	54	
N	1.64	1.14	1.6	1.4	0.43	0.2	
S	0.4	1.03	2.85	0.3	0.9	0.03	
Al ₂ O ₃	28.7	24.2	13.7	28	19.4	4.6	
CaO	4.8	2.6	4	4	16.2	25.6	
Fe ₂ O ₃	5.2	8.7	14.3	5.3	3.1	12	
K ₂ O	1.2	3.0	2.5	1.1	0.04	22	
MgO	1.0	2.0	0.8	1.6	1.02	6.7	
P ₂ O ₅	1.8	0.9	0.05	0.7	0.1	6.7	
SO ₃	2.3	5.0	33	2.5	9.0	0.0	
SiO ₂	53.0	51	30	52	49.5	21	
TiO ₂	1.4	1.05	0.87	2.36	1.05	0.08	

In order to determine the corrosion behaviour of several materials in boiler tubes in different types of combustion processes defined by fuel and in different boundary atmospheres, the cooled and un-cooled probes were introduced to level 11 of the test rig for around 100 hours. The corrosion rate was calculated by collecting empirical values of oxide scale thickness per several time steps (duration). More information about these techniques, theory and the results are given in [16,17].

Also, a deposition rate probe (described in Appendix 1) was used to determine the real deposition rate. The probe was exposed inside the burning chamber at different levels, at sub stoichiometric (L11) and over stoichiometric (L21) conditions. The measured (real) deposition rate and, then, the theoretically possible deposition rate (maximum) were calculated.

The results of the deposition rates and collection efficiency from the 0.5 MW USTUTT pilot facility are shown in [16] and are also presented in Fig. 2.1 (left). For comparison, slagging intensities obtained for three fuels from the IEN 20 kW stand are shown in the same figure (right). It can be seen that results from the two stands give the same tendency for slagging intensity at over stoichiometric conditions. The highest deposition rate was measured for Sebuku coal, a lower deposition rate for Opole (OPP) coal and the lowest for US coal. A similar order of slagging intensity was obtained at the IEN 20 kW stand, where Sebuku coal had the lowest temperature of slagging beginning (T_{be}) and the highest slagging intensity while US coal had the highest T_{be} and the lowest slagging intensity.

The very important output from the deposition tests in the USTUTT 0.5 MW pilot plant proved that results from the small scale IEN 20 kW stand are applicable to large scale slagging predictions. This also provided confirmation that IEN's slagging database (64 fuels) could be used for ANN training in development of the slagging module in CIBOP.

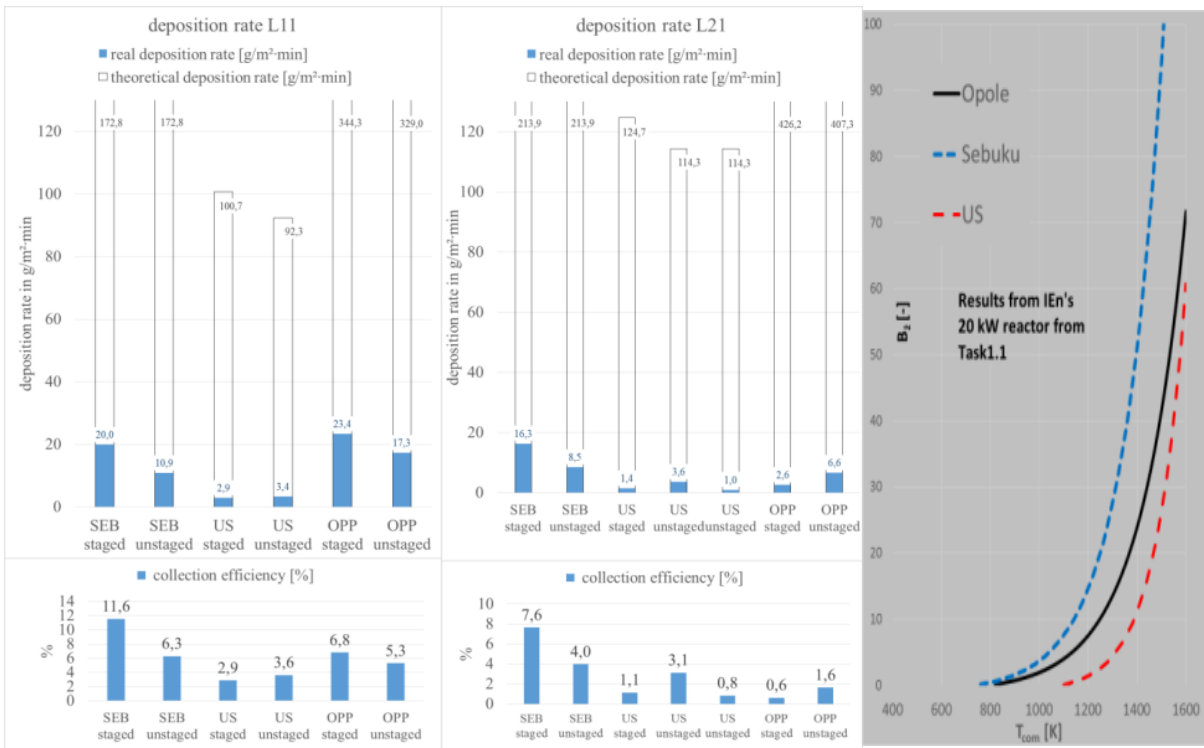


Fig. 2.1 Deposition rates and collection efficiency at levels 11 and 21 with deposition probes in USTUTT 0.5 MW test rig

Task 1.3 Real scale diagnostics campaigns

Several measuring campaigns were run: three in Bełchatów Power Plant (BPP) boiler no. 5 and two in Opole Power Plant (OPP) boiler no. 3, as shown in Tab.2.2 below. The cases in the table denote different boiler operating conditions: boiler load, configuration of coal mills, air distribution, etc.

The campaigns had three main aims: (i) determine the risk of slagging and corrosion in both boilers, (ii) obtain data for ANN training and validation in WP3, and (iii) gather data for CFD calculations in WP3. The campaigns were prepared by PGEGIEK and IEN and all other project partners participated in them. The scope of measurements carried out by each partner is listed in brief next:

- IEN1 Measurement of gas species, temperature and ash suction in the boundary layer of the combustion chamber, temperatures in the combustion chamber, mills investigations, fuel-ash analysis, gaining data from boiler DCS.
- IEN2 Measurement of O₂ & CO in the boundary layer of the combustion chamber, fuel-ash analysis, gaining data from boiler DCS.
- USTUTT Cooled and uncooled deposition probes for a range of specimens, ash suction probe.
- TNO Mobile diagnostic probe application for the determination of deposition rates, fouling factors. Deposit chemical composition investigation.
- HF+PWR unplanned in Task 1.3 preliminary tests of some sensors and corrosion devices/probes (described in WP4).

Tab. 2.2 General matrix for all full scale measurement campaigns (✓ – carried out, X – not carried out)

Campaigns	OPP					BPP					
	IEN1	IEN2	USTUTT	TNO	HF+PWR	Campaigns	IEN1	IEN2	USTUTT	TNO	HF+PWR
2016 3 cases	✓	✓	✓	✓	✓	2015 4 cases	✓	✓	✓	✓	✓
2016 21 cases	X	✓	X	X	X	2015 8 cases	X	✓	X	X	X
						2017-2018 12 cases	X	✓	X	X	X

The campaigns included:

- measurement of O₂, CO, CO₂, H₂S and temperature in the boundary layer of four walls (IEN),
- suction of fly ash from the boundary layer of three boiler walls (IEN),
- measurement of SO₂, NO, NH₃, HCN, H₂O, HCl, HF in several points in the boundary layer of one boiler wall (IEN),
- measurement of O₂ and CO and temperature in the combustion chamber at two locations (IEN),
- measurement of air-dust flows from two mills and determination of temperature and O₂ concentration in selected ducts and dryers (IEN),

- long term collection of the deposits and fly ashes by cooled and un-cooled probes at several locations, SEM WDX and EDX analysis of the samples and collected deposits (USTUTT),
- long term measurement of flue gases and fly ashes at two locations, SEM deposit sample analysis (TNO),
- acquire the working parameters data of the boiler and fundamental parameters of unit (IEN),
- collecting fuels, bottom and fly ashes samples (IEN).

Measurements in the OPP.

Figure 2.2 presents the view of the combustion chamber of boiler no. 5 in Belchatów Power Plant, a lignite fired steam boiler with capacity of 1150 t/h of steam (pressure of primary steam 180 bar, temp. of primary steam 560 C deg.). It is a tangentially fired unit with eight columns of burners located on the walls at between 17 and 27 m. Eight fan mills (called NL1...8) feed the burners with pulverized lignite. Coal is dried in dryers fed by flue gases taken from the boiler from level 47 m. There are two levels of OFA ports (41.4 m and 54 m) and additional wall protection nozzles at levels 19, 27 and 34 m. The first superheaters are located at level 54 m. 220 adapters with diameter of around 16 mm between membrane wall pipes were mounted on four walls of the boiler to allow measurement of the concentration of flue gases and temperature in the boundary layer of the combustion chamber.

Moreover, additional openings with diameter of around 100 mm at levels 27, 54 and 57 were made for the purpose of measuring the concentration of flue gases and temperature inside the combustion chamber as well as for introducing the deposition probe and the ash suction probe.

All measurement places were shown in detail in [18].

The main campaign at this boiler took place in 2015, when the abovementioned measurements were made. Four measurement cases were carried out, each lasting 24 hours as shown in Tab. 2.3, two for a high load of 380 MW (100%) and two for a low load of 230 MW (60%).

Two additional campaigns (shown in Tab. 2.2) took place in 2015 and 2017/2018. Their purpose was to gather more data on O₂ and CO concentrations in the combustion chamber near the walls in various operation conditions of the boiler. In total, 24 cases of O₂ and CO concentrations were collected for ANN training

Detailed measurement results and fuel and ash analysis as well as a description of the results obtained are presented in [18].

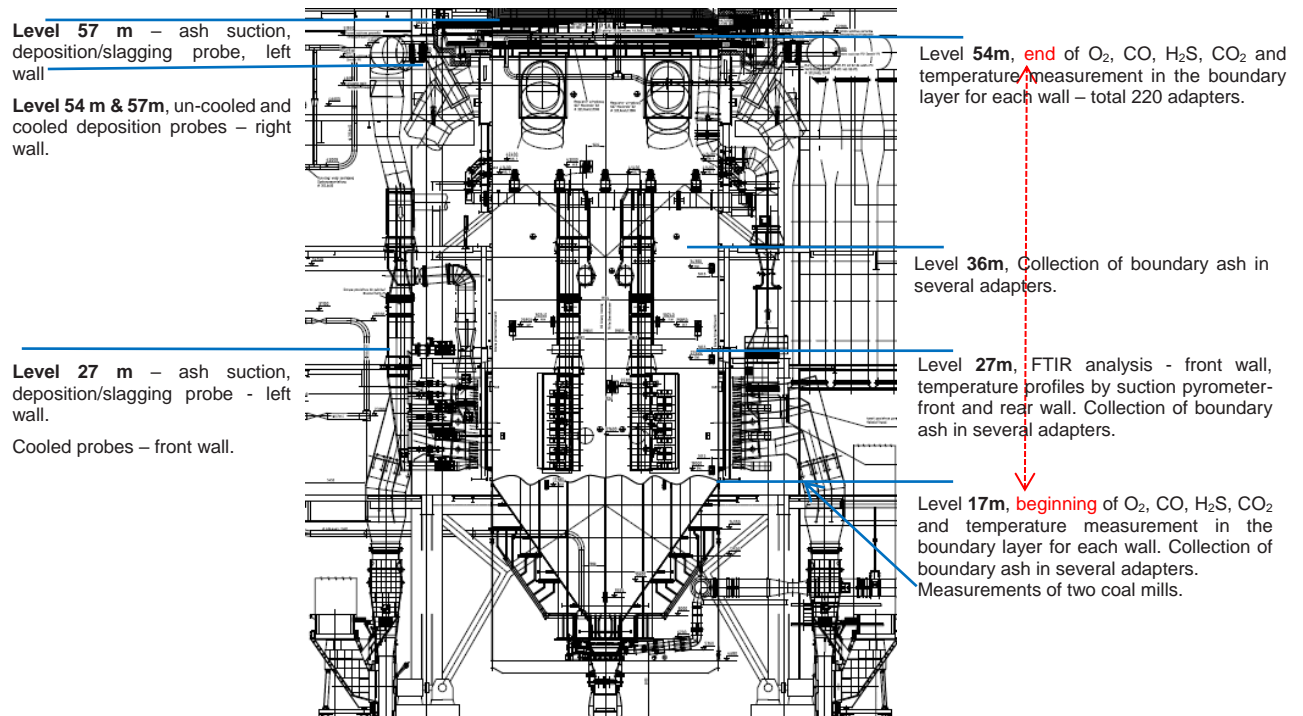


Fig. 2.2 View of the combustion chamber of boiler no. 5 in BPP with location of some measurements

Tab. 2.3 General data for the measurement campaign in BPP in 2015

Case no	Capacity MW _e	Excess air up to OFA	Time of experiment	Averaged NO _{x,outlet} mg/m ³ _n	Averaged CO _{outlet} mg/m ³ _n	Averaged O _{2,outlet} , %
Case 1	380	According to expl. manual	24 hours	203	160	2.04
Case 2	380	Increased (lower OFA flow)	24 hours	205	92	1.8
Case 3	230	According to expl. manual	24 hours	170	34	2.23
Case 4	230	Increased (lower OFA flow)	22 hours	194	20	2.22

The investigations carried out in boiler no. 5 in BPP led to the following main conclusions:

- There is a risk of corrosion for each evaporator wall between levels 17 and 45 m. Areas of high risk of corrosion were determined.
- Relatively low temperature of flue gases prevailing in the boundary layer of the evaporator can decrease the risk of corrosion. The slag/ash accumulating on the probes did not melt and was rather fragile and easy to remove.
- High fluctuations of coal quality and thus the overall amount of air to boiler markedly affects the behaviour of gas species concentration in the boundary layer. Once the given area is determined as with certain risk of corrosion within minute may change to no corrosion risk at all.
- Data for CFD simulation and for online corrosion detection system were gained.
- Measurements with TNO's mobile diagnostic probe had showed very little deposition taking place in the vicinity of the walls, hence slagging-related corrosion problems does not occur.
- Deposits formed are largely made up of calcium species, aluminosilicates and iron, none of which is known to promote corrosion.
- No corrosive attacks of the deposition substrate could be detected, provided that the protective oxide layer on the deposition substrate was intact.
- On sites where the oxide layer was destroyed (by detachment due to mechanical or thermal stress forces) sulphation of the metal surface was detected which could be seen as the onset of corrosion. This implies that thermal stresses should be minimised during start/stop procedures and load changes in order to prevent detachment of the protective oxide layer on the boiler walls.

Measurements in the OPP

Figure 2.3 presents the view of the combustion chamber of boiler no. 3 in Opole Power Plant, which is hard coal fired steam boiler with capacity of 1150 t/h of steam (pressure of primary steam 180 bar, temp. of primary steam 560 C deg.). It is tangentially fired unit with four columns of burners located between 19 and 32 m. Five mills feed the burners with coal dust (each mill for each raw of burners). There is one level of OFA located at level 32 m and ROFA (34.3, 39.2), and ROTAMIX (39, 44.7 and 50.5 m) installation up to 50.5 m. First superheaters are located on the level of 47 m (except wall superheater between levels 38-46 m). In 2010 boiler was modernised in order to reach emission of NO below 200 mg/m³_n by primary methods which forced lower excess air in the combustion chamber and SNCR method (above mentioned ROTAMIX). This increased markedly the risk of low emission (high temperature) corrosion. In 2017 boiler was further modernised (mainly ROFA) to reach 150 mg/m³_n.

116 adapters with diameter 14 mm between membrane walls tubes were mounted on four walls of the boiler to allow the measurement of concentration of flue gases and temperature in the boundary layer of the combustion chamber.

Moreover, additional openings with diameter around 100 mm at levels 30, 51 and 60 were done for measurement of flue gases concentration and temperature inside the combustion chamber, and for deposition and ash suction. All measurement places were shown in detail in [19].

The main campaign at this boiler took place in 2016 year, when full set of measurements had been carried out.

Three measurement cases were carried out, first lasting 14 hours, second 24 hours and third 22 hours as shown in Tab. 2.4. One for high load of unit 380 MW (100%), one for 300 MW (80%) and one for low load of unit 230 MW (60%).

Additional campaign aimed for collecting data for ANN training took place also in the year 2016, which had allowed for collection in total of 24 cases of O₂ and CO concentrations

Detailed measurement results and fuel and ash analysis as well as description of the results obtained had been presented in [19].

The investigations carried out in boiler no. 3 in OPP had allowed for formulation following main conclusions:

- There is a high risk of corrosion for each wall of evaporator between levels 19 and 36 m. Areas at high risk of corrosion were determined.
- High temperature of flue gases in the boundary layer of the evaporator increases the risk of corrosion. The slag/ash accumulating on the probes melted, was difficult to remove, almost embedded into the material of the pipe, the deposition rate was high.
- Data were gathered for CFD simulation and for the online corrosion detection system.

- Measurements with TNO's mobile deposition probe showed that at level 60m no harmful deposit is formed that would either cause significant corrosion or fouling.
- In contrast, deposits formed at level 30m were made up of molten and iron-rich particles closely attached to the steel surface. The close attachment of the deposit to the steel surface can cause diffusion of steel constituents such as chromium and nickel into the deposit, effectively deteriorating the steel. The origin of the iron-rich particles is unclear, but most likely they originate from pyrite in the fuel.
- Sulphur was only found at one location in the vicinity of the steel surface. Chlorine was not found.

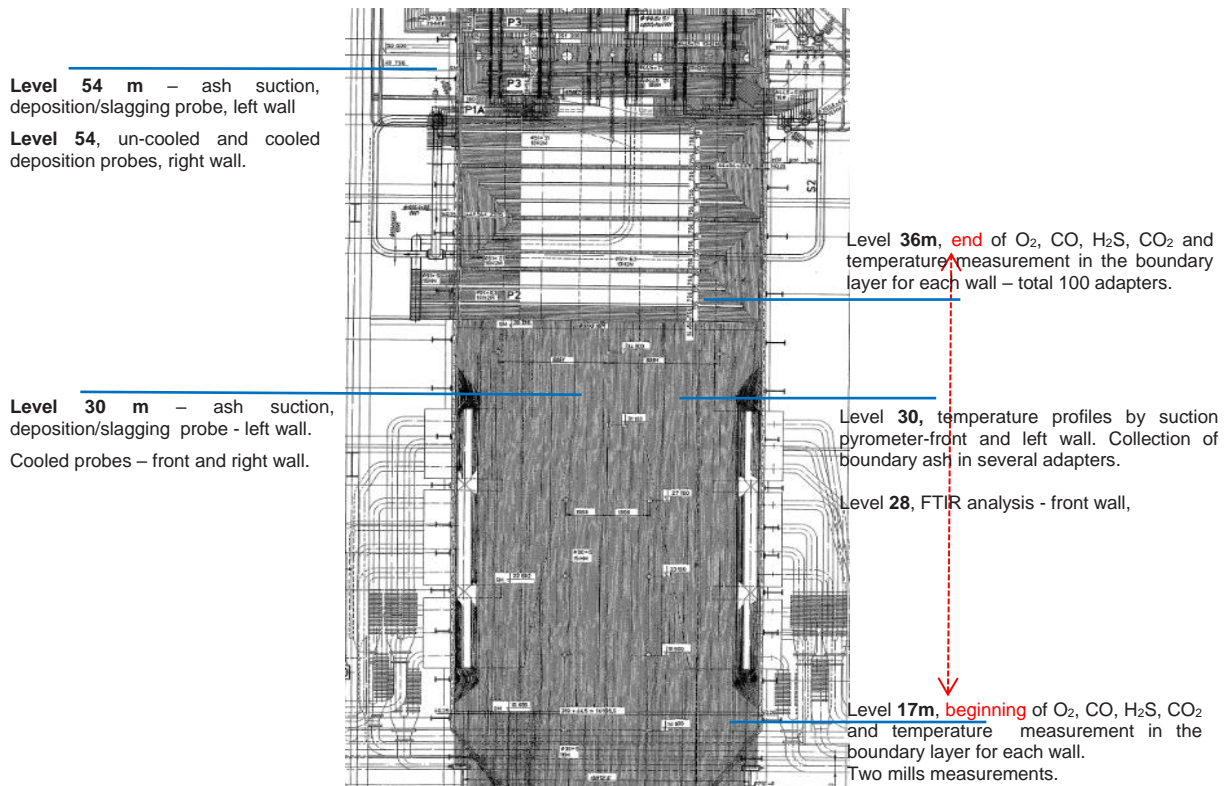


Fig. 2.3 View of the combustion chamber of boiler no. 3 in OPP

Tab. 2.4 General data for measurement campaign in OPP in 2016

Case no	Capacity MW _e	Excess air up to ROFA	Time of experiment	Averaged NO _{x,outlet} mg/m ³ _n	Averaged CO _{outlet} mg/m ³ _n	Averaged O _{2,outlet} , %
Case 1	380	According to expl. manual	14 hours	177	73	2.28
Case 2	300	According to expl. manual	24 hours	183	40	2.55
Case 3	230	According to expl. manual	22 hours	204	5.5	4.0

Discussion of WP1 results.

Work package WP1 was very informative and gave background and reference for planned and conducted measurements with various online corrosion detection systems which were developed in the project in WP2 and also supported development of the whole concept of online corrosion detection systems in WP3.

Determination of corrosion, slagging and fouling behaviour under different emission regimes (NO_x, CO₂) was done for different types of tube materials and different fuels (Tasks. 1.1, 1.2 and 1.3). This activity was carried out by collection and subsequent chemical/physical analyses of fly ash deposits in the 0.5 MW pilot plant at USTUT and in the both investigated boilers during measurement campaigns. Cooled and uncooled probes with deposition rings made from different steels were used. In addition, deposition probes were used to determine the rate of deposit growth. Samples from the deposition probe taken by TNO during boiler measurements were also subject to chemical/physical analyses. The selected steel materials were also examined in the USTUT laboratory corrosion test rig. In general, the results obtained broadened knowledge about corrosion mechanisms, in particular those occurring in the investigated boilers. Among others, they confirmed that sulphur corrosion is a prevailing mechanism in these boilers.

Some disappointing results were obtained from joint measurement campaigns in the case of corrosion estimation on the basis of cooled probe exposure. Corrosion rates determined on that basis were very often markedly higher in BPP than in OPP which was contrary to real measurements of wall thickness loss in recent years. The reason might lie in overly short probe exposure or significantly different conditions, affecting the alloys on the probe differently to the materials in the evaporator tubes (temperature, flow direction, erosion). It is thus difficult to estimate the real corrosion rate

based on such measurements - all measurements indicated higher corrosion rates in BPP than in OPP. For these reasons cooled probes took no further part in the diagnostic system under development.

A very important output from the deposition test in the 0.5 MW pilot plant was the similar assessment of deposit growth for different coals as for the IEN 20 kW slagging reactor, which was used for generation data for ANN training for the CIBOP slagging module.

Another very important output WP1 was acquiring voluminous, real scale data from the two utility boilers where finally the CIBOP was to be applied and tested.

2.3.2 Development, intra-validation and integration of different corrosion and flow sensors - WP2

In WP2 the most promising sensors for applications in utility boilers were selected with particular attention to the extreme power plant conditions. The work conducted focused on development, manufacturing and testing of the various sensors, as well as the measurement devices and sensing platforms based on them. The testing of these developed elements of the future diagnostic system was carried out first in laboratory conditions and then in pilot scale conditions.

An important part of WP2 was conceptual integration of different measurement techniques in sensor platforms, enabling prediction of the corrosion rate.

Task 2.1 - Definition of sensors to be investigated.

A broad range of sensors and sensing equipment to determine either directly the corrosion rate or to monitor the indirect risk of corrosion of evaporators in thermal power plants were evaluated in this task. Furthermore, a novel sensor to measure steam flow was taken into account for assessing the rate of slagging or fouling of a boiler. The analysed measurement principles are generally known, but their specific combination for application in thermal power plants was central for their selection and is truly novel.

The key was simultaneous use of direct and indirect sensors, enabling direct prediction of the corrosion rate of entire membrane walls of a boiler.

The sensors and measurement methods selected and then were investigated in the project are listed in Tab. 2.5 below.

Tab. 2.5 Overview of methods and sensors investigated in WP2

Method/sensor	Measured variables	Sensor type	Derived quantities	Beneficiary
Electrical resistance of boiler wall – own sensors	Resistance, temperature	Direct	Corrosion rate	HF
Corrosion probe - electrical resistance of sensor from boiler strel – own sensor	Resistance, temperature	Direct	Corrosion rate	PWR
Ultrasonic wall thickness measurement – commercial sensor	Wall thickness	Direct	Corrosion rate	IEN
Reduction conditions at boiler wall - different types of commercial sensors (zirconium and electrochemical)	O ₂ , CO, H ₂ S concentration	Indirect	Corrosion risk	IEN, PWR
Steam flow – own sensor	Heat flux, temperature	Indirect	Steam mass flow, (deposit built-up)	TNO

Direct corrosion sensors:

- HF engaged in developing a boiler wall resistivity measurement system based on measuring the electrical resistance of the actual boiler wall (Corrosion Monitoring System CMS). The wall temperature was measured simultaneously with the electrical resistance of the wall. By correcting for the temperature dependence of the resistivity of the membrane wall, the corrosion rate could be determined since the resistivity of the boiler wall is a function of its thickness. The big advantage of the system was that the corrosion rate of the boiler wall was monitored directly.
- PWR engaged in investigating the same corrosion rate measurement principle as HF, but as opposed to the previously described system, the boiler wall is not monitored; instead, a corrosion probe is used. Both electrical resistance of the corrosion ring (mounted on the probe) and its temperature are monitored. By correcting for the temperature dependence of the resistivity of the corrosion ring, the corrosion rate can be determined. This system has the advantage that temperatures of metal of the corrosion ring are relatively constant and easy to measure.
- IEN engaged in investigating an alternative measurement system to determine the wall thickness by means of ultrasonic acoustic waves. The sensor requires a special connection to the membrane wall of a boiler. Like the HF sensor, the ultrasonic sensor gives direct information on actual wall thickness and hence the corrosion rate can be determined via the change in wall thickness over time. The big advantage of the system is that it can be online used during normal boiler operation

since the measurement of fireside wall thickness is made by a device located outside the boiler combustion chamber.

Indirect corrosion sensors:

- IEN and PWR engaged in investigating gas analysis equipment suitable for long-term online monitoring of flue gases in near wall layer. Indications of possible corrosion problems of furnace walls can be derived from online analysis of the gas atmosphere in the flue gases layer near a wall of the boiler combustion chamber. Sub-stoichiometric conditions indicate an increased risk of corrosion. The presence of hydrogen sulphide poses an additional risk for rapid evaporator wall corrosion. An array of electrochemical sensors for the determination of the local redox conditions by means of measuring concentrations of O₂, CO and H₂S was tested. Also, several different zirconium probes were investigated. Subsequently, IEN engaged in developing its own gas composition monitoring systems basing on chosen zirconium and electrochemical sensors integrated in one suitable device.
- TNO engaged in developing a Non-Invasive Steam Flow Meter (NISTFLOM or NF for short) for application in thermal power plants. The flow meter is capable of detecting changes in steam flow in individual steam pipes. If the properties of the working medium are known, the steam flow can also be monitored quantitatively. The measurement principle was based on a heat flux measurement between the steam pipe and the cooled sensor. When the steam flow changes, the convective heat transfer coefficient changes too, and hence, a change in heat flux could be detected. In combination with a heat flux measurement mounted directly on the steam pipe of the boiler, deposit build-up and fouling phenomena could be detected (fouling sensor).

Task 2.2 - Development and laboratory testing of O₂/CO/H₂S probes.

The activity in this task was comprised of developing a single system for gas analysis.

There were no cheap gas analysers available on the market that were dedicated to online measurement of very hot flue gases taken from a boiler combustion chamber. Such gas samples are loaded with dust and moisture, which causes the analyser to clog and can destroy its sensors. So, analysers of this type require additional systems to enable them to cope with long-term operation in extreme conditions

The gas analysis system that was developed consisted of a gas suction pipe mounted in the membrane wall of the boiler – a so-called adapter – gas sensors and a set of subsystems enabling permanent gas analysis by these sensors. This is schematically shown in Fig. 2.4, with red and blue arrows indicating two considered approaches to the gas analysis system: one with a pump, the other with an injector.

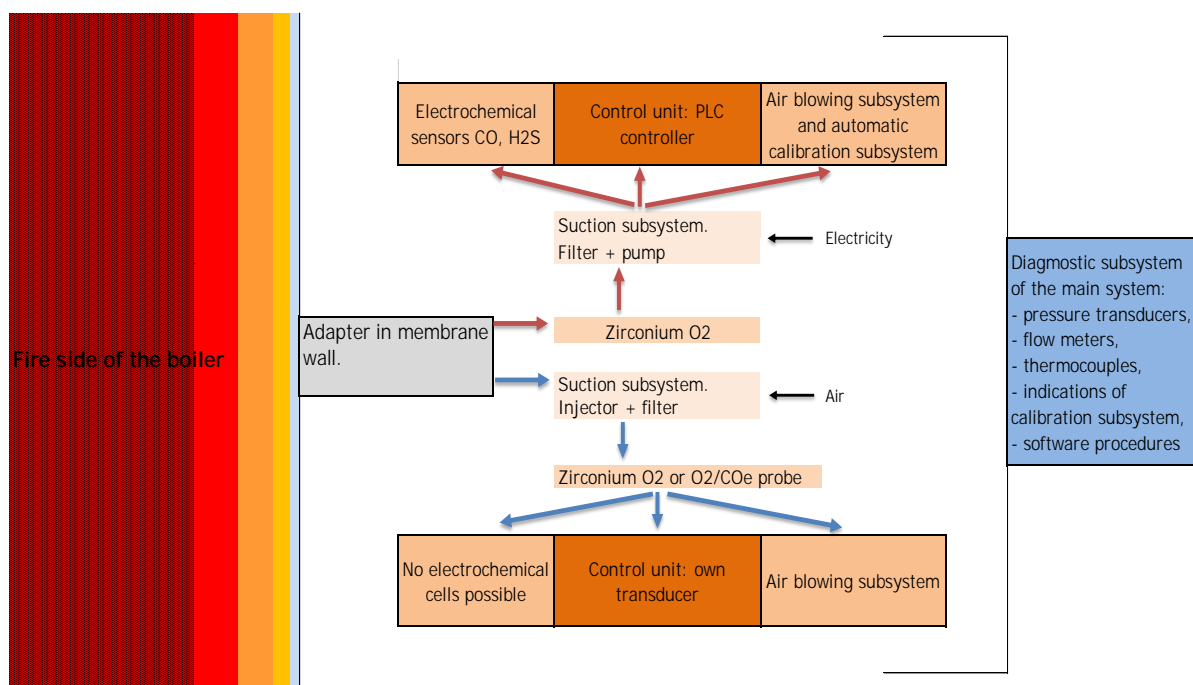


Fig. 2.4 Development chart for gaseous sensors and probes

Thus, the research activity carried out could be grouped into five subtasks:

- Development of zirconium and electrochemical sensors in the sense of testing them in different and variable laboratory and real boiler conditions,
- Development of a flue gas suction subsystem,
- Development of an air blow/calibration subsystem,

- Development of control systems of developed devices, on the basis of either own manufactured control transducers (PWR) or PLC controllers available on the market (IEN) (more expensive but more flexible for future commercial utilisation in boiler conditions),
- Development of a diagnostic sub system informing the user about possible incorrect operation of the gas analyser.

Initially, gas sensors of various types from different supplier were selected and tested in laboratory conditions. The main specifications of the investigated sensors are given in Tab. 2.6. Output from the sensors were compared with indications of professional gas analysers like Siemens Ultramat 23. Some results of these test are shown in Appendix 2.

Tab. 2.6 Main specification of gas sensors

Species measured	Operation principle	Range	Error
O ₂	Narrow zirconium	0-20.9%	Max. ±0.5% O ₂
O ₂	Wideband zirconium	0-20.9%	Max. ±0.13% O ₂
O ₂	Electrochemical	0-30%	Max. ±1% FS
CO	Electrochemical	0-10% (non-continuous measurements)	< 500 ppm at 1% CO
H ₂ S	Electrochemical	0-10 000 ppm (non-continuous measurements)	< 40 ppm at 2 000 ppm H ₂ S
O ₂ /CO _e	Wideband zirconium (KS1D Lamtec)	0-20.9% O ₂ 0-1% CO	n.d.

Tests of different gas sensors were also conducted in real scale in boiler no. 5 in BPP. Despite the extreme conditions (high temperature, dust) the results obtained for wideband zirconium 1 and also for a simple electrochemical O₂ sensor were very close to the reference results (Appendix 2).

One of the important parameters for CO and H₂S electrochemical sensors was their response time. A special measurement chamber was designed and manufactured for these sensors. In the design process CFD was used to optimise flue gas flows, which in the case of electrochemical cells is very important (faster reaction, faster purging).

Beside the sensors, an important and at the same time the most difficult element of Task 2.2 was development and construction of specified subsystems for assembling the complete gas analyser. This was due to the requirements of these devices. It was necessary to reconcile the aspiration of keeping costs down with the requirement of long-term, reliable operation of these devices in the extreme conditions of a coal-fired power plant. Many alternative options of these subsystems were designed, manufactured and tested, as described in [20] and Appendix 2. Some examples of issues which had to be worked out are given below.

One of the main problems of continuous measurement of the exhaust gas composition in the boundary layer is clogging of the measurement points (adapters in membrane walls or places close to adapters, especially connectors (Fig. 2.5). In order to overcome this problem a new adapter was designed and manufactured as presented in Fig. 2.5 (right side), featuring an internal filter in the connector and pump-free suction of flue gases using an ejector.

Air blow (for purging) and automatic calibration subsystem is a very important part of the main system. When electrochemical cells are used, the system becomes more complicated. Different pneumatic schemes of the developed subsystems (depending on configuration of used gas sensors) were tested in laboratory and real scale conditions

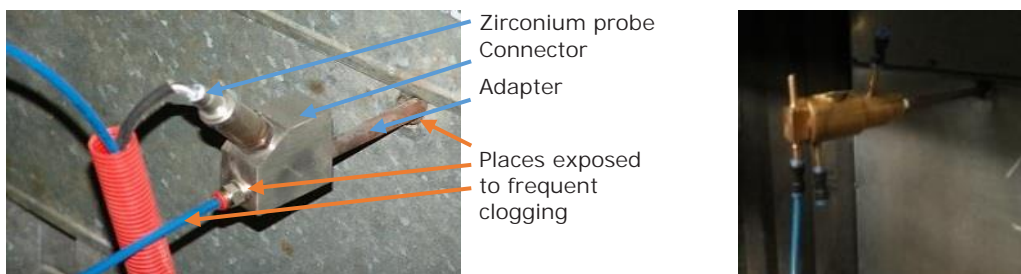


Fig. 2.5 View of the typical connector with zirconium O₂ probe (left) and the new design (right)

One of the most important features of the measuring system that was developed was the diagnostics of its condition during normal operation. The diagnostics referred to clogging of the measuring port or pipes by ash, and failure of the sensor, pump and other parts. The diagnostic system informed the user about possible issues.

The development works and tests had resulted in the construction of two types of specially designed gas analysers (Fig. 2.6) equipped with the abovementioned subsystems.

The type 1 gas analyser is designated for the zirconium wideband O₂ sensor and equipped with the researchers' own manufactured controller. The type 2 gas analyser equipped with a PLC controller available on the market had three versions adapted for different sets of sensors:

- O₂ wideband zirconium sensor,

- O₂ and CO - wideband zirconium and electrochemical sensors respectively,
 - O₂, CO, H₂S - electrochemical sensors.
- All analyser types were tested and verified in laboratory and real scale conditions.

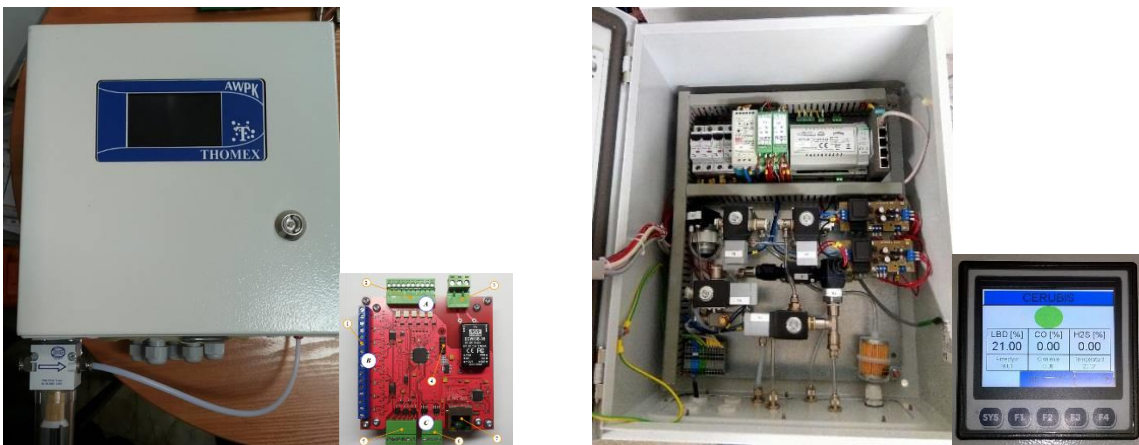


Fig. 2.6 Gas analysers designed and manufactured in the CERUBIS project: type 1 (left) and type 2 (right)

Task 2.3 Development and laboratory testing of online corrosion/sludging sensors.

Online corrosion probe.

The technique for measuring the corrosion rate is long-established, but mainly for measurements at low and constant temperatures, for example in water tanks, pipelines or underground steel constructions. The sensors were mostly based on electrical resistance or electrochemical principles (for example, electrochemical noise measurement or linear polarisation resistance measurement). For such cases, commercial measuring systems were available and many companies provide ready-made solutions.

At the time the project proposal was prepared, several institutes and companies were developing corrosion monitoring systems using corrosion probes for high temperatures. The sensors were typically based on electrochemical principles that are well known from corrosion in electrolytes. These methods were very complicated and expensive at high temperatures, are still under development and their reproducibility is sometimes quite low.

Some of these techniques are already commercially available, but are very expensive. At that time, no cost-effective high temperature corrosion monitoring system based on electrochemical methods was available.

The challenge was to produce a probe in which the sensing element placed in the boiler combustion chamber would be electrically insulated and cooled in order to stabilise the temperature.

The corrosion probe was designed to directly measure the electrical resistance of the sensor. The sensor is made of boiler steel (the same material as the material of the boiler evaporator) and electrically insulated from the rest of the probe, as shown in Fig. 2.7.

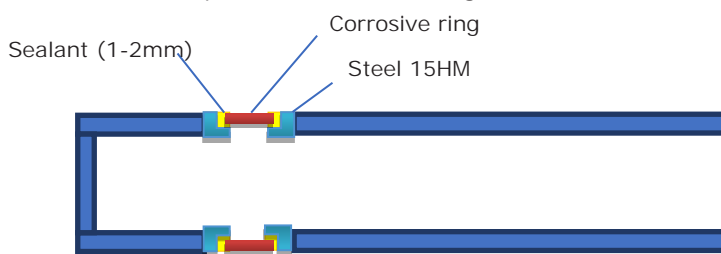


Fig. 2.7 Schematic diagram of the corrosive ring (sensor) on the probe

In the designed resistance probe, in order to measure the loss of thickness of the sensor (and thus evaporator pipes) 4-wire resistance measurement was used (separate pairs of current-carrying and voltage-sensing electrodes).

Preliminary tests were carried out in the laboratory to find out how changes in dimensions of the selected material affect its electrical resistance and how the resistance level depends on the thickness of the probe. During this test the recorded probe resistance changed by mechanical treatment (reducing the thickness). Since the resistance of the sensor is strongly dependent on temperature, the sensor has to be constantly cooled by air and its temperature has to be measured. The automatic adjustment of the cooling system was intended to provide a constant temperature of the sensor (approx. 350-400°C), depending on the type of boiler. Both resistance and temperature were taken into account when calculating the corrosion rate. An automatic control system, with a 2/2-way proportional solenoid valve and regulator of temperature was designed and manufactured (A4) in order to provide continuous control of the sensor temperature [21].

Online electric resistance measurement of the evaporator wall (CMS)

Corrosion on the inside of a boiler wall will lead to a reduction of wall thickness over time, as schematically shown in Fig. 2.8 (left). This reduction of wall thickness is measured by the CMS system, which measures changes in electric resistance between points located on membrane walls of the boiler, as shown in Fig. 2.8 (right). According to the Ohm law, a decrease in wall thickness results in higher electrical resistance, as the cross-section of the steel material between the measurement points becomes smaller.

The advantage of this system is the potential to work in an installation long-term, because it works on the outside of the boiler. Moreover, the system does not require openings in the boiler wall, which is also a big advantage. However, it is extremely challenging to measure very low resistance of the order of single $\text{m}\Omega$ in the presence of very high signal-to-noise ratio and influence of temperature, which changes very often and rapidly during boiler operation.

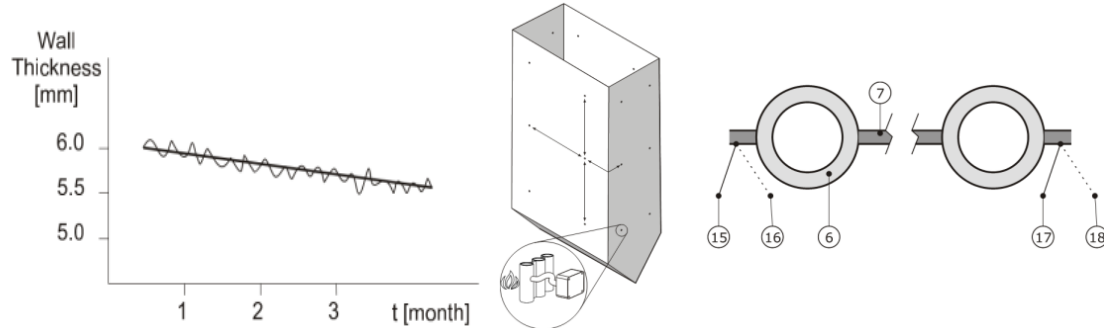


Fig. 2.8 Schematic diagram of the measurement principle, resistance is measured between the points 15/16 and 17/18. Wall temperatures are also measured at the connection points

A bridge circuit method was used to measure resistance and overcome the problem of the small magnitude of the signal. Three different implementations of the method were considered and investigated during laboratory tests. Initial laboratory tests were done on a metal plate of $28 \times 15 \times 1$ mm, with two copper cables attached to the sides of the plate and three thermocouples spot welded on the plate itself (Fig. 2.9). Electrical resistance was **about $0.8 \text{ m}\Omega$** . For the second round of laboratory tests, a second prototype was made (also Fig. 2.9). It was a stainless steel plate of $61 \times 10 \times 1$ mm with 5 connection points. Electrical resistance was **about $4 \text{ m}\Omega$** . In order to continuously measure the resistance, two versions of the measurement control box were built, called a long-term corrosion monitoring system (CMS). One system is able to supply 15 V and 40 A. The second system is built with a 35 V, 45 A power supply.



Fig. 2.9 First and second prototype for laboratory tests and CMS control box

The current through the boiler wall can be determined by measuring the voltage drop over a shunt resistor with known resistance in series with the boiler wall. A mathematical analysis was conducted on the settings for minimum uncertainty when taking 4-wire resistance measurements with a CR6 and a CR1000 data-logger. Based on this analysis, it was decided to go with the Campbell Scientific CR6 data-logger for further development of the measurement system.

Temperature differences induce thermal offset voltages. A model to describe this effect was developed and tested on the second laboratory prototype. The effect of thermal voltages by averaging over two measurements with reversed current direction was removed.

Capacitive coupling between two close wires, one carrying a large current, leads to capacitive effect, which has an impact on settling times of measured resistance. This effect was subject to laboratory investigation [21]. On this basis it was supposed that the capacitive effect is contained solely in the wires. It was finally decided not to use the same cables for current injection and voltage sensing altogether. A dedicated wiring configuration was established, ensuring that the capacitive effect disappeared completely.

First measurements with hot flue gases with the CMS were carried out at the laboratory reactor. The electrical resistance and temperature of the TNO deposition probe, consisting of a pipe and a deposition sample of stainless steel 310 (non-preoxidised), were measured.

The results of the laboratory testing were promising. It was possible to measure few- $\mu\Omega$ resistance changes on a signal in the m Ω range. The signal-to-noise ratio of the resistance measurements was around 300 and the four-wire method used to measure the resistance is very stable with respect to changing the external voltage and the value of the shunt resistor.

Online ultrasonic tube thickness measurement

Fig. 2.10 shows the concept of direct measurement of wall thickness loss using the ultrasonic measurement of pipe thickness from the outside of the boiler through a special connection welded to the membrane wall. This could be the simplest of all the direct methods developed, but an accurate model of calculation of real wall thickness is vital in this method. Another challenge is measurement itself. Measurement could be carried out online during normal boiler operation, but the issue is the temperature. On the one side, a shorter connector welded to the pipe gives better accuracy of measurement. On the other side the shorter connector results in the higher temperature of the ultrasonic probe. The estimated temperature of the 30 mm connector located in the insulation of the combustion chamber is only around 25 °C lower than the temperature of the tube. This can destroy the ultrasonic probe or, even if it does not destroy it, the surface of the connector may be covered by some oxide leading to measurement failure. High temperature may also cause some chemical reactions of the paste used to ensure a good connection between the probe and connector.

To mitigate the temperature effect, measurement could also be carried out during short boiler outages (even during a weekend), at several points normally covered by insulation — but during measurements they would be opened and the ultrasonic probe would be attached to the connector. Although it would no longer be an online method, it is still interesting because it can be carried out from outside of the boiler. The core of the method is proper recalculation of the values obtained into inner wall thickness. It is very important to know exactly where the connector is welded and where the probe is attached to the connector.

To check the method, two connectors were welded to used and new tubes from OPP. The experiment relied on attaching the probe to the connector by hand every 10 second during a period of time. Big differences in measurement results were noticed, and more importantly, the measurement frequently failed. The issue was that during welding not all material/weld is melted between the connector and tube material, leaving empty gaps between them. For the ultrasonic method this is the barrier. Obtained values close to the range 26 to 28 mm corresponded to the height of the welded connector itself, and the thickness of the tube itself was not visible. Moreover, BPP and OPP specialists had some concerns relating to welding such connectors directly to tubes working in high pressure conditions. For these reasons this method was developed no further and was not used in WP3 or WP4.

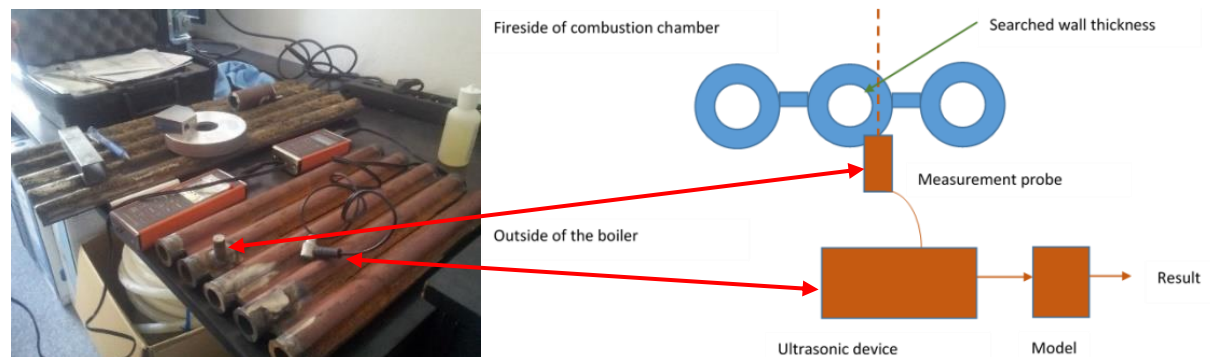


Fig. 2.10 The ultrasonic method of online wall thickness measurement

Task 2.4 - Development and bench-scale testing of online steam flow metering sensors.

Non-invasive Steam Flow Metering

A Non-Invasive Steam Flow Metering (NISTFLOM) system was developed and tested. This system is meant to give precise, real-time insight into the steam flow in a single pipe of the steam heat exchanging system. At the heart of the sensor is a heat flux sensor manufactured by HF. A schematic diagram of the sensor is given in Fig. 2.11.

The heat flux sensor is enclosed in a small chamber, through which a small reference medium flow is passed. The reference medium flow through the chamber is controlled in such a way as to obtain sufficient signal-to-noise ratio and response time, while minimising the medium use. The output of the sensor, a microvolt-range signal, is measured by a self-contained electronic unit, which digitises and logs the data. The unit makes it possible to transmit the data to the boiler control room or to a remote location, where the data can be processed further. This signal can be translated into steam mass flow, based on a multipoint calibration.

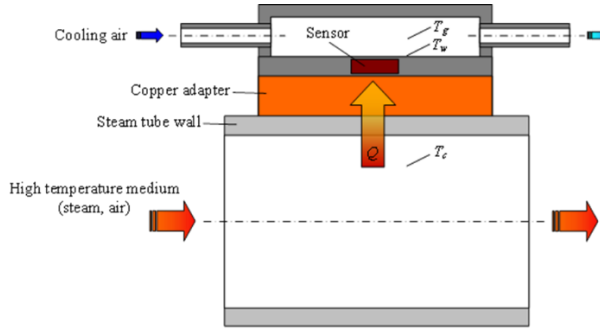


Fig. 2.11 Schematic diagram of the NISTFLOM sensor

In order to withstand high-temperature conditions found in heat exchanger sections of a thermal power plant, the online stem flow sensors need to have a robust design while at the same time maintaining optimal functionality, i.e. an optimal thermal design of the sensor has to be preserved. The latter implies ideally one-dimensional heat flux through the sensor and minimal thermal inertia. A sensor fulfilling these requirements was designed and prototypes of the sensor were manufactured. The measurement principle is based on the measurement of the heat flux between the steam pipe and the heat sensor and its theory was described in detail in [22].

The recorded heat flux signal from the sensor is proportional to the true heat flux and the temperature difference between the sensor and the working medium. Hence, an experimental overall heat flux coefficient can be determined as:

$$k_{t,exp} = \frac{SS}{\Delta T_s}$$

where SS is the sensor signal and ΔT_s is the temperature difference between the sensor and the working medium. The experimental overall heat coefficient $k_{t,exp}$ can be calibrated against the theoretical values, which in turn can be used to calculate the flow velocity and hence determine the mass flow rate.

In order to calibrate the sensors two test rigs were constructed. Both rigs consisted of an electric gas heater connected to an electrically traced steel pipe on which a NISTFLOM sensor was mounted. The sensor and its connecting adapter were well insulated in order to mimic realistic high-temperature conditions occurring in heat exchanger sections in a thermal power plant. Nitrogen was used as the medium.

Several tests were carried out, varying medium flow and cooling flow of the sensor, keeping the temperatures constant at 350 °C (maximum temp. of the first laboratory rig). Experimental overall heat transfer coefficients were measured and compared with the theoretical values (A6). The tests confirmed that the procedure applied was capable of correlating the experimental values with the theoretical ones.

The second laboratory rig achieved a temperature of up to 570 °C. The first tests on this rig were carried out using a copper adapter piece connecting the sensor with the pipe carrying the medium. After a few hours of testing at 540 °C the copper adapter was visibly corroded due to contact with air at high temperatures. Hence, it was decided to change the adapter material to aluminium. Aluminium has, like copper, a significantly higher thermal conductivity than steel, hence is a suitable material for using in combination with the NISTFLOM sensor, since it will add only a little additional thermal resistance to the heat transfer from the hot medium to the sensor.

Calibrations of the sensors were carried out at 540 °C and 570 °C after the decision was taken that the sensors would be placed in the reheating section in OPP for additional preliminary tests in February 2016. Two sensors were calibrated, because it was decided that two sensors would be mounted just after an inlet header in the reheat-section, while two other sensors would be placed on the membrane wall. The latter two sensors were intended to deliver qualitative information about the water/steam flow in the membrane wall. It was confirmed that the sensors can be calibrated also at the higher temperatures and higher Reynolds numbers via a linear correlation. It was shown that each individual sensor, even though they were apparently identically constructed, needs individual calibration. Apparently, the way each individual sensor was constructed, in particular the supply of cooling air, plays a crucial role for the sensor output. Nevertheless, as could be seen from the calibration curves, both sensors could be calibrated with simple linear regression, yielding very high coefficients of determination (R^2), indicating very good correlation. Calibration results for abovementioned experiments are given in Appendix 5.

A sensor platform for the measurement of steam flow in heat exchanger pipes in thermal power plants was developed further, based on the calibrated sensors. Alongside constructive optimisations, the necessary theory to operate the sensor was developed and validated by means of calibration trials. The resulting sensor platform could detect changes in steam flow and was able to quantify them, provided that the physical properties of the working medium were known. The latter implies that the sensors should be mounted on steam pipes leaving inlet headers, since the steam parameters are uniform throughout the header and logging of the necessary parameters (pressure and temperature) is present in power plants.

Task 2.5 Different sensors integration and validation

All sensors and measurement devices were developed and tested under laboratory conditions and in some cases in power plant conditions. After these works preferable sensors and solutions for measurement devices were known. On the basis of the experience gained, different possible combination of sensors was analysed from the point of view of the requirements of the final diagnostic systems. The sensors were grouped into sensor platforms. A sensor platform denotes the conjunction of at least two sensors from which the rate of corrosion can be estimated for a wider area of the membrane wall of the boiler, not only locally. Direct corrosion sensors (wall resistance measurement, corrosion probe) determine the corrosion rate locally and a long exposure time is needed to estimate the corrosion rate. On the other hand, indirect methods (O_2 , CO, H_2S concentration measurements) can almost immediately determine the corrosion risk for a wider area, like whole evaporator walls. Thus, the combination of direct and indirect methods was necessary for a proper and economically reasonable diagnostic system configuration and operation.

As a result of the analysis, eleven possible sensor platforms were defined (Tab. 2.7). This formed a basis for further tests and improvements of the sensors and measurement devices, as well for shaping two final diagnostic systems – one for boiler no. 3 in BPP and the second for boiler no. 3 in OPP. Table 2.7 shows which platforms were later chosen for pilot scale experiments and for boiler diagnostics.

Tab. 2.7 Sensor platforms defined/further developed in CERUBIS project

Sensors	Platform No.										
	1	2	3	4	5	6	7	8	9	10	11
Boiler wall electric resistivity measurement	✓	✓	✓							✓	✓
Wall corrosion probe	✓			✓	✓	✓					✓
Online ultrasonic measurement			✓			✓	✓	✓			
Online steam flow sensors				✓					✓	✓	
O_2 concentration measurement using zirconium probes	✓		✓			✓	✓			✓	
O_2 concentration measurement using zirconium probes and CO measurement using electrochemical sensors			✓	✓				✓			
O_2 concentration measurement using zirconium probes and CO, H_2S measurement using electrochemical sensors					✓						✓
O_2 concentration measurement using zirconium probes and CO measurement using IR sensors									✓		
Platforms to be tested at laboratory scale		0.5MW USTUTT			0.5MW IEN						0.5MW USTUTT
Platforms to be tested at real scale	BPP	OPP		OPP					BPP	OPP	

Task 2.6 Pilot scale multi-sensors investigations.

From the eleven sensor platforms specified in Task 2.5, three were chosen as the most promising for pilot scale experiments. The objectives of pilot scale experiments with sensor platforms were as follows:

- investigation of integration possibilities and compatibility issues,
- adequate analysis of data obtained and corrosion evaluation,
- longer tests of the sensors in more extreme conditions compared to a typical laboratory,
- test of sensor platforms against different fuel types and gaseous atmospheres,
- verification of sensor platforms indications.

All these objectives were met during the tests. Due to difficulties with testing the NISTFLOMS on 0.5 MW test facilities (the highest possible temperature of steam on 0.5 MW test facility was 250 °C. instead of at least 500), NISTFLOMS were tested in OPP, part of Task 2.6 and Task 3.3.

Pilot scale measurements were conducted at two 0.5 MW test facilities in IEN and USTUTT (A3). IEN carried out measurements mainly with the combustion of lignite (with different levels of moisture) and biomasses, also including some oxy combustion tests, while USTUTT conducted investigations with hard coal with different amount of ash for air mode only. In total 18 cases were investigated: 12 at IEN (Tab. 2.8) and 6 at USTUTT (Tab. 2.9) test facilities. Descriptions of the tests and their results are given in [23].

Tab. 2.8 Schedule of the investigations carried out at the IEN 0.5 MW test facility

Case no	Time, h	Date	Fuel	Combustion mode
1	30	05-06.05.2016	LC BPP (LC2)	Air, low O ₂
2	30	10-11.05.2016	LC BPP (LC2)	Air, high O ₂
3	6	12.05.2016	Torrefied straw	Air, low O ₂
4	6	16.05.2016	Torrefied straw	Air, high O ₂
5	7	17.05.2016	Torrefied beech	Air, low O ₂
6	7	18.05.2016	Torrefied beech	Air, high O ₂
7	5	02.06.2016	HC from ZM	Air, low O ₂
8	7	21.05.2016	LC BPP (LC2)	Oxy, low/high O ₂
9	4	24.05.2016	LC BPP (LC2)	Oxy, prim. & second. recirc., low O ₂
10	4	30.05.2016	LC BPP (LC2)	Oxy, prim. & second. recirc., low O ₂
11	24	30.05.2016	LC BPP (LC2)	Oxy, second. recirc., low/high O ₂
12	5	01.06.2016	HC from WM (HC1)	Oxy, second. recirc., low O ₂
Total	135 hours			

Tab. 2.9 Schedule of the investigations carried out at USTUTT 0.5 MW test facility

Case no	Time, h	Date	Fuel	Combustion mode
1	8.5	12-13.09.2016	HC Sebuku (HC9)	Air, staged
2	7.5	13.09.2016	HC Sebuku (HC9)	Air, unstaged
3	20	13-14.09.2016	HC US (HC8)	Air, staged
4	16	14.09.2016	HC US (HC8)	Air, unstaged
5	20	14-15.09.2016	HC OPP (HC7)	Air, staged
6	10	15-16.09.2016	HC OPP (HC7)	Air, unstaged
Total	82 hours			

Pilot tests - IEN

The measurements in the 0.5 MW IEN test facility relied mainly on:

- comparison of indications of investigated gas sensors with indications of reference analysers in different combustion regimes and conditions in an environment of lignite coal combustion (air and oxy, low and high O₂),
- behaviour analysis of different parts of prototype gas analysers (filters, solenoid valves etc.) in an environment of lignite coal combustion (air and oxy, low and high O₂),
- analysis of corrosion probe behaviour in different combustion regimes and conditions with simulations of starting up and shutting down of the boiler in an environment of lignite coal combustion (air and oxy, low and high O₂),
- SEM analysis of corroded ring from the corrosion probe.

The corrosion probe.

Testing with the corrosion probe was carried out in order to examine the probe behaviour in different combustion regimes and to investigate the ring itself after tests. The probe was located in the second duct of the 0.5 MW test facility in the range of temperature 800-1000 C deg. This version of the probe was cooled by air, so the efficiency of the cooling system and temperature sensor stabilisation were tested as well. The temperature of sensor and the temperature of measuring probe tube were measured during the tests. Resistance of the sensor is strongly dependent on temperature, so a reference test was conducted to determine the temperature coefficient of the sensor. The dependence of sensor resistance changes to sensor temperature was linear, so the coefficient was calculated based on these results. This approximation was useful for temperature differences in a narrow range of sensor temperature (300-400 °C) and slight fluctuations of temperature sensor could be compensated in this way. The temperature coefficient was used to recalculate measured resistance of the sensor in real conditions for reference conditions at temperature 350 °C. More details and some measurements results are given in Appendix 3.

The gas analysers.

The indirect sensors listed in Appendix 2 (namely gas sensors) as well as pumps, filters, valves elements etc. were tested in pilot scale conditions. All of the elements used were carefully evaluated during the tests and their advantages and disadvantages were described from the point of view of application in a power plant. The most promising elements were chosen to upgrade the gas analysers developed in Task 2.2 and to prepare them for the pilot tests in USTUTT and for long-term power plant tests in WP4.

The pilot tests – USTUTT.

The tests were carried out at the same time (in parallel) as those in Task 1.2. More detailed descriptions of the tests and their results are given in [23].

The chosen combustion conditions ensured several cases in which the tested sensor platforms could be checked against specific aspects, like excess O₂, ash content or temperature (by location of ports). The ports where the sensors were located were selected in the respective favoured temperature range and local excess O₂. Some redundant systems were placed in parallel in sub- and hyper stoichiometric levels (Appendix 1).

Beside the measuring values from sensor platforms, permanent gas analysis was conducted at the end of the combustion chamber and part time with the profile measuring probe at Levels 6 and 10 of the species CO₂, O₂, CO and SO₂. The measurements mainly relied on:

- comparison of indications of investigated gas sensors with indications of reference analysers in different combustion regimes and conditions in an environment of hard coal air combustion (staged and unstaged),
- behaviour analysis of different parts of prototype gas analysers (filters, solenoid valves etc.) in an environment of hard coal air combustion (staged and unstaged),
- analysis of corrosion probe behaviour in different combustion regimes and conditions with simulations of starting up and shutting down of the boiler in an environment of hard coal air combustion (staged and unstaged),
- analysis of electric resistance measurement in an environment of hard coal air combustion (staged and unstaged).

The tested IEN gas analyser (O₂, CO and H₂S) and all its subsystems worked properly in all test conditions. Measured temporary O₂ and CO values (not averaged like in the tests at the 0.5 MW IEN facility) were in good coincidence with those measured by the reference gas analyser (Appendix 2). Also, investigation of the corrosion probe confirmed that this measurement device was ready for power plant tests. The methodology of recalculation of sensor resistance for the reference temperature 350 °C was also confirmed. This test showed that a clear change in the measuring signal was obtained in a relatively short measurement time, which was promising in the context of long-term research in the steam boilers (Appendix 3).

The main goal of electric resistance measurement was to develop the system so it would be able to withstand power levels of 200 W or higher without overheating (Appendix 4). Three measurement tubes were made specifically for these 0.5 MW pilot tests. The tubes were designed to be placed through the burner. The idea was to measure the resistance of a stainless-steel tube that is exposed to extreme conditions.

Two tubes survived the campaign and were used to further develop the theory of online long-term corrosion measurement using an electrical resistance measurement. One tube burned during the second night of the campaign.

To adapt the system to withstand higher power levels, the shunt resistors were moved outside of the system, the shunt resistors to units with a higher power rating were changed, and they were thermally glued to the shunt resistors, to an aluminium heatsink that is actively cooled with a fan. The prototype of the online long-term corrosion monitoring system was successfully adapted to withstand power levels of 200 W without overheating. The limiting components during tests were the relays used to switch main power. These had to be replaced by units with a higher power rating for running in real scale boilers during WP4. The shunts were actively cooled. This solution was effective, but not suited for long-term operation in the dusty boiler environment. A decision was taken to make three measurement systems work on 200 W power for the long-term measurement campaign in the power plant, with the option of 300 A. Also, the systems were to operate in a quasi-continuous state. This allowed the use of shunts resistor without active cooling. The measurement campaign proved very useful for the purpose of developing the theory of online corrosion monitoring by measuring electrical resistance. A detailed look at measured data of a failure event (breaking tube) highlighted the usefulness of this method.

Discussion of WP2 results.

The first important output from WP2 was confirmation of the usefulness of the sensors developed and measurement methods for future diagnostic systems. Most of the hardware part of the systems were developed, manufactured and tested in this WP. This denotes not only sensors and measurement systems, but first of all fully equipped measurement devices for each of the sensing methods. They were successfully tested during pilot test in 0.5 MW stands at IEN and USTUTT and it should be underlined here that a total of 217 hours of very valuable pilot scale experiments were conducted. Also preliminary tests of these new devices were conducted in the power plants. The expertise acquired helped determine which basic sensor platforms would be used in the diagnostic systems.

2.3.3 Development of intelligent software tools for visualisation, monitoring, control and optimisation and its integration with different sensing systems - WP3

WP3 encompassed the integration of the earlier developed sensor platforms with the existing boiler control and diagnostic systems and the creation of a Common Intelligent Boiler Operation Platform – CIBOP.

Task 3.1 & 3.2 - Integration of developed sensing systems.

Five sensor platforms were chosen to be installed and tested during a half year of operation in full scale boilers in OPP and BPP, as was shown in Tab 2.7: two platforms at boiler no. 5 in BPP and three platforms at boiler no. 3 in OPP. More platforms were envisaged in OPP due to the higher corrosion risk observed there, compared to BPP.

Figure 2.12 presents the location of sensor platforms in boiler no. 5 in BPP. The first platform consisted of wall electric resistance measurement, corrosion probe and O₂ measurements by zirconium probes. O₂ probes were located on every wall (five per wall) whilst wall electric resistance measurement and the corrosion probe were located on the right wall at levels 36 m and 27 m respectively. It was envisaged that these direct corrosion measurements located on the right wall would be used to evaluate the risk of corrosion for the whole boiler on the basis of O₂-CO maps created by ANN on the basis of O₂ measurements.

The second platform consisted of four zirconium sensors of O₂ located on the level 45 m and two steam flow meters NISTFLOMs located at level 56 m on one of the super heaters. This platform was to be used to determine the slagging risk at the outlet from the combustion chamber. However, more than two steam meters (preferably around 20) are required for good estimation of steam flow. Due to the limited budget that was not possible, but the idea was checked and the results obtained discussed.

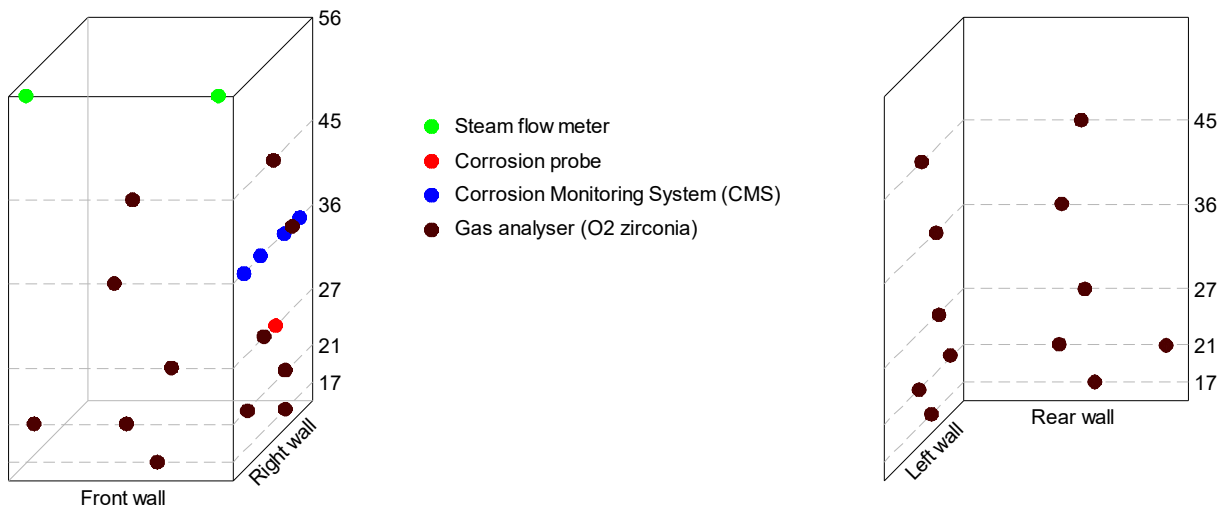


Fig. 2.12 Sensor platforms deployment in boiler no. 5 in BPP

Figure 2.13 presents the location of sensor platforms in boiler no. 3 in OPP. The first platform consisted of O₂ (zirconium) and CO (electrochemical) sensors (one per each wall on the level 23 m) and wall resistance measurement located on the right wall at the level 23 m.

It was planned that this direct corrosion measurements located on the right wall would be used to evaluate the risk of corrosion for the burners belt of the whole combustion chamber on the basis of O₂-CO maps created by ANN on the basis of O₂-CO measurements.

The second sensor platform consisted of a wall corrosion probe located on the right wall at level 30 m, four steam meters (two located on the right wall of the combustion chamber at level 30 m and two located on the rear wall at level 60 m in one of the superheaters) and four O₂ gas sensors located on each wall between 19 and 30 m.

On the basis of data from this platform an evaluation of slagging risk in the outlet form combustion chamber in the upper part of the burners belt was planned. In that case the corrosion probes were planned to be used as slagging probes.

The third sensor platform consisted of a corrosion probe and wall resistance measurement located on front wall at levels 30 and 27 m respectively and O₂, CO and H₂S sensors located at level 30 m on each wall. On the basis of data from this platform and also some other sensors from the two abovementioned platforms, evaluation of the corrosion risk for the whole combustion chamber was planned. It must be underlined that signals from particular sensors could be utilised in every platform, since the whole system was integrated.

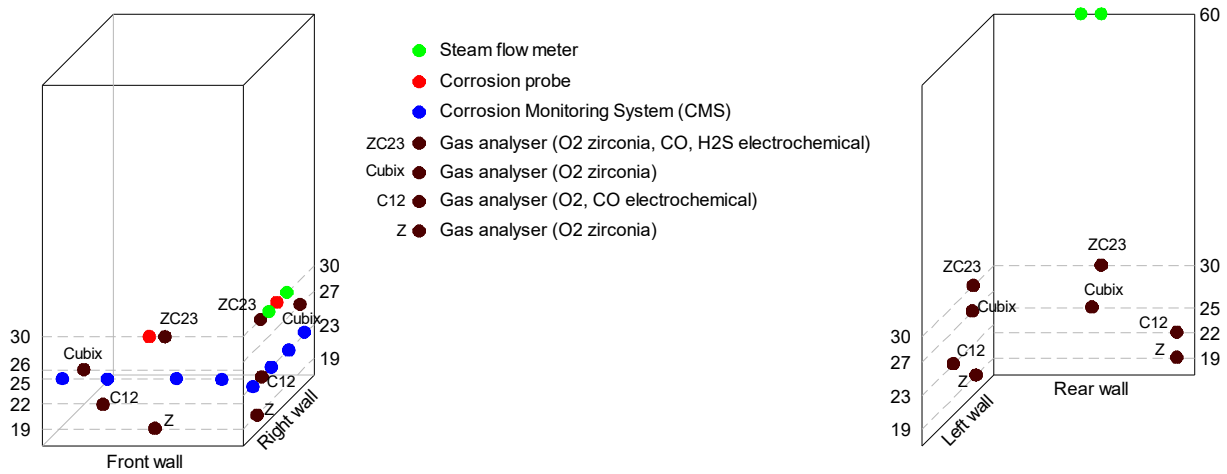


Fig. 2.13 Sensor platforms deployment in boiler no. 3 in OPP

The sensor platforms form part of the sensing systems. The single sensing system consists of: the sensor platforms, hardware, local control systems, and data handling. In order to run the system and have online determination of corrosion or slagging risk based on continuous measurements and continuous analysis of data, good integration is vital (hardware, local control, data handling, main control, software). Each sensor to be used in real scale application (O_2 , CO, H_2S , steam flow; ring in corrosion probe, junction for resistance in membrane wall) possesses necessary hardware like pumps, solenoid valves, different mechanical parts for assemblies, cooling systems etc. which together create the measuring device. All this hardware was successfully developed and tested in laboratory activity and finally verified in pilot scale tests in WP2. All the above-mentioned hardware elements and sensors needed local control systems, which also formed part of the measurement device. Such control systems were necessary for proper control of the measurement, e.g. controlling the temperature of the sensor, air purging, amount of cooling air, recalculations of some signals, diagnostics of sensors etc. Each measurement device possesses its own local control system, working independently of the main data collection system of the sensing systems. Such control systems were developed and manufactured together with the measurement devices for pilot scale experiments and in WP3 they were upgraded slightly to meet stricter real scale conditions and power plant demands. All such devices from the implemented platforms were connected to the main server by a Modbus TCP/IP connection for further data handling, creating together the sensing systems. In the BPP and OPP power plants the sensing systems themselves were also connected to the boiler and power plant environment, like data handling, electricity, air.

Moreover each emergency state of the sensing system was also monitored, enabling rapid reaction. The whole system could be also monitored by remote access.

The sensing systems could collect and store data from the sensor platforms and the power plant DCS system, but they did not give any interpretation in terms of rate or risk of corrosion.

Specific features of the integrated system are listed next.

The gas analysers.

Each gas analyser operated autonomously and did not require any host system to carry out measurements. The master application of CIBOP was used only to retrieve and process measurement data, and it worked for diagnostics and optimisation purposes. The gas analysers communicated with the master application via Ethernet, using the Modbus TCP/IP. In addition, analysers communicated with each other, delivering synchronisation of their working cycles. The protocol used was EGD (Ethernet Global Data).

The PLC was equipped with a colour touch screen, presenting all the parameters of the analyser. The touch screen could be used to change parameters and operating mode directly. Access to the parameters of the analyser was protected by a three-step password. The ability to change operating parameters was also available from the host control and measurement system.

In the client application there were default settings related to the measurement cycle such as:

- measurement time (suction of flue gases),
- number of air blows and breaks,
- time of one air blow,
- time of one break,
- time of the whole cycle,
- time and frequency of flushing the measuring element,
- time and frequency of automatic calibration.

The measurement system was maintenance-free during standard operation. It was able to switch to the appropriate working mode based on data gathered from the plant control system (DCS). This included starting-up or shutting down of the boiler, operation of the heavy oil support burners and

water injectors. It did not have to be switched off during outages of the boiler that did not affect the measurement system directly.

The corrosion probes.

Each corrosion probe was equipped with a control cabinet with a PLC with a colour touch screen. It was responsible for controlling the corrosion probe temperature and for calculating the change in resistance. The PLC could be used to change the main operation parameters including:

- resistance measurement frequency,
- temperature setpoint,
- PID regulator parameters,
- start and stop of the measuring cycle.

Data exchange between the PLC and the CIBOP server application was carried out using the Ethernet connection. Data provided by the corrosion probe controller included:

- reference resistance measurement,
- means resistance measurement,
- probe temperature,
- compressed air pressure,
- position of the cooling probe valve.

The steam flow meters.

Steam flow meters were equipped with a data logger with Modbus TCP. Data exchange between the PLC and CIBOP server application was carried out using the Ethernet connection. Data provided by the steam flow data logger included:

- steam flow sensor temperature (a direct-measured signal, ideally very close to the actual steam temperature at the specific installation point),
- steam flow sensor heat flux signal (also a directly measured parameter, but heavily depending on the local installation settings/geometry and the flow of the cooling medium).

The measurement system was maintenance-free system during standard operation. It did not have to be switched off during outages of the boiler that did not affect the measurement system directly.

The wall resistance measurements.

Electrical resistance sensors were connected with a datalogger equipped with a Modbus TCP. Data exchange between the PLC and the CIBOP server application was carried out using the Ethernet connection. Data provided by the electrical resistance measurement system included:

- electrical resistance of the boiler wall,
- electrical resistance of the boiler wall, corrected to temperature,
- boiler wall temperature at adapter 1,
- boiler wall temperature at adapter 2,
- boiler wall temperature at adapter 3,
- boiler wall temperature at adapter 4,
- temperature of the datalogger,
- current through the boiler wall,
- voltage drop over the shunt resistor.

Electric power integration.

The power supply of each measurement system was delivered by electric cabinets for power distribution in OPP and BPP installed as part of the project. All of the systems were powered by 230VAC single phase. The power consumption of each system (based on the maximum power supply specs) was approximately:

- Gas analyser: 200W,
- Corrosion probe measurement: 400W,
- Electric resistance measurement: 250W,
- Steam flow measurement: 200W,

At BPP total power did not exceed 1850W.

At OPP total power did not exceed 3100W.

Communication integration.

Integration of all elements of the sensing system is shown in Fig. 2.14. As was mentioned, each measurement device is equipped with a controller able to communicate via Modbus TCP/IP using the Ethernet connection with the main application running on a server computer located in the control cabinet. For proper operation of the system there is also a need to collect some data from the power plant control system DCS (Digital Communication System). Connection with DCS depends on the power plant and local conditions (2.14)

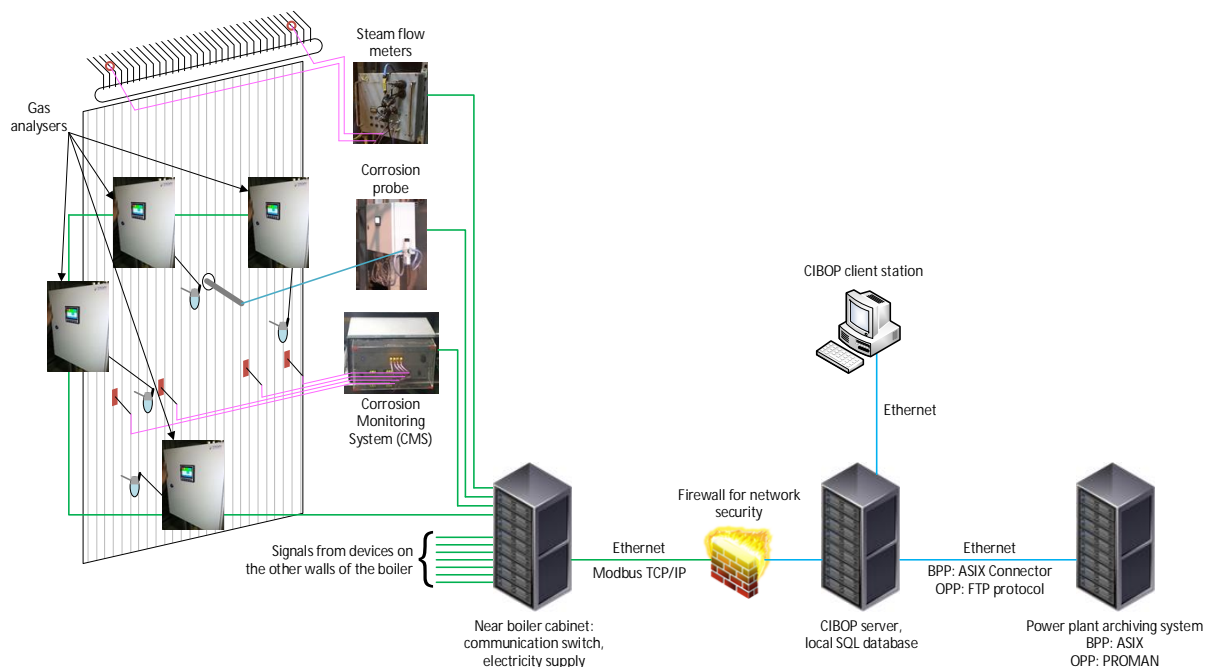


Fig. 2.14 Sensing systems in BPP and OPP – an overview schematic not including real numbers of sensors or their location

In the case of BPP there is a large distance between the boiler and the control room, but there is no need to use optic fibre for data transmission to the server because existing network infrastructure near to the boiler was available for use. The BPP is equipped with the ASIX system for control and data archiving. Data exchange between the ASIX and CIBOP system was carried out with the use of the Microsoft SQL database.

In the case of OPP the distance between the boiler and the control room is not so big, so the connection between the server and the measurement devices was made by the Ethernet twisted pair cable. The BPP is equipped with the PROMAN system responsible for control and data archiving. Data exchange between the PROMAN and CIBOP system was carried out using Modbus TCP/IP.

A major challenge was to get formal access to boiler operation data from its DCS saved in power plant archiving systems (**different at Opole and Bełchatów**) and install the CIBOP servers directly in the control rooms.

Due to the increasing risk of terrorism and cyber-attacks in 2017 PGEGIEK (owner of both power plants and partner of the CERUBIS project) drastically enhanced the safety policies and requirements regarding access to power plant network and its particular subnetworks.

An additional difficulty in the implementation of communication with existing archiving systems, but also with measuring devices mounted on the boilers in the CERUBIS project, was the structure of administration of power plants Ethernets, which is divided into two parts:

- the industrial one **near boilers' networks**, administered by the power plant IT Department and power plant Security Department,
- office networks, but also connections to global network (internal PGE WAN and Internet), administered by outsourcing sister company PGE SYSTEMY, with its own planning, infrastructure and security departments.

This administrative structure meant that the decision path was very long and time-consuming.

In the end, in the case of OPP the CIBOP system was placed on two servers: one temporary/auxiliary, where data from CIBOP measurements devices mounted on boiler no. 3 was gathered and analysed and second one which had access only to DCS boilers operation data (Fig. 2.14).

In the case of BPP the CIBOP system had access to current boiler data, but they could only be uploaded to the CIBOP server periodically and manually (Fig. 2.14).

Summarising, it was not possible to design and integrate CIBOP as originally planned in both OPP and BPP boilers to enable online monitoring and optimisation of the boilers performance, because the CIBOP systems were not connected to the DCS in the control rooms. This deviation was accepted by RFCS officials.

During tests and the long-term run, the CIBOPs were operated online locally in both power plants, collecting data from all measurement devices of the sensing system. The servers were located in the electric cabinets installed close to the boilers, and DCS data of boiler operation parameters were uploaded from time to time to the servers. After collecting a complete set of the data for the given time period, the data was analysed and optimisation of the boiler was carried out on that basis.

Task 3.3 - Pilot scale testing of the measurement devices at the boilers.

It was originally assumed that measurement devices would be tested and verified only at the pilot scale. However, it proved more productive to carry out such tests on real scale conditions, since more insightful conclusions and indications could be determined on the basis of such tests. In fact, all of the measurement devices developed were tested in the BPP and OPP in Task 3.3 [24]. The context of the “**pilot scale**” was retained in a sense, since particular measurement devices were tested as single systems, not integrated with others or the boiler measurement system

Gas analysers capable of measuring concentrations of O₂, CO and H₂S were tested in OPP. After many combinations of different elements and subsystems were tested in Task 2.2, finally four types of fully equipped gas analysers were developed and manufactured: two types measuring O₂ (wideband zirconium sensor), one type measuring O₂ and CO (wideband zirconium and electrochemical sensors) and one measuring O₂, CO & H₂S (electrochemical sensors). In total, 16 gas analysers were manufactured for long-term experiments in the boilers.

All developed types of the gas analysers were installed on each wall of the boiler in the locations already chosen for CIBOP. Example results of concentration measurements are shown in Appendix 2. During the tests of the gas analysers systems it was found that, for high boiler loads, ambient temperature inside the gas analyser box was increasing in some cases, reaching almost 55 °C. High temperature inside the gas analysers could have substantial influence on overall device behaviour, for example slower response and measurement errors.

Moreover, the Ibd O₂ zirconium sensor should be located near the gas analyser, not close to the wall adapters as was originally assumed, as this location enhances the life span of the sensor and its general performance.

Regarding filters, it was found that even 5 µm filter is insufficient to provide 100% protection for the flue gas pump, whose life span was estimated as several months. It was necessary to install an additional ash trap located close to the wall adapter, which allows for longer gas analyser operation without service.

Tested electrochemical cells had a long stability time during measurements of O₂ and very rarely reached a 0 % value of O₂ even when the zirconium probe at the same time showed “**deep zero**” which suggests that zirconium sensors would be more preferable for the CIBOP.

After successful testing and calibrating of the NISTFLOM steam flow sensors at laboratory scale, four NISTFLOM sensors were mounted at boiler no. 3 in the OPP during an outage. After running the boiler it was found that all four sensors were operational, but the sensors mounted at level 60 m could not be supplied with sufficient cooling air due to a rupture in the feeding line, created probably while closing the thermal insulation. The sensors at level 30m (evaporator) were fully functional and accessible, hence it was possible to connect both cooling air and the data acquisition system.

Measurements of steam flow on the evaporator wall over several days indicated that the sensor was well capable of monitoring constant load cases as well as dynamic load changes. However, it was not possible to draw quantitative conclusions due to: (i) sensor signal analysis being based on single phase medium properties (as is the case in the superheated and above all in a supercritical steam environment), and (ii) the exact steam quality (phase balance-wise) at the location being unknown. However, even under two-phase conditions the sensors proved to deliver high definition qualitative data regarding flow changes in the evaporator (Appendix 5).

During a maintenance shut-down of boiler no. 3 (after 8 months of sensors operation) an in-depth inspection and re-connection of two NISTFLOM sensors at level 60 m was carried out. This was done in order to check their status (material damage etc.) to enable the full operation after the earlier-mentioned cooling/reference air feed failure. The sensors were in good condition in spite of the lack of cooling air. After fixing the issues with cooling air and attachment of new connectors to the sensor tubes, tests were repeated with those two NISTFLOMs located at level 60 m.

The NISTFLOM sensors were operated in OPP in total for more than one year. After finishing the above test, they were investigated for a detailed long-term stability evaluation and re-calibration. Initial visual inspection revealed no damage after real full-scale exposure.

The corrosion probe was tested (for several hours) in boiler no. 5 in BPP. During the test the corrosion probe was inserted into a measuring port on the left wall (level 30m) for several hours.

In the normal position of the probe in the combustion chamber (approx. 5 cm from the surface of the evaporator) the probe temperature was easily kept at a stable level of approx. 300-350°C. After inserting the probe deeper (more than 10cm), the temperature increased to more than 500°C (instead of the expected increase to 400°C) and it was deemed necessary to increase the efficiency of the cooling system. It was therefore decided to modify the tip of the probe to minimise the surface heat transfer. The tip of the probe was shortened and the location of the measuring sensor ring changed before more trial measurements in OPP (Appendix 3).

A comparison was made between the power plant relationships observed and those obtained in laboratory conditions, and the differences were noted. Although a linear relationship was obtained in both tests, under real conditions the values of resistance were higher at a given temperature than in the laboratory test. This could be caused by radiation exposure in the boiler furnace and the specific thermocouple location. This might be the result of difficulties with the cooling system and maintaining a stable temperature of the resistance probe. Therefore, the location of thermocouples in the probe needs to be carefully chosen.

The last test was carried out in OPP (left wall at level 30m) after modifications of the corrosion probe prior to its final performance in WP4. The results are given in Appendix 3.

Electric resistance measurements of membrane wall were carried out after lab scale experiments and before 0.5 MW pilot tests for preliminary checking of the system in real boiler conditions.

The first experiments were carried out in boiler no. 5 in BPP on the front wall at level 54 m. The CMS 3545 measuring system was used, with four connection points to the boiler wall.

Measurements were taken during two nights, the first night with a current supply of 1 A, the second night with a current supply of 2 A. The measurement results are presented in Appendix 4.

In order to check how increasing the current supply would affect the resistance behaviour another real scale experiment was carried in boiler no. 3 in OPP. The test levels of current were respectively 4.6 A, 7.7 A and 11.6 A. The results showed a significant increase in performance of the method, especially for higher current.

Task 3.4 - Intelligent systems development – Common Intelligent Boiler Operation Platform – CIBOP.

One central aspect of the project was development of software based on artificial intelligence and creating an intelligent system for data processing and interpretation, which together with the above-mentioned sensing system creates an integrated boiler diagnostic system called Common Intelligent Boiler Operation Platform – CIBOP.

This software was developed in Task 3.4 and was partially based on software developed earlier, like Slagann (model of slagging), Dawid (model of high temperature corrosion determination) and Rachel (model of utility boiler optimisation). All this software was further improved in the project and new components were added, such as diagnostics for the sensing system and models of wall thickness loss. This last one was a very important part, elaborated on the basis of investigation of correlations between indirect and direct sensor indications (short and long term) gathered among others in Task 3.3.

In the earlier version of the software, only O₂ concentrations and corrosion risk were determined. Work in the CERUBIS project had enabled a transition to assessment of current and predicted rate of the walls thickness loss in mm/year. It is also possible to assess the total loss of wall thickness over a given period of time.

Thus, one of the important challenges for the new software was integration of all single computer programs developed thus far with simultaneous development in the CERUBIS with new programs created in CERUBIS and with control systems of new measurement devices and power plants.

Figure 2.15 presents the main concept of the CIBOP. There are two major blocks: one concerning the corrosion issue and the second concerning the slagging issue. They are connected to boiler data from the DCS and to the optimiser module of the boiler. The accuracy and creditability module checks the quality and reliability of indications of all sensors.

Figures 2.15 and 2.16 highlight a role played in the CIBOP by the individual sensing method, i.e. what kind of output information is available after intelligent software processes the data gathered by the sensing system.

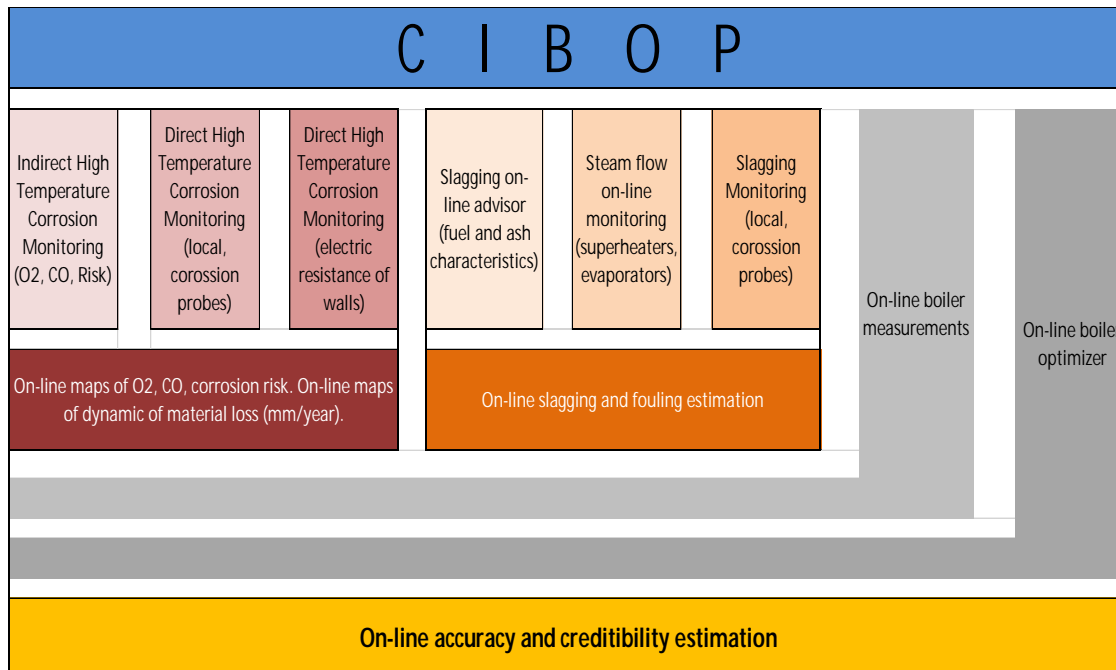


Fig. 2.15 Conceptual chart of CIBOP working principles

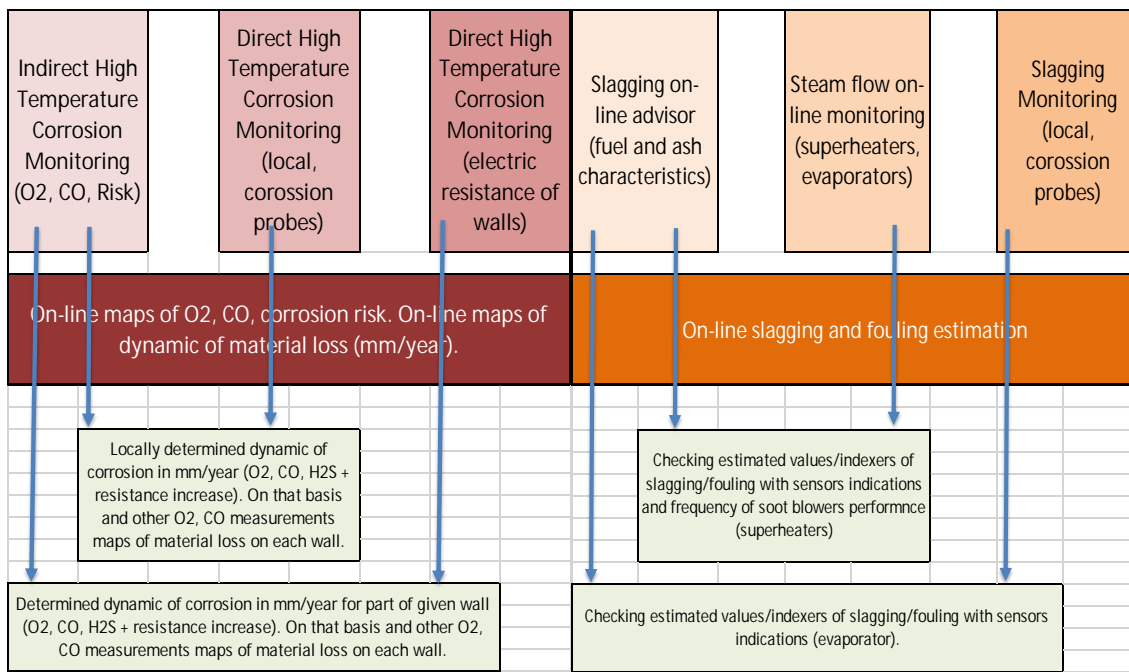


Fig. 2.16 General block chart flow scheme of sensor indications for corrosion (left) and slagging (right) assessment

Intelligent software was developed based on this idea. The software consists of four main modules listed and described in brief below. A more detailed description of the modules and works carried out in their development are given in Appendix 6.

1) Corrosion risk module (name Rachela).

This module shows all current measurements carried out by the installed sensors, the most important data from the boiler DCS, and maps of the concentration of O_2 at the wall layer, the risk of corrosion and the dynamics of the evaporator wall thickness loss determined based on the O_2 model.

It is possible to plot the above maps for different periods of time as averages e.g. daily, monthly or yearly. The program also displays suggested values of new air distribution to the boiler combustion chamber proposed by the optimiser for current boiler operation parameters (power, configuration of working mills and carbon feeders) to reduce emissions NO and enhance the protection of the evaporator walls against corrosion. All reported values can also be generated in the form of reports in an Excel file.

2) Slagging risk module (name Slagann).

This module shows some current data from the boiler DCS and predicts the risk of slagging for a given fuel: temperature of beginning of slagging, slagging intensity and flue gases temperature at outlet of the combustion chamber. Final result: the risk of slagging is shown in four colour-coded hazard classes and can be calculated by three different models. A user can also check how changing some parameters may affect the risk of slagging.

3) Measurement accuracy module (name Accuracy).

This module displays the level of reliability of all measurements from the installed sensors in four colour-coded classes. The classification into the relevant group (scale) is done by comparing the measured value against historical values obtained for similar boiler operation parameters.

In addition, the program determines the accumulated average reliability for each of the walls of the chamber and it is possible to plot a map of reliability of measurements, but only for measurements of O_2 concentrations, because such maps can only be created on the basis of a greater number of measurements.

4) Module integrating data from all implemented measurements systems (name Integration)

This module displays all measurement values and boiler operating parameters, similar to that in the Rachel module together with the optimisation part and maps.

The module was extended to predict the evaporator wall thickness loss, determined on the basis of four models: O_2 , $O_2 + CO$, CMS, corrosion probe (currently, the O_2+CO model is not active).

Based on each of the three models, one can plot a map of the rate of loss of the wall thickness of the evaporator in the current state or as a mean loss from the last specified period, optionally from a few hours to one year.

It is also possible to predict loss in future periods in two options: when the boiler is running according to the DCS settings or when the boiler is running according to the settings of the genetic optimiser, but the program predicts such dynamics only for the given power of the boiler and configuration of working mills. If a user wishes to specify the future rate of corrosion for a variable boiler operation, this must be done separately for each power range and configuration of working mills and then summed up.

Task 3.5. CFD computations.

As can be seen, the ANN is a crucial part of the developed diagnostic system. Its prediction quality depends very much on having a sufficient amount of data for training. Since power plant measurements campaigns are expensive and time-consuming, CFD analysis was introduced in order to supply more training data with regard to O₂ and CO in boundary layers, outlet temperature from combustion chamber as well as NO_x and CO emissions.

In Task 3.5 CFD modelling of both boilers used in the project was conducted [25] using Fluent (ver. 17.1) - commercial software ANSYS Inc.®. Fluent employs the finite-volume method to discretise the partial differential equations of mass, momentum, energy conservation, and species concentrations. The simulations included in detail all phenomena occurring inside the boiler such as: devolatilisation and char combustion of coal, homogeneous chemical reactions, turbulent flow, heat exchange by convection and radiation and pollutant formation (CO, NO_x).

The detailed geometries for both boilers were created and the computational domains extended from the furnace hopper to the outlet from an economiser.

The first stage of the simulations was to validate the results obtained based on experimental data from real scale measurements, while the goal of simulation was to generate results for different boiler loads, mill configurations and air distributions to the burners.

In particular, the following information was desirable:

- O₂ and CO profiles in the boundary layer of the combustion chamber (for Rachel),
- flue gas temperature at the outlet from the combustion chamber (for Slagann),
- NO_x and CO emissions and loss on ignition LOI (for Rachel),
- all above parameters for self-diagnostics of the CIBOP system.

In order to estimate how close CFD calculations are to real measured values of O₂ and CO, probe points were defined close to the walls at the same position as in the real scale boiler (in the real boiler: the places of the adapters). The values from those points as averages for the whole wall were compared with the experimental results.

Results for boiler no. 5 in BPP.

The calculated O₂ concentrations (2.6-5.8%) had much higher values than the measured ones (1.6-2.3%). Unfortunately, no modification of the tested combustion parameters, like kinetic data or amount of volatiles, was able to improve the results.

There were some qualitative common features of O₂ and CO behaviour in the boundary layer between CFD and real data, but no quantitative compatibility was found. Thus, more effort was made to improve the results obtained. The following modifications were made:

- change of computational mesh (different meshing schemes, number of cells, etc.),
- modifications of combustion parameters (kinetics constant of volatile and CO combustion, mixing rate, etc.),
- change of some air arrangements inside burners,
- modifications of coal parameters.

None of the tested modifications caused a significant improvement in the results. Due to those problems the training of neural networks for boiler no. 5 in BPP was done only based on experimental results (as reported to the EU Project Officer). As a compensation, optimisation of the boiler in BPP using CIBOP was carried out (see chapter 2.3.4).

Results for boiler no. 3 in OPP.

For this boiler the results of O₂ measurements and CFD results were relatively similar. However, the qualitative behaviour of CO in CFD calculations compared to real measurements could not be viewed as promising. Due to computational difficulties in predicting CO, the combustion model was modified. Modifications to the combustion model resulted in increased CO which was slowly oxidised, so that the CO and O₂ mole fraction were better predicted than previously. CFD calculations were also carried out for several other cases, using data from additional measurements of the boiler (Tab. 2.2). Averages of O₂ and CO for each wall were calculated for these cases. O₂ concentrations calculated by CFD were higher, while CO was lower when compared to real scale experiments. It was also noticed that errors of computation increased as boiler load decreased.

The resulting absolute errors at levels of 15 to 30% for CFD estimation of O₂ and CO were considered satisfactory and such results could be used for ANN training. The validity of this assumption was also proved in operation of the CIBOP in WP4.

With this improved model more cases were calculated in order to collect data for training of the ANN, as is described in Appendix 6.

Besides O₂ and CO predictions in the boundary layer, another important issue was to obtain the outlet temperature from the combustion chamber and CO, NO_x emission and LOI. In the case of the outlet temperature from the combustion chamber, no real scale measurement was carried out inside the boiler, firstly due to overly long distances in the boiler (measurement by a suction pyrometer probe up to 4 metres long), secondly due to the very high temperature. Thus, the data for training of ANN in the SLAGGAN module was obtained only on the basis of CFD calculations.

Discussion of WP3 results.

The core product of the CERUBIS project, namely CIBOP, was developed in this WP. In addition to the creation of a common diagnostics platform for all developed measurement devices, a core achievement was the conceptual linking of instantaneous measurements of O₂ and CO concentration with time-consuming direct measurements of the corrosion rate by two resistance methods.

Another achievement was the extended use of artificial intelligence, in particular ANN, to transform data – gathered from a limited number of measurement devices installed in the boiler – into valuable information which can be used by a boiler operator or for planning boiler maintenance.

The possibility of creating – through CFD modelling – an increased amount of boiler operation cases for teaching the ANN was confirmed. However, it was also found that CFD modelling was not as easy and reliable as originally supposed at the beginning of the project, especially regarding the near wall flue gases layer.

Graphical interface was created to enable use of the developed CIBOP software modules by a final user. The interface makes it possible for a user to work with historical data gathered by CIBOP during boiler operation, but also to assess future risk and rate of corrosion on the basis of current data or data generated by the boiler optimiser.

Regarding the hardware part of CIBOP, all kinds of the measurement devices were integrated with the boiler infrastructure and checked in difficult real operational conditions. Shortcomings of the equipment were removed when they occurred.

2.3.4 Full-scale tests of the developed monitoring and optimisation systems at two locations - WP4

WP4 focused on testing and optimisation of the newly-developed systems at real scale conditions. The conducted work encompassed:

- carrying out wall thickness measurements in order to validate and check sensing systems and intelligent software (CIBOP),
- testing and validating of sensors and measurement devices performance in extreme boiler conditions,
- investigating of corrosion/sludging phenomena in the real scale conditions under low emission demands for hard coal and lignite combustion,
- validating and further improving the intelligent software tools – CIBOP and supportive numerical models,
- long-term testing of CIBOP in the power plants.

The testing and validation were carried out in two separate boilers of partner PGEGIEK, firing different coals: **hard coal (Opole) and lignite (Bełchatów)**. This made it possible for the project to cover a broader fuel and technology portfolio. Furthermore, these two installations were equipped with different low NO_x systems. Also, the high moisture flue gas resulting from the lignite combustion added to the challenge of testing the mechanical durability and longevity of the sensors.

Task 4.1 & 4.2 - Wall thickness measurements and first stage of system operation

Many boiler inspections took place in order to prepare the boilers both for measurements in WP1 as well as for installation of the measurement devices and the diagnostic systems. New openings were made and adapters installed in both BPP and OPP. Wall thickness measurements were also conducted and historical data were used as well. In the case of BPP the rate of wall thickness loss is very small, not more than 0.08 mm/year, on average 0.02 mm/year.

At OPP the corrosion rate is ten times higher. Tab. 2.10 shows the corrosion rate for periods from 2007 to 2017 in % of controlled area of the walls (200-230 m²) for four levels of corrosion rate: more than 0.7 mm/year, 0.7 to 0.3 mm/year, 0.3 to 0.05 mm/year and below 0.05 mm/year. In the meantime, some areas of the evaporator were exchanged, usually if the thickness of tube was lower than 3.4 mm. In total, 60% of the measured area is continuously under low O₂ conditions, exposed to corrosion processes. 20-30 % of the measured area is subject to intensive corrosion processes. In 2015 more than 200 m² of the walls were exchanged due to corrosion. Between 2015 and 2017 rapid increase in the loss of wall thickness was observed, especially for high corrosion rates, i.e. >700 µm/y as is graphically presented in Fig. 2.17. It was noticed that the highest corrosion occurs more on right sides of walls, which was with good agreement with O₂/CO measurements presented in detail in [19]. The right wall was the one most attacked by corrosion [26].

To recap, wall thickness measurements of the evaporator in boiler no. 3 in OPP showed intensive high temperature corrosion while the corrosion rate in boiler no. 5 in BPP is very low. While the latter boiler should not be considered as a high corrosion risk, attention should still be paid to the relatively high CO concentrations in the boundary layer, as was confirmed by boiler measurements in WP1. Several measurement devices of different types were installed temporarily or permanently in boilers no. 5 in BPP and no. 3 in OPP in the preliminary stage of the project. Some were tasked with testing the sensors and measurement devices, as described in chapter 2.3.2 which was connected with WP2 activity. Others were tasked with making a preliminary determination of the corrosion risk in the

boilers. Three different types of gas analysers were tested in OPP. Electric resistance measurement, corrosion probe and measurement of steam flow were tested, mainly during the first OPP measurement campaign.

Tab. 2.10 Evaporator walls thickness loss rate in boiler no. 3 in OPP

Front wall					Right wall						
Parameter	Unit	2007-2010	2010-2012	2012-2015	2015-2017	Parameter	Unit	2007-2010	2010-2012	2012-2015	2015-2017
Average	um/year	-54.6	-53.6	-72.7	-146.8	Average	um/year	-6.1	-37.7	-126.6	-209.6
Max	um/year	-633	-500	-667	-2500	Max	um/year	-267	-450	-967	-1500
> 700 um/y	%	0.00	0.00	4.98	4.56	> 700 um/y	%	0.00	0.00	2.74	6.64
300-700 um/year	%	2.27	6.98	10.65	12.03	300-700 um/year	%	0.00	2.89	17.32	14.72
50-300 um/year	%	46.15	39.13	34.44	32.92	50-300 um/year	%	30.68	42.86	28.86	53.82
< 50 um/year	%	52.57	52.89	19.93	50.48	< 50 um/year	%	69.32	54.26	51.08	24.82
Rear wall					Left wall						
Parameter	Unit	2007-2010	2010-2012	2012-2015	2015-2017	Parameter	Unit	2007-2010	2010-2012	2012-2015	2015-2017
Average	um/year	-58.5	-20.4	-94.8	-259.6	Average	um/year	-15.5	-76.7	-73.8	-251.0
Max	um/year	-433	-800	-733	-1600	Max	um/year	-400	-750	-800	-1500
> 700 um/y	%	0.00	0.26	0.68	11.49	> 700 um/y	%	0.00	0.29	0.00	13.58
300-700 um/year	%	2.45	6.72	14.86	15.95	300-700 um/year	%	2.46	8.8	8.38	15.17
50-300 um/year	%	33.04	27.54	38.92	29.32	50-300 um/year	%	31.25	46.32	27.17	35.98
< 50 um/year	%	64.51	65.48	45.54	43.24	< 50 um/year	%	68.75	44.59	64.45	35.26

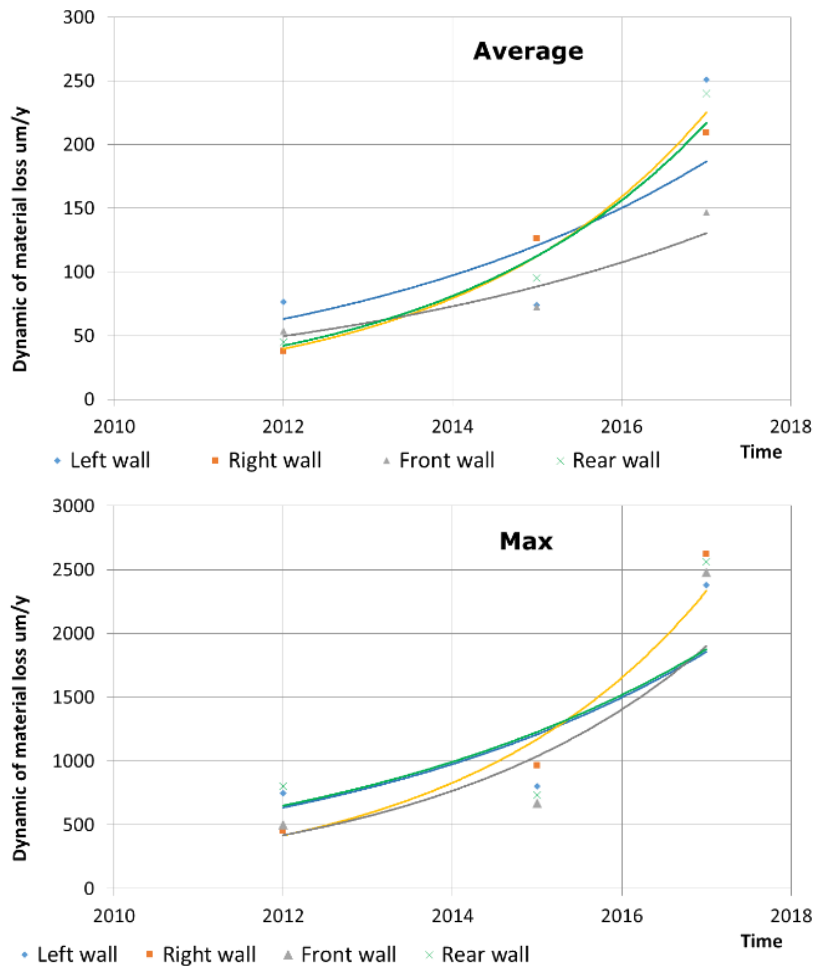


Fig. 2.17 Average and maximum rates of evaporator's wall thickness loss for all walls 2010-2017 during operation of boiler no. 3 in OPP

In the case of BPP, O₂ gas sensors were already mounted as part of other self-financed work, pre-dating the CERUBIS project. Indications from O₂ sensors were gathered during a 12 month period. At OPP, electric resistance measurements of wall and the corrosion probe were also tested. Steam measurement sensors were not tested in BPP in the preliminary stage of the project.

Task 4.3 - Final mounting of the systems on two utility boilers.

The CIBOP systems were fully mounted on two utility boilers in OPP and BPP in the way described in chapter 2.3.3. The number of measurement devices manufactured and mounted is summarised for each boiler in Tab 2.11. Figures 2.18 to 2.21 present example views of the measurement devices mounted in the OPP and BPP boilers.

Tab. 2.11 The measurement devices installed in the boilers

Method/sensor type	Bełchatów Power Plant	Opole Power Plant
O ₂ concentration (old type)	24	
O ₂ concentration (type 1)		4
O ₂ concentration (type 2)		4
O ₂ , CO concentration		4
O ₂ , CO, H ₂ S concentration		4
Corrosion probe	1	2
Wall resistance	1	2
Steam flowmeters	2	4

In both OPP and BPP, cabinets with an electric power supply and internal communication system for all measuring devices have been manufactured and mounted near boiler (at level 30 m). All sensors and sensing systems were connected to the central cabinet (schematic diagram in Fig. 2.14) and supplied with electricity and pressurized air where necessary.

To mount the sensors for **Hukseflux's Corrosion Monitoring Systems (CMS)** (Fig. 219) and TNO's NISTFLOM (Fig. 2.21), a few days breaks in operation of the boilers (to cool them down) were needed in both power plants. As the **Bełchatów and Opole power plants belong to those operating in the electricity supply base for polish power system**, all available boilers (including unit No. 3 at Opole and unit No. **5 at Bełchatów**) operated continuously during the summer peak demand for electricity. PGEGIEK, specially for the needs of the CERUBIS project, made accessible (out of operation, cooled down) boiler No. **5 at Bełchatów power plant on 23 of July 2017**, and boiler No. 3 at Opole power plant from 24 to 27 of July 2017. On those days the assembly of the above-mentioned sensors was carried out. At that time, however, the final version of the electrical and communications systems was not ready yet. Due to the very long procedures in power plants regarding electrical and communication installations (also their safety), the need for multi-level documentation acceptance, absence of personnel responsible for approving documentation (vacation time), installations were ready at the end of August/September. Unfortunately, in September there was serious failure of boiler No. 3 at Opole power plant.

After a long repair of the boiler superheater, it was back in operation on 31 of October. A visit of TNO and Hukseflux was necessary to launch and run NISTFLOM and CMS systems. This was scheduled **for 24 of October at the Opole power plant and 25 of October at the Bełchatów power plant (when both boilers should work)**. As mentioned, the return to operation of boiler No. 3 in Opole was delayed, however, in order to avoid further delays, it was decided to keep the planned visit times of partners from the Netherlands. The commissioning and starting up of the NISTFLOM and CMS systems was successful (however in Opole on boiler out of operation).

After partially solving the problems with communication with the power plant archiving systems, servers operation in restricted industrial environment, the final launch of the CIBOP was completed in January 2018.



Fig. 2.18 Gas analysers mounted in OPP (left) and BPP (middle). Location of adapter (zirconium O₂ sensor) in the evaporator wall (right) in the direct vicinity of the two NISTFLOMs



Fig. 2.19 Installed wall resistance measurements (CMS) in OPP (Opole 1) mounted on 28 m front wall (left) and (Opole 2) mounted on 23 m right wall (middle), CMS installed in BPP mounted on 36m right wall (right)



Fig. 2.20 The resistive corrosion probes located in OPP at level 30 m on the front wall OP1 (left) and on the right wall OP2 (middle), the corrosion probe located at level 27 m in the right wall in BPP (right)



Fig. 2.21 NISTFLOM sensors installed in OPP on the **evaporator's right wall** at level 30m (left) and on superheater tubes rear wall at level 60 m (middle), NISTFLOM sensors installed on superheater tubes, front wall at level 60 m at BPP (right)

Task 4.4 - Half year system operation in two utility boilers.

For the reasons mentioned earlier, the systems were not run in full mode from July 2017 (although parts of the systems worked previously). All circumstances were reported to the EU Project Officer and finally 0.5 year of operation of the whole systems was accepted. The systems were run in January 2018 and were in operation also after 30.06.2018 (end of the project), but mainly data from the first half year were analysed.

Figure 2.22 presents the electricity production of power plant units powered by the investigated boilers in the OPP and BPP through the first half of 2018. In total, boiler no. 5 from BPP worked almost 4100 h and boiler no. 3 from OPP less than 3900 h. Many shutdowns of boiler no. 3 were noted, in contrast to boiler no. 5. Shutdowns of boiler 3 were rather short: several hours during the night or weekend. The boiler shutdowns were forced by an operator of the Polish energy system. During operation of the CIBOP systems, several failures of each of the installed sensor platforms or measurement devices occurred. The main cause of failure was overheating, particularly concerning power supply and high-powered switching relays. This was primarily due to the high ambient temperature inside the boiler house. Also, non-responsive software made it sometimes necessary to restart the sensing and data acquisition systems, as for instance was the case for the NISTFLOM

platform. In spite of that, the gathered data enabled analysis of more than 2500 hours of operation of the CIBOP systems and their work at each boiler.

In this chapter results from corrosion measurements and steam flow sensors are described and then their use together with results from gas analysers on the CIBOP platform was analysed.

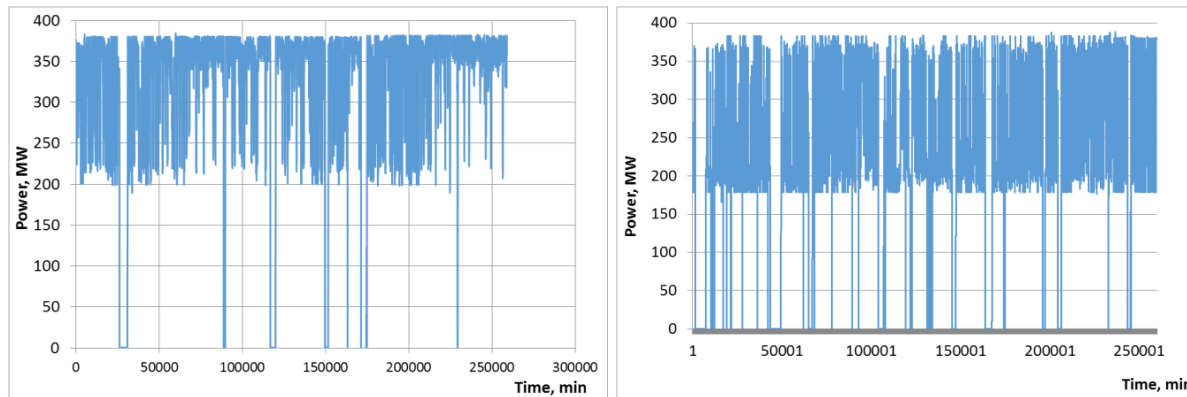


Fig. 2.22 Electric power for units of boiler no. 5 in BPP (left) and of boiler no. 3 in OPP (right) through 0.5 year work of CIBOP systems

Wall resistance measurements (CMS).

The corrosion monitoring system (CMS) measurement unit had 4 adapters welded to the boiler wall (described from A to D) – Fig. 2.23. A current was supplied through the two outer adapters, and the voltage drop between adapter B and C was measured. This gave a measurement of the electrical resistance of the piece of boiler wall between adapter B and C. The system also measured the temperature of the four adapters, plus data logger temperature and supplied current. The system carried out these measurements every 4 seconds, for 5 minutes at the start of every hour. Sample results are shown in A4.

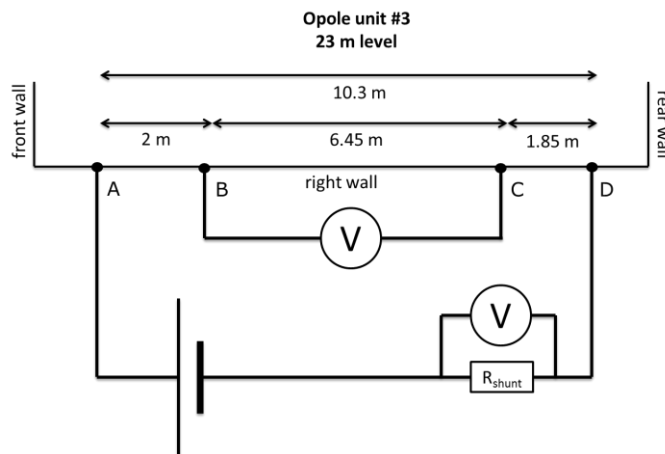


Fig. 2.23 Online resistance measurement setup with four connection points to the boiler wall

The system suffered from smaller or bigger failures. It was found that the mechanical relays used did not have a sufficient lifetime. They were rated for 70000 to 300000 cycles, which for the current method of operation translates to 2 to 6 months. When the relays failed, it was often possible to get the system back online by replacing the relays. However, in the Opole 1 system, the failure of the mechanical relays created a short circuit that resulted in the measurement drawer melting down. The upgraded system was re-installed in the Opole power plant.

The Bełchatów system showed signs of impending failure at the end of measurement period and was turned off. Moreover, because the measurement is sensitive to boiler wall temperature, stable boiler conditions are necessary to be able to perform a good analysis. If the temperature changes are too high, the model of a linear dependence of boiler wall resistance on temperature no longer applies. This was especially an issue in Opole, as the Bełchatów unit ran in more stable fashion during the campaign. Finally, for Opole 1, 162 days of good data were found, of which 107 with stable boiler conditions. For Opole 2, 129 days of good data were found, of which 89 with stable boiler conditions. For Bełchatów, 189 days of good data were found, of which 173 with stable boiler conditions.

Fig. 2.24 presents the results of analysis of CMSs - normalised resistance measurements and remaining wall thickness are both plotted as a function of time for all three systems. In the case of Opole 2 the line for "maximum" values was plotted (hatched). The results are also shown in Tab. 2.12. The value behind the \pm symbol is 2 times the standard deviation of the residuals of the

fit. Temperature dependence is similar for all three systems. The values from this table were used to analyse the dynamic of wall thickness loss.

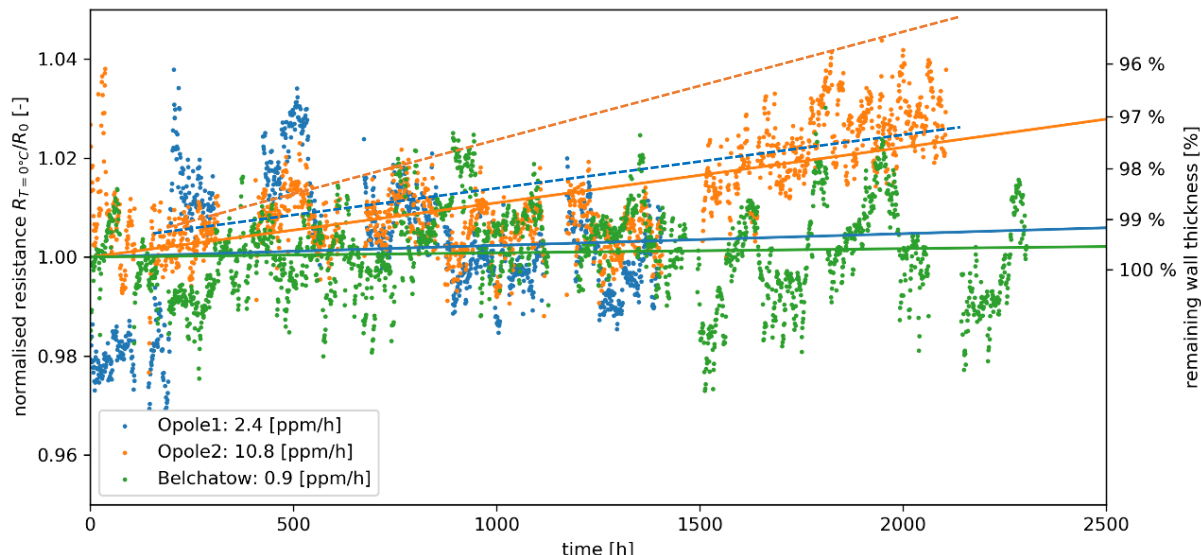


Fig. 2.24 Normalised resistance measurements and calculated remaining wall thickness as a function of time for OPP and BPP

Tab. 2.12 Fit results for CMS in OPP and BPP

CMS	R_0	a	b
Opole1	$11.5 \mu\Omega \pm 0.7 \mu\Omega$	$6.0 \times 10^{-3}/^\circ\text{C} \pm 0.7 \times 10^{-3}/^\circ\text{C}$	$2.5 \text{ ppm/h} \pm 2.0 \text{ ppm/h}$
Opole2	$9.9 \mu\Omega \pm 0.3 \mu\Omega$	$6.5 \times 10^{-3}/^\circ\text{C} \pm 0.3 \times 10^{-3}/^\circ\text{C}$	$10.8 \text{ ppm/h} \pm 0.6 \text{ ppm/h}$
Belchatów	$7.9 \mu\Omega \pm 0.2 \mu\Omega$	$6.9 \times 10^{-3}/^\circ\text{C} \pm 0.3 \times 10^{-3}/^\circ\text{C}$	$0.9 \text{ ppm/h} \pm 0.6 \text{ ppm/h}$

The corrosion probe.

During BPP campaign one probe (BP1) worked in the period from 15.12.2017 to 29.05.2018. The second probe (BP2) worked from 29.05.2018 to 15.12.2018. Two probes were tested in this boiler and were mounted one after the other in the same place. During testing of the first probe (BP1), a problem with data logging occurred, therefore the resistance measurements were made periodically during the inspection and the corrosion rate was determined on this basis. Continuous registration of temperatures and resistance was carried out during testing of the second probe (BP2).

After the first test with BP1 probe lasting 162 days, a 0.07 mm change in thickness of sensor was found, meaning a corrosion rate of approximately 0.16 mm/y.

The BP2 probe tests lasted 195 days. After finishing the test with probe BP2, a 0.055 mm change in thickness was determined, meaning a corrosion rate of approximately 0.12 mm/y. The results of the corrosion rate calculation for both probes are shown in Tab. 2.13. Figures presenting data recorded during the experiments are given in Appendix 3.

Tab. 2.13 Results of the corrosion probe tests in BPP

Probe	Time, days	R_{ox} , mΩ	R_{xend} , mΩ	ΔR_x , %	ΔG , mm	Corrosion rate, mm/y
BP1	162	2.9646	3.1065	4.79	0.072	0.16
BP2	195	3.4037	3.5294	3.69	0.055	0.12

Generally, no intensive slagging was observed on the surface of the sensor during the tests. Low alkali content and no potassium and no chlorine content in the ash deposit on the surface of sensor was found. But high sulphur content was present in the deposit, both in the external and internal layer. The results indicate a lack of high risk of corrosion caused by the chemical composition of the ash deposit on evaporators. For boiler no. 3 in OPP campaign, two probes were installed at level 30 m on the front and right walls. The probe mounted on the front wall was marked as OP1, while the probe on the right wall was marked as OP2. In the initial test period, the calculated corrosion rate was 0.39 mm/year for the OP1 probe (112-day test) and 0.48 mm/year for the OP2 probe (212-day test).

For the longer test the calculated corrosion rates were lower: 0.22 mm/year for OP1 probe (351-day test) and 0.22 mm/year for OP2 probe (436-day test) respectively, but this period covered several weeks of boiler outage. The average resistance measurement results and determined corrosion rate are shown in Table 2.14.

Figures with the probe temperature and resistance measured during the test as well as results of SEM/EDS analyses for cross-sections of corrosion sensors OP1 and OP2 are presented in [27], and Appendix 3.

Tab. 2.14 Results of the corrosion probe tests in OPP

Probe	Time, days	R_{ox} , mΩ	R_{xend} , mΩ	ΔR_x , %	ΔG , mm	Corrosion rate, mm/y
OP1	112	3.4116	3.6815	7.91	0.119	0.39
	269*	3.4116	3.8207	11.99	0.180	0.24
	351*	3.4116	3.8937	14.13	0.212	0.22
OP2	212	3.2051	3.7514	17.04	0.256	0.48
	436*	3.2051	3.7391	16.67	0.250	0.22

*(time including boiler outage)

Steam flow meters

A total of six NISTFLOM sensors together with two data loggers were installed in the OPP and BPP boilers. The data loggers acted both as online data acquisition systems for direct integration into the CIBOP system as well as locale data storage devices for manual data transfer via FTP for external checks and quality assurance. Both installations were fully installed in late October 2017 due to the maintenance schedule of the boilers that had to be followed by the investigation teams.

Measurement data was not accessible directly from TNO, but was sent in bulk in intervals by project partner IEN. When analysing the data obtained from the power plants, it was concluded that the calibration of the NISTFLOM sensors had shifted again compared to the previous re-calibration at TNO. The latter is probably due to oxide layers formed on both the sensor body and the adapter piece as well as the different contact interface steam pipe – sensor as compared to the ideal situation used at laboratory scale for calibration of the sensors. Hence, it can be concluded that, at least with the current methods and materials used, an absolute steam flow measurement was not possible. A description of some results from long-term NISTFLOM work is given in Appendix 5.

As demonstrated in the long-term testing in WP4, the NISTFLOM sensing platform is sufficiently robust and reliable to record flow changes in steam pipes under realistic full-scale conditions. Unfortunately, technical and accessibility reasons meant that NISTFLOM systems could not be mounted on steam pipes just after the inlet headers. Hence, the evaluation of the recorded signals could not be completed since the steam temperature in an individual pipe, which is unknown just before entering the collection header, forms crucial input for further data analysis and interpretation

Since the absolute values of steam flow and heat uptake are of less interest for determining dynamic changes in the boiler in terms of fouling, it is sufficient to be able to monitor the relative changes in steam flow and heat uptake. When a series of NISTFLOM sensors are well distributed over the steam pipes of a heat exchanger, not only the fouling rate of the heat exchanger can be monitored, but also the location where deposit build-up takes place. The latter enables the development of a smart soot blowing strategy, optimising the soot blowing intervals and soot blowing locations. The latter can lead to higher power plant efficiencies and lower CO₂ emissions (due to less soot blowing), longer up-time and lower maintenance costs (due to reduced thermal stress of the steam pipes, hence reducing spalling).

Determination of the corrosion rate in the CIBOP systems

Three models of rate of wall thickness loss were implemented in the Integration module of CIBOP. They were developed on the basis of periodic ultrasonic measurements of the boiler evaporator (O₂ model), electric resistance measurement of the wall evaporator (CMS model) and electric resistance measurement of the corrosion probe (CP). All models can be treated as empirical models.

The O₂ model was developed by comparison of O₂ concentrations in the boundary layer of the evaporator and real wall thickness loss. This model can be treated as the most realistic, because it is determined on the basis of real measurement of wall thickness loss.

CMS model and corrosion probe models are based on correlation between local O₂ concentration and corrosion rate determined for given O₂ concentration by the direct (resistance) methods during long-term measurements.

In the case of BPP, data from only one CMS system and one corrosion probe were available. For their particular location O₂ concentration was determined by CIBOP as an average from long-term experiments. The results from the direct corrosion measurements were extrapolated for other O₂ concentrations, assuming that for O₂=2 % the corrosion rate is equal to 0 (Fig. 2.25).

On the basis of these extrapolations CIBOP calculates the corrosion rate in mm/y for all places on the walls of the combustion chamber from the O₂ concentration at the wall determined by ANN.

It is also possible to calculation and display values of averages for each wall of O₂ concentration and corrosion rate calculated according to different models.

Ideally such CMS and corrosion probe models should be determined for several levels of O₂ concentrations. That means that more sensors should be installed in the boiler in areas of different O₂ levels. In the CERUBIS project, but also in future applications, the number of direct corrosion sensors is limited mainly for cost reasons.

It should be noticed that local O₂ CO and H₂S concentrations at a given point near the wall can differ greatly for different operational conditions of the boiler, as was confirmed by measurements. For this reason, an assumption that O₂ concentration is averaged for a longer time, when the boiler was being run in different conditions, could be quite representative for long-term predictions of the corrosion rate. The results had been obtained from CIBOP for long-term experiments in boiler no. 5 in BPP are given in Tab. 2.15 and example figures next.

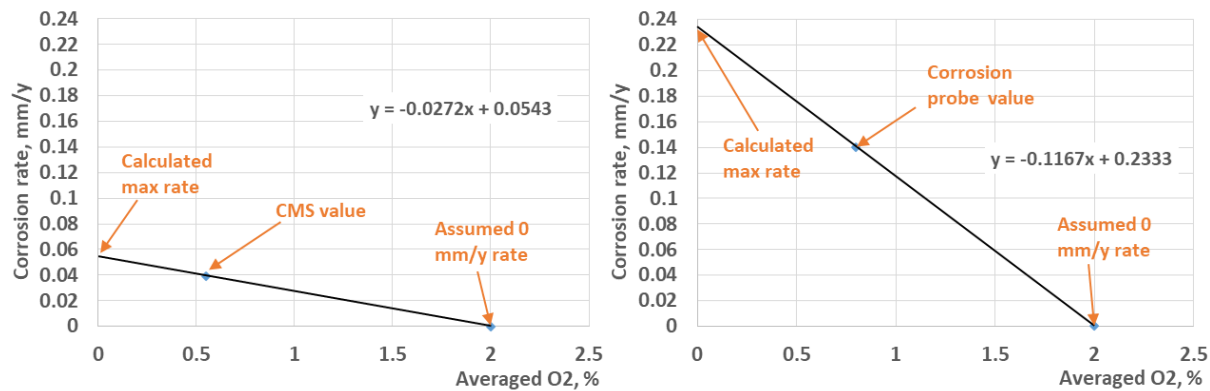


Fig. 2.25 Extrapolation of the corrosion rate for CMS (left) and corrosion probe (right) experimental results

Tab. 2.15 Overview of averaged concentrations of O₂ and CO in the boundary layer of the evaporator and the rate of wall thickness loss calculated on the basis of O₂, CMS and corrosion probe approaches over 0.5 year of operation of boiler no. 5 in BPP

Parameter and unit	Wall	Front	Right	Rear	Left	All
Average O ₂ concentration in boundary layer, %	1.25	0.86	1.92	1.71	1.435	
Average CO concentration in boundary layer, %	1.18	1.22	1.08	0.74	1.055	
Average dynamic of wall thickness loss mm/year (O ₂ model)	0.016	0.017	0.010	0.014	0.0142	
Max dynamic of wall thickness loss mm/year (O ₂ model)	0.032	0.039	0.034	0.038	0.0357	
CMS, level 36 m, right wall, wall thickness loss mm/y (O ₂ -0.55%)		0.0394				
CMS, average dynamic of wall thickness loss mm/year	0.028	0.034	0.017	0.0077	0.02	
CMS, max dynamic of wall thickness loss mm/year			0.0482			
Corr. probe, level 27 m, right, wall thickness loss (O ₂ - 0.8%)		0.14				
Corr. probe, average dynamic of wall thickness loss mm/year	0.11	0.136	0.068	0.033	0.082	
Corr. probe, max dynamic of wall thickness loss mm/year			0.19			

Figures 2.26 presents the half-year averaged maps of O₂ concentrations in the boundary layer of the evaporator for boiler no. 5 in BPP. Figure 2.27 presents the related rate of wall thickness loss determined by the O₂ model. The maximum dynamic reaches not more than 0.03-0.04 mm/year, which is a very small value for high temperature corrosion. This means that some tubes might reach their critical thickness (assumed 3 mm) after 50-70 years of operation; if the average is taken into account, after more than 120 years. Moreover, there are also areas with corrosion dynamic equal to almost 0.

For CMS located on the right wall, at level 36 m, the corrosion rates were equal to almost 0.04 mm/year, which is 2-3 times higher than the values obtained by the O₂ model. However, the maximum value obtained by CMS was only 1.5 times higher than the one obtained by the O₂ model. On the basis CMS model maps of the corrosion rate could be created, as shown in Fig. 2.28, and averages for the whole walls, as shown in Tab. 2.15.

A comparison of the rate of wall thickness loss in Fig. 2.27 and Fig. 2.28 obtained by the O₂ model and CMS model shows their similarity in the case of boiler no. 5 in BPP. Maximum corrosion rates for those models do not exceed 0.04 mm/year in some places of the evaporator where very low O₂ was measured.

A similar approach was used in CIBOP for the corrosion probe model, whose results are also shown for comparison in Tab. 2.15. The corrosion rate obtained for the corrosion probe was around 0.14 mm/year, with the maximum rate of 0.23 mm/y. This is almost four times higher than for CMS, in spite of the fact that the O₂ concentration at level 27 m was a little higher than at level 36 m, which runs counter to the results of wall thickness measurements. One of the reasons for such behaviour could be intensified erosion of the probe due to the different position of the probe relative to the evaporator tubes.

In boiler no. 3 in OPP, two CMS systems and two corrosion probes were implemented. So, two values of the rate of corrosion at two different averaged O₂ concentrations were obtained for each measurement method. An extrapolation of the corrosion rate for other O₂ concentration is shown in

Fig. 2.29 for CMS and in Fig 2.30 for the corrosion probe. Linear and exponential correlations were considered for both measurement techniques. Directly measured values of the corrosion rates, averaged O₂ at these points and selected results from CIBOP system are given in Tab. 2.16, which also shows for comparison real averaged rates of corrosion for two periods determined by ultrasonic measurements

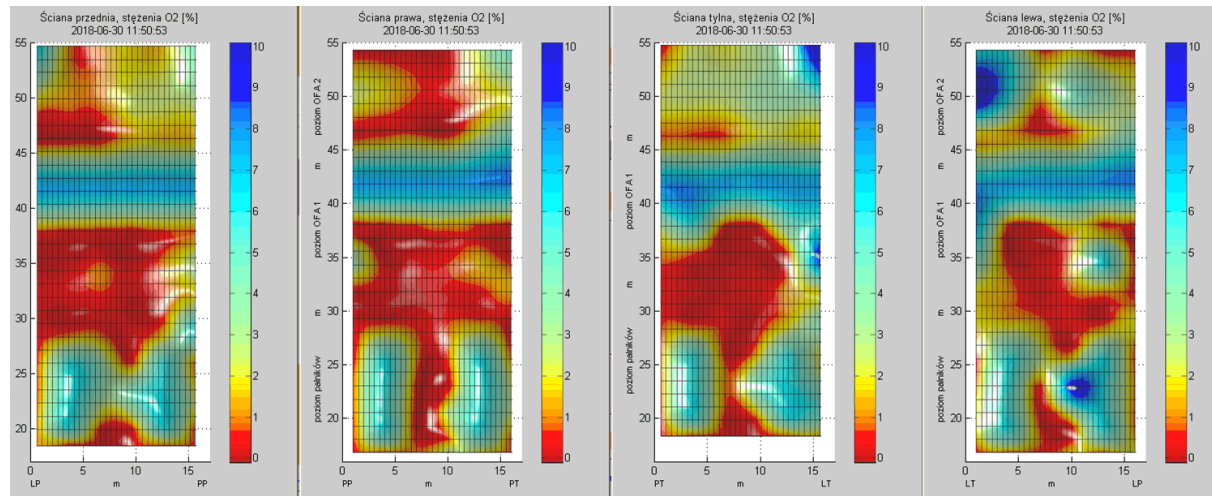


Fig. 2.26 Half-annual averages of operation maps of O₂ concentrations (%) in the boundary layer for all four walls in boiler no. 5, BPP (taken directly from CIBOP, view from outside of the boiler)

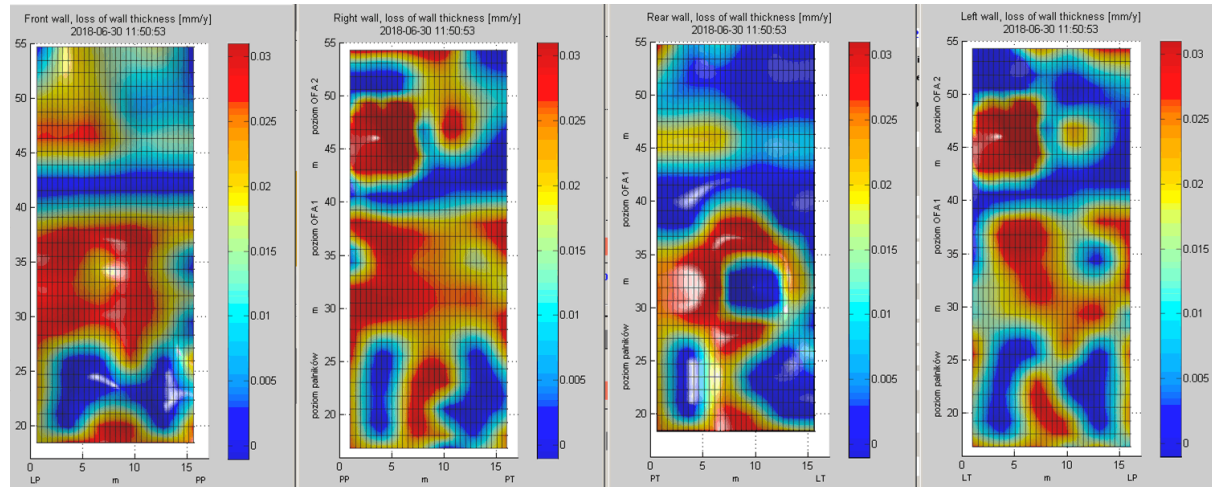


Fig. 2.27 Half-annual averages of operation maps of the rate of wall thickness loss (mm/y) for all four walls in boiler no. 5, BPP (taken directly from CIBOP, view from outside of the boiler) – O₂ Model

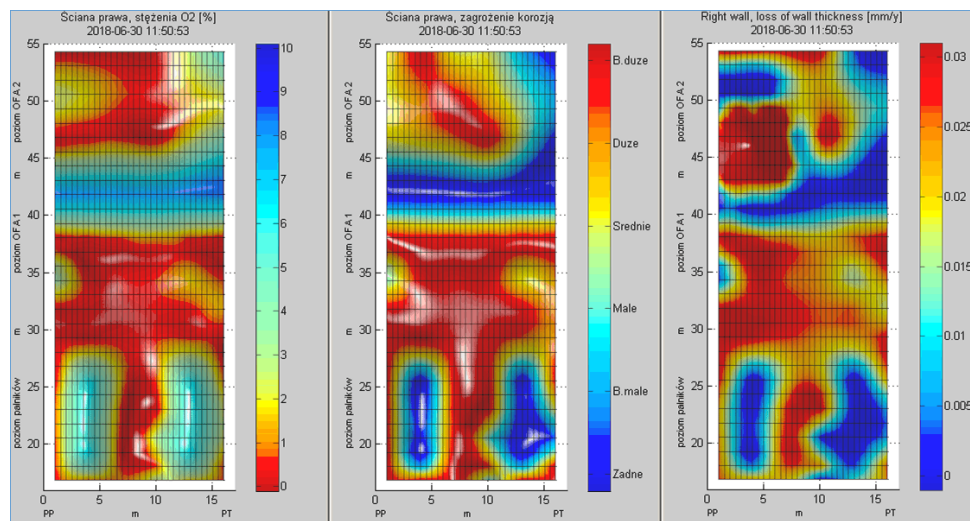


Fig. 2.28 Half-annual averages of operation maps of O₂ concentration (left), the risk of corrosion (middle) and the rate of wall thickness loss (right) for right wall at boiler no. 5, BPP (taken directly from CIBOP) - CMS Model

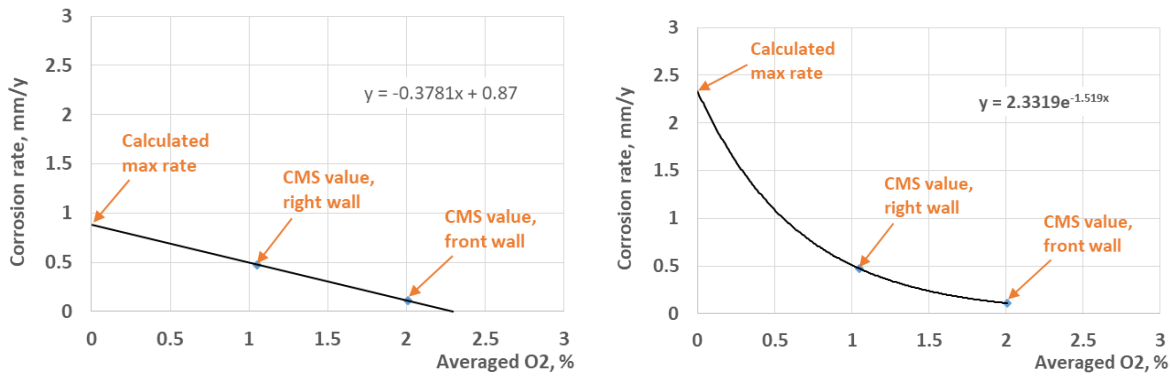


Fig. 2.29 Extrapolation of the corrosion rate for CMS: linear (left) and exponential (right)

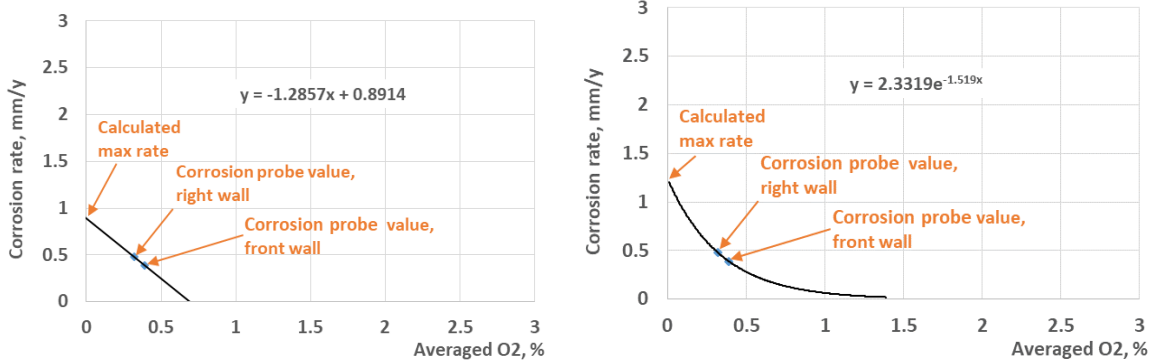


Fig. 2.30 Extrapolation of the corrosion rate for the corrosion probe: linear (left) and exponential (right)

The corrosion rates determined by CIBOP for boiler no. 3 in OPP were much higher than in BPP. Figure 2.31 presents O_2 concentrations in the boundary layer of the evaporator averaged over a half year and Fig. 2.32 the rate of wall thickness loss resulting from the O_2 model. At some points maximum corrosion rates reach more than 0.5 mm/year. The corrosion rates averaged for the whole walls area are in the range of 0.2 to 0.3 mm/year - Tab. 2.16. The table also highlights the area affected by particular corrosion rates, which can be compared to the real one from Tab. 2.17.

Tab. 2.16 Overview of averaged concentrations of O₂ and CO in the boundary layer of the evaporator and the rate of wall thickness loss calculated on the basis of O₂, CMS and corrosion probe approaches over 0.5 year of operation of boiler no. 3 in OPP

Parameter and unit	Wall	Front	Right	Rear	Left	All
Average O ₂ concentration in boundary layer, %	1.98	1.66	1.64	1.95	1.8	
Average CO concentration in boundary layer, %	3	2.72	2.9	3.18	2.95	
O₂ model						
Average dynamic of wall thickness loss mm/year (O ₂ model)	0.281	0.227	0.264	0.231	0.272	
Max dynamic of wall thickness loss mm/year (O ₂ model)	0.41	0.46	0.32	0.51	0.35	
Approx. area with corrosion >700 um/year, % of wall	0	0	0	0	0	
Approx. area with corrosion 300-700 um/year, % of wall	32	34	22	27	31	
Approx. area with corrosion 50-300 um/year, % of wall	46	44	55	41	42	
Approx. area with corrosion <50 um/year, % of wall	22	22	23	32	27	
CMS model						
CMS, level 23 m, right wall, wall thickness loss mm/y (O ₂ – 1.05%)		0.473				
CMS, level 28 m, front wall, wall thickness loss mm/y (O ₂ – 2.01%)	0.11					
Linear correlation						
CMS, average dynamic of wall thickness loss mm/year	0.478	0.414	0.47	0.368	0.432	
CMS, max dynamic of wall thickness loss mm/year	0.838	0.749	0.767	0.87	0.806	
Approx. area with corrosion >700 um/year, % of wall	35	21	20	29	26.25	
Approx. area with corrosion 300-700 um/year, % of wall	35	43	55	21	38.5	
Approx. area with corrosion 50-300 um/year, % of wall	4	11	5	7	6.75	
Approx. area with corrosion <50 um/year, % of wall	26	25	20	43	28.5	
Exponential correlation						
CMS, average dynamic of wall thickness loss mm/year	0.853	0.592	0.692	0.754	0.722	
CMS, max dynamic of wall thickness loss mm/year	2.053	1.434	1.544	2.332	1.84	
Approx. area with corrosion >700 um/year, % of wall	52	43	50	36	45.25	
Approx. area with corrosion 300-700 um/year, % of wall	13	21	25	14	18.25	
Approx. area with corrosion 50-300 um/year, % of wall	9	11	5	25	12.5	
Approx. area with corrosion <50 um/year, % of wall	26	25	20	25	24	
Corr. probe model						
Corr. probe, level 30 m, right, wall thickness loss mm/y (O ₂ -0.32%)		0.48				
Corr. probe, level 30 m, front, wall thickness loss mm/y (O ₂ -0.39%)	0.39					
Linear correlation						
Corr. probe, average dynamic of wall thickness loss mm/year	0.242	0.117	0.132	0.223	0.178	
Corr. probe, max dynamic of wall thickness loss mm/year	0.784	0.48	0.543	0.891	0.674	
Approx. area with corrosion >700 um/year, % of wall	13	0	0	21	8.5	
Approx. area with corrosion 300-700 um/year, % of wall	22	25	30	7	21	
Approx. area with corrosion 50-300 um/year, % of wall	17	18	10	4	12.25	
Approx. area with corrosion <50 um/year, % of wall	48	57	60	68	58.25	
Exponential correlation						
Corr. probe, average dynamic of wall thickness loss mm/year	0.29	0.143	0.17	0.304	0.227	
Corr. probe, max dynamic of wall thickness loss mm/year	0.967	0.48	0.55	1.24	0.809	
Approx. area with corrosion >700 um/year, % of wall	22	0	0	25	11.75	
Approx. area with corrosion 300-700 um/year, % of wall	13	25	30	3.5	17.88	
Approx. area with corrosion 50-300 um/year, % of wall	30	25	40	21.5	29.1	
Approx. area with corrosion <50 um/year, % of wall	35	50	30	50	41.25	

Tab. 2.17 Real averaged corrosion rates determined for two periods, boiler no. 3, OPP

Parameter and unit	Wall	Front	Right	Rear	Left	All
Real measurement (2015-2017)						
Average dynamic of wall thickness loss mm/year	0.147	0.210	0.260	0.251	0.217	
Max dynamic of wall thickness loss mm/year	2.5	1.5	1.6	1.5	1.775	
Area with corrosion >700 um/year, % of wall	4.56	6.64	11.49	13.58	9.07	
Area with corrosion 300-700 um/year, % of wall	12.03	14.72	15.95	15.17	14.47	
Area with corrosion 50-300 um/year, % of wall	32.92	53.82	29.32	35.98	38	
Area with corrosion <50 um/year, % of wall	50.48	24.82	43.24	35.26	38.45	
Real measurement (2012-2015)						
Average dynamic of wall thickness loss mm/year	0.073	0.127	0.095	0.074	0.092	
Max dynamic of wall thickness loss mm/year	0.667	0.967	0.733	0.8	0.792	
Area with corrosion >700 um/year, % of wall	4.98	2.74	0.68	0.00	2.1	
Area with corrosion 300-700 um/year, % of wall	10.65	17.32	14.86	8.38	12.8	
Area with corrosion 50-300 um/year, % of wall	34.44	28.86	38.92	27.17	32.3	
Area with corrosion <50 um/year, % of wall	49.93	51.08	45.54	64.45	52.75	

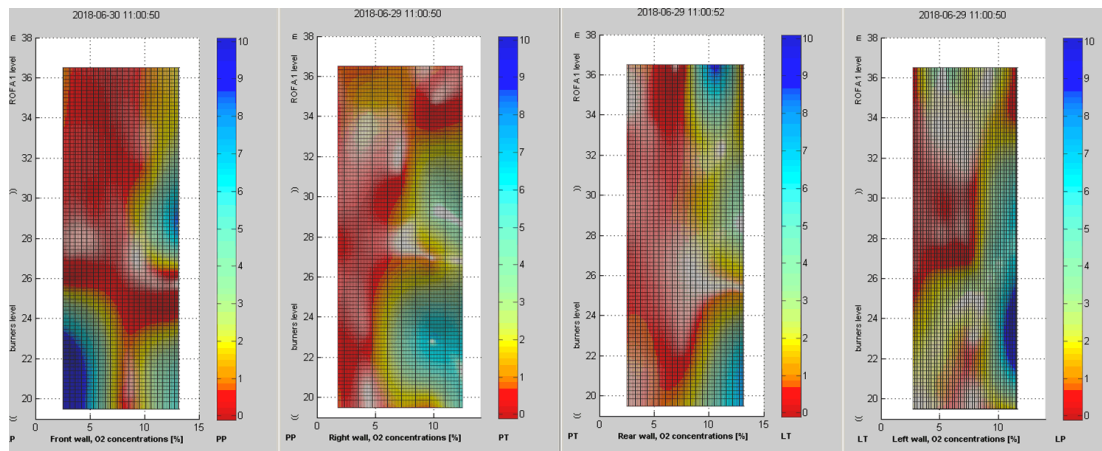


Fig. 2.31 Half-annual averages operation maps of O₂ concentrations (%) in the boundary layer for all four walls in boiler no. 3 in OPP (taken directly from CIBOP, view from outside of the boiler)

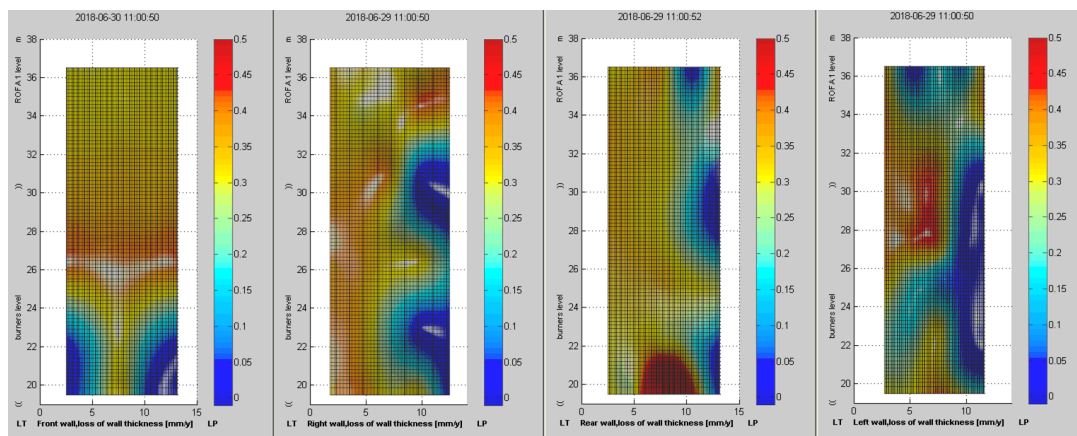


Fig. 2.32 Half-annual averages of operation maps of the rate of wall thickness loss (mm/y) for all four walls in boiler no. 3 in OPP (taken directly from CIBOP, view from outside of the boiler) – O₂ model

The O₂ model in CIBOP does not indicate any rates greater than 0.7 mm/y which is contrary to real measurements of wall thickness from the last two years. Areas affected by corrosion rates of 0.3 - 0.7 mm/y are overestimated around twofold. However, if real measurement rates for the ranges >0.7 and 0.3-0.7 are added together, they are closer to the 0.3-0.7 obtained by the O₂ model, especially for left and rear walls. The corrosion rates for the range 0.05-0.3 mm/y from the O₂ model are also overestimated, compared to real values except for the right wall where the situation is the opposite. The corrosion rates for the range < 0.05 mm/y are for the O₂ model in all cases less than in reality but for right and left walls they are close to each other.

The situation differs as regards CMS and the corrosion probe, for which results were also shown in Tab. 2.16. These corrosion rates are higher compared to the O₂ model and closer to those obtained from real measurements in the years 2012-2017. It might be seen that linear extrapolation of CMS model is closer to 2012-2015 data for maximum values, but the averages are over 4 times overestimated.

If data for 2015-2017 are taken into account, exponential extrapolation gives values from the CMS model closer to maximum values, but the averages are also overestimated almost four times (or eight times if 2012-2015 is taken into account).

The type of extrapolation also influences the area of the walls subject to the corrosion rates from the particular range. The areas of higher corrosion rates are markedly overestimated.

Such overestimation, in spite of good correlation for maximum values, might be caused by wrong O₂ concentration estimations or possibly a wrong assumption that in points with similar O₂ concentrations the same corrosion rate of CMS method can be applied. Some correction factors might be applied, but then maximum values will be underestimated.

In fact, maximum corrosion rates are very important, even if the area affected by such rate is very small, because this is direct information about the appearance of possible damage to tubes which can occur after 1-2 years of boiler operation after exchanging the water walls.

On the other side, averaged on the whole wall corrosion rates are also important but, in that case, it is more important to properly determine the area affected by the corrosion in order to focus on a given part of the wall during the next maintenance outage.

Better results were obtained for the corrosion probe, also included in Tab. 2.16. In both approaches, linear and exponential, averages are very close to real ones. Maximum values are comparable to those obtained from real measurements in the years 2012-2015, but for those from 2015-2017 they are underestimated. Good agreement of the areas affected by corrosion is also very important.

To recap, in spite of some underestimation of maximum values, corrosion probes gave better results compared to the CMS method.

Boiler optimisation.

Optimisation trial was carried out in boiler no. 5 in BPP using CIBOP for three different boiler loads.

Table 2.18 presents initial data resulting from boiler operation according the DCS system settings for four cases which were optimised. This table also shows the corrosion rates estimated by CIBOP according to CMS and corrosion probe models. For these cases the boiler was optimised in a two-step approach: in the first step the optimiser was run and the boiler was set for conditions indicated by the optimiser, then after 2-3 hours the optimiser was run again and the boiler was again set to new optimiser settings. The results of the optimisation averaged for the whole combustion chamber are also given in Tab. 2.18 and they can be compared against the initial values. More details for the optimised cases, like initial and optimiser-provided air settings, O₂ and CO concentrations as well as the corrosion rates averaged for each wall are given in Appendix 7.

Tab. 2.18 Results of the optimisation of boiler no. 5 in BPP using CCIBOP optimisation module

Case number	Load MWe	Number of working mills	Outlet emissions in mg/m ³ n, ref. 6% O ₂				Outlet O ₂ emission, %		Averages concentrations in boundary layer for all walls, %				Average corrosion rate for all walls, µm/y			
			NO _x		CO		O ₂		O ₂ , all		CO, all		CMS model		Corr. probe model	
			Base case	Optimis. case	Base case	Optimis. case	Base case	Optimis. case	Base case	Optimis. case	Base case	Optimis. case	Base case	Optimis. case	Base case	Optimis. case
Case 1	370	7	165	175	81	70	1.85	2.3	1.62	2.63	1.07	0.65	22.1	6.3	87.9	25.5
Case 2	370	6	172	169	273	56	2.1	2.5	2.38	3.18	1.015	0.70	9.9	3.0	39.5	25.0
Case 3	340	6	149	140	110	79	2.7	2.1	1.98	2.91	1.32	0.93	16.4	1.5	65.1	6.5
Case 4	245	5	131	187	129	82	2.2	2.2	1.92	2.84	0.94	0.89	17.2	3.2	68.6	13.0

In all cases, beside different air settings (secondary air and OFA), the optimiser also increased total amount of air to the combustion chamber. This had increased NO_x emission but only in cases 1 and 4 where NO_x emission was still below 200 mg/m³n. In all cases, increase of O₂ concentration near the walls could be observed together with some decrease of CO concentration. CO emissions from the boiler also decreased (except in case 4). Most importantly, for all cases use of the optimiser markedly decreased the risk of corrosion. This was achieved not only through adding more air to the combustion chamber, but also through appropriate distribution of the secondary air to the boiler.

Task 4.5 - Techno-economic evaluation of the system.

Techno-economic analysis was carried out for the OPP boiler with three possible scenarios for the next twelve years of boiler operation with regard to the low O₂ corrosion issue:

- implementation of CIBOP with some minor wall tubes replacement every 3 years,
- extensive wall tubes replacement every three years, as is done currently (min. scenario – 450 m²/12 years, max. scenario – 1500 m²/12 years), no implementation of CIBOP,

- evaporator covered by three different coatings, no wall tubes replacement at all, no implementation of CIBOP.

CIBOP was considered in two configurations:

- with 16xO₂/CO gas analysers, 4xCMS, 2x Corrosion probe and 10xNISTFLOM,
- with 16xO₂/CO gas analysers, 2xCMS, 2x Corrosion probe and no NISTFLOM.

Tab. 2.19 show assumed CAPEX costs for all above-mentioned scenarios while Tab. 2.20 shows OPEX costs for CIBOP in different configurations. This table also includes two scenarios (min. / max.) for necessary replacement of evaporator walls if CIBOP is installed as part of 20%, 30% and 40% of the walls area which would have to be replaced if CIBOP were not installed.

With regard to the coatings, a 4-6 year guarantee was assumed for Hybrid MD and thus this coating should probably be applied twice. Other coatings can have 8-10 years' warranty and thus only one application in 12 years period was assumed. In sum, 2 000 m² of evaporator wall was assumed to be covered by coatings.

Tab. 2.19 CAPEX for 3 different scenarios of boiler operation with regard to low O₂ corrosion for the next 12 years

Scenario	CIBOP	Replacement of evaporator walls		Coatings		
		EUR	EUR/m ²	EUR/m ²	Type	Company
CIBOP 16xO ₂ /CO, 4xCMS, 2xCorr.Pr., 10xNF	500 000		1 975 (2018 year) 2 450 (2027 year)	1 400	Hybrid MD	Enter-Eko
				1 630	SUME BOIL	Sulzer Metko Coating GmbH
CIBOP 16xO ₂ , 2xCMS, 2xCorr.Pr.	341 500			2 325	Inconel 622	Aquilex Welding Service Poland

Tab. 2.20 Main assumptions for techno-economical calculations with regard to CIBOP OPEX

Kind of cost	Personal costs		Energy costs	Average maintenance cost per year					Wall replacement if CIBOP installed (if not installed)			
	Man hours per month	Hourly rate		1 MWh in PP	O ₂ /CO	O ₂	4xCMS	2xCorr. Pr.	10xN	Cost	3rd year	6th year
Scenario	h/month	EUR	EUR	EUR	EUR	EUR	EUR	EUR	EUR/m ²	m ²	m ²	m ²
Min	160	16	41.9	9 872	6 078	2 958	4 292	1 054	1 977	20 (100)	48 (150)	80 (200)
Max	160	16	41.9	9 872	6 078	2 958	4 292	1 054	1 977	80 (400)	150 (500)	240 (600)

Fig. 2.33 presents for each of the scenarios the sum total of calculation of CAPEX costs and cumulated OPEX costs over 12 years of operation.

The cheapest scenario features minimum evaporator wall tubes replacement without CIBOP and coatings. However, this scenario is rather unlikely due to the fact that NO_x emissions will be further decreased and the operating conditions of the walls could only become worse.

More likely is the max. scenario, with total costs reaching 3 500 000 Euros over 12 years of operation. If this scenario is taken into account, CIBOP installation in both configurations and for both scenarios of walls tubes replacement is cost-effective (two times lower costs of OPEX + CAPEX). Coatings always have the highest CAPEX but there are no OPEX costs. This expensive technique has a very big advantage – the lowest probability of tube failure compared to other techniques. It must be underlined that an emergency three day outage costs the power plant around 500 000 Euros. So, if coatings decreased the number of emergency outages to at most 6-8 through the 12 years of operation, they can be considered cost effective. However, there is no currently guarantee that coatings will survive 12 years of operation. A comparison of CAPEX and OPEX costs for advanced and basic CIBOP scenarios is given in Tab. 2.21.

Tab. 2.21 Comparison of CAPEX and OPEX for two CIBOP configurations

CIBOP configuration	Advanced	Basic
	16 O ₂ /CO gas analysers, 4 CMS 2 corrosion probes, 10 NISTFLOM	16 O ₂ /CO gas analysers, 2 CMS 2 corrosion probes
CAPEX	500 000 EUR	341 500 EUR
OPEX	770 000 EUR	572 000 EUR

A more detailed structure of the OPEX costs is shown in A9. High OPEX is related to personnel costs which are on average one half of the total OPEX costs. Energy costs (electricity to the system itself and pressurised air) are relatively low. Other costs are related to raw materials/consumables necessary for services and also for control measurement of O₂/CO in the boundary layer every three years. The highest cost in raw material/consumables is cost of O₂ and CO sensors and pumps. CO sensors should be replaced every year, O₂ sensors and pumps every two years.

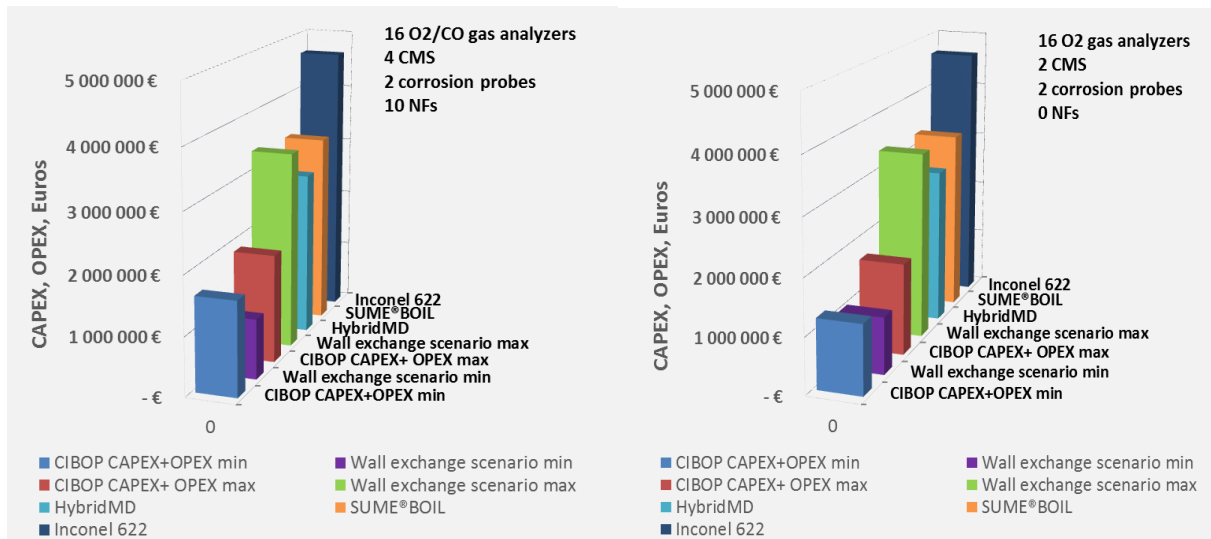


Fig. 2.33 CAPEX + OPEX cost for the different scenarios of protection of boiler no. 3 in OPP against low O₂ corrosion

2.3.5 Project management - WP5

The project was coordinated and controlled according to the WP5 description. All necessary meetings, especially those in both power plants were held. All reports, some with delays, were successfully delivered except for progress reports, which were not necessary under RFCS rules. The progress was estimated on the basis of yearly reports and intensive email exchange among all partners. A project website was set up and run. Data exchange between partners was organised through a login-based part of this webpage. One workshop, instead of two (approved by the EU officer), was organised in **Wrocław**, Poland, in June 2018. Several national and international articles were written. The project partners attended several conferences. Marketing leaflets and other materials were created and distributed at conferences and trade fairs. A “mobile trade facility” highlighting some components of the system was manufactured. Moreover, IEN applied for two patents concerning gas analysers developed in the CERUBIS project. An exploitation road map was also created, highlighting the most promising and valuable directions for future development and industrial applications of results of the CERUBIS project

Discussion of WP4 results.

From the technical point of view, four significant components of the diagnostic system were implemented in each boiler and their usefulness was proved during long-term operation, i.e. gas analysers, wall resistance measurements, corrosion probe and steam flow meters. If we count four type of gas analysers, then even eight significant system components were successfully assessed. These components were unique constructions with specific features, which meant that they could not be bought on the market that time. In the case of gas analysers two IEN patent applications (P-417989 and P-419387 from 2016) confirm their novelty.

An important methodology achievement was confirmation that direct corrosion measurements can give valuable results after a longer time of operation, and not only noise was registered but also change in resistance over time. The results of these measurements were used to calibrate the corrosion rate models implemented in CIBOP.

From the methodology point of view, the idea of coupling quick indirect gas analysis with slow direct measurement of the corrosion rate was confirmed by experimental data. CIBOP calculation of the corrosion rate was done using data gathered by CIBOP during a half year campaign, plus calibrated corrosion models and tube thickness measurements. Broad analysis of the results obtained and comparison of them with the real corrosion rates obtained from tube thickness measurements showed the usability of the method and of the software tools created. Some of the quantitative results obtained by different corrosion models might be questionable, but the diagnostic system is up, running and works.

For BPP, CIBOP predictions of corrosion rates were very similar to real ones when the CMS model was used. In the case of OPP, CMS predictions usually overestimated real corrosion rates but satisfactory results were obtained for the corrosion probe. The reason for some deviations might lie in the assumptions for extrapolation of CMS/corrosion probe results to whole boiler walls. Also CMS and corrosion probe techniques should be tested and verified for several different O₂ and CO concentration levels in the boundary layer, where the measurements were taken. In places where current CMS and corrosion probe were installed, very low O₂ was usually observed. Moreover, as regards the corrosion probe the O₂ average through the period of time was calculated only locally – in fact at one point where the probe was inserted. With the CMS method, an O₂ time average was calculated as the average for 4 - 6 metres of evaporator wall and the direct route of current through the evaporator wall was unknown.

Almost all developed models in CIBOP are based on AI techniques, so there is no need to determine a detailed mathematical model, formulate equations etc. AI techniques provide an opportunity to create models on the basis of real data through training processes. This is a big advantage of such modelling, especially when the phenomena are complex and not all parameters influencing the process are known. It is obvious that the more measurements are carried out, the better the prediction results are, including corrosion rates and affected areas. When a low amount of data is known, the performance of the trained ANN is rather poor. However, it was confirmed, at least for the OPP boiler, that CFD techniques work. After good calibration of the model regarding real cases, the model can supply more data (test errors up to 20%) which can be used to train and test the ANN, instead of very costly full-scale measurements.

Very promising results were obtained from CIBOP in BPP when the optimisation module was tested. Setting the boiler parameters according to CIBOP decreased the averaged corrosion rates 3-4 times, keeping the NO_x below 200 mg/m³ and in some cases even decreasing the NO_x emissions compared to DCS set cases. This is one of the very promising results of CIBOP performance. However, there were still some places on the evaporator when corrosion rates were very similar to the initial ones (the total average was reduced).

The slagging part of CIBOP was investigated, but not to the extent initially envisaged. In general, steam flow meters —which have the potential to determine the deposition, slagging and fouling issues in evaporators or superheaters — were tested positively for a very long time (almost two years in total) with quite good performances. However, due to inaccessibility of the proper measurement locations, the full potential of the sensors could not be exploited. Furthermore, the determination of deposit build-up on the basis of two or four signals the assessment of slagging risk in the boiler was rather not possible. For a realistic assessment, at least 10-20 pipes coming through the boiler should have been monitored. Such determination could give a direct signal to steam guns or acoustic devices to be switched on in order to remove deposit/dust.

Nevertheless, other features of the slagging part of CIBOP were tested to determine slagging properties of fuels which could be directly used in boilers instead of currently fired slagging fuel. This was done mainly for OPP, where acoustic dust removers are usually switched on every 3-4 hours and steam guns at least two times per day.

2.4 Conclusions

Thanks to the development and test work carried out within the CERUBIS project, and in particular through long-term operational trials, a number of new diagnostic systems were developed to the point nearing the commercial design. It was confirmed that it is technically feasible to construct, install and use the intelligent system for monitoring of in-boiler corrosion in a full-scale power plant environment. The new knowledge concerns both the course of corrosion in the boiler, the construction and mounting solutions for the sensors as well as the corresponding measurement methods and the integration of the entire new system of corrosion diagnostics of the boiler.

Next to long term test runs with the integral diagnostic system, several measurement campaigns were carried out in two full-scale power plants, namely the lignite-fired Belchatow PP (BPP) and bituminous-coal-fired Opole PP (OPP). The measurements were carried out employing various types of short-term deposition probes. The subsequent SEM/EDX metallographic analyses of collected deposits and tube materials provided important information helping to determine the corrosion and slagging behavior under recently implemented, deep-staged low NO_x emission regime. These results showed that the leading corrosion mechanism in both investigated boilers is sulphuric corrosion but only within the combustion chamber of the boiler. In the area of the first superheaters, there were generally no corrosive factors, which finding was also confirmed by boiler inspection and tube material measurement data. Also, SEM studies showed that corrosion processes for both BPP and OPP is not an intensive process in this area.

Furthermore, the above described investigations demonstrated that assessment of corrosion rates on the basis of calculations of dynamics of oxide layer growth on the deposition probes does not correspond with the real corrosion rate determined on the basis of periodic (every 2-3 years) ultrasonic measurements of the evaporator wall tubes thickness. The results from the short-term measurement were significantly too high. Translating directly the results from deposition probes gives an average corrosion rate of 50-230 mm/year for BPP and 70-120 mm/year for OPP while maximum actual defects are 2.5 mm/year for OPP and only 0.02 mm/y for BPP. Moreover, the obtained results showed that the rate of high-temperature corrosion is higher in the BPP than in the OPP, which is not in line with reality.

These discrepancies could, amongst others, be due to:

- The relatively short exposure time of the probe in the combustion chamber (max. 20 h), resulting in an initial rapid formation of (unstable) oxides, which is not limited by the diffusion of oxygen and corrosive species. This process later becomes significantly slower, both due to the further stabilization (disproportionation/dissolution of alloys etc.) of the oxide layer as well as diffusion limitations for the corrosive species. Hence, based on the initial corrosion rate the long-term rate cannot be adequately assessed.
- The specific location of the probe e.g. in the dust eroding stream, which may result in an increase in the degradation of the oxide layer, hence increasing the wear of the tube material.
- Probe physical settings deviating from that of the evaporator wall tubes (i.e. the position of the probe perpendicular to flue gases flow, while parallel for the evaporator wall) which generated additional physical-chemical processes absent during the normal operation of the boiler evaporator.
- More frequent and faster thermal stresses resulting from the nature of the measurement itself.
- A higher temperature difference between the surface of the probe deposit ring and the cooling medium.

In sum it can be concluded, that although such measurements are invaluable in order to assess the mechanism of the corrosive attack, by producing real-life deposits, such short-term deposition diagnostic methods may not reflect the actual corrosion process and may not be used directly for assessment of the long-term corrosion rate.

A much more reliable approach than the above mentioned is the estimation of corrosion rate based on long-term resistance methods, i.e. resistance corrosion probes or the method of measuring the resistance of the membrane walls of the boiler (CMS).

Such methods allow to directly determine the rate of the thickness loss of evaporator material in mm/y independent to the nature of the corrosion/erosion process itself and only on the basis of a change in resistance or measuring element of the corrosive probe introduced into the boiler or part of the boiler screen. Both methods were developed within the project and successfully tested and applied in CIBOP during powerplants campaigns.

Based on the observations and development of the resistive-based systems within CERUBIS project, the main characteristics and requirements for measuring equipment was identified, allowing them to be practically used in energy boilers. These characteristics are briefly discussed below

The resistivity-based corrosion probe.

The measuring sensors of the resistance corrosion probes are preferably to be made of the same material as the evaporator (in this case 15HM steel). The probes construction should be such as to allow for easy replacement of each of their elements on-site and without applying force/heat, i.e. avoiding any welded or screw connections and favoring sleeve-type connections with an external tightening system to provide good electric contact.

The measuring system should be equipped with a resistance meter adapted for industrial applications (i.e. dust-tight yet preferably with adequate ventilation to prevent aggregation of corrosive gasses), a temperature control system and a PLC controller (located in an individual control cabinet). The data recording system allows to record the resistance value with a minimal frequency of 1 per minute, wherein each measurement recorded is an average of three measurements taken. The measurement results are saved locally on the memory card in the controller and sent to the central unit of the CIBOP system. The measuring system can operate as a standalone system or under the control of the CIBOP system using the Modbus protocol. The main control parameters are the temperature settings of the sensor and the frequency of the resistance measurement itself.

For operational reasons, the probe is cooled with compressed air which is the most technically feasible solution, given the fact that each power plant is equipped with compressed air system. It is also the safest in that respect, that no water spillage over the sensitive and high-current intensity elements can occur.

One of the most important operational issues is precisely maintaining a stable temperature of the sensor corresponding to the temperature of the evaporator tubes because all sensor temperature fluctuations have a significant impact on the deviations of the resistance measurement results.

The recommended thickness of the resistance sensor is 2.5–5 mm, wherein for smaller thickness a higher measurement sensitivity is possible. When using a 5 mm thick sensor (tested at OPP and BPP) **the range of the measured resistance was in the range of 6–8 mΩ** (approx. 8 mΩ at 320 °C sensor temperature). Under such conditions, the corrosion rate can be determined during operation of the probe during at least one month. With a smaller sensor thickness this time will be shorter.

Evaporator wall resistance measurements (CMS)

The CMS Corrosion Monitoring System developed and demonstrated within the CERUBIS project uses an electrical resistance measurement based on a refined four-wire method and it is able to measure electrical resistance of the order of μOhms when operated at 200 W power input.

To account for the temperature dependence of the resistivity of stainless steel, the resistance measurement must be combined with temperature measurements on the boiler wall itself.

To relate the electrical resistance into material loss, a theoretical model with a linear corrosion rate and a linear temperature dependence of the resistivity of the material was developed based on pilot-scale tests. Used in full-scale power plant, this method gave good results.

When applied on a single tube, the developed corrosion monitoring system (CMS) is able to successfully predict tube failure and is able to detect different rates of material loss at different fuel conditions.

The following was observed and concluded when applying the CMS on a real-scale boiler wall, such as tested in OPP and BPP power plant,

- Long-term stable datasets of about one year are required to determine corrosion rates in the order of 1 ppm/h with a satisfactory statistical significance.
- A setup as tested in BPP, with four connection points spaced at 2 m, 6 m and 2 m on one boiler wall, gives a boiler wall resistance of about 8 μOhm . This results in a current draw of the system of 6.6 A and a voltage drop over the boiler wall of about 50 μV .
- To achieve good electrical contact with the boiler, adapters can be welded onto the membrane wall, preferably on the so-called spacers, between the boiler tubes. These adapters should be shaped conically such to accommodate the welding process. Adapters made of electrolytical copper are feasible, but for optimal results adapters should be made from the same material as the boiler wall.
- A quasi-continuous operating mode combined with active cooling of the shunt resistors allows the system to operate at a minimum 200 W electrical power level required to reach the desired resolution and accuracy.
- To reach system lifetimes of multiple years, solid state relays are required instead of mechanical relays due to the vast number of cycles required to operate the system.

The gas analysers

The project confirmed previous observations from other researchers that the concentrations of O₂ and CO in the evaporator wall layer are a valuable indicator for assessing the risk of high-temperature corrosion. Besides O₂ and CO concentration, data on H₂S concentrations were demonstrated to be important as well, as H₂S is responsible for sulphuric corrosion under reducing conditions (typical for the lower part of a deep--staged furnace), which was confirmed to be the prevailing mechanism in the boilers investigated in the project. However, the project showed that H₂S measurement is unnecessary in assessing the rate of corrosion due to well-established coinciding nature of H₂S concentration profiles (both spatial as well as temporal) with CO concentrations. Hence it can be argued that CO is a good enough H₂S indicator.

Moreover, during laboratory research and in-boiler measurement campaigns, a large disturbance due to high concentrations of CO, SO₂, on the H₂S measurement itself was found, giving improper quantification of the signal.

Removing the H₂S measuring cell from the gas analyzer altogether reduces its production costs and significantly operating costs, amongst others due to avoiding expensive and hazardous gas for H₂S calibration.

The undoubted achievement of the project is the development of low-cost gas analyzers for measuring O₂, CO (optionally H₂S) in the combustion chamber of pulverized-coal fired boilers. The unit cost of such an analyzer system for the delivery and installation of 16-20 units is estimated at 4 to 5 thousands EURO per piece. It should be strongly emphasized that such analyzer is adapted to extremely harsh conditions for measuring O₂ and CO concentrations in the combustion chamber (temperatures above 1200 °C, dusty environment, presence of slag and flames, active chemical reaction zone). For comparison, the current generation of commercially available analyzers is generally adapted to measure emissions in relatively cool and chemically stabilized exhaust gases at the exit of the boiler. The price of such units varies between 8 to 15 thousands EURO per piece depending to the manufacturer. Such commercial analyzer is typically not equipped with an automatic cleaning system of the entire sampling and measurement path, which is the feature of the analyzer developed in the project, and incorporated in the above mentioned affordable price.

The estimated measurement error demonstrated in lab-scale tests and in full-scale trials during the development and the validation of the analyzers was found to be slightly greater compared to commercial analyzers (Siemens Ultramat U23). Nonetheless, this increased measurement uncertainty does not significantly affect the final result of determination of corrosion risk nor the corrosion rate.

Since the measurement itself does not apply to emissions, hence has no formal/legal requirements as to the sensitivity etc., it only serves to assess the concentrations of gases in the wall layer of the evaporator. For example, the O₂ indication of the developed analyzer equal to 0, compared to the actual, measured concentration of 0.2 %, will not have a significant impact on the risk or the rate of corrosion, which for the entire wall of the combustion chamber is estimated on the basis of the stochastic/empirical methods.

As one of the tangible deliverables of the project, an owing this result greatly to the extensive laboratory, pilot and power plant tests, prototypes of analyzers for O₂, CO and H₂S (optional) were created. The following most important observations can be formulated:

- It is very important to be able to diagnose on-line the status of the integral sampling and measuring track of the analyzer (by measuring pressure, gas flow rate and temperature). This gives essential information about the quality of the measurement and warns in advance about the upcoming clogging event. A purging system always has to be used between the live measurements.
- The shape of the gas sampling duct and its track onto the sensor, together with the damping chamber is important for the speed of measurement and its stabilization time.
- When selecting critical components like filters and pumps, the most economically-sound results were obtained using pneumatic trap chamber directly attached to the measuring points on the membrane wall and a set of two MINDMAN filters 40 µm and 5 µm, in combination with THOMAS pumps without rotating elements.
- For long-term work of the analyzer, it is fundamental to compromise between the measurement time (extracting the gas sample), time of purging and idle operation in order to stabilize the system. The right compromise will give sufficient accurate measurement and long life of the analyzer and measurement sensors in particular.

Too short a measurement time is not adequate, because stabilization is insufficient and the average measurement result could be statistically unsound. Too long a time is also detrimental contributing to the increased overall wear and tear, because the analyzer, pump and filters are operating excessively.

Long purging time is undesired for zirconium sensors (causing excessive cooling, thermal stress and hence cracking of the sensor body itself), as well for pumps and filters, resulting in more frequent revision. Too short a purging time can result in clogging of the measurement duct.

Another significant advance was achieved in the application of the zirconium sensors. Recommendation is to use zirconium sensor in the analyzer alone, without the electrochemical CO sensor. The addition of the CO sensor requires the analyzer to be adapted and equipped with electric and electronic interface for electrochemical sensors. The use of O₂ zirconium sensor alone simplifies the analyzer and decreases costs significantly. In such case CO can be assessed reliably by deployment of neural network (ANN) based on the O₂ concentration measurement reaching a satisfactory overall Mean Square Prediction Error (MSPE) of 15%.

In the course of the long-duration tests it was found, that the measurement of CO concentration can be valuable for situations when low O₂ concentrations occur together with low CO concentrations and risk of corrosion is not so evident. Adding a CO sensor does improve credibility of the results, but is associated with higher investment in the hardware and the exploitation costs.

Steam flow meters.

NISTFLOM sensors were demonstrated successfully on full-scale. The sensors are based on a novel approach to correlate heat transfer from a steam pipe to the sensor with the actual steam flow in the steam pipe. The latter information - in conjunction with simple temperature and pressure

measurements - can be used to monitor the heat uptake of individual steam pipes or whole tube banks. While the sensors proved excellent long-term mechanical and operational stability, it was found that lab-scale calibrations cannot be used for full-scale measurements directly, i.e. no quantitative information of the steam flow could be derived. Furthermore, a slight signal drift was observed during the course of operation. The latter was caused by the formation of a porous layer of magnesium oxide on the surface of the adapter plate due to segregation of magnesium from the used aluminum alloy. However, despite these setbacks, it was demonstrated that normalized steam flows can be monitored reliably. The latter are sufficient for the implementation of a smart soot blowing strategy. In order to be able to perform quantitative measurements, a number of necessary changes to the sensor platform were identified. This includes the production of aluminum adapters from pure aluminum (1000 series alloys), the controlled formation of sufficiently strong passivation layers on both the sensor body and the adapter plate surface that can withstand the conditions present in power plant heat exchangers and a better thermal insulation of the cooling air supply to prevent excessive heating up of the cooling air before it reaches the sensor, resulting in the loss of measurement sensitivity.

Summarizing the above conclusions, it should be underscored that specific measuring devices were developed during the CERUBIS project, matching in full the specific features of the pulverized-coal-fired boilers and working in a fully automated manner. This applies namely to all the gas analyzers adapted for the measurement within the combustion chamber, the tested resistivity-based corrosion probes and the global evaporator wall measurement, as well as the non-invasive steam flow meters. Long term investigations in both power plant, in particular in the OPP, confirmed the reliability of these devices, each within its own unit operations limits, as well as integrated into the CIBOP diagnostic platform. Such devices, ready for installation on the boiler and equipped with unique features integrated into the CIBOP system, were not available on the market prior to the completion of the CERUBIS project.

Moreover, when comparing prices of the gas analyzers developed within this project to similar commercial equipment, with similar analytical features and sensitivity, it can be concluded that the newly-developed product is nearly 50 % less expensive. At the same time, the newly-developed analyzers are much more fit for the purpose of in-boiler, hot, raw flue gas quality monitoring, when compared with the reference Siemens analyzers, typically used for cooled flue gas quality monitoring.

Besides the achieved technical progress, the knowledge gained in the project enables the estimation of costs of components of sensing systems and whole diagnostic system CIBOP and their exploitation costs, which was used in the economic analysis.

The developed measuring systems can be used successfully in pulverized-coal-fired boilers, each for its own scope of analyses. The corrosion rate and concentration of gases can be assessed for each location separately and in real time. Integrated in CIBOP system (vide infra) the overall information on O₂ and CO concentrations and the steam flow can be monitored on-line and in real-time as soon as the appropriate analyzers/sensors are installed, while the corrosion rate in mm/y using the corrosion probe and CMS give a valuable long-term behavior insight.

Furthermore, it was demonstrated that training the ANN Artificial Neural Network (vide infra) systems based on data from in-boiler raw flue gas compositions can be done in a very cost effective way using the newly-developed, affordable measurement units, instead of laborious and discontinuous diagnostic methods used currently.

Another important lesson learned from the work performed is that set of the training data should include also some additional essential data from the boiler control system DCS like boiler load, air distribution and load of coal feeders, and not only from O₂ and CO sensors.

Good results were achieved in the project for 47 data sets (15 inputs for each data set) for BPP boiler and 24 sets (16 inputs for each data set) for OPP boiler respectively.

The project also explored the possibility of replacing labor-intensive and hence costly investigations in the power plant by Computer Fluid Dynamics (CFD) modelling. To date, the use of CFD does not always yield satisfactory results, especially in terms of the determination of O₂ and CO concentrations in the wall layer of the combustion chamber of a typical pulverized-coal-fired boiler. Despite significant effort invested into both grid optimization and appropriate definition of all variable in several models and runs, it proved almost impossible to obtain quantitative results similar to the actual measurements in the boiler. Nonetheless in the case of OPP qualitatively good results were achieved. The OPP example shows that the use of CFD data may be acceptable for ANN training in terms of O₂ and CO prediction in the wall layer. It was demonstrated that by using such carefully constructed and externally validated CFD model results a decrease in ANN verification errors (MSPE) can be obtained, reaching for O₂ from 7.53 to 5.98 and for CO from 7.14 to 4.17. These results were reached when using additional 11 variants received from CFD modelling in combination with 24 real-scale variants from boiler measurements.

The use of CFD modelling may hence indeed limit the minimum required volume of in-boiler characterisation in order to get enough operation cases for training of ANN, which significantly reduces costs.

A great achievement of the project is the development of a method for the determination of the corrosion rate on the entire surface of the walls of the boiler's combustion chamber. This is based on real-time measurements of O₂ concentrations only at several measuring points per wall. The method requires simultaneous, longer (several months, yet not further verified by physical measurements of the wall material thickness) measurements of the corrosion rate and O₂ concentration in the combustion chamber in at least two locations with different oxygen concentrations.

Based on the results of the measurements, the corrosion model was developed in the form of functional dependencies of corrosion rate on the concentration of oxygen averaged for the entire measurement time. Such a functional representation allows for the prediction of the corrosion rate anywhere in the boiler wall, as long as oxygen concentration is known there. This method is applied on the CIBOP platform, which uses the idea of matching the quick indirect gas analysis with slow direct measurement of the corrosion rate.

The calculation of the corrosion rate for the entire wall surface of the boiler was done by CIBOP subroutine, using O₂ concentration data gathered by CIBOP during a half year campaign and CMS model and the corrosion probe models calibrated according to above mentioned method during this campaign.

In contrast to the purely statistical/signal-based method described above, yet another method for the determination the corrosion rate was also tested. This particular method was depending on the local O₂ concentration in relation with the results of periodic measurements of pipe thickness loss in the boiler. This model was then fed with O₂ concentrations calculated and averaged by CIBOP for the period of the half year measuring campaign. This has been also implemented into CIBOP as an O₂ model, which gave also reasonable agreement with the real-life verification data

Another central aspect of the CERUBIS project was the development of software based on Artificial Intelligence (AI) algorithms and creating an intelligent system for data processing and interpretation. This software interface together with the earlier described sensing systems, forms the main deliverable of this project, namely the integrated boiler diagnostic system called Common Intelligent Boiler Operation Platform – CIBOP.

Artificial Neural Networks (ANN) are successfully used in utility boilers since several decades. The existing systems are commonly applied for NO_x reduction optimization and occasionally for the optimization or heat exchanger cleaning. The newly developed CIBOP system follows the same mechanistic approach, but reaches out further by incorporating corrosion, slagging, and fouling effects next to the commonly used tasks as well, forming a more complete diagnostic system with which utility boiler operation can be optimized automatically.

CIBOP is hence a sophisticated diagnostic system enabling continuous and long-term monitoring of boiler corrosion and slagging risk. CIBOP consists of:

- Measurement devices of different types installed in the boiler, i.e. different types of sensors with all necessary auxiliary equipment, each of which forms a separate sensing platform usable for diagnostics within its own analytical boundaries.
- Data acquisition system for each measurement platform.
- Data acquisition system collecting selected data from the power plant DCS system.
- Dedicated software for analysis of the acquired data and further translation to information displayed at the dedicated Graphical User Interface (GUI), directly usable for boiler operators, boiler maintenance and analytical equipment servicemen.

The overall operating strategy of CIBOP is as follows:

- Initially, CIBOP collects signals from all different implemented sensors, subsequently checks their credibility (measurement accuracy module is a part of the intelligent diagnostic system) and archives them for further use. This data relates to the current state and place in the combustion chamber where the individual sensors are located.
- CIBOP also collects the boiler's operational data at the same time, on the one hand to monitor its operation, but also to provide additional data for use by smart software included in the system.
- Thanks to the use of Artificial Intelligence (ANN and GA – hence the name CIBOP - Common Intelligent Boiler Operation Platform), the diagnostic platform software processes data from the sensors and the boiler into useful information for the visualisation of the current and predicted status of the boiler combustion chamber.

Admittedly, not all integrations were fully realised within the project duration. Such was the case with the NISTFLOM system as the steam flow meters signals, were recorded diagnosed, and displayed, but not further integrated into predictive and decisive CIBOP routines. This mostly in view of the signal drift issues and lack of quantitative translation of the signal into the actual stem flow at the time. Nevertheless, it was demonstrated that normalized steam flows can be monitored reliably. The latter are sufficient for the implementation of a smart soot blowing strategy in future applications.

Within the project duration, there was no possibility of a direct (on-line) interpretation of resistance measurement signals (CMS and the resistivity-based corrosion probe) in the form of the rate of loss of pipe thickness. This proved impossible due to the nature of the signal, i.e. very slow change over

time. These signals are diagnosed, displayed and recorded for subsequent processing and development or updating corrosion models.

Despite the shortcoming described above the current developed diagnostic system has a number of very useful functionalities that allow for:

- The assessment of the risk of corrosion and the rate of loss of the thickness of the tubes for the entire walls of the boiler combustion chamber (i.e. not only locally within the sensors operating area) based on the method previously presented, using the historical data collected by the system from gas concentration sensors,
- The prediction of the values of the above-mentioned variables forward for the specified time horizon for the existing parameters of operation of the boiler or parameters optimized according to the indications of the optimizer,
- The optimization of the operation of the boiler, i.e. CIBOP proposes recommended air flow distribution to the boiler in order to simultaneously minimize NOx emissions and corrosion hazard of the walls of the combustion chamber.
- The assessment of the slagging risk, based on boiler operating data and detailed actual composition of the current fuel blend, including the effect of the slagging phenomena on the temperature of the exhaust gases at the furnace exit (FET). This is one of the crucial diagnostic parameters important used for the assessment of heat exchanging efficiency throughout the boiler. Thus, it gives the possibility to select fuel or blends of fuels for the boiler targeted to limit the formation and deposition of slag, which also may have an impact on the rate of corrosion.

The use in CIBOP long-term corrosion measurement methods combined with artificial intelligence methods and the expert "know-how" gained during the project, gives reliable results not only in sensor locations, but also on the entire evaporator wall, which has not yet been the result of any other R&D project in coal-fired systems.

The method becomes fully on-line in terms of corrosion rate measurement within the first few months of the use of the system, when the first changes in resistance are reliably detectable. On the other hand, the system measures in real time and immediately after launch the concentrations of O₂, CO which together with the historical measurement of thickness loss evaporator screens tubes can be used to estimate indirectly the actual corrosion rate, even before statistically-sound data are obtained from the resistive-based measurement.

The integral CIBOP system was implemented on two different large utility boilers (hard coal and lignite fired) and operated for a six month period. It should be stressed that despite some periodic failures of certain components of the CIBOP system during its half-year operation, the overall CIBOP measurement accuracy module worked correctly. For example, prior to the gas analyzer failure, its first signs were correctly observed and identified by the system, e.g. reduced flue gases flow in the analyzer or increased pressure of purging air (as a rule, more than 0.5 bar). Such information is very valuable for timely system maintenance.

Moreover, for O₂ and CO measurements, it was observed that when the DCS measurements were less reliable due to components failure, the predictive value developed by CIBOP using the ANN routine deviated from the actual verified one by approximately 0.5 % vol. CIBOP develops the predictive values based on the collected historical data, current DCS data on air flow and load of carbon feeders and the trained relevant ANN.

When replacing uncertain measurement of CO, these differences were greater and for CO above 10% reached up to 1.5 %. However, as already mentioned, such an error did not have much impact on the risk assessment and the rate of corrosion. Independent on whether for 10% or for 11.5% or for even up to 15% of CO concentration in a layer, the risk of corrosion was estimated as very high and measured defects in wall thickness in these areas are similar to one another other (about 1 mm/year).

The measurements of the actual losses of the thickness of the membrane wall tubes in the tested OPP and BPP boilers were the reference point for the research methods and diagnostic systems developed in the project.

Although CIBOP operation were limited to half a year the calibration of its corrosion models was completed. The studies carried out made it possible to compare the corrosion rate determined by CIBOP according to the developed sub-routines (based on different inputs) with the actual rate determined on the basis of the aforementioned measurements of the thickness of the evaporator pipes. The corrosion rate values averaged for all evaporator walls as derived from CIBOP sub-routines are compared to averaged real values from the thickness loss measurements in the Tab. 2.22.

Tab. 2.22 Comparison of results of corrosion rate

BPP boiler	Real values	Corrosion probe model	CMS model
Average corrosion rate mm/year	0.02	0.08	0.02
Maximal corrosion rate mm/year	0.08	0.18	0.05
OPP Boiler	Real values	Corrosion probe model	CMS model
Average corrosion rate mm/year	0.1-0.22	0.17-0.23	0.43-0.72
Maximal corrosion rate mm/year	0.8-1.78	0.67-0.81	0.81-1.84

These results confirm in general a good alignment of the prediction of corrosion rate using long-term results from CMS and corrosion probe combined with the CIBOP software.

First of all, a right level of corrosion rate was obtained, which reflect situation in the boilers, i.e. almost no corrosion in BPP and relatively intensive corrosion in OPP.

Two values for each model in the case of OPP correspond to two extrapolation approach (linear and exponential). For CMS, good simultaneous compatibility of medium and maximum corrosion rate was not received. Better results were received for corrosion probes, but there in turn the maximum value is understated.

More accurate results using the methodology developed can be expected by using more corrosion probe or CMS measurements in the boiler in areas with significantly different average oxygen concentrations, which would allow for a better description of corrosion rate dependence on oxygen concentration. However, this is somewhat contrary to the idea of CIBOP diagnostic system, which is based on minimizing the number of measuring devices used. Each time a compromise should be sought between costs of the system and the credibility of its indications, keeping in mind potentially possible technical and economic benefits.

An important feature of the CIBOP system, either when integrated fully with the plant controls or **simply by using the parameters for aiding operator's decisions, is its possibility to reduce the** corrosion rate in the boiler by direct optimization of the boiler working parameters. Setting the boiler parameters according to CIBOP indications substantially decreases the averaged corrosion rates compared to operation of the boiler according to boiler DCS settings.

During the tests of this "Optimizer" feature in the BPP boiler, the corrosion rate was reduced 3 to 11 times, while maintaining the required NOx and CO emissions, and unburned carbon in ash by changing redistribution of air within the combustion chamber.

It was also demonstrated that it is feasible to reduce CO emissions (except for low-load variants), which may suggest that the redistribution of the air indicated by CIBOP improved the overall combustion efficiency in the combustion chamber. In several cases this was accompanied by measurable decrease of NOx emissions; the lowest obtained NOx emission was 140 mg/m³n for cases with intermediate-to-full boiler loads.

In practice, the air redistribution resulted mainly in increasing the amount of secondary air within the combustion chamber for specific, individual burner columns in operation (not all but only some of them involved) and decreasing amount of OFA air. In some cases however, the "Optimizer" suggested to increase slightly the total volume of air to the boiler, which unfortunately resulted in a decrease in the efficiency of the boiler (albeit due to pumping losses and larger loss in discharge flue gas and not due to poorer combustion). This was nonetheless not a subject of optimization within the CERUBIS project integration and tests. It was also observed that all CIBOP-optimized cases were characterized by less "false air", i.e. unwanted air leak into the boiler or improper mixing resulting in unused combustion air discharge in the flue gas, compared to the initial boiler operation.

These results were obtained in the real power plant right after starting work of the CIBOP "Optimizer", which is truly significant practical result, because of the substantial reduction in the risk of corrosion and with the concurrent NOx emissions reduction of up to 175 mg/m³n.

In the case of OPP, no full optimization was carried out on the boiler as in the case of BPP, but the **CIBOP "Optimizer" was started and its indications were analyzed.**

The indications included suggestion as to the burner zone air and fuel staging of the combustion process. For instance, for the best overall efficiency with the lowest emission while operating the boiler with three out of five mills, the CIBOP suggested to use the burner rows 1, 3 and 5, with the parallel increase of primary air to non-active burners in rows 2 and 4.

Such operation in partial load guaranteed the best protection of walls against corrosion, the smallest corrosion rate and NOx emissions below 200 mg/m³n.

Summarizing the conclusions concerning CIBOP:

- The assumed research methodology was confirmed to be able to deliver the right input data for the assessment of the processes in the boiler. While the detailed processes of corrosion or deposit formation may not be known in full detail as yet, the measurements of O₂ and CO in near-wall layer combined with the resistance measurements can give very good estimators of corrosion.
- The risk and the actual corrosion rate are determined/predicted by CIBOP for the entire walls of the combustion chamber. This is a very practical and usable result enabling to produce an assessment of corrosion rate in mm/year and not only an assessment of the corrosion risk.
- The use of CIBOP allows the plant operator to identify areas at risk of corrosion and can help in planning maintenance of the boiler on the basis of historical data collected during the operation of the system in the boiler where it is installed.
- CIBOP allows also to predict the impact of the change in boiler operating parameters on the future corrosion rate in different time horizons as well as to optimize boiler operation for limitation of the corrosion rate as well the flue gas emissions.

- A reliable and continuous determination of corrosion rates and spatial distribution of corrosion affected areas offers the greatest added value for power plant operations. The integral CIBOP system and each part of it separately, can readily be installed at utility boilers on a commercial basis, however the full economic evaluation could not be provided, within the limited time span and the extend of the integration of the CIBOP in the two power plants Nevertheless, the evidence was generated that CIBOP is capable of reducing potential corrosion and better predict its course, making it possible to plan maintenance shutdowns, before emergency situations arise.

2.5 Exploitation and impact of the research results

Exploitation of the results.

The consortium conducted a high-tech research project with reasonable and promising results. The important fact is that the project was created to meet demand from power plant services, which were recognised by the consortium. This was also confirmed by the participation of PGEGIEK in the consortium, which also made its boilers available for experiments and CIBOP implementation.

The results of the project, i.e. the CIBOP diagnostics system, can solve two problems with regard to the boiler corrosion/sludging phenomena:

- unplanned outages of boilers due to tube faults (in such case at least 72 hours out of operation),
- necessity of exchanging the water walls of evaporators or covering them with very expensive coatings.

The consortium as a whole created an effective approach to: investigate, determine, control, and finally eliminate the corrosion/sludging issues in base load coal fired boilers.

The whole development effort, knowledge and expertise were linked in one product – the Common Intelligent Boiler Operation Platform – CIBOP, which was successfully tested through a half year in two utility high capacity boilers. The consortium estimates that – for the CIBOP – TRL on level 8 was achieved. At the beginning of the project the TRL of the diagnostic system was between 3 and 5 depending on the particular method.

Extensive and fully elaborated methodology for determination of low O₂ corrosion/sludging using CIBOP is ready for use in other power plants as a commercial system.

This methodology includes the following subsequent steps:

Analysis of boiler operating data together with analysis of historical data related to the tube thickness loss caused by corrosion. If no loss is observed, there is no corrosion risk and periodical checking of the thickness of the tubes is sufficient.

If there are reasonable tube thickness losses, the following actions are envisaged:

- 1) Multi variant boiler investigation (at least 30 cases) in different boiler conditions gathering data for CFD modelling and O₂ and CO concentration for ANN learning. Optionally 1 to 2 months' measurements with a corrosion probe assisted with local O₂ concentration measurement.
- 2) Analysis of the data and additional CFD simulations.
- 3) Development of the CIBOP concept depending on preference of the client and the risk of corrosion. O₂ sensors on their own make it possible to estimate the corrosion risk, or alternatively the full system with resistance measurements and corrosion probes. A decision must be taken on the number of different sensors and their deployment. The minimum is four O₂ sensors for each wall and two resistance measurement units located in an area of different O₂ concentration.
- 4) Assembly of the system
- 5) Adaptation of the CIBOP software and teaching the ANNs.
- 6) Running the system.
- 7) Yearly review and verification of the system and replacement of spare parts.

Besides the whole system, particular individual measurement devices were developed in CERUBIS to a level enabling them to be offered on the market.

An especially big step forward was made in direct measurement of the corrosion rate, i.e. electric resistance measurement of evaporator walls and the corrosion probe. The partners involved – HF and PWR – started from TRL 3 and through the four years of the project developed the professional systems, tested in extreme boiler conditions for months or even years in some cases, finally reaching levels TRL 7 and TRL 8 respectively.

HF also obtained a side product, namely a temperature measurement system for steel (boiler) tubes, which was necessary for the developed resistance measurement system. The product is called the Tube Temperature Measuring System or TTMSYS and is ready for commercial deployment (TRL 9). Other developed techniques started from TRL levels 4-5 and were finished at levels 7-8. They are all listed in Tab. 2.23, where their readiness for implementation is indicated and further R&D needs are mentioned.

All these products performed in full-scale, real life boiler environment conditions and were successfully tested and verified over extended periods.

Tab. 2.23 List of CERUBIS project physical products, their TRL levels at the starting and the end of the project, with projected further development indication

Product	Partners	Readiness foreground (Background)	Further development or research needs	Description
CIBOP	IEN (All)	VIII (IV)	Yes	Common Intelligent Boiler Operation Platform
GAN	IEN	VII (III)	Yes	Gas Analyser
CPO2	PWR	VIII (III)	Yes	Corrosion Probe with O ₂ measurement
LOCMS	IEN&PWR	IX (VII)	No	Low O ₂ corrosion monitoring system (O ₂ /CO gas analysers + Rachel with O ₂ corrosion rate model)
TTMSYS	HF	IX (VI)	NO	Tube temperature measuring system
CMC (TCORSYS)	HF	VII (III)	Yes	TCORSYS-new commercial name of the product) – Corrosion Monitoring System
NISTFLOM	TNO&HF	IX (V)	Yes	Steam Flow meters

Application readiness of the system or its parts had been already confirmed to some extent by interest from potential users. IEN and PWR were invited three times to make an offer for a corrosion monitoring system in three Polish Power Plants: Opole Power Plant (new units 5 and 6), Łagisza Power Plant and Bełchatów Power Plant. In the case of the Opole Power Plant a tender was announced in which IEN participated, but failed to win (around 210 000 EUR was estimated for O₂/CO monitoring for each of two boilers). In the Łagisza Power Plant a new evaporator was finally covered by coatings and the diagnostic system was deemed not necessary. In the case of Bełchatów Power Plant the system was partially installed.

Looking at the supplementary research needed to improve the commercial offer of the consortium, its partners declare themselves willing to seek financing for a new project where all CERUBIS products could be moved into TRL 9 level. The new project would focus on superheaters and the convective area of the boiler as well as flexibility issues. It was recognised that the most sought-after product for power plants is a system to predict tube failures (due to corrosion, erosion, slagging, thermal tension etc.). A properly-functioning system could save yearly up to 1-2 million Euros per boiler.

Project impact

Despite EU decarbonisation policy, coal fired power plants will remain important source of energy for years to come, at least in some countries.

These power plants will work in difficult operation conditions and they will need more diagnostics and more sophisticated diagnostic systems. After the CERUBIS project some ready solutions can be offered to them. Distribution of the results of the project among potential users increased awareness and led them to consider alternative ways to protect boilers against low O₂ corrosion. Some techniques covered by the CERUBIS project, like O₂/CO measurements are already included as required equipment for newly-designed boilers. Diagnostic methods are also compared with other anti-corrosion approaches.

The application of research and technological results of the project should decrease the cost of energy production in EU power plants due to decreased frequency of emergency outages, better scheduled evaporator maintenance and fewer replacement of water walls tubes. Financial concerns will determine the outcome in power plants with high corrosion rates as to whether a CIBOP or special coatings approach should be selected.

3 List of figures

1.1	Sensor platforms deployment in boiler no. 5 in BPP	10
1.2	Sensor platforms deployment in boiler no. 3 in OPP	10
1.3	Sensing systems in BPP and OPP – overview chart does not include real numbers of sensors or their location	11
2.1	Deposition rates and collection efficiency at levels 11 and 21 with deposition probes in USTUTT 0.5 MW test rig	21
2.2	View of the combustion chamber of boiler no. 5 in BPP with location of some measurements	22
2.3	View of the combustion chamber of boiler no. 3 in OPP	24
2.4	Development chart for gaseous sensors and probes	26
2.5	View of the typical connector with zirconium O ₂ probe (left) and the new design (right)	27
2.6	Gas analysers designed and manufactured in the CERUBIS project: type 1 (left) and type 2 (right)	28
2.7	Schematic diagram of the corrosive ring (sensor) on the probe	28
2.8	Schematic diagram of the measurement principle, resistance is measured between the points 15/16 and 17/18. Wall temperatures are also measured at the connection points	29
2.9	First and second prototype for laboratory tests and CMS control box	29
2.10	The ultrasonic method of online wall thickness measurement	30
2.11	Schematic diagram of the NISTFLOM sensor	31
2.12	Sensor platforms deployment in boiler no. 5 in BPP	35
2.13	Sensor platforms deployment in boiler no. 3 in OPP	36
2.14	Sensing systems in BPP and OPP – an overview schematic not including real numbers of sensors or their location	38
2.15	Conceptual chart of CIBOP working principles	40
2.16	General block chart flow scheme of sensor indications for corrosion (left) and slagging (right) assessment	41
2.17	Average and maximum rates of evaporator's wall thickness loss for all walls 2010-2017 during operation of boiler no. 3 in OPP	44
2.18	Gas analysers mounted in OPP (left) and BPP (middle). Location of adapter (zirconium O ₂ sensor) in the evaporator wall (right) in the direct vicinity of the two NISTFLOMs	45
2.19	Installed wall resistance measurements (CMS) in OPP (Opole 1) mounted on 28 m front wall (left) and (Opole 2) mounted on 23 m right wall (middle), CMS installed in BPP mounted on 36m right wall (right)	46
2.20	The resistive corrosion probes located in OPP at level 30 m on the front wall OP1 (left) and on the right wall OP2 (middle), the corrosion probe located at level 27 m in the right wall in BPP (right)	46
2.21	NISTFLOM sensors installed in OPP on the evaporator's right wall at level 30m (left) and on superheater tubes rear wall at level 60 m (middle), NISTFLOM sensors installed on superheater tubes, front wall at level 60 m at BPP (right)	46
2.22	Electric power for units of boiler no. 5 in BPP (left) and of boiler no. 3 in OPP (right) through 0.5 year work of CIBOP systems	47
2.23	Online resistance measurement setup with four connection points to the boiler wall	47
2.24	Normalised resistance measurements and calculated remaining wall thickness as a function of time for OPP and BPP	48
2.25	Extrapolation of the corrosion rate for CMS and corrosion probe experimental results	50
	Half-annual averages of operation maps of O ₂ concentrations (%) in the boundary layer	
2.26	for all four walls in boiler no. 5, BPP (taken directly from CIBOP, view from outside of the boiler)	51
	Half-annual averages of operation maps of the rate of wall thickness loss (mm/y) for all	
2.27	four walls in boiler no. 5, BPP (taken directly from CIBOP, view from outside of the boiler) – O ₂ Model	51
	Half-annual averages of operation maps of O ₂ concentration (left), the risk of corrosion	
2.28	(middle) and the rate of wall thickness loss (right) for right wall at boiler no. 5, BPP (taken directly from CIBOP) - CMs Model	51
2.29	Extrapolation of the corrosion rate for CMS: linear (left) and exponential (right)	52
2.30	Extrapolation of the corrosion rate for the corrosion probe: linear (left) and exponential	52
	Half-annual averages operation maps of O ₂ concentrations (%) in the boundary layer for	
2.31	all four walls in boiler no. 3 in OPP (taken directly from CIBOP, view from outside of the boiler)	54
	Half-annual averages of operation maps of the rate of wall thickness loss (mm/y) for all	
2.32	four walls in boiler no. 3 in OPP (taken directly from CIBOP, view from outside of the boiler) – O ₂ model	54
2.33	CAPEX + OPEX cost for the different scenarios of protection of boiler no. 3 in OPP against low O ₂ corrosion	57

4 List of tables

1.1	Overview of methods and sensors investigated in WP2	9
1.2	Measurement devices installed in the boilers	9
2.1	Overall matrix of pilot scale investigations and fuel/ash data of investigated fuels; (✓ – carried out, X – not carried out)	20
2.2	General matrix for all full scale measurement campaigns (✓ – carried out, X – not carried out)	21
2.3	General data for the measurement campaign in BPP in 2015	23
2.4	General data for measurement campaign in OPP in 2016	24
2.5	Overview of methods and sensors investigated in WP2	25
2.6	Main specification of gas sensors	27
2.7	Sensor platforms defined/further developed in CERUBIS project	32
2.8	Schedule of the investigations carried out at the IEN 0.5 MW test facility	33
2.9	Schedule of the investigations carried out at USTUTT 0.5 MW test facility	33
2.10	Evaporator walls thickness loss rate in boiler no. 3 in OPP	44
2.11	The measurement devices installed in the boilers	45
2.12	Fit results for CMS in OPP and BPP	48
2.13	Results of the corrosion probe tests in BPP	48
2.14	Results of the corrosion probe tests in OPP Overview of averaged concentrations of O ₂ and CO in the boundary layer of the evaporator and the rate of wall thickness loss calculated on the basis of O ₂ , CMS and corrosion probe approaches over 0.5 year of operation of boiler no. 5 in BPP	49
2.15	Overview of averaged concentrations of O ₂ and CO in the boundary layer of the evaporator and the rate of wall thickness loss calculated on the basis of O ₂ , CMS and corrosion probe approaches over 0.5 year of operation of boiler no. 3 in OPP	50
2.16	Real averaged corrosion rates determined for two periods, boiler no. 3, OPP	53
2.17	Results of the optimisation of boiler no. 5 in BPP using CIBOP optimisation module	54
2.18	CAPEX for 3 different scenarios of boiler operation with regard to low O ₂ corrosion for the next 12 years	55
2.19	Main assumptions for techno-economical calculations with regard to CIBOP OPEX	56
2.20	Comparison of CAPEX and OPEX for two CIBOP configurations	56
2.21	Comparison of results of corrosion rate	64
2.22	List of CERUBIS project physical products, their TRL levels at the starting and the end of the project, with projected further development indication	66

5 List of acronyms and abbreviations

CERUBIS project partners	
IEN	Institute of Power Engineering – Leader of the Project
USTUTT	IFK, University of Stuttgart – project partner
TNO	the Netherlands Organisation for Applied Scientific Research TNO – project partner
HF	Huxeflux Thermal Sensors B.V. – project partner
PGE GIEK	PGE Mining and Conventional Energy JSC
PWR	Wrocław University of Science and Technology – subcontractor of IEN
AI	Artificial intelligence
ANN	Artificial neural network
BPP	Bełchatów power plant
CAPEX	Capital expenditures
CFD	Computer fluid dynamics
CIBOP	Common intelligent boiler operation platform
CMS	Corrosion monitoring system
DCS	Distributed control system
EDS, EDX	Energy-dispersive X-ray spectroscopy
EGD	Ethernet global data
ES	Expert system
ETS	EU emission trading scheme
FTP	File transfer protocol
GA	Genetic algorithm
GUI	Graphical user interface
LOI	Loss of ignition
MSPE	Mean squared prediction error
NISTFLOM	Non-Invasive Steam Flow Metering

OFA	Over fair air
OPEX	Operating expenditures
OPP	Opole power plant
PID	Proportional-integral-derivative controller
PLC	Programmable logic controller
RFCs	Research Found for Coal and Steel
ROFA, ROFAMIX	Trade names of low NO _x emission combustion technologies
SEM	Scanning electron microscope
SNCR	Selective noncatalytic reduction
TA	Technical annex
TCP	Transmission control protocol
TRL	Technology readiness levels
WAN	Wide area network

6 List of references

- [1] Pronobis M., 2001. **Modernizacja Kotłów Energetycznych**, WNT, Warszawa (in Polish)
- [2] Kordylewski W. (Eds.), 2000. Niskoemisyjne techniki spalania w energetyce, Oficyna Wydaw. Politechniki Wrocławskiej, 2000 (in Polish)
- [3] Adamiec J., 2009. High temperature corrosion of power boiler components cladded with nickel alloys. Materials characterization, 60, 1093-1099.
- [4] Kruczak H., 2006. Effect Of Staged Combustion In Pct- Boilers On Rate Of Fireside Corrosion, 7th European Conference On Industrial Furnaces And Boilers, Porto Tuela – Portugal 18-21 April 2006.
- [5] Bryers R.W. 1996. Fireside slagging, fouling and high-temperature corrosion of heat-transfer surface due to impurities in steam-raising fuels, Prog. Energy Combust. Sci. Vol.22, pp.29-120, 1996
- [6] Pronobis M., Litka R., 2012. Rate of corrosion of waterwalls in supercritical pulverized fuel boilers. Chemical and Process Engineering, 33 (2), 263-277.
- [7] Pronobis M., Hernik B., Wejkowski R., 2010. Kinetics of low NO_x corrosion of waterwalls in utility boilers. Rynek Energii, 6 (91), 121-128.
- [8] Bukowski P., Hardy T., Kordylewski W., Evaluation of corrosion hazard in PF boilers applying the oxygen content in flue gases, Archivum Combustionis, Vol29, No1-2, 2009
- [9] Wejkowski R. et al. 2013. The control of high temperature corrosion phenomenon in boundary layer using different measurement methods, Modern energy technologies, system and units, Cracow University of Technology, Kraków 2013.
- [10] Kakietek S. et al. 2014. The on-line system for monitoring of low emission corrosion of water walls in the case of boiler no 5 in Belchatów Power Plant, 12th International Conference 4 on Boiler Technology 2014
- [11] Ostrowski P., Kalisz S., Wejkowski R. 2011. Investigations of low NO_x corrosion hazards in boiler op650 of the Rybnik power plant using a mobile monitoring system, Rynek Energii, nr 3, 2011
- [12] Hardy T., Kordylewski W., Thoma K., Kowalski M., Pietrzyk M., System do pomiaru stężenia tlenu w warstwie przyściennej ekranów kotła w celu kontroli on-line zagrożenia korozyjnego, Kontrola sterowanie i automatyzacja procesu spalania w kotłach energetycznych, Szczyrk, 4-6 czerwca 2007 (in Polish)
- [13] Sucharda E. 2013. Monitor warstwy przyściennej GM960, X S-T Conference - Materiały i technologie w modernizacji (in Polish)
- [14] Kakietek S., Golec T. 2007. Sztuczna inteligencja w eksploatacji i optymalizacji pracy kotła, Konferencja Eksploatacja maszyn i urządzeń energetycznych, Szczyrk 2007 (in Polish)
- [15] Deliverable 1.1, Circabc
- [16] Midterm Report, Circabc
- [17] Deliverable 1.3, Circabc
- [18] Deliverable 1.2-BPP, Circabc
- [19] Deliverable 1.2-OPP, Circabc
- [20] Deliverable 2.2, Circabc
- [21] Deliverable 2.4, Circabc
- [22] Deliverable 2.3, Cicabc
- [23] Deliverable 2.5, Circabc
- [24] Deliverable 3.3, Circabc
- [25] Deliverable 3.6, Circabc
- [26] Deliverable 4.2, Circabc
- [27] Deliverable 4.5, Circabc

7 Appendices

A1. The research stands used in the project

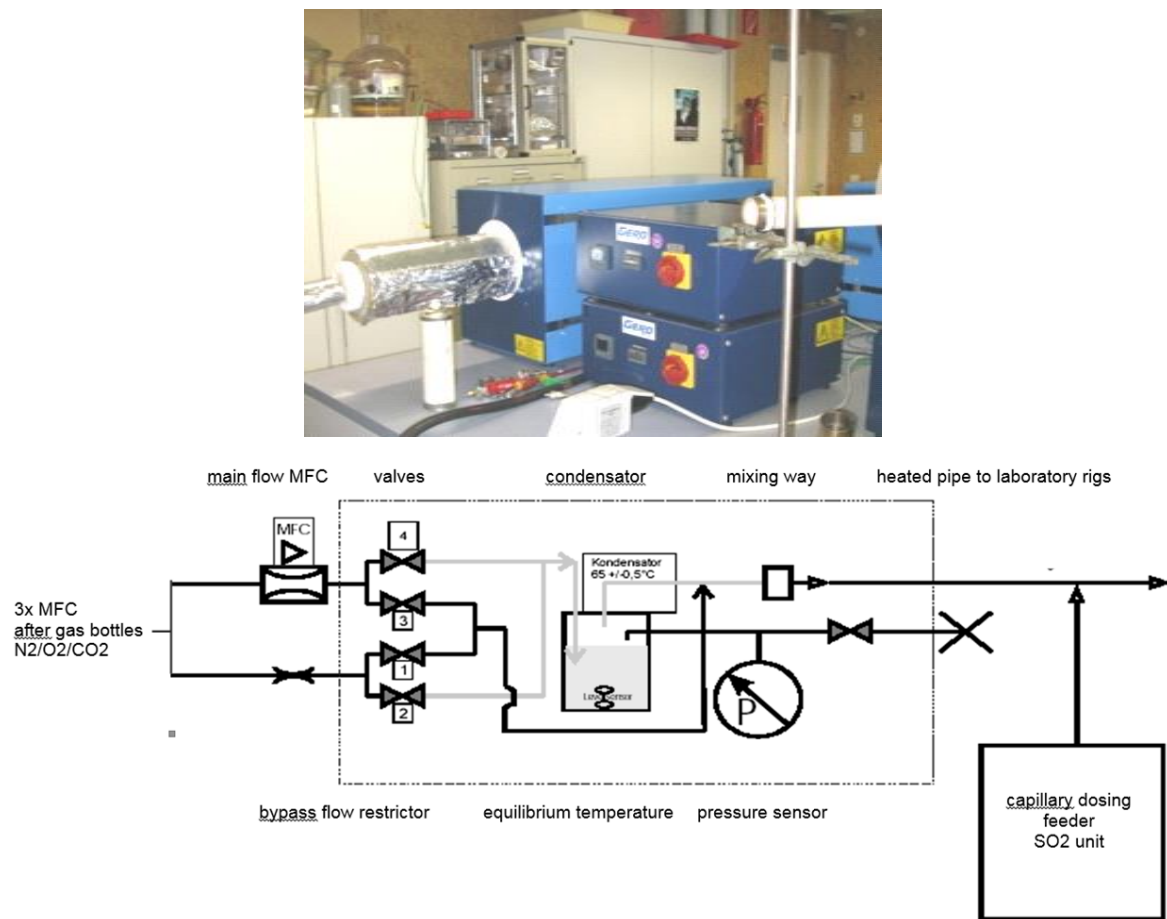


Fig. A1.1 General view and a schema of the USTUTT corrosion research stand.

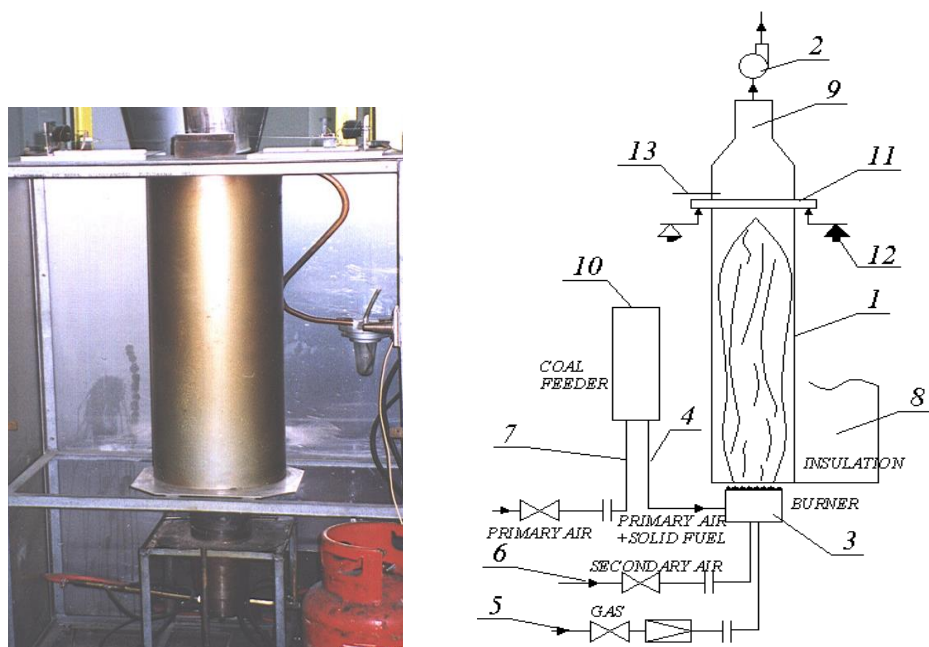


Fig. A1.2 General view and a schema of the IEN slagging research stand

The cylindrical ceramic combustion chamber (1) has inner diameter of 100mm. Flue gases leave combustion chamber (1) through exhaust fan (2). In the bottom part there is a flat flame gas burner (3). Through the axis of the burner solid fuel dust (4) is supplied into the combustion chamber. Gas

fuel (5) (propane) is mixed with secondary air (6) in the mixing chamber of the burner (3) and afterwards through stabilising cartridge gets into the chamber (1) where it is ignited. The gas burner (3) generates flue gases at the specific temperature and gas composition to make the ignition of solid fuel possible. By change of gas (5) or secondary air (6) the temperature of flue gases, excess of air, quantity of supplied heat into the chamber (1) and temperature at the outlet of chamber (9) may be controlled. The solid fuel is supplied through a coal dust feeder (10) which is used to change the fuel feed rate and quantity of primary air (7). About one metre from the front of the burner (3) there is a ceramic deposition pipe of 10 mm diameter (11) suspended on beams of the extensometer balance (12). The slag deposit bends the beams causing the resultant voltage, which is the function of mass increase of deposit pipe. The temperature of flue gases is measured close to deposit pipe by thermocouple (13).

IEN's slagging facility is oriented for investigations of pulverised solid fuel combustion. It is used to obtain solid fuel slagging properties for various temperatures of combustion. On the basis of experimental results, the beginning temperature of slagging (T_{beg}) and an indicator of slagging intensity (k_z) are obtained.

Investigations of solid fuels consist of burning samples of fuel with quantity of about 0.41-0.55 g/s (1.5 - 2 kg/h) in a preheated combustion chamber in suitable conditions that are variable during the duration of experiments (excess air, temperature) and in this way obtaining the rate of accumulation of slag for various temperatures and the beginning temperature of slagging.

T_{beg} and k_z , which are respectively, the beginning temperature of slagging and index of slagging intensity are determined by the following equations:

$$B_z = \frac{M_z \cdot F_k}{M_p \cdot F_r}$$

$$B_z = e^{k_z \left(\frac{T_{sp}}{T_{beg}} - 1 \right)} - 1$$

where:

B_z – relative slagging intensity,

M_z – collected mass of slag on deposition pipe [g],

M_p – mass of ash flown through the combustion chamber of the slagging test facility [g],

F_k – area of the cross section of the combustion chamber of the slagging test facility [m^2],

F_r – active area of pipe [m^2],

T_{beg} – beginning temperature of slagging [K],

k_z – index of slagging intensity

T_{sp} – temperature of combustion (e.g. T_{out}) [K].

A pilot scale facility of 0.5 MW in IEN is shown in Fig. A1.3 while Fig. A1.4 is a chart of the facility. Coal or biomass dust is introduced to the swirl burner located on the front wall by a primary, usually preheated, gas agent. A secondary gas agent is usually preheated to 315 °C. The secondary agent can be introduced to the burner by one or two ducts depending on particular needs. An OFA air can be introduced to the combustion chamber by three independent OFA nozzles 2 to 3 metres behind the burner.

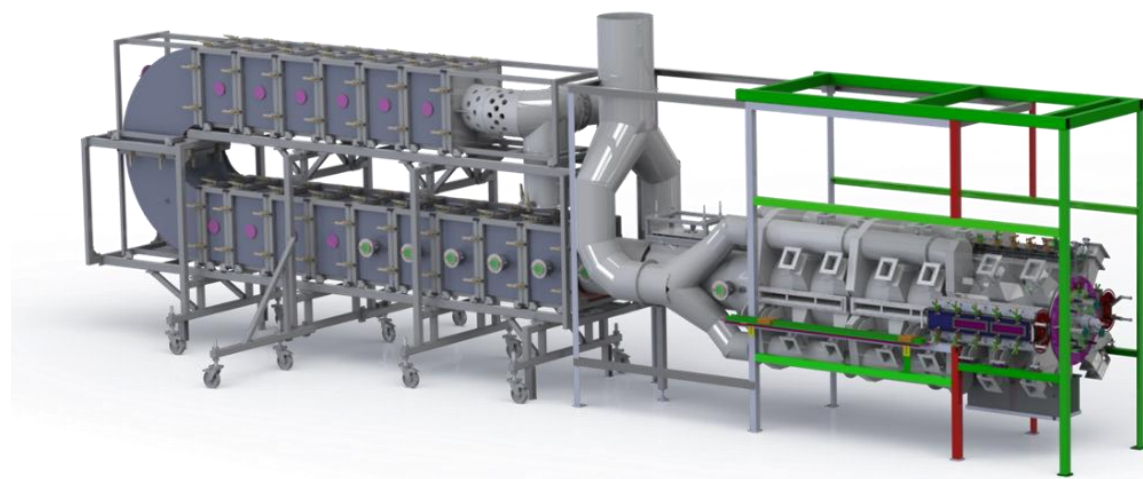


Fig. A1.3 General view of 0.5 MW pilot test stand in IEN

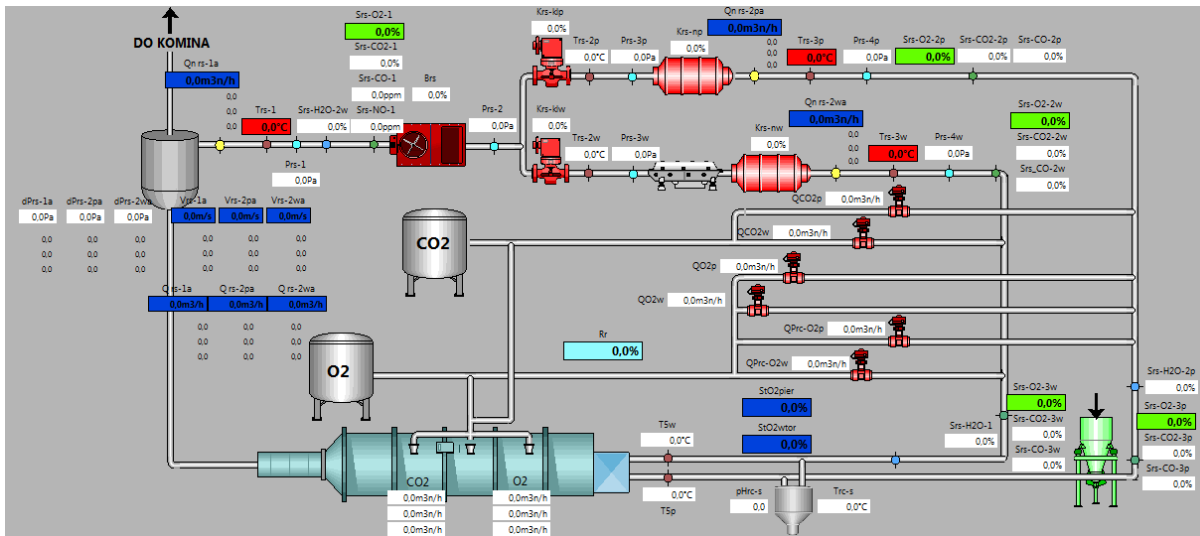


Fig. A1.4 Chart of the 0.5 MW IEN test facility



Fig. A1.5 Front view of the combustion chamber with and recirculation installation (left), investigated gas analysers (middle), and the corrosion probe (right) at IEN 0.5 MW test facility

The 0.5 MW pilot scale facility in USTUTT is shown in Fig. A1.6 while Fig. A1.7 shows a chart of the facility.

This is a top fired vertical combustion chamber constructed for combustion of pulverised solid fuels. The combustion chamber has a total length of 7,000 mm and an inner diameter of 800 mm. A refractory lining covers the inner surface of the upper segments of the combustion chamber to a distance of 4,000 mm from the burner. A water jacket is integrated into the double-wall of the reactor. Numerous measurement openings are integrated into the reactor wall with distances between each level of 150 to 170 mm. In several segments there are up to three ports per level, oriented at 90° to one another.

The ports for the selected sensor platforms shown in Fig. A1.6 were chosen relative to the desired temperature range and local excess of O₂.

A deposition rate probe which was schematically shown in the Fig. A1.8 has been used for determination of real deposition rate. The probe was exposed inside the burning chamber at a sub stoichiometric (level 11 in the Fig. A1.6) and over stoichiometric (level 21 in the Fig. A1.6) level.

The measured (real) deposition rate is calculated after the following equation:

$$\alpha_{tat} = \frac{\Delta M_{tat}}{A_{sonde} \cdot \Delta t} \quad \left[\frac{g}{m^2 \cdot min} \right]$$

with

ΔM_{tat} $\left[\frac{g}{m^2} \right]$ - real specific deposit mass

A_{sonde} $[m^2]$ - cross section of the probe

Δt [min] - corresponding period.

The theoretically possible deposition rate (maximum) is calculated by the following equation:

$$\alpha_{theo} = \frac{\dot{M}_A \cdot \gamma_A}{A_{DE}} \quad \left[\frac{g}{m^2 \cdot min} \right]$$

\dot{M}_A , $\left[\frac{g}{m^2 \cdot min} \right]$, ash mass flow per corresponding period, mean value

γ_A , [-] ash content in coal

A_{DE} , $[m^2]$, cross section of furnace.

The collection efficiency is $\xi = \frac{\alpha_{tat}}{\alpha_{theo}} [\%]$.

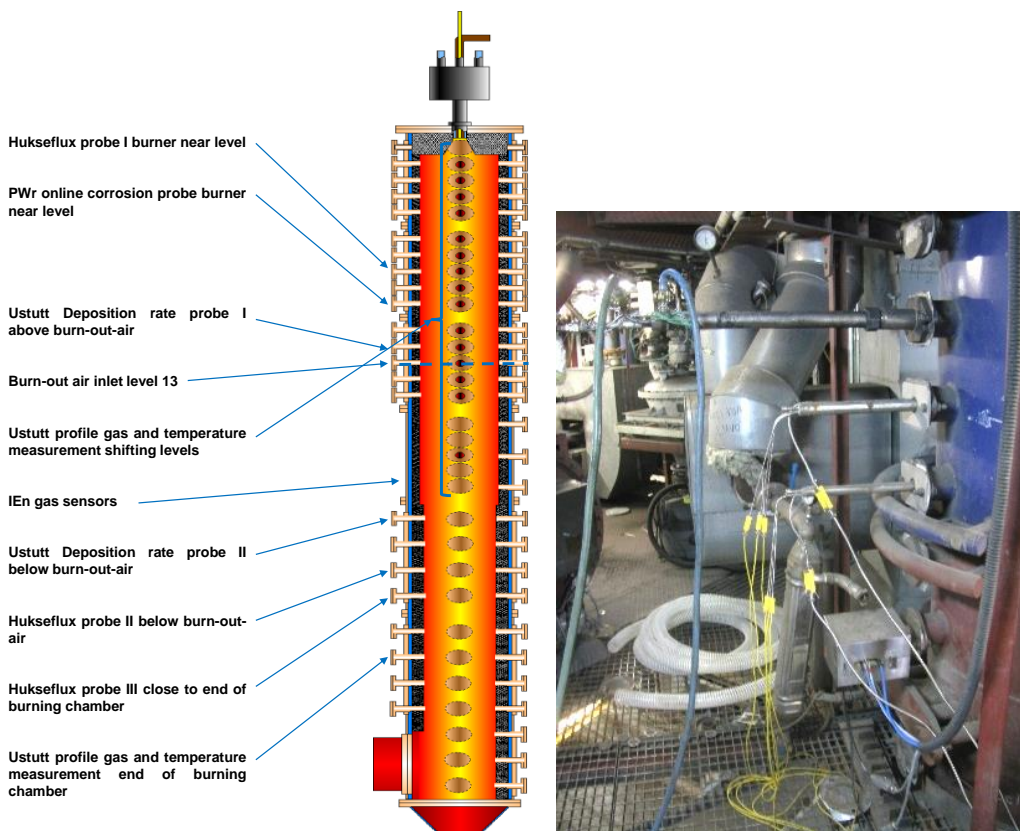


Fig. A1.6 Ports location of specific measure points (left) and deposition rate probe (right) in 0.5 MW USTUTT pilot scale research facility

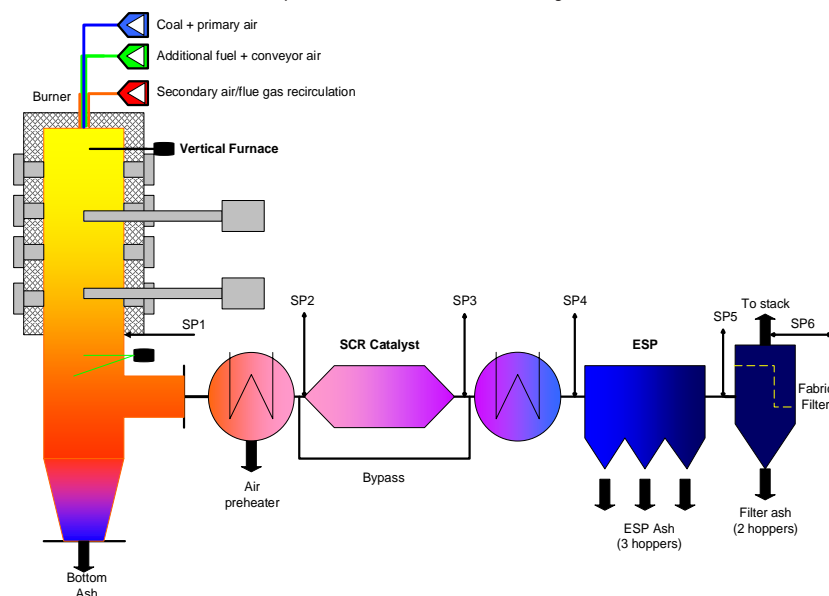


Fig. A1.7 Chart of 0.5 MW USTUTT down fired test facility

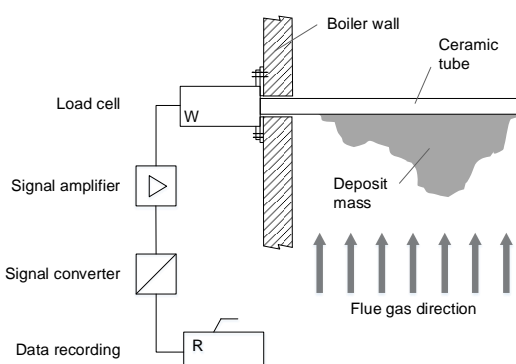


Fig. A1.8 Schematic diagram of the on-line deposition probe

A2 – Development of the gas analysers

Introduction

The corrosion hazard control system developed in recent years by IEN and PWR was based on the continuous measurement of O₂ concentration in the boundary layer by simple zirconium sensors. Many issues were encountered during the operation of this system such as clogging, poor reliability of zirconium sensors and of the whole system as well.

Appropriate selection of the gas sensors and the design of the measurement ports are crucial to reliable operation of the whole measurement system. Flue gas probes consist of flue gas sensors (zirconium) and suction-filtering systems, which are very important in light of the extreme utility boiler conditions.

The various gas sensors (O₂, CO, H₂S) and probe designs were developed and tested in laboratory, pilot and real scale conditions as part of the CERUBIS project. The measurement system with a suction pump and injector and various systems for the purification of flue gas were investigated too. Development of the gas analysers was carried out in two parallel ways, using continuous results from the ongoing research:

- creating a new generation having an O₂ analyser based on a zirconium sensor (O₂ type 1) with own control unit,
- creating from scratch a gas analyser with PLC controller able to work with different types of gas sensors, including zirconium sensor (O₂ type 2).

This appendix shows examples of works carried out and the results obtained.

The analyser with new control unit.

The assumption of building a new control unit/converter at least enabled the continuous measurement of two or three components of flue gases, additional monitoring of blowing air pressure, flue gas flow and enabled the use of automatic sensor calibration. Fig. A2.1 shows the chart of the analyser with new options. The general description of connectors in the new electronic control unit is shown in Fig. A2.2. An analyser based on the new electronic control unit (with 8 analogue inputs) was fabricated and is shown in Fig. A2.3.

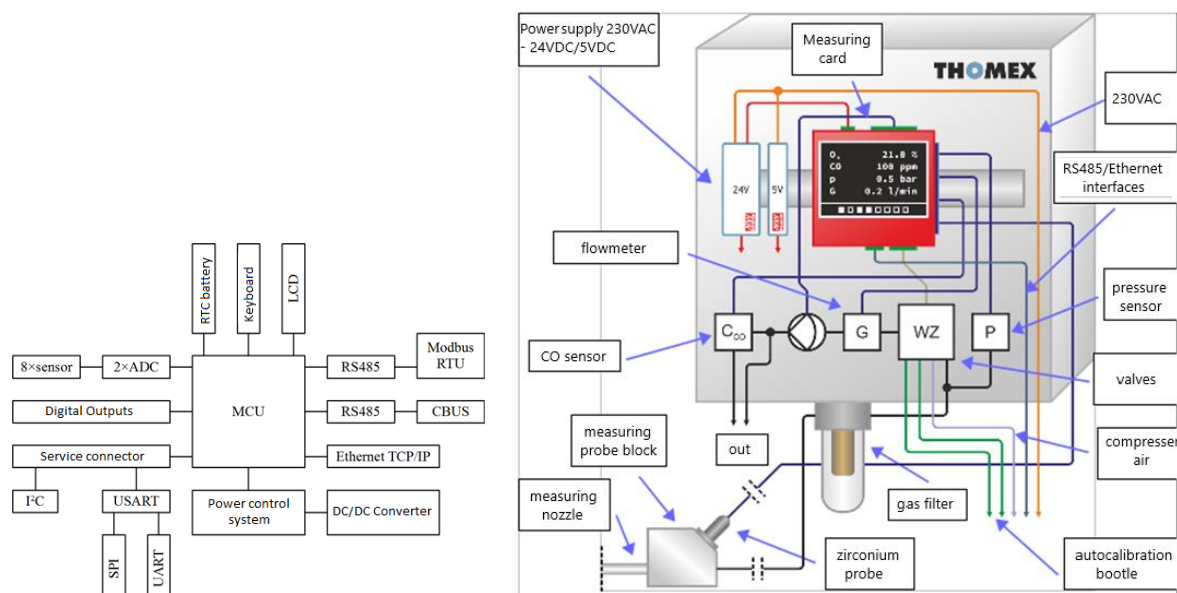
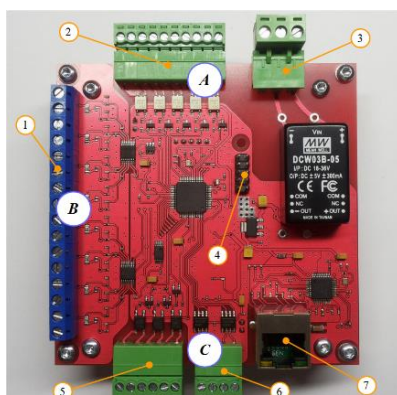


Fig. A2.1 Chart of the gas analyser (type 1) based on the new control unit



Description of configuration connectors	
Clamp	Description
1	analog input connectors
2	digital output connectors
3	power connection
4	servicing connector
5	digital output connectors
6	serial interface connector
7	etherent interface (MODBUS TCP/IP)

Fig. A2.2 New control unit specification



Fig. A2.3 View of the new measurement system with new electronic transducer

Diagnostics of the zirconium probe failures.

The development and laboratory tests carried out led to two diagnostic subsystems being proposed for the fault diagnosis of sensors. The first enables continuous measurement of internal resistance of the wide band zirconium probe, as shown in Fig. A2.4, whereas Fig. A2.5 presents the results of the operation of this subsystem.

The second one compares the sensor output with the desired value during the calibration process. If the difference is too high, **the sensor will be determined "with failure"**.

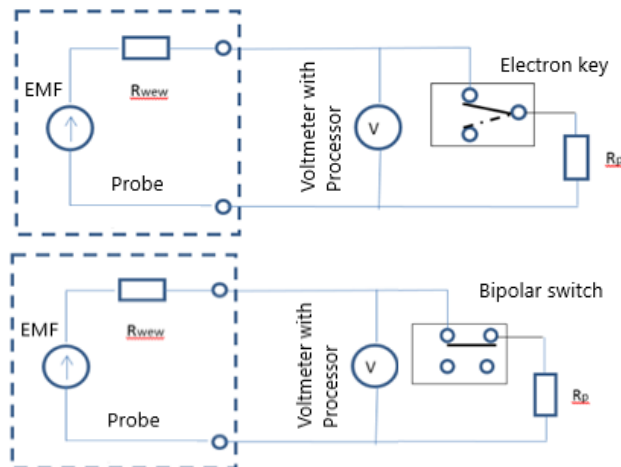


Fig. A2.4 Schematics of measuring systems for continuous and automatic control of internal resistance of the zirconium probe for implementation with FRT02 converter

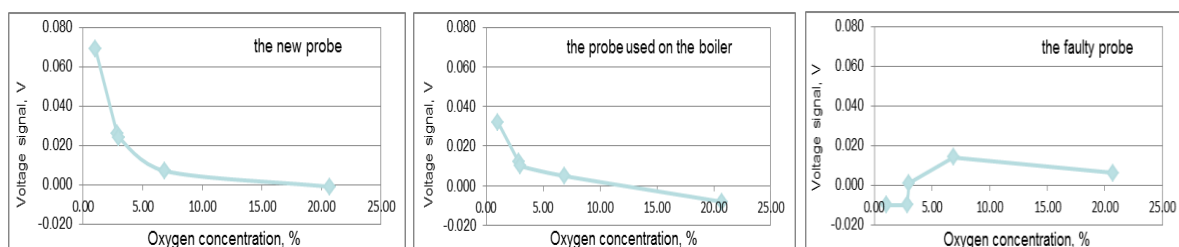


Fig. A2.5 Laboratory tests with the reference gases - detection of probe failure

Diagnostics of the pump and clogging of pneumatic path

One way to detect blockage of the pneumatic path (measuring port and/or pneumatic pipes) is by monitoring vacuum changes before the suction pump or changes in the load of the electric engine of the suction pump (current of the engine). In this example two types of suction pumps were tested in terms of impact of pneumatic pipe clogging on pump operation:

Schwarzer Precision SP600EC (12V, flow up to 3l/min, negative pressure 600mBar)

Thomas - type110 (230V, flow up to 4.3l/min, negative pressure 280mBar)

The first pump was used in the monitoring system in BPP, but quite rapid wear-out of pumps was observed. Therefore, a new pump was selected in the CERUBIS project. The impact of pneumatic resistance of pipes on the current of the pump engine is shown in Fig. A2.6. In the case of the

Schwarzer pump, when the resistance of flue gases flow increases, the gas flow decreases and a change in current can be observed. However, in the case of the Thomas pump with vibrating drive, the current is constant and this signal is not usable. It must also be underlined that the Thomas pump is believed to have a longer life span than the Schwarzer pump. For this reason an electronics flow meter to control the flow of gas sucked by the pump from the combustion chamber and pressure sensor to vacuum control was developed and successfully tested.

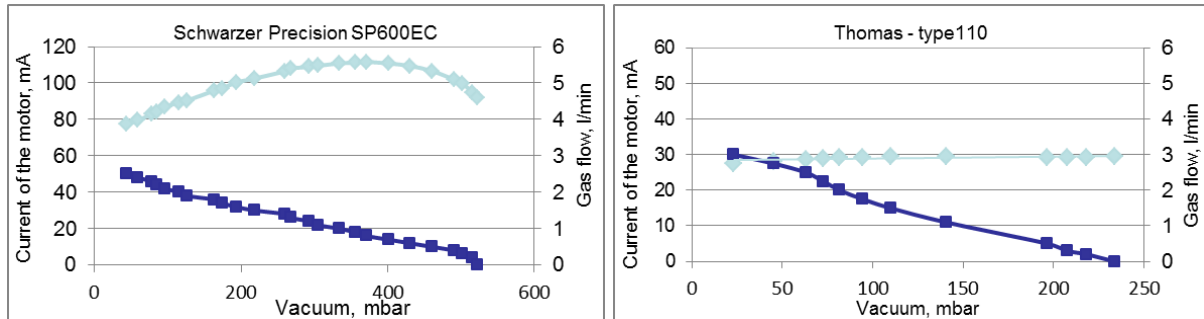


Fig. A2.5 Impact of pneumatic resistance of the pipe on the current of the pump engine

Development of the analyser with PLC control unit

Three prototypes of gas analyser with PLC control units were created with different sensor configurations:

- wideband zirconium O₂ sensor, electrochemical CO and H₂S sensors,
- electrochemical O₂ and CO sensors,
- wideband zirconium O₂ sensor (O₂ type 2)

A pneumatic diagram of one of them is shown in Fig. A.2.6. On the left side there is the boiler wall, with the zirconium sensor (S) mounted nearby. Other elements are placed near the **analyser's** control cabinet (filters – FS1, FS2) or inside it. Solenoid valves (Y1-Y4) allow for reconfiguration of the system when automatic calibration or de-clogging is needed. Flue gases from the analyser are redirected to the boiler after measurements.

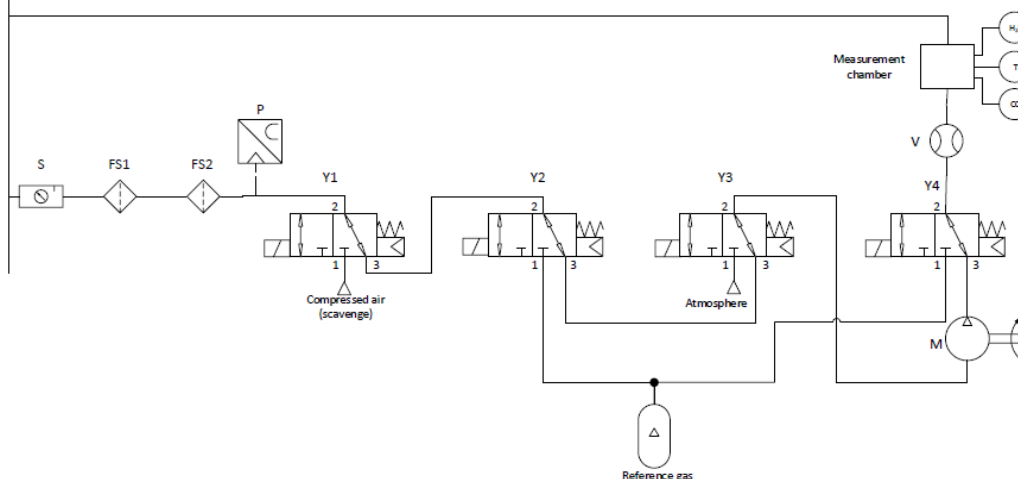


Fig. A2.6 Pneumatic schematic of the ZC23 analyser

The measurement chamber was designed and manufactured as part of the gas analyser. It allowed for two electrochemical sensors to be mounted in the analyser. The manufactured measurement chamber is shown in Fig. A2.7. After several tests the slow response of the sensor was noticed.

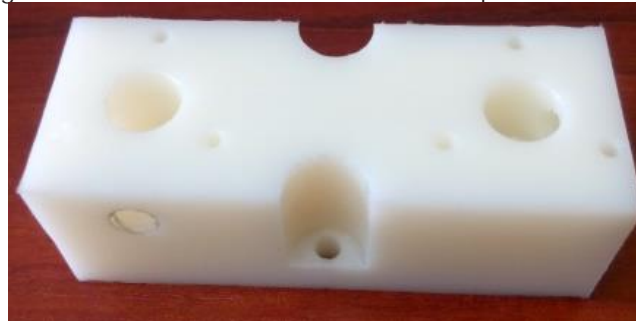


Fig. A2.7 First version of the measurement chamber for the electrochemical sensors

CFD calculations were carried out in order to find the answer to this issue. Example results presented in Fig. A2.8 show low turbulence intensity, especially near the second and third sensor. The path

lines are mostly straight. After several modifications of the design, the final version was developed with asymmetrical connections between sensor chambers. The electrochemical sensors generated signals that had to be processed by a potentiostatic circuit. These circuits were designed for the analysers. They balance the currents flowing through the sensor and generate output voltage proportional to the concentration of the measured gas. The electrical part of the analyser consists of the abovementioned PLC controller, power devices, fuses, etc. and was designed using Eplan Electric CAD software. Fig. A2.9. shows the prototype of the new gas analyser with PLC controller.

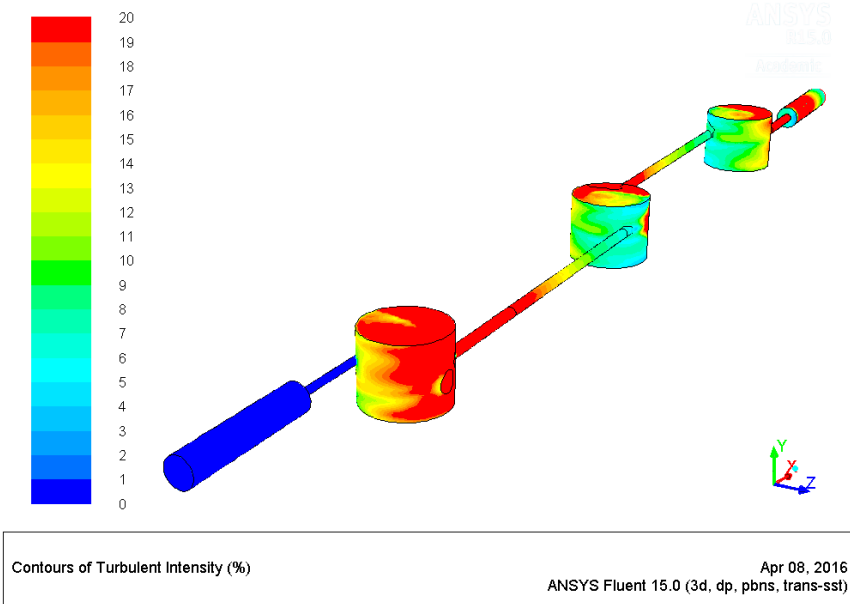


Fig. A2.8 Turbulence intensity in the final measurement chamber design

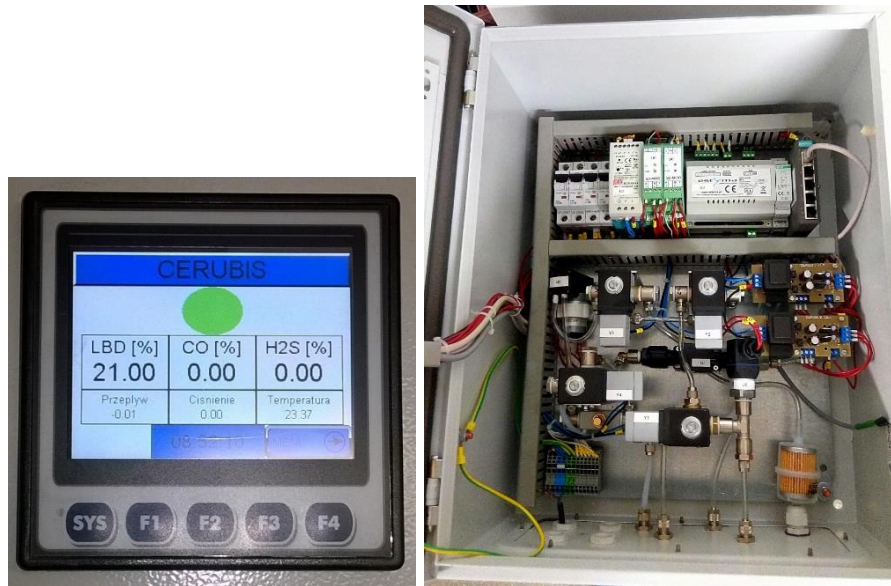


Fig. A2.9 Main screen of the ZC23 analyser's controller and inside of this analyser

Gas sensors testing

Investigations of O₂ sensors are only one example of the tests carried out. Output from the sensors were compared to a typical Siemens Ultramat 23 gas analyser (U23). Figure A2.10 shows the absolute errors of sensors at different concentrations of O₂, as compared to the reference U23 indications. The plot shows very small differences between the reference U23 indications and wideband zirconium 1 sensors (blue line). Tests were also conducted in real scale in BPP on boiler no. 5. Figure A2.11 shows the results of several O₂ sensors, while the grey line shows results from the reference U 23 gas analyser. Despite the extreme conditions (high temperature, dust) the results obtained for wideband zirconium 1 and for a simple electrochemical O₂ sensor were very close to the reference results.

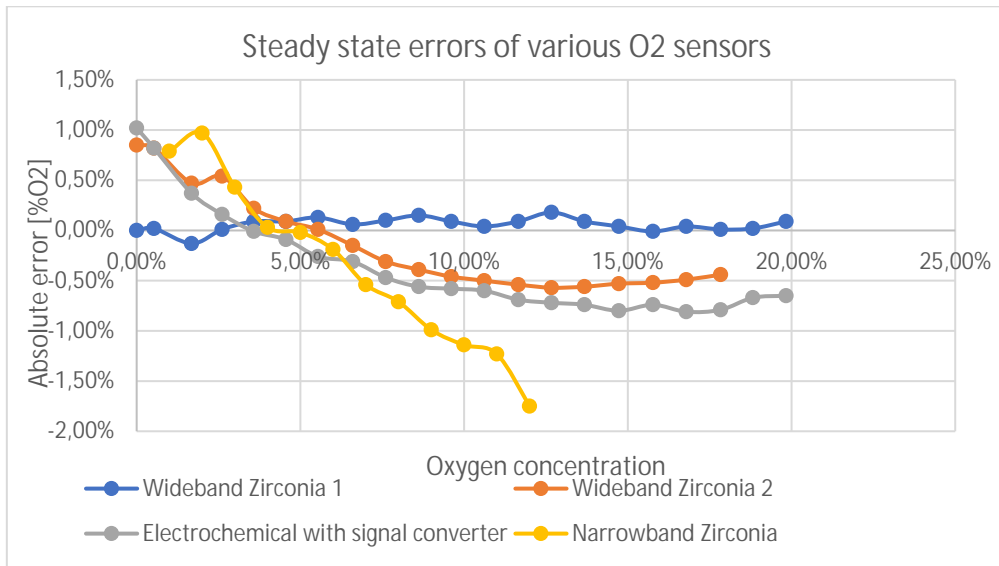


Fig. A2.10 Absolute errors of various O_2 - sensors compared to a reference analyser U23

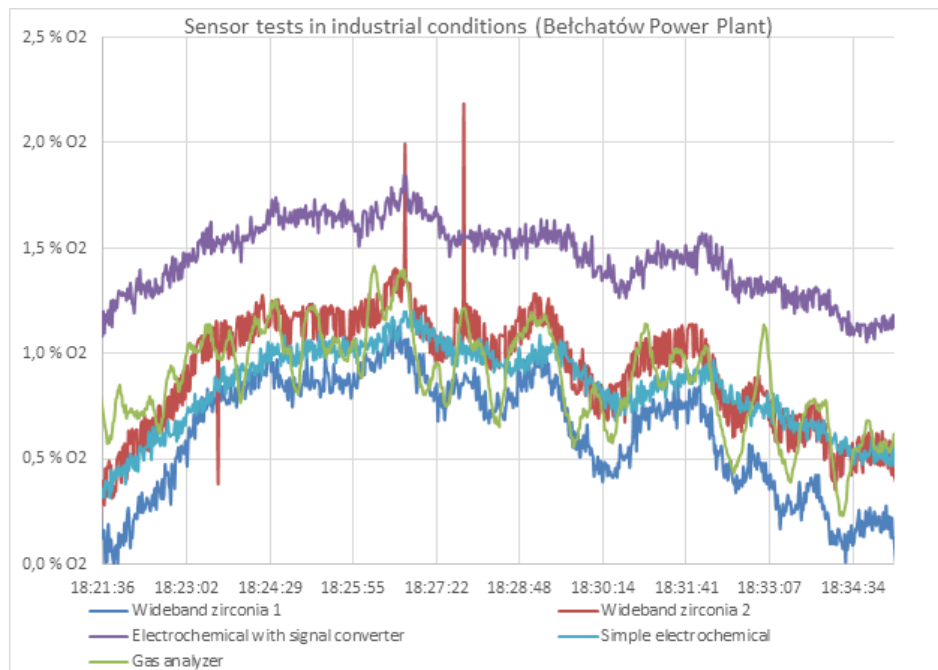


Fig. A2.11 Different O_2 sensors outputs in industrial conditions (flue gas in BPP).

Since information about the current concentration of H_2S in the flue gases in the boundary layer can be used as an indicator of the corrosion risk, a trial assembly of an electrochemical sensor (H_2S) in the analyser was made. The additional sensor was installed in portable housing of the analyser for measurement of O_2 . The first test of this analyser together with measurements of CO was carried out on boiler no. 1 in EC Wroclaw (heat and power plant). High similarity was found between the H_2S and CO maps. It was considered whether it was worthwhile to measure both of these flue gas components simultaneously or to select and measure the gas which is more valuable for analysis of the corrosion risk. Beside its high sensitivity to pressure changes, the H_2S sensor also exhibit more problems with cross-sensitivity to gases such as NO , NO_2 , SO_2 and CO , which is difficult to overcome. Looking at these issues it was concluded that measurement of H_2S gives little additional information to determine corrosion risks in the developed system.

An alternative probe to the electrochemical CO sensor is the use of a zirconium probe like KS1D, manufactured by Lamtec company. The KS1D probe consists of solid electrolyte from stabilised zirconium dioxide (ZrO_2) with electrodes for simultaneous measurement of O_2 and combustible flue gas components (CO/H_2) denotes as CO -equivalent (COe). This type of sensor measures O_2/CO in wet flue gas up to $450^\circ C$ which reduces its cost of application. However, the biggest disadvantage is the high cost of purchase. Figure A2.12 presents the laboratory test results of the KS1D probe. The characteristics are not fully advantageous for CIBOP application, especially at high levels of CO concentration when the change in output signal is very small. However, such a probe can be used under conditions of large fluctuations of CO concentration in flue gases, e.g. from zero to 1-1.5%.

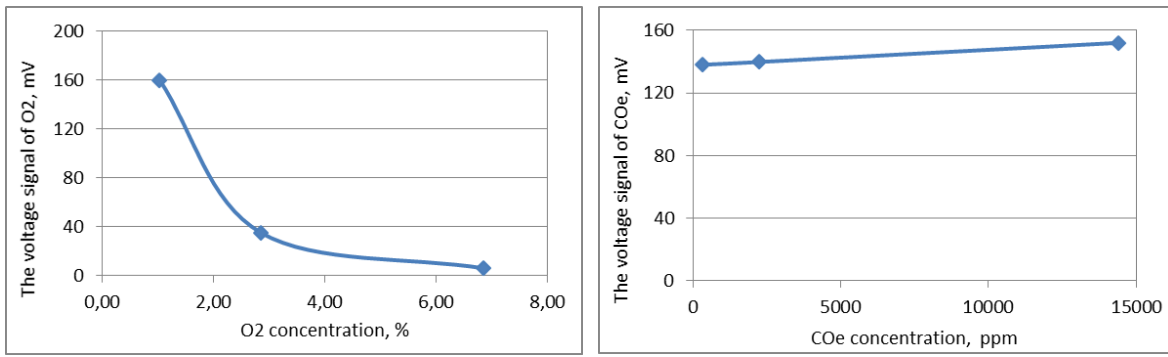


Fig. A2.12 Characteristics of O_2 and CO signals from KS1D probe

The air blow/calibration.

The air blow and automatic calibration subsystems are very important for the reliability and durability of the main system. This is especially important when electrochemical sensors are used. In this case a more sophisticated air blow/calibration subsystem had to be developed and verified.

A good solution to avoid use of the suction pump is to use an injector. Various construction solutions of the measuring connector with injector (with internal filter) were developed and tested. Results ensured long-term operation of such solution without maintenance, which was also confirmed in the test in real scale boiler conditions. However, in this case electrochemical sensors cannot be used.

After successful laboratory tests of the first version of the measuring unit, it was decided to build a new device containing an exhaust filter in front of the zirconium probe. To increase reliability modifications were made to the entire device, compressed air nozzle and ejector parameters. The manufactured unit is shown in Fig. A2.13. Because of the large weight of the injector tested, its design was modified slightly and a new device was made, as shown in Fig. A2.14. This device was used during the tests in EC Wrocław.



Fig. A2.13 Second version of the measuring device with ejector



Fig. A2.14 The injector device was used in tests on a boiler in EC Wrocław

Pilot tests – IEN.

The indirect sensors (namely gas sensors), pumps, filters, valves elements etc. presented in Tab. A2.1 were tested during pilot scale conditions. All elements used were carefully evaluated during

the tests and their advantages and disadvantages were described from the point of view of application in power plants. The most promising elements were chosen for upgrading gas analysers from Task 2.2 and long-term power plant tests in WP4

Tab.2.1. Indirect sensors and other elements tested during the 0.5 MW IEN test campaign

Device	Name	Advantages	Disadvantages
Flow meter	Honeywell AWM5101VN	Flow range to 3 l/min.	Result of measurement depends on ambient
		Result of measurement not depended on ambient temperature. Flow range to 3 l/min. Easy to mount.	Flow range to 3 l/min. Difficult to mount. Breaks in signals.
	Honeywell AWM3300V	Result of measurement not depended on ambient temperature. Flow range to 3 l/min. Easy to mount.	Probably neccesity to filter flue gases up to 1 um.
Pump	Schwarzer Precision SP270 EC-LC-HR	Small, 12 V power supply.	Too low capacity up to 1l/min. Frequent and high pulsations. Brush rotary motor.
	Schwarzer Precision SP620 EC-HR-DV	Capasity up to 3l/min. Small. Possibility to change the membrane. 24 V power supply.	Brush motor. Fast degradation of viton membranes. Rarely degradation of bearings.
	Schwarzer Precision SP620 EC-BL-DU-HR-DV	Capacity 4 or 8 l/min. No brush motor. Two cylinders. Power supply 24 V.	Big dimensions. Neccesity to change pneumatic connections before current application.
	THOMAS Typ 302	No rotary elements. Capacity up to 3 l/min.	Too big. Power supply 230 V.
	THOMAS Typ 303	No rotary elements. Capacity up to 3 l/min.	Too big. Power supply 230 V.
Solenoid valves	KNF N3 KPE 115/230V	Capacity up to 3l/min. Low pulsations.	Big, upper temperature of operation too low (40 C deg.)
	A7544/1002/012-UN	Two ways, direct operation, no pneumatic support needed, low flow resistance.	Operating pressure up to 6,5 bar. High emission of heat, high dimensions.
	Mindman MVDC-220-3E1	Small, low emission of heat, pressure operation up to 7 bars.	High flow resistance, one way operation.
CO cell	Alphasense CO-CE	Range 0-2%. Shotly up to 10%. Easy to mount.	High influence of pulsations on measurements.
	Cititel 4MF	Range 0-10%. Easy to mount. Fast reaction. Stability of measurement.	Some influence of pulsation on measurement. Expensive.
H ₂ S cell	Alphasense H2S-AE	Range 0-1000 ppm. Easy to mount. Cheap.	Long time of purging. High influence of pulsations and CO on measurement.
	Membrapor H2S/M-2000	Range 0-1000 ppm. Easy to mount. Short time of purging.	High influence of pulsations and CO on measurement. Probably short life span.
	Honeywell 4H2S-1000	High range. Stability of measurement. Low influence of CO on measurement.	Necesity to use special converter. Expensive.
O ₂ cell	Figaro oxygen SK-25F	Cheap	Long time of reaction during measurement.
	Cititel 4OxLL	Not tested yet.	Not tested yet.
Lambda	Estyma Electronics ML-2 V-2.7	Fast response. Good accuracy. Two possibilities of communication. Wide range of ambinet temperature 0-60 C deg.	bad influence on cell of air blows. Preferable fFiltration of solid particles.
Filters	Mindman MAF401-8A-G	Big area of filtering. Good efficiency of air blows	Not defined.
	Mindman MAF401A-8A-G	Big area of filtering. Good efficiency of air blows	Not defined.
	Festo MS4-LFM-1/8-B-R-M	Compact housing.	Small area of filtering. Poor efficiency of air blows.
	Festo MS4-LF-1/8-C-R-M	Compact housing.	Small area of filtering. Poor efficiency of air blows.

Some examples from the carried out tests of gas sensors are given below.

Fig. A2.15 and A2.16 show the comparison between reference measurements (O₂, CO and H₂S) and tested gas sensors for two pilot long-term cases, namely 1 and 2 (Tab. 2.8). The reference values are 0.5 h averages on the basis of measurements with two seconds interval while investigated ones are 0.5 h averages but on the basis of intervals of 30 s for measurements lasting usually 3-4 minutes in a 15 minute cycle. The length of this cycle resulted from the breaks needed to deliver air blows to clean the developed gas analysers. Thus it was difficult to directly compare given measurement results but some conclusions could be drawn. In general, the investigated O₂ gas sensors understated measured values, especially for low O₂ concentration. In the context of the corrosion risk, it was better than overstating. In the case of CO sensors, the measured values for low CO content were understated. For higher CO, the values were overstated. Good correlation was found for H₂S sensors thus, they were also used further in realisation of WP4.

For oxy fuel combustion case 11, long term results are shown in Fig. A2.17. The behaviour of gas sensors was similar to this and was analysed for the air cases.

During the tests at IEN 0.5 MW facility several gas sensors were investigated and finally qualified for real scale applications. It was discovered that with Ibd (lambda O₂ sensor) it is beneficial to use a preliminary filter, as it gives better indications, and less service of subsequent filters. In parallel with gas sensors, pumps, filters, solenoid valves and other parts were tested and their functionality verified. As was original presumed, the solid particles filters were the most problematic and required careful optimisation of the amount of air blows for cleaning.

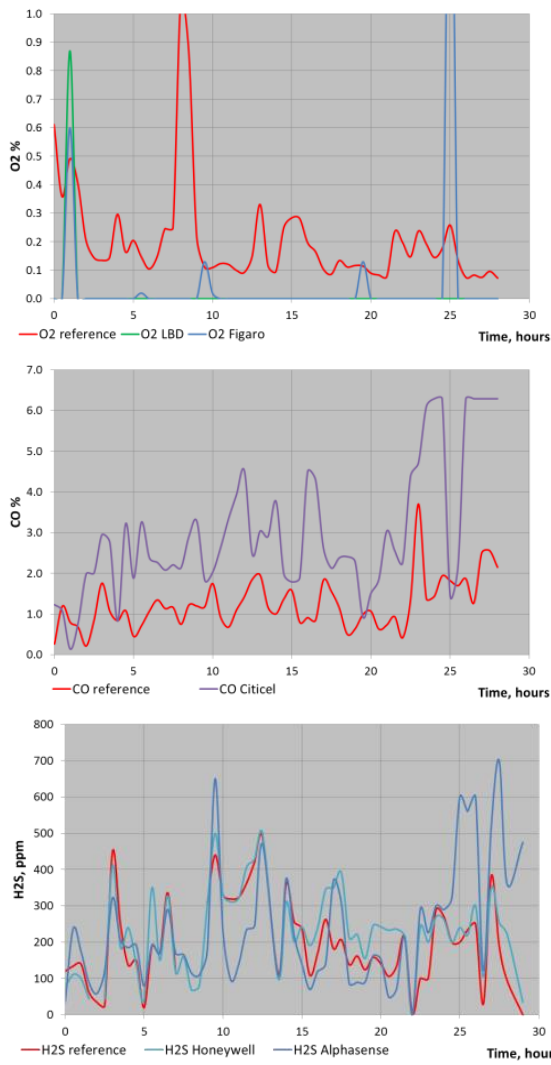


Fig. A2.15 O₂, CO and H₂S measurement of tested sensors versus reference measurements (red curves), case 1 (air), 0.5 MW IEN test facility

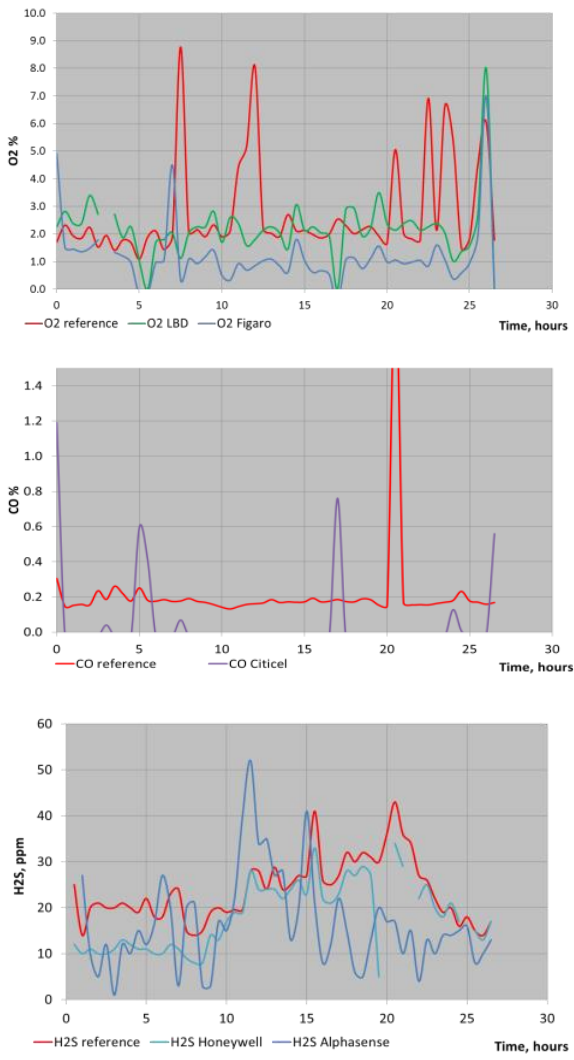


Fig. A2.16 O₂, CO and H₂S measurement of tested sensors versus reference measurements (red curves), case 2 (air), 0.5 MW IEN test facility

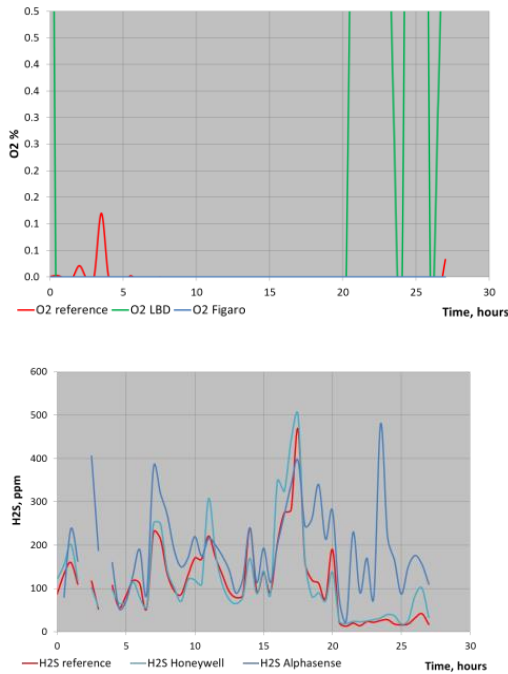


Fig. A2.17 O₂, CO and H₂S measurement of newly developed sensors versus reference measurements (red curves), case 11 (oxy), 0.5 MW IEN test facility

The pilot tests - USTUTT

Table A2.2 shows an example of momentary, not averaged as at IEN pilot tests, measurement results from the developed gas analysers and corresponding reference values (Ultramat 23). Good coincidence between these measurements can be seen. The tested IEN gas analyser (O_2 , CO and H_2S) and all its subsystems were working properly in all test conditions.

Tab. A2.2 Comparison of O_2 , CO and H_2S measurements at 0.5 MW USTUTT test facility

Date	Time	λ	Fuel	Ultramat 23		IEN developed gas analyser		
				O_2	CO	O_2 -LBD	O_2	CO
2016-09-12	18:58:00	0.80	Sebuku	0.00	1.84	0.00	0.83	1.74
2016-09-12	19:10:00	0.80	Sebuku	0.00	1.51	0.00	0.77	1.90
2016-09-12	19:24:00	0.80	Sebuku	0.00	1.54	0.00	0.81	1.84
2016-09-13	09:27:00	1.15	Sebuku	4.20	0.10	7.94	4.55	0.00
2016-09-13	09:42:00	1.15	Sebuku	4.17	0.10	7.98	4.59	0.00
2016-09-13	09:57:00	1.15	Sebuku	4.32	0.10	8.03	4.66	0.00
2016-09-13	11:35:00	0.80	US HardCoal	0.00	1.61	0.00	0.21	1.68
2016-09-13	11:50:00	0.80	US HardCoal	0.00	1.99	0.00	0.23	1.99
2016-09-13	12:05:00	0.80	US HardCoal	0.00	1.73	0.00	0.40	1.76
2016-09-13	12:20:00	0.80	US HardCoal	0.00	1.80	0.00	0.36	1.99
2016-09-13	18:55:00	0.80	US HardCoal	0.00	1.64	0.00	0.85	2.03
2016-09-13	19:10:00	0.80	US HardCoal	0.00	1.81	0.00	0.70	2.19
2016-09-13	19:25:00	0.80	US HardCoal	0.00	2.07	0.00	0.67	2.25
2016-09-13	19:40:00	0.80	US HardCoal	0.00	1.81	0.00	0.62	1.81
2016-09-13	19:57:00	0.80	US HardCoal	0.00	2.19	0.00	0.61	2.20
2016-09-14	10:41:00	1.15	US HardCoal	2.28	0.15	4.96	2.48	0.03
2016-09-14	10:56:00	1.15	US HardCoal	2.28	0.18	4.84	2.34	0.03
2016-09-14	11:11:00	1.15	US HardCoal	2.07	0.16	4.41	2.18	0.02
2016-09-14	15:20:00	1.15	US HardCoal	2.84	0.20	5.02	2.77	0.01
2016-09-14	15:35:00	1.15	US HardCoal	3.00	0.20	5.92	3.15	0.01
2016-09-14	15:50:00	1.15	US HardCoal	3.20	0.20	5.60	3.15	0.02
2016-09-15	13:03:00	0.80	OPP hardcoal	0.10	0.14	1.26	0.45	0.01
2016-09-15	13:18:00	0.80	OPP hardcoal	0.15	0.22	1.02	0.34	0.05
2016-09-15	13:30:00	0.80	OPP hardcoal	0.51	0.18	1.31	0.56	0.01
2016-09-15	23:06:00	1.15	OPP hardcoal	3.86	0.10	7.08	3.83	0.00
2016-09-15	23:22:00	1.15	OPP hardcoal	3.60	0.10	6.56	3.53	0.00
2016-09-15	23:37:00	1.15	OPP hardcoal	4.10	0.09	6.90	3.95	0.00
								9.34

Tests in Opole and Bełchatów Power Plants

At BPP O_2 gas sensors were mounted under the aegis of other self-financed work before the CERUBIS project started. Indications from the O_2 sensors were gathered within a 12 month period.

Three different types of gas analysers were tested at OPP. Gas analysers capable of measuring concentrations of O_2 , CO and H_2S were tested in OPP. All developed types of gas analysers were installed in the boiler on each wall (zirconium O_2 , electrochemical O_2 and CO, and electrochemical CO and H_2S). Fig. A2.18 shows exemplary results for the left wall from one point over a period of several days. Very high concentrations of CO (>11%) and H_2S (>500ppm) were recorded. O_2 obviously in such cases reached 0 %. In general, the H_2S concentration picture follows the pattern for CO. The figures show changes in concentrations of flue gases components over time. Low CO and sometimes O_2 reaching 1 to 2 % probably denote cases of low boiler capacity or unstable conditions like changing the mills configuration etc.

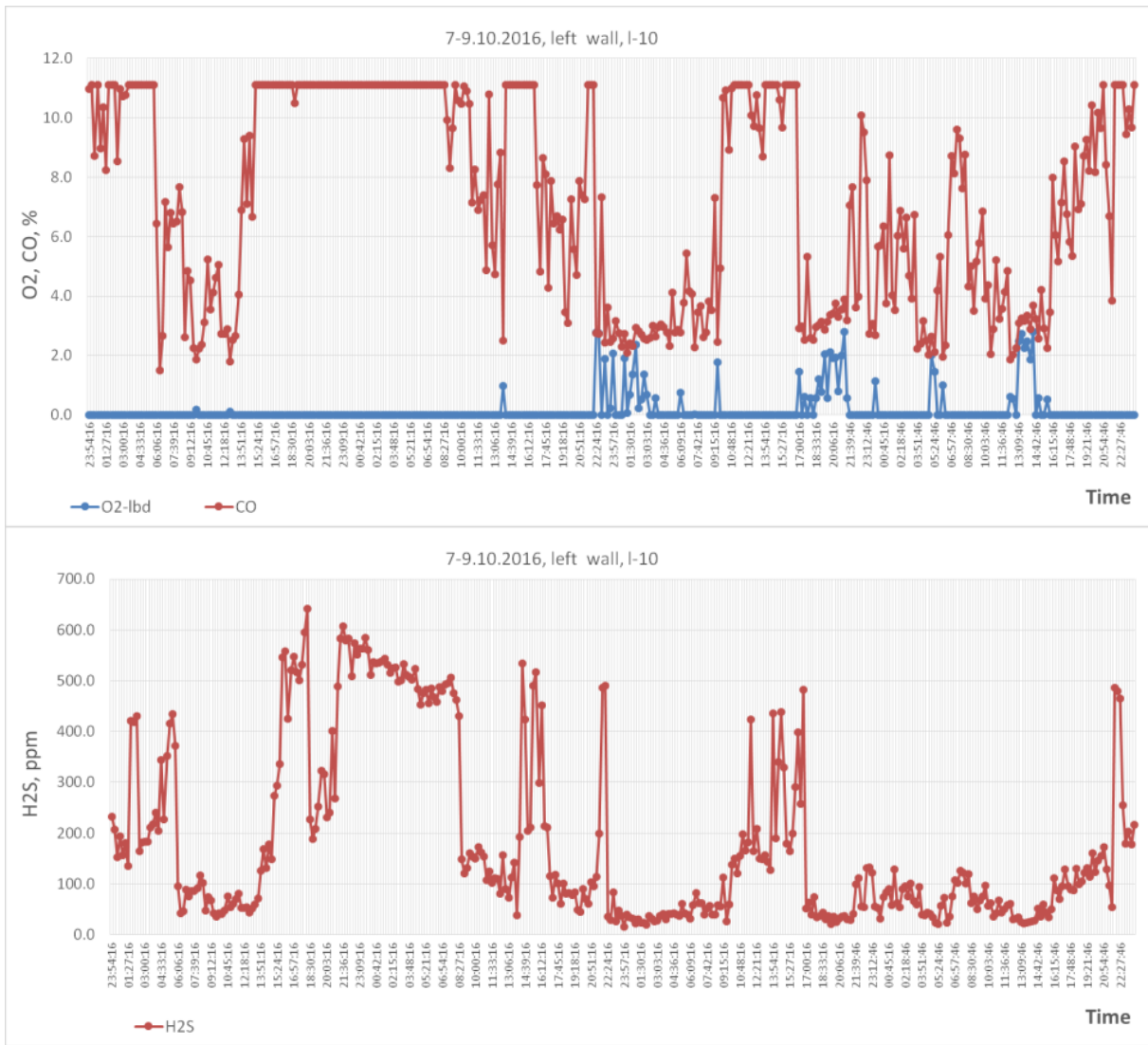


Fig. A2.18 Example results of O₂, CO and H₂S measurements

A3 - Development of the corrosion probe

Laboratory tests

Preliminary tests were conducted in the laboratory in order to find out how changes in the dimensions of selected material affect its electrical resistance and how the resistance level depends on the thickness of the probe. During these tests, recorded probe resistance changed through mechanical treatment (reducing the thickness).

Figure A3.1 (left) presents exemplary results of resistance change versus loss of probe volume. Since the resistance of the sensor is strongly dependent on temperature, the sensor must be constantly cooled by the air and its temperature measured. Automatic adjustment of the cooling system was intended to provide constant temperature of the sensor (approx. 350-400°C), depending on the type of boiler. Both resistance and temperature were taken into account when calculating the corrosion rate. The automatic control system was designed and manufactured, featuring the use of a 2/2-way proportional solenoid valve and regulator of temperature [8].

Figure A3.1 (right) shows the linear relationship between the temperature and resistance of measuring element during laboratory tests with flue gases. The resistance increases with an increase in temperature. The test determined the resistance value of the ring at a certain temperature when the corrosion reaction does not proceed.

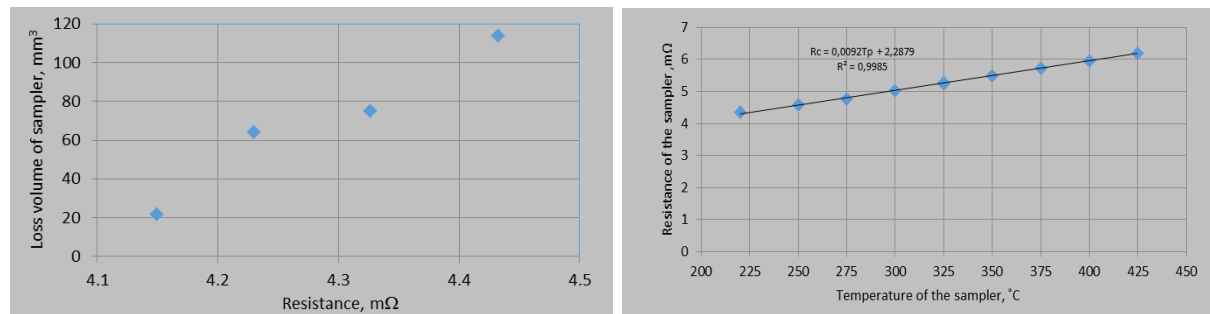


Fig. A3.1 Changes in resistance of the tested sample depending on its changes on volume (left). The relationship between the temperature and resistance of measuring element in temperature range from 200 to 425°C (right)

Pilot tests - IEN

Testing with the corrosion probe was carried out to examine the behaviour of the corrosion probe in different combustion regimes and to investigate the ring itself after tests. The probe was located in the second duct of the 0.5 MW test facility in the range of temperature 800-1000 °C. This version of the probe was cooled by air, so the efficiency of the cooling system and temperature sensor stabilisation were tested as well.

The temperature of the sensor and the temperature of the measuring probe tube were measured during the tests. Example results of temperature measurements of both are shown (for one test) in Fig. A3.2. The temperature of the probe tube follows the temperature of the sensor so it could be used to adjust the cooling of the probe. Adjusting the cooling based on measurement of the probe tube temperature instead of direct measurement of the sensor temperature could significantly simplify the replacement of sensors during normal operation. Due to the need for fast thermal stability during operation of the measuring system, the point at which the temperature is measured and used to control the cooling system of the probe had to be carefully selected. The benefits from facilitating the replacement of sensors made it worthwhile to further develop and apply such measurement of probe pipe temperature

Resistance of the sensor is strongly dependent on temperature, so the reference test was carried out to determine the temperature coefficient of the sensor (Fig. A3.3). The dependence of sensor resistance changes on sensor temperature is linear, so the coefficient was calculated based on these results.

This approximation was useful for temperature differences in a narrow range of sensor temperature (300-400 °C) and slight fluctuations of temperature sensor could be compensated for in this way. The temperature coefficient was used to recalculate measured resistance of the sensor in real conditions for reference conditions at temperature 350 °C.

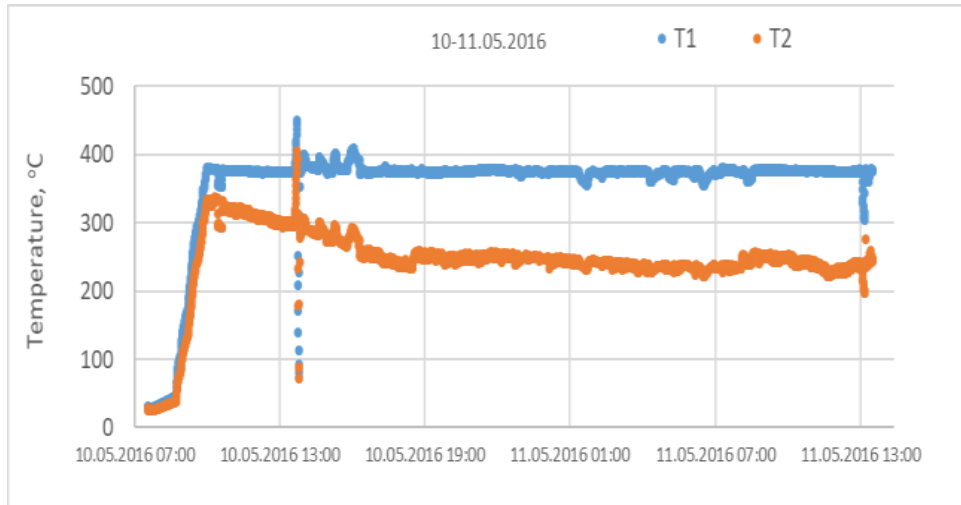


Fig. A3.2 An example of changes in temperature of sensor (T1) and probe (T2) during testing

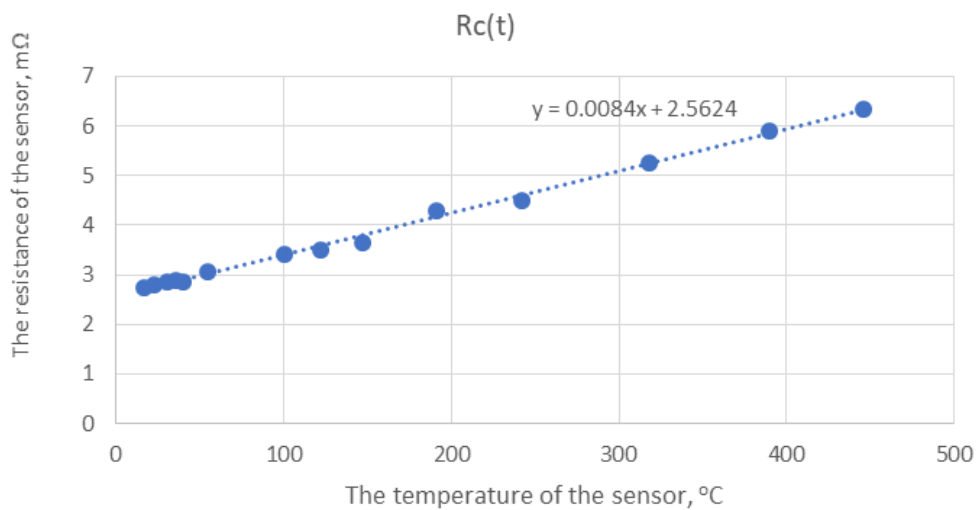


Fig. A3.3 Results of calibration of the temperature coefficient of the sensor

Fig. A3.4 gives a view of the corrosion probe and ring itself, with definition of additionally investigated sides of the ring with SEM mapping [9]). Analysis of the ring led to determination of the material loss presented in Tab. A3.1. in the column denoted by 135 hours. The table also presents the results of a simple recalculation of what would happen if the probe were operated longer, eg. one month or one year. It shows a rather high dynamic of corrosion, reaching in excess of 2 mm per year of tube material loss.



Fig. A3.4 Corrosion probe and ring sides defined for SEM analysis

Tab. A3.1 Recalculation for longer operation of corrosion probe

Side of ring	135 hours	1 month	1 year
Wind side	22 µm	117 µm	1404 µm
Lee side	35 µm	186 µm	2240 µm
Tangent side	7 µm	37 µm	446 µm

Pilot test - USTUTT

Fig. A3.5 presents a comparison of measured and recalculated resistance for two measuring cases. The measured resistance (R_c) was recalculated (denoted as R_t) according to constant reference conditions (constant temperature of 350 °C). It shows that it is worthwhile to present measurement results as values recalculated to reference temperature.

This test showed that the clear change in measuring signal was obtained in a relatively short measurement time, which is promising in the context of long-term research in steam boilers.

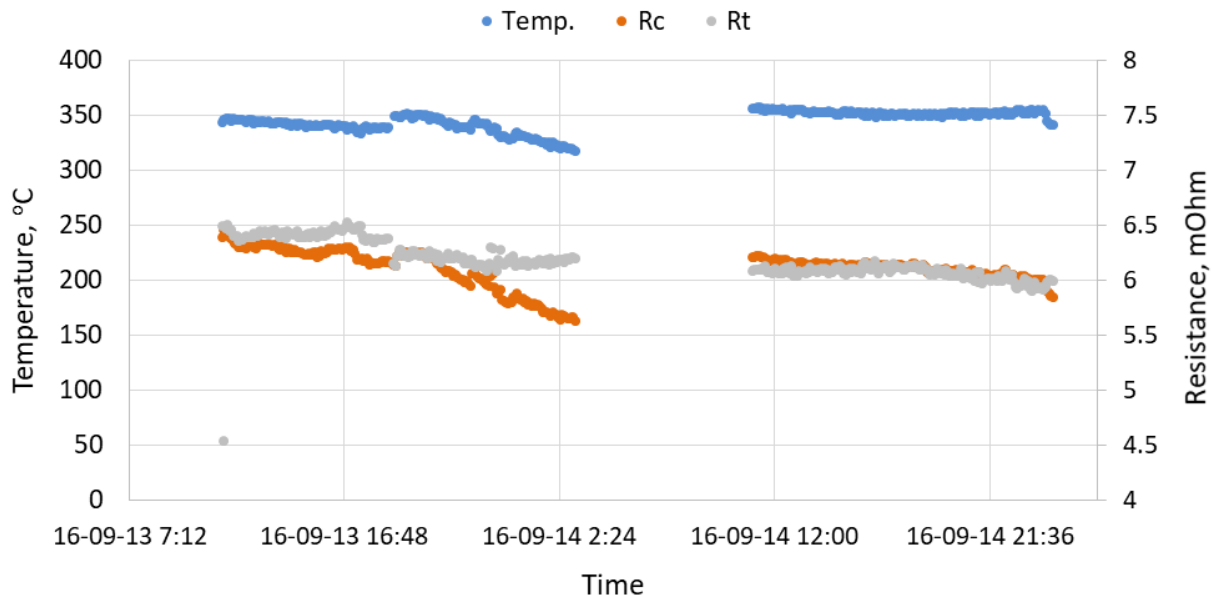


Fig. A3.5 Comparison of the measuring results of sensor resistance (R_c) and resistance value recalculated for the reference temperature of 350 °C (R_t), 0.5 MW USTUTT test facility

Power plant tests.

In order to check probe performance, it was tested (for several hours) in BPP on boiler no. 5. During the test the corrosion probe was inserted into a measuring port on the left wall (level 30m) for several hours – see Fig. A3.6.



Fig. A3.6 3D visualisation of the corrosion probe located in the measuring point (left). Assembly of the corrosion probe in the boiler wall, BPP (middle). View of the tip probe after end of test (right)

In the normal position of the probe in the combustion chamber (approx. 5 cm from the surface of the evaporator) the probe temperature was easily maintained at a stable level of approx. 300-350°C. After inserting the probe deeper (more than 10cm), the temperature increased to more than 500°C (instead of the expected increase to 400°C) and it was necessary to increase the efficiency of the cooling system. It was therefore decided to modify the tip of the probe to minimise the surface heat transfer (the tip of the probe was shortened and the location of the measuring sensor ring was changed before other trial measurements in OPP). Figure A3.7 presents the changes in resistance of the ring versus temperature during BPP measurements.

Comparing these relationships to those obtained in laboratory conditions, differences between the results were observed. Although a linear relationship was obtained during both tests, under real conditions the values of resistance are higher for a given temperature compared to the laboratory test. This could be caused by radiation exposure in the boiler furnace and the specific thermocouple location. This may result in hindering the cooling system and cause problems with maintaining the stable temperature of the resistance probe. Therefore, the location of thermocouples in the probe must be carefully chosen.

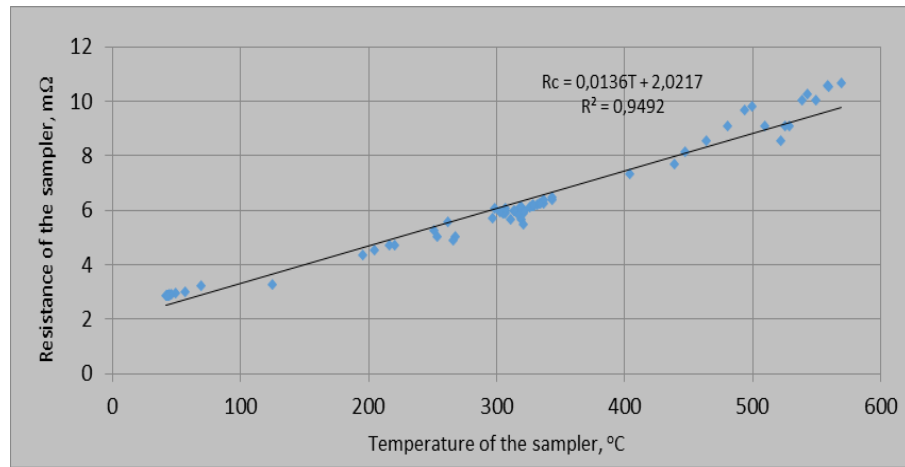


Fig. A3.7 The relationship between the temperature and resistance of the measuring element in a temperature range from 40 to 570°C during tests in the combustion chamber at BPP

The last test of the corrosion probe was carried out in OPP (left wall at level 30m). The relationship between the temperature and resistance of the measuring element is shown in Fig. A4.8. During the test, high slagging in the combustion chamber was observed. The effect of slagging on the probe was visible after half an hour. This implies that the corrosion probe could also be used as a "slagging probe" and that the location of the probe has to be carefully chosen.

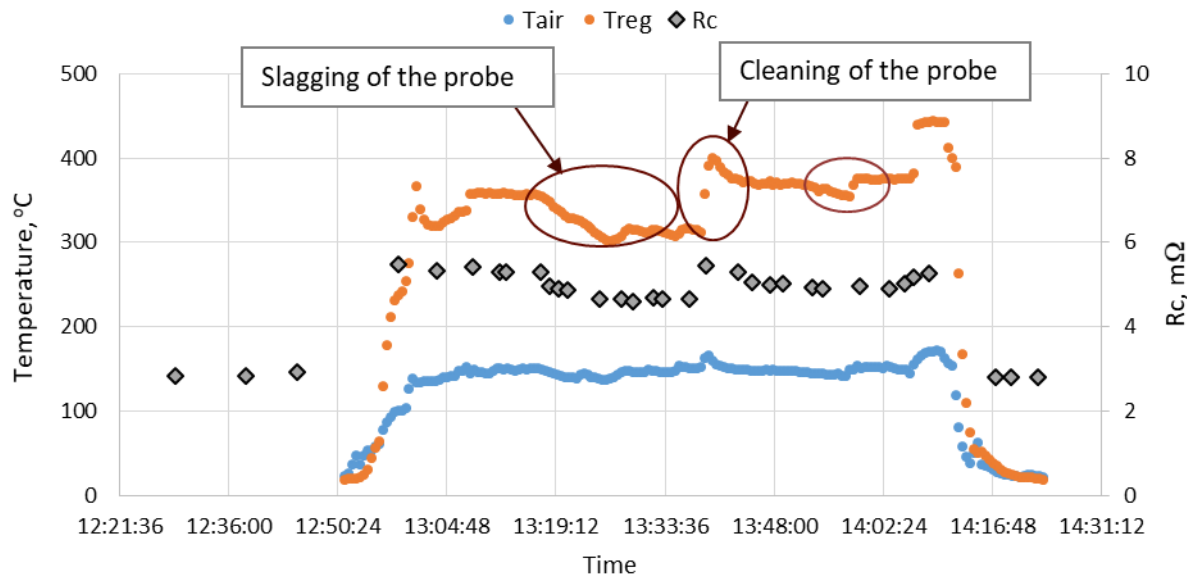


Fig. A3.8 Changes in temperature of the probe and resistance of the measuring element (R_c) during tests at OPP

Long-term power plant tests - Boiler no. 5 I BPP

In the case of corrosion probe and BPP one probe (BP1) worked in the period from 15.12.2017 to 29.05.2018. The second probe (BP2) worked from 29.05.2018 to 15.12.2018. Two probes were tested in this boiler and were mounted one after the other in the same place. During testing of the first probe (BP1), a problem occurred with data logging, therefore the resistance measurements were made periodically during the inspection and on this basis the corrosion rate was determined. Continuous registration of temperatures and resistance was carried out during testing of the second probe (BP2).

Fig. A3.9 shows the sensor temperature changes (denoted T_{kr}) in the selected period of time, O₂ concentration (denoted O₂_4) measured half a metre from the probe and electric power of the unit for the first month of BP1 operation. As can be seen, operating conditions (and gas atmosphere) were changing with the change in boiler capacity. The O₂ concentration varied in the range from 0 to 2 %, with the average value being around 0.8 %. Stabilisation of the temperature seems to be quite good.

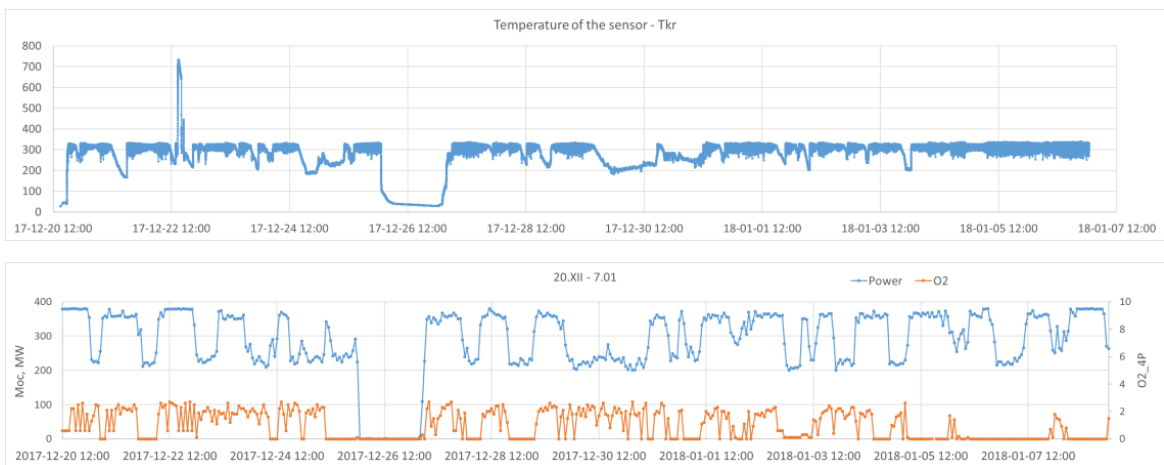


Fig. A3.9 Changes in BP1 probe temperature and boiler working conditions during testing of the probe (in the initial period of the test)

After the first test with the BP1 probe lasting 162 days, the sensor was dismantled and analysed. Changes in sensor resistance value of 4.8% were observed during this test. Assuming even wear of the ring (in this case sensor wear was fairly even and low), it would mean a change in thickness of 0.07 mm, meaning approximately 0.16 mm/y.

The BP2 probe tests lasted 195 days. In Fig. A3.10 the changes in temperature and resistance of the sensor during the test are shown, as well as the changes in electric power of the unit during the test. After finishing the test with probe BP2 (test lasting 195 days), the change in resistance of the sensor was determined as 3.7%. Assuming even wear of the ring, it would mean a change in thickness of 0.055 mm, meaning approximately 0.12 mm/y.

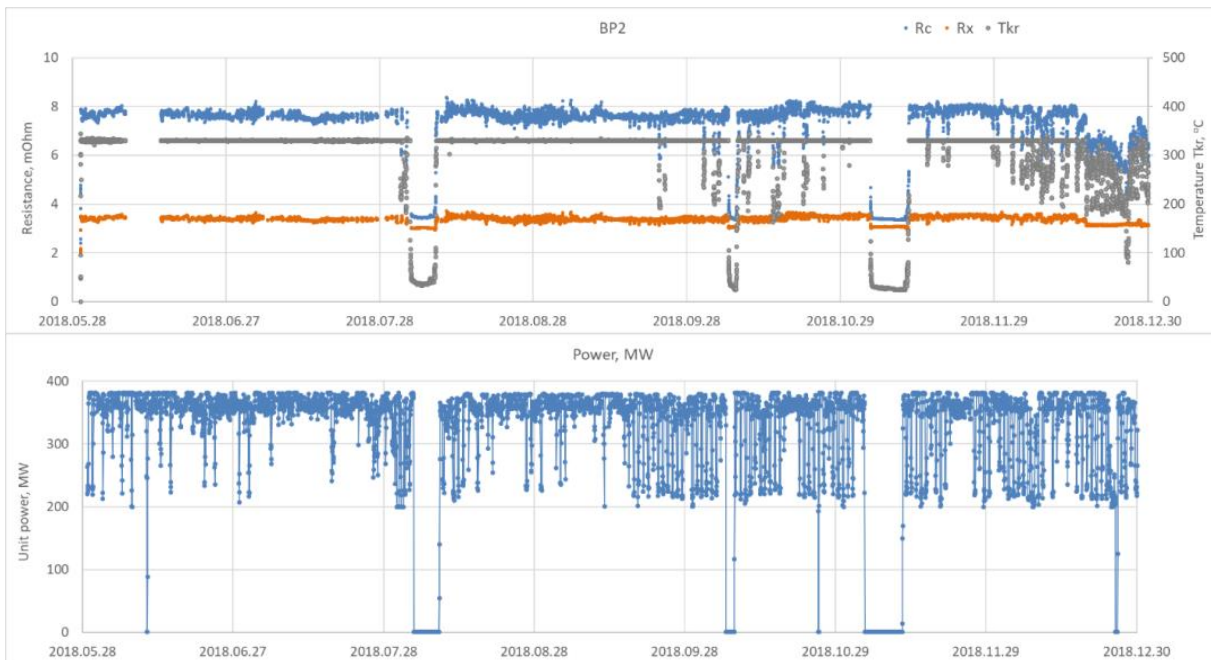


Fig A3.10 Changes in BP2 probe temperature and resistance during the test (195 days) (up) and the electric power of the BPP unit during the test (bottom).

Long-term power plant tests - Boiler no. 3 in OPP.

Two probes were installed at level 30 m on the front and right walls. The probe mounted on the front wall was marked OP1, while the probe on the right wall was marked OP2. Figures A3.11 to A3.14 show temperature and resistance measured during the test. In the initial test period, the calculated corrosion rate was 0.39 mm/year for the OP1 probe (112-day test) and 0.48 mm/year for the OP2 probe (212-day test).

In the long-term test, the calculated corrosion rates are lower: 0.22 mm/year for OP1 probe (351-day test) and 0.22 mm/year for OP2 probe (436-day test), respectively, but this period covered several weeks of boiler outage.

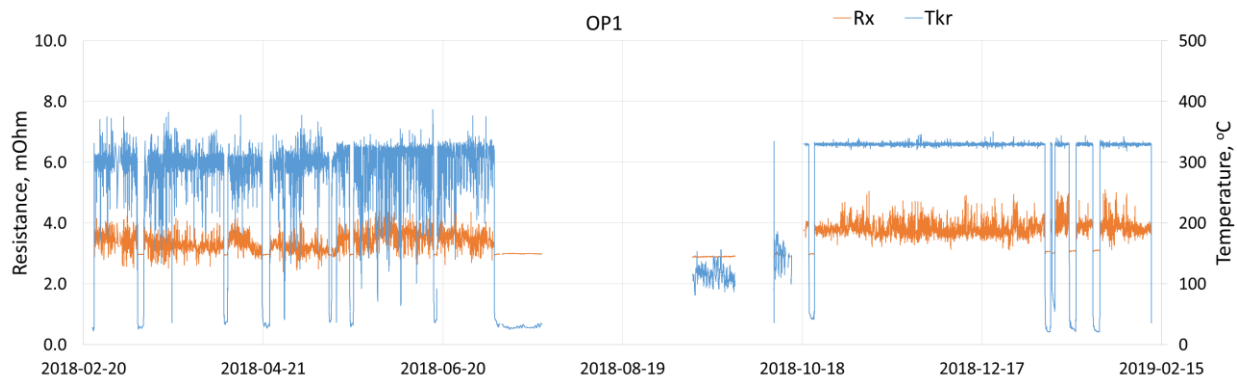


Fig. A3.11 Changes in probe temperature and resistance during testing of the OP1 probe

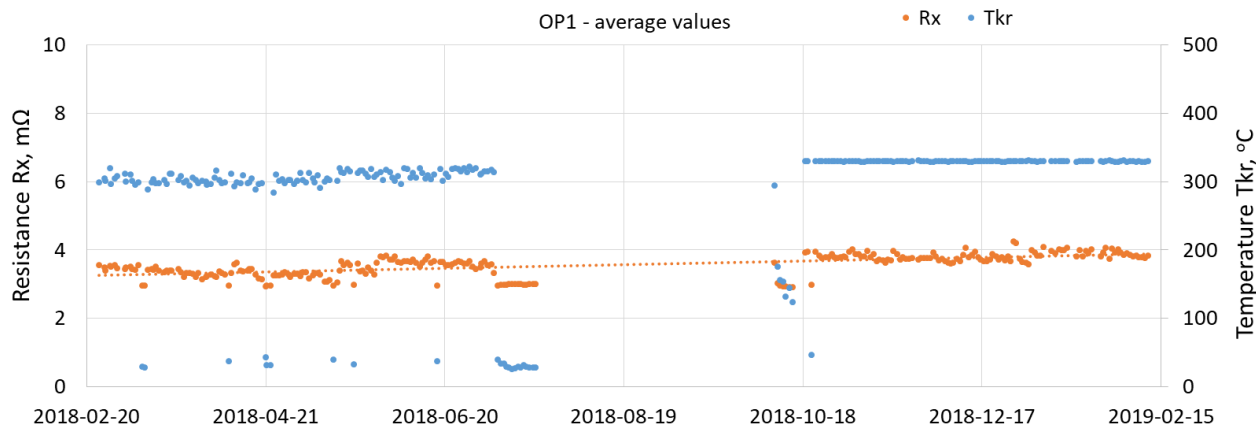


Fig. A3.12 Daily average values for the measured resistance during testing of probe OP1

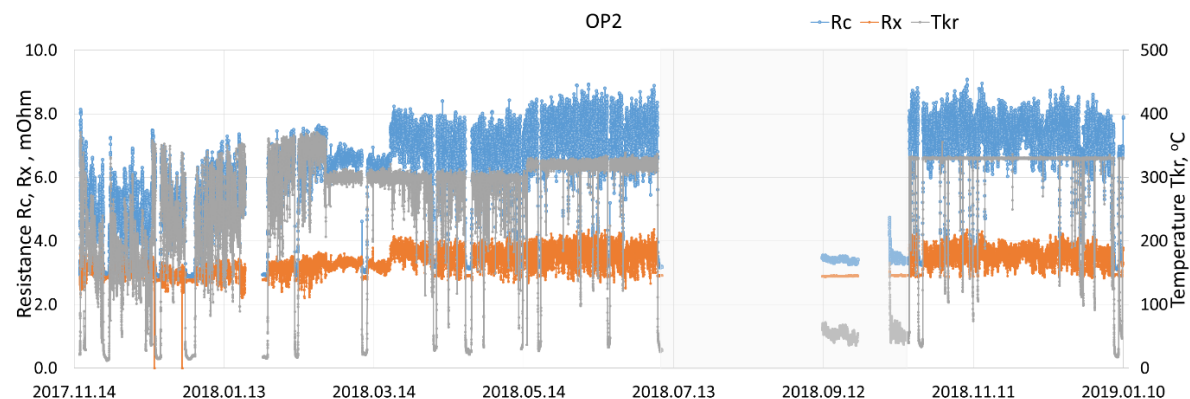


Fig. A3.13 Changes in probe temperature and resistance during testing of probe OP2

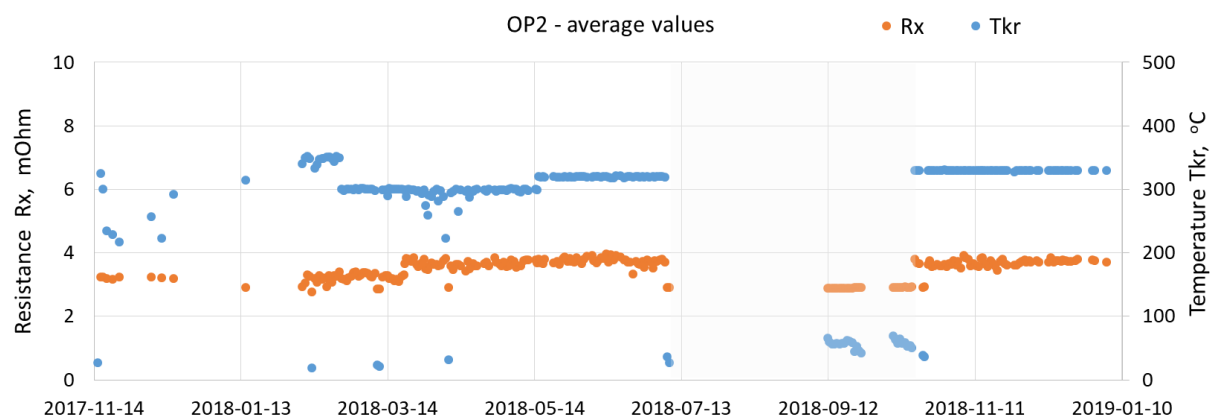


Fig. A3.14 Daily average values for the measured resistance during testing of probe OP2

A4 – Development of the resistance method

Results of the preliminary power plant tests.

Electric resistance measurements of the membrane wall were carried out after laboratory scale experiments and before 0.5 MW pilot tests for preliminary checking of the system in real boiler conditions.

First experiments were carried out at boiler no. 5 in BPP on the front wall at level 54 m, as presented in Fig. A4.1. CMS 3545 was used with four connection points to the boiler wall. Current was supplied to the boiler wall between P1 and P5. The voltage drop between P2 and P4 was used to calculate the resistance of the boiler wall. The distance between P1 and P5 was 12 metres, between P2 and P4 6 metres.

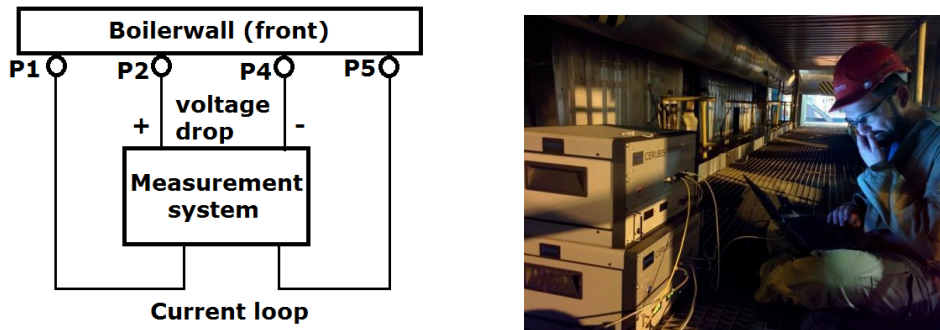


Fig. A4.1 Real scale experiments at boiler no. 5 in BPP

Measurements were taken during two nights, the first night with a current supply of 1 A, the second night with a current supply of 2 A. The results of the measurement are presented in Fig. A4.2. The electrical resistance of the boiler wall between two connection points spaced 6 metres apart (P2 and P4) was measured at $15.5 \mu\Omega$. With a current supply of 2 A it was able to detect variations of $2.3 \mu\Omega$ (15 %) with a level of significance of 95 %. The measured value of $15 \mu\Omega$ was much lower than single $m\Omega$, which was originally set for measurement. To be able to detect smaller variations it was considered to increase the distance between connection points. Also, by further increasing the current supply, the noise on the measured signal might be further reduced.

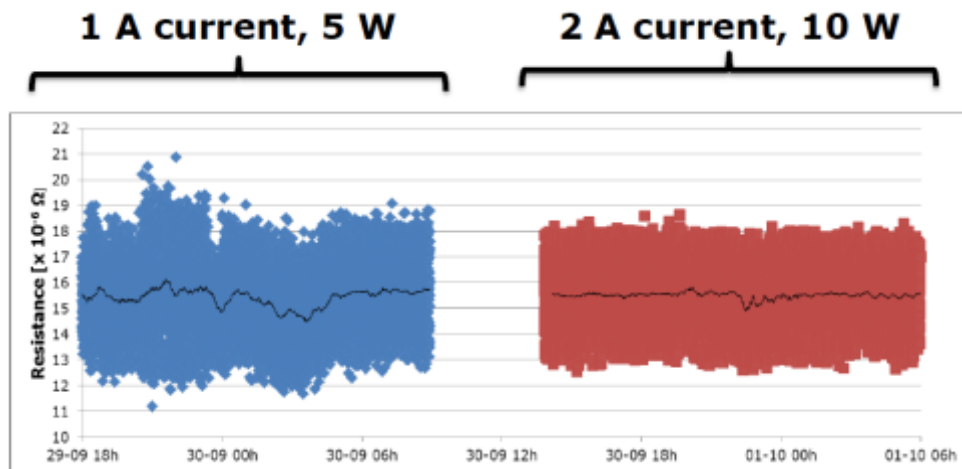


Fig. A4.2 Measured resistances as a function of time for real scale experiments, black lines show moving averages over 255 samples

In order to check how increasing the current supply will affect resistance behaviour, another real scale experiment was carried in boiler no. 3 in OPP (Fig. A4.3). Test levels of current were respectively 4.6 A, 7.7 A and 11.6 A. The results are shown in Fig. A4.4 and Tab. A4.1. The increase in performance of the method is significant, especially in the last step.

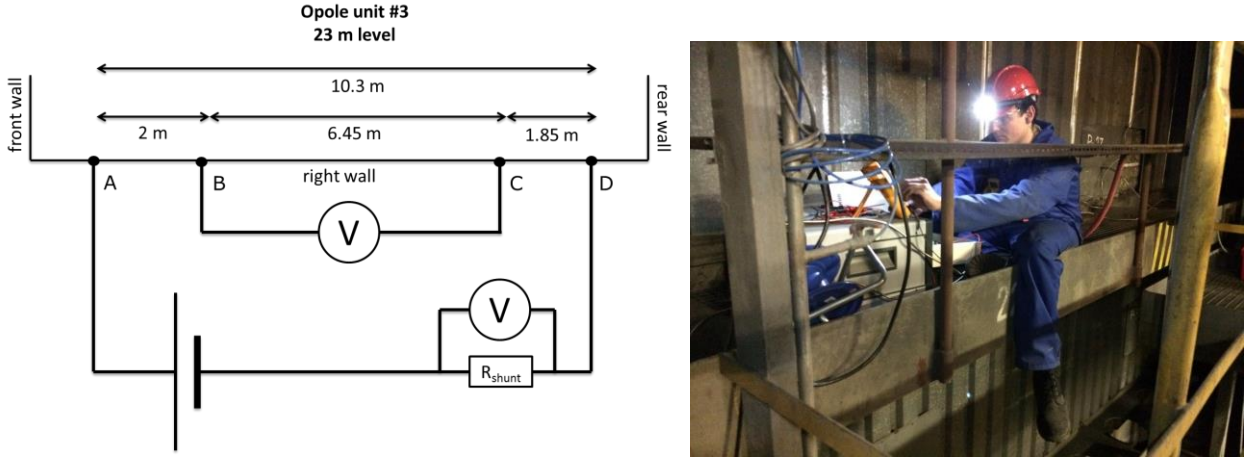


Fig. A4.3 Real scale experiments at boiler no. 3 in OPP, right wall, level 23 m.

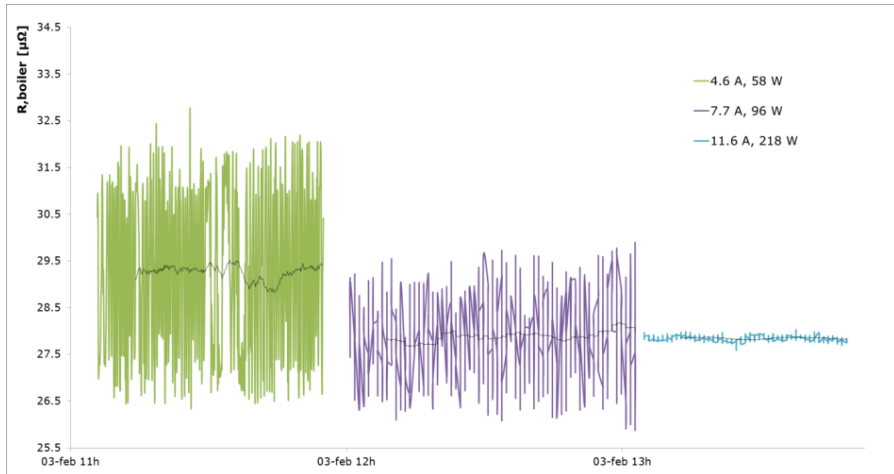


Fig. A4.4 Measured resistances as a function of time for experiments in OPP, black lines show moving averages

Tab. A4.1 Results of OPP experiments

No	Current supplied	Power	Resistance measured	2σ	Signal to noise ratio	Peak to peak value
A	W		$\mu\Omega$	$\mu\Omega$	-	$\mu\Omega$
1	4.6	58	29.3	3.3	18	6.3
2	7.7	96	27.9	1.6	35	4.0
3	11.6	218	27.8	0.1	524	0.4

Regarding capacitive effects, an experiment was conducted to quantify capacitive effects in the boiler wall. First, the resistance between point B and point C with current supply between points A and D was measured (see Fig. A4.5). In this setup, there is no current flowing through the cables used for measuring resistance. Measured resistance between B and C is 30 μ Ohm. The measured resistance between A and D is 220 μ Ohm.

Assuming the resistance measured between B and C is correct, and that the resistance of the wall is constant, you would expect a resistance value between A and D of:

$$\frac{10.3 \text{ m}}{6.45 \text{ m}} \cdot 30 \mu\Omega = 48 \mu\Omega$$

where 10.3 and 6.45 m are the distances between A and D and between B and C, as before.

The capacitive effect in the measured resistance value of AD is $220 - 48 = 172 \mu$ Ohm.

Next, the resistance between point B and point C with current supply also between points B and C was measured. In this setup, there is current flowing through the cables used for measuring resistance. Measured resistance is 205 μ Ohm. This suggest the magnitude of the capacitive effect in the second setup is $205 - 30 = 175 \mu$ Ohm. Both experiments give roughly the same result, which gives confidence in the theory.

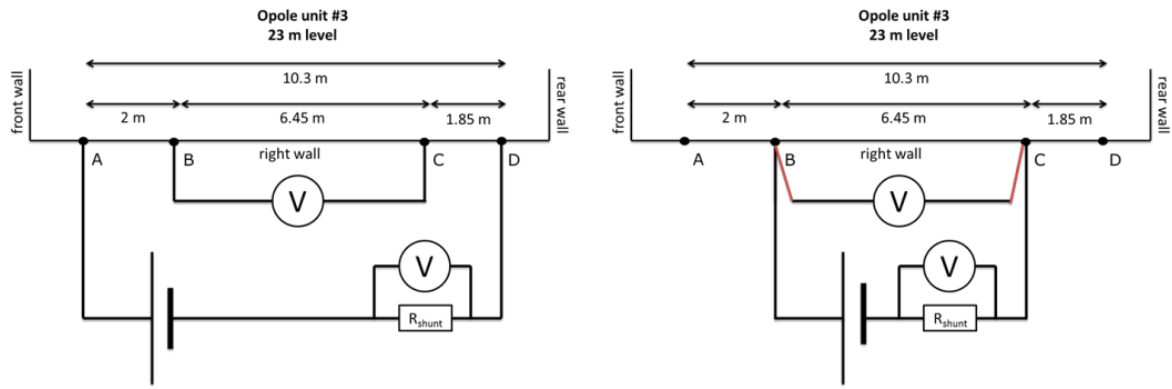


Fig. A4.5 Sketch experiment to quantify capacitive effects. First setup (left) gives $R_{AD,1} = 220 \mu\text{Ohm}$ and $R_{BC,1} = 30 \mu\text{Ohm}$ for a theoretical capacitive effect in the AD sensing wires of 172 μOhm . Second setup (right) gives $R_{BC,2} = 205 \mu\text{Ohm}$ for a capacitive effect in the BC sensing wires of 175 μOhm .

Pilot tests - USTUTT.

The main goal of electric resistance measurement was formulated after the OPP measurement campaign in Task 3.3: to develop the system to be able to withstand power levels of 200 W or higher without overheating. Three measurement tubes were made specifically for these 0.5 MW pilot tests. The tubes were designed to be placed through the burner. The idea was to measure the resistance of a stainless-steel tube exposed to extreme conditions.

All tubes (Fig. A4.6) were 2 m long, with connection points welded on the sides to be able to supply current to the tube. The tubes had 5 thermocouples on the inside of the tube.

The tubes are named A, B and C as shown in Tab. 4.2. The tubes were installed in the burner at level 8 (tube B), level 23 (tube C) and level 24 (tube A) as already presented in Appendix 1. Tube A and C survived the campaign, and they were used to further develop the theory of the online long-term corrosion measurement using wall resistance measurement. Tube B burned during the second night of the campaign, when temperatures reached above 1000 °C, which caused the tube to break. 5-second measurements were taken on the tube during this process, which gives insight into the usefulness of resistance and temperature measurements.

To adapt the system to withstand higher power levels the shunt resistors for units with a higher power rating were changed. The new shunt resistors were moved outside of the system: and were thermally glued to the shunt resistors for an aluminium heatsink, which was actively cooled with a fan.

Fig. A4.7 (top) presents the behaviour of tube C for 200 W test. The system ran on 200 W power for 18 hours without problems. The changes made to the system described above were successful in preventing overheating. Combing two systems made it possible to test higher power ratings. A successful run on 400 W for about 1 hour on tube C was made as well – Fig. A4.7 (bottom). A run at 600 W caused the system to fail. The shunt resistance did not overheat, but the relays that switch the main power burned.

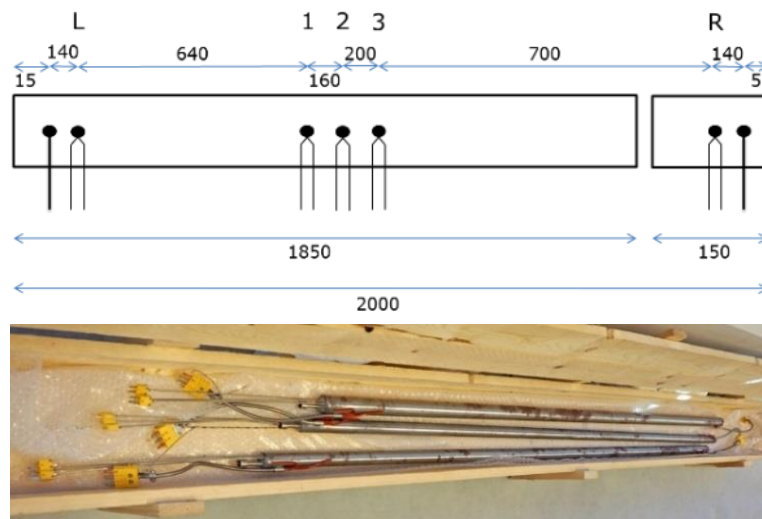


Fig. A4.6 Schematic drawing of measurement tubes. Thick black lines indicate connection wires (Cu or Ni), thin black lines indicate thermocouple wires. Measurement points are labelled L, 1, 2, 3 and R.

Tab. A4.2 Tube materials, dimensions and connection wires

Tube	Material	Length	Outer diameter	Inner diameter	Thickness	Connection wires
A	16Mo3	2 m	30 mm	20 mm	5 mm	Ni
B	16Mo3	2 m	30 mm	20 mm	5 mm	Cu
C	13CrMo4-5	2 m	38 mm	26.8 mm	5.6 mm	Cu

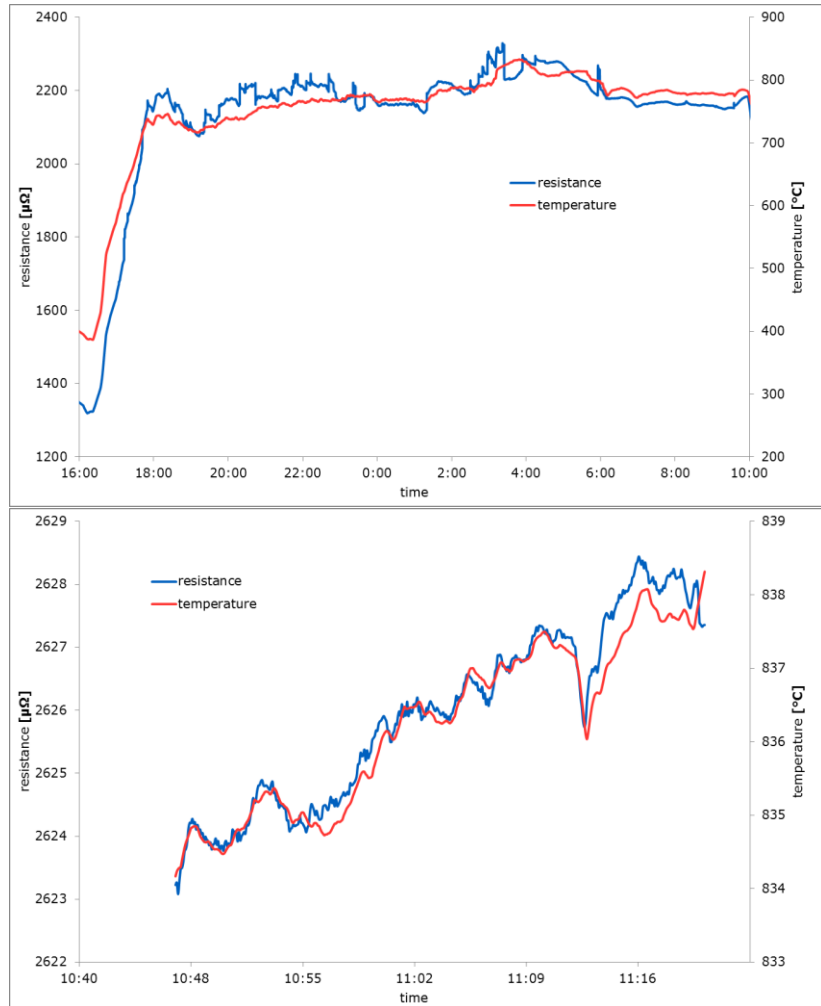


Fig. A4.7 Measurement of tube C resistance and temperature at 200 W (top) and 400 W (bottom)

The baseline resistance at room temperature is calculated from material properties:

$$R_{\text{baseline}}(T_0) = \rho(T_0) \frac{L(T_0)}{A}$$

with ρ the specific electrical resistivity at 20 °C, L the length of the tube, A the surface area of the tube. To determine the α value for both tubes, data from the first day of the measurement campaign with single gas flame (no coal dust) at 600 °C as R_{baseline} (600 °C) was used. Tab A4.3 presents the results of theoretical analysis. Fig. A4.8 shows the resistance and temperature from the experiments. To determine resistance change (red line, primary axis) during the campaign, the following function was plotted:

$$\frac{R(T_0)}{R_{\text{baseline}}(T_0)} = \frac{R(T)}{1 + \alpha(T - T_0)} \frac{1}{R_{\text{baseline}}(T_0)}$$

Temperature (blue line, secondary axis) is also shown. Different coal feeds are separated by vertical black lines. It is possible to make quantitative statements on how the tubes are affected. For tube A, there is no data from 'Sebuku staged' and 'Sebuku unstaged'. During 'US staged', resistance increases strongly, 5 % in 8 hours, before stabilising. During 'US unstaged' and 'Opole staged', the resistance of the tube remains constant. For tube C an increase of resistance during the gas flame period was monitored. There is no visible resistance change during 'Sebuku staged' and 'Sebuku unstaged'. There is no data for 'US staged' and 'US unstaged'. For the last part of 'Opole staged' and during 'Opole unstaged' a slight trend of increasing resistance was noticed.

Tab. A4.3 Tube parameters and results of theoretical analysis

Tube	ρ^*	L	A	$R_{\text{baseline}}(T_0)$	$R_{\text{baseline}}(600 \text{ }^\circ\text{C})$	α
A	$0.19 \Omega \cdot \text{mm}^2/\text{m}$	2 m	398.6 mm^2	$945 \mu\Omega$	$2174 \mu\Omega$	$2.27 \times 10^{-3} \text{ }^\circ\text{C}^{-1}$
C	$0.24 \Omega \cdot \text{mm}^2/\text{m}$	2 m	570.0 mm^2	$842 \mu\Omega$	$1642 \mu\Omega$	$1.16 \times 10^{-3} \text{ }^\circ\text{C}^{-1}$

*value for 13CrMo4-5 from ThyssenKrupp Material Data Sheet P12/T12 (13CrMo4-5). Because literature values for ρ of 16 Mo3 vary greatly, the ρ value for tube A to match the resistance measurement on the tube of 842Ω at room temperature before the campaign was set.

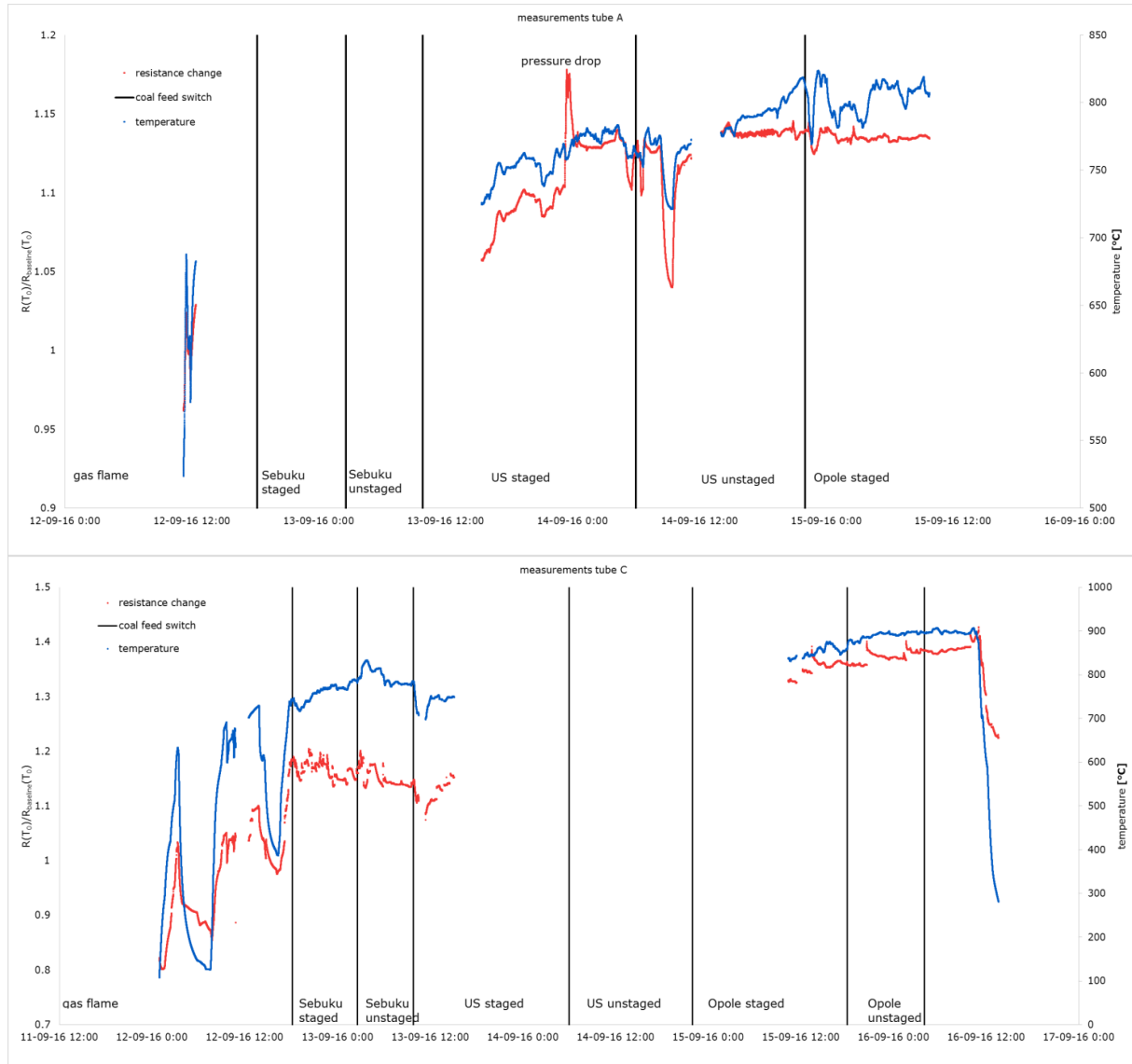


Fig. A4.8 Temperature measurements and calculated resistance change of selected data on tube A during the entire campaign (top). Temperature measurements and calculated resistance change of selected data on tube C during the entire campaign (bottom). Vertical black lines indicate coal types switches.

Fig. A4.8 also highlights the practical limits of this measurement. For high temperature gradients, the linear temperature dependence correction based on one thermocouple is not sufficient. When applying this method in a boiler environment, this should be less critical. On a boiler wall, temperature gradients will be smaller and temperature conditions should be more stable. During this campaign, several settings were tried and different configurations were used. This can also induce biases in the measurement, which makes a qualitative statement on metal loss highly uncertain. During online long term monitoring, this will not play a role, as the system will run in one configuration.

For tube A (16Mo3), a resistance change of 14 % during the campaign was measured (see Tab. A4.4). This corresponds to a thickness loss of 10 %, assuming an uniform loss of thickness. For tube C (13CrMo4-5), a measure a resistance change of 40 % during the campaign was measured. This corresponds to a thickness loss of 25 %, assuming a uniform loss of thickness.

Tab. A4.4 Quantitative and qualitative results of resistance change analysis

TUBE	A	C
Material	16Mo3	13CrMo4-5
EFFECT ON RESISTANCE		
Sebuku staged	no data	no change
Sebuku unstaged	no data	no change
US staged	strong increase	no data
US unstaged	no change	no data
Opole staged	no change	no data
Opole unstaged	no data	small increase
EFFECT OF WHOLE CAMPAIGN		
Resistance change	14 %	40 %
Corresponding thickness loss	10 %	25 %

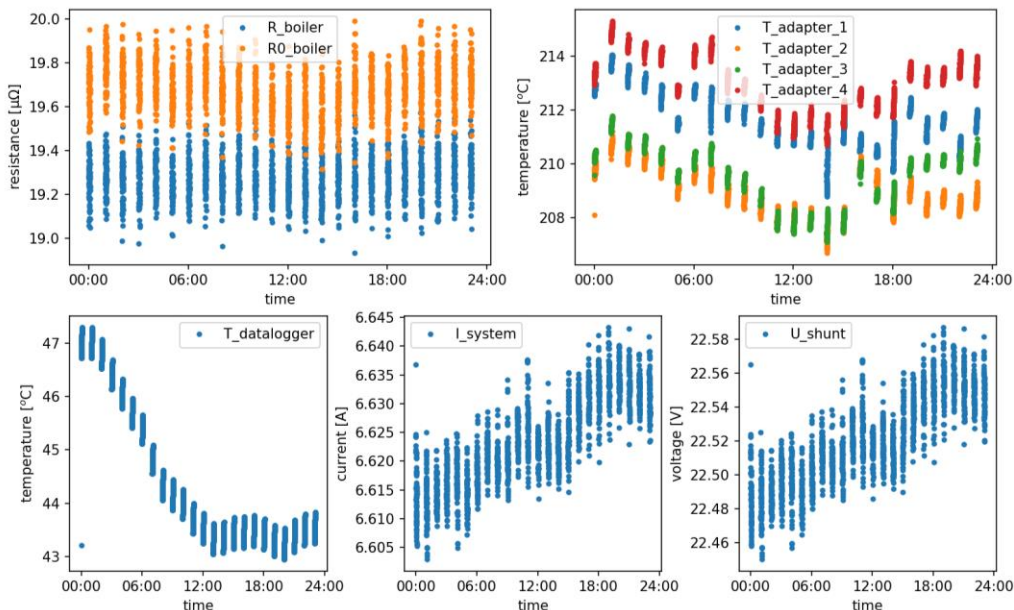
Long-term test in the power plants

Fig. A4.9 Sample data file for one day from BPP

A reduction in the thickness of the boiler wall should lead to increase in the electrical resistance. It is known that the resistance of a boiler wall also depends on temperature. A basic model to describe this process, with linear temperature dependence and a constant rate of wall thickness reduction, was introduced:

$$R(T, t) = R_0 \cdot (1 + a \cdot T) / (1 - b \cdot t)$$

where $R(T, t)$ is the resistance of the boiler wall in Ω as a function of temperature T in $^{\circ}C$ and time t in s, R_0 the resistance of the boiler wall in Ω at $0^{\circ}C$ and at the start of the data analysis. A is the temperature dependence of the resistivity of the boiler wall in $\Omega/{}^{\circ}C$ and B the reduction in wall thickness in ppm/h . For temperature T , the average temperature of adapter B and C was used. In the analysis all days except those with a validity classified as 'FAIL' were included. Applied criteria to the data points to filter out noise were highlighted in Tab. A4.5. The model can be fitted to the data, with R_0 , a and b as free variables. From the value of b , it was possible to calculate remaining wall thickness x with respect to the start of the measurement in % as $x = 100 \cdot b \cdot t / 10000$. From the value of b , it is possible to set a maintenance interval for a certain wall thickness reduction. If, for example, one wants to perform maintenance after a 10 % reduction in wall thickness, the time for maintenance $t_{10\%}$ in hours is $100000/b$. For example, with a wall thickness reduction rate of 4 ppm/h , this would come down to $t_{10\%} = 100000/4 = 25000$ hours = 2.8 years.

Tab. A4.5 Applied data analysis criteria

CMS	standard deviation R	T	standard deviation T
Opole1	< 2 $\mu\Omega$	> 210 $^{\circ}C$	< 5 $^{\circ}C$
Opole2	< 2 $\mu\Omega$	> 230 $^{\circ}C$	< 5 $^{\circ}C$
Belchatow	< 2 $\mu\Omega$	> 170 $^{\circ}C$	< 5 $^{\circ}C$

Several major difficulties were met during operation of the CMS, especially in the case of OPP. Figures A4.10 to A4.12 present the data validity features from all measurements. The left axis determines the feature of the gained data:

- NOMINAL CMS working, boiler running normally
- FAIL CMS not working (no communication, no proper readings)
- COOLDOWN CMS working, boiler cools down during the day
- COLD CMS working, boiler not running
- WARMUP CMS working, boiler warms up during the day
- TEMPERATURE_CHANGES CMS working, large temperature changes in boiler

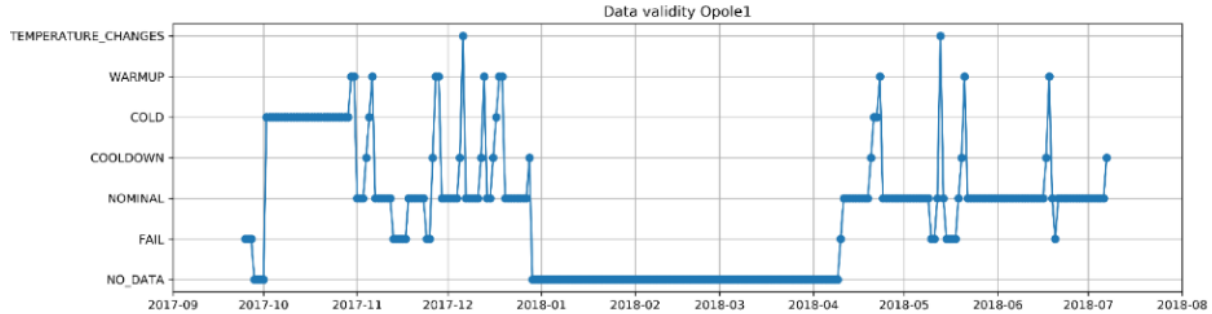


Fig. A4.10 Data validity graph for Opole1

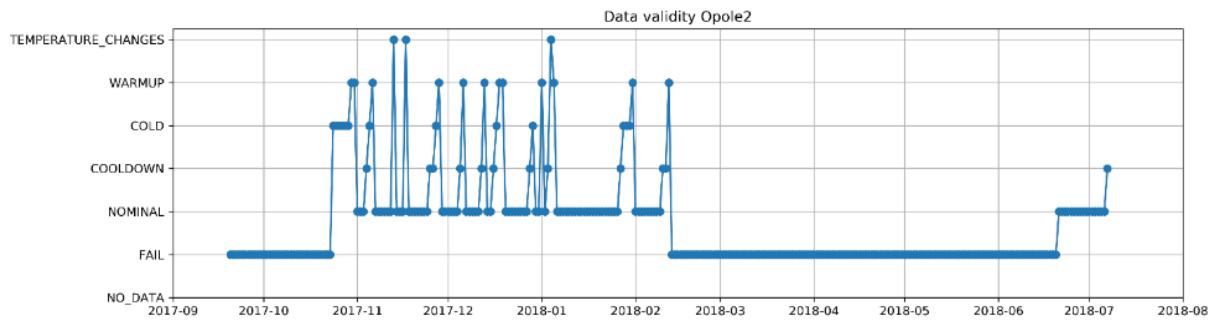


Fig. A4.11 Data validity graph for Opole2

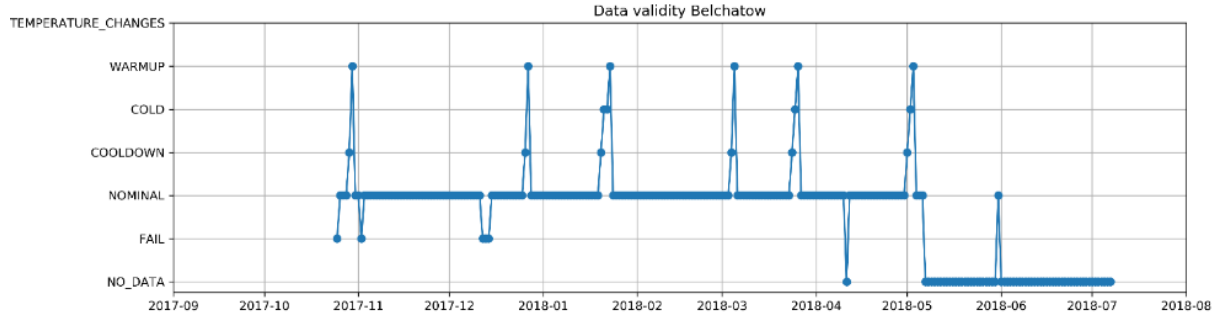


Fig. A4.12 Data validity graph for Belchatów

A5 – DEVELOPMENT OF THE STEAM FLOW METERS

Laboratory experiments.

Several tests were carried out varying medium flow and cooling flow of the sensor, keeping the temperature constant at 350 °C (maximum temp. of first laboratory rig). Using the procedure described above, experimental overall heat transfer coefficients could be measured and compared with the theoretical values as shown in Fig. A5.1 (top). It can be seen that the values of the experimental overall heat transfer coefficient fall on a line, despite the fact that the sensor temperatures and the sensor signals were different for each experiment, indicating that the procedure applied is capable of correlating the experimental values with the theoretical ones. Without this treatment, the sensor signals differ significantly, as shown in Fig. A5.1 (bottom).

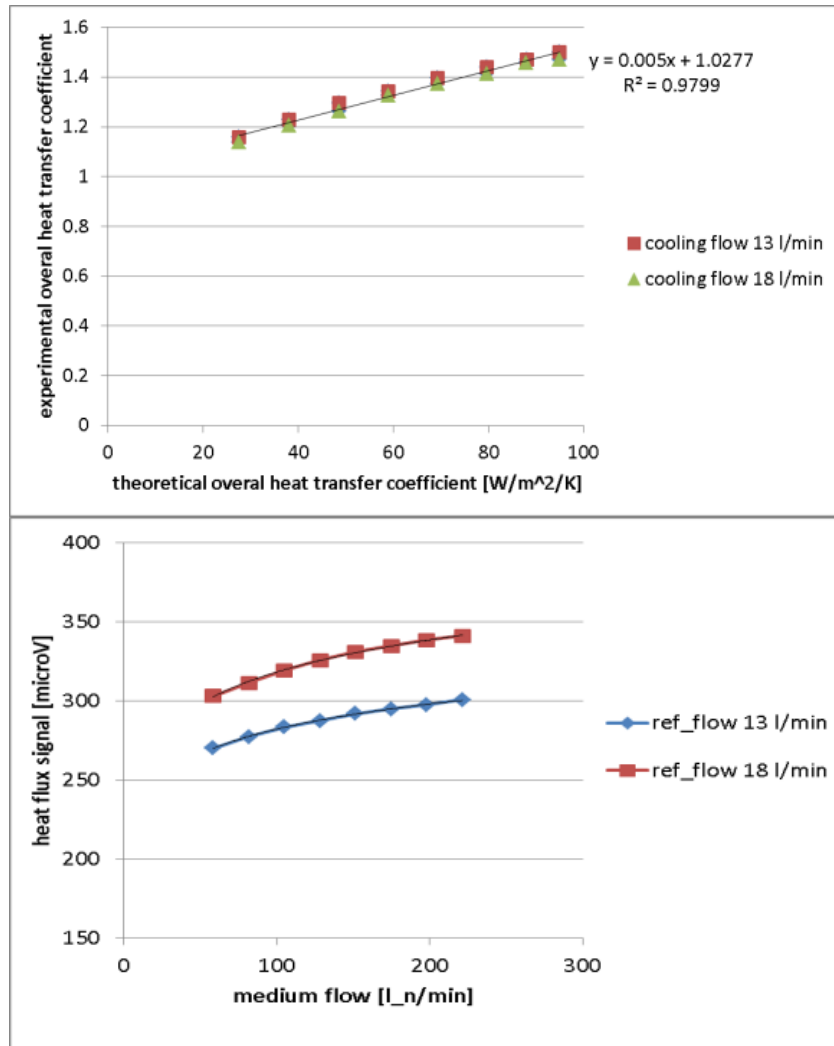


Fig. A5.1 NISTFLOM test results for two different cooling flows varying the pipe flow at constant medium and pipe temperature of T = 350 °C (top); heat flux signals "as recorded" during tests varying the cooling flow (bottom)

The second laboratory rig enables temperatures of up to 570 °C to be reached. Calibrations of the sensors were carried out at 540 °C and 570 °C. Two sensors were calibrated, because it was decided that two sensors would be mounted just after an inlet header in the reheat section, while two other sensors would be placed on the membrane wall. Figures A5.2 and A5.3 show the calibrations of NISTFLOM #1 (the prototype sensor) and NISTFLOM #2.

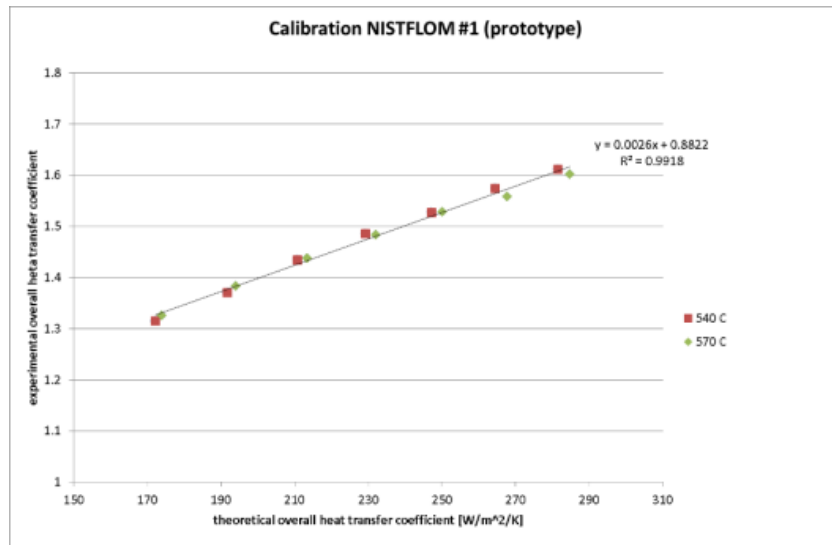


Fig. A5.2 Calibration curve for NISTFLOM #1 (prototype).

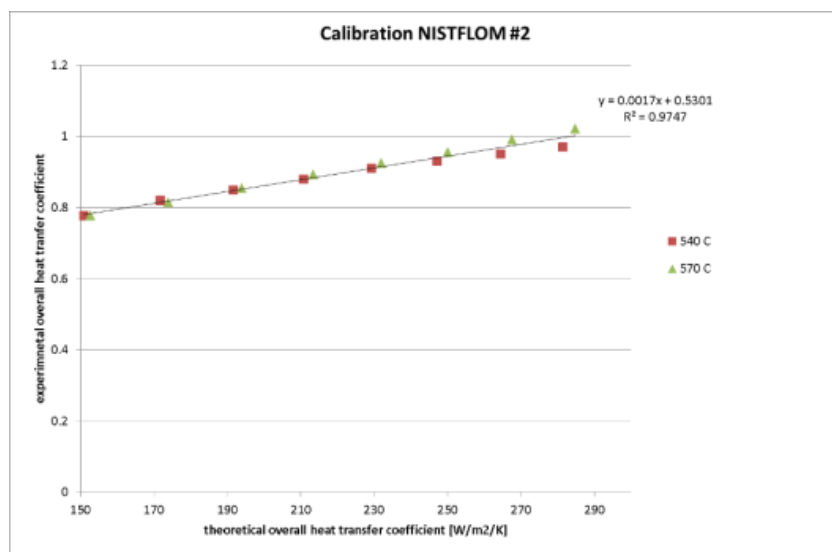


Fig. A5.3 Calibration curve for NISTFLOM #2

Pilot scale tests in boiler no. 3 in OPP

The sensors at level 30m (evaporator) were fully functional and accessible, hence it was possible to connect both cooling air and the data acquisition system

Figure A5.4 shows a measured overall heat transfer coefficient profile as a function of time during a period of several days under full-scale conditions in the boiler. One can see that the overall heat transfer coefficient – which is a function of the Reynolds number (amongst others) which in turn is proportional to the flow velocity and thereby to the flow rate – is fairly constant at the start of the measurement until approximately 10:00h on 04-02-2016. During this period the power plant was operated at constant load and consequently the steam flow was also constant, as can be seen in the figure. From approximately 10:00h until 11:15h a load change took place. Load changes in power plants follow a ramp, which is correctly captured by the steam flow sensor. From 11:15h on 04-02-2016 onwards the plant was operated at constant load again, as indicated by constant steam flow. Measurements of steam flow on the evaporator wall over several days indicate that the sensor was fully capable of monitoring constant load cases as well as dynamic load changes. As (i) the sensor signal analysis is based on single phase medium properties and (ii) the exact steam quality at the location is unknown, it is not possible to draw quantitative conclusions. However, even under two-phase conditions the sensors proved capable of delivering high definition qualitative data regarding the flow changes in the evaporator.

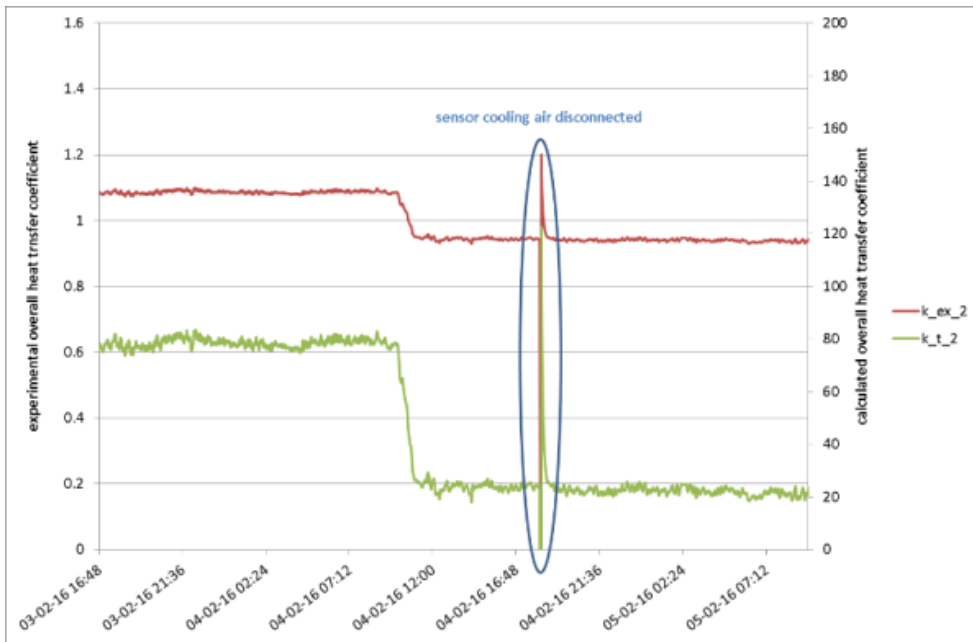


Fig. A5.4 Overall heat transfer coefficient of steam flow in the evaporator measured at OPP using NISTFLOM sensors

During a maintenance shutdown of boiler no. 3 (after 8 months of sensors operation) re-connection of two NISTFLOM sensors at level 60 m was carried out in order to check their status (material damage etc.). Figure A5.5 shows a view of the sensors. The sensors were in good condition despite the lack of cooling air. After fixing the issues with cooling air and attaching new connectors to the sensor tubes, the tests were repeated with those two NISTFLOMs located at level 60 m.

The measured overall heat transfer coefficients of the two sensors installed are shown in Figure A5.6 (top) for the period ranging from 11 November to 28 December 2016. It can be seen from the data that measurement of steam flow over a period of approximately one and a half months is reliable, i.e. no drift of the overall heat transfer coefficient occurs. Furthermore, repetitive load cycles can be captured reliably. Additionally, two (probably unplanned) shutdowns of the power plant were recorded on 15 November 2016 and 3 December 2016. Greater temporal resolution is given in Figure A5.5 (bottom) for the measurement period between 24 December 2016 and 28 December 2016. Fairly dynamic behaviour of the stream flow in the course of the measurement period can be seen with clearer load change patterns until 25 December 2016, followed by a steadier period onwards. The latter was probably due to lower electricity demand during the period between **Christmas and New Year's Eve**.

Figure A5.6 also gives an indication of the measured effective heat transfer coefficient, since the steam parameters (temperature and pressure) change depending on the load regime in which the boiler operates. For construction of the plots, a fixed steam temperature of 540°C was assumed. Once detailed operational data of the power plant is available, the actual steam flow can be analysed in detail and quantified, as will be described in chapter WP4. The NISTFLOM sensors operated in OPP for more than one year. After finishing the above test, they were investigated for a detailed long-term stability evaluation and re-calibration. Initial visual inspection (Fig. A5.5) revealed no damage after real full-scale exposure.



Fig. A5.5 Photograph of NISTFLOM sensor after more than one year of real full-scale exposure

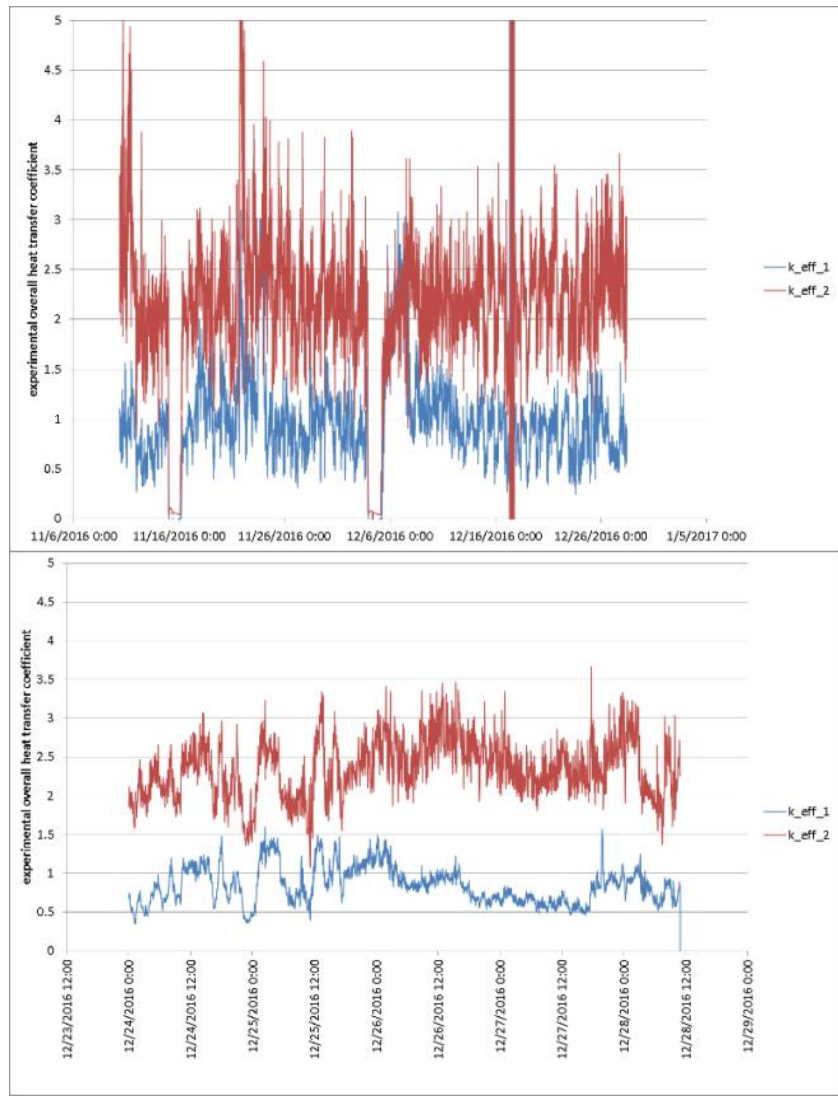


Fig. A5.6 Overall heat transfer coefficient of steam flow in the superheater measured at OPP using NISTFLOM sensors. Measurement period 11/11/2016 – 28/12/2016 (top), measurement period 24/12/2016 – 28/12/2016 (bottom).

Long-term test in the power plants.

A total of six NISTFLOM sensors together with two data loggers were installed in OPP and BPP. Tab. A5.1 gives an overview of the individual pieces of equipment and their locations. The data loggers act both as online data acquisition systems for direct integration into the CIBOP system as well as local data storage devices for manual data transfer via FTP for external checks and quality assurance. Both installations were fully installed in late October 2017 due to the maintenance schedule of the boilers that had to be followed by the investigation teams.

Tab. A5.1 Overview of installed steam flow sensing equipment

identifier	location/level	PP
NISTFLOM #1	superheater/60m	OPP
NISTFLOM #2	superheater/60m	OPP
data logger #1	30m	OPP
NISTFLOM #3	evaporator/30m	OPP
NISTFLOM prototype	evaporator/30m	OPP
identifier	location/level	PP
data logger #2	54m	BPP
NISTFLOM #4	superheater/54m	BPP
NISTFLOM #5	superheater/54m	BPP

When analysing the data obtained from the power plants, it was concluded that the calibration of the NISTFLOM sensors had shifted again, compared to the previous re-calibration at TNO. The latter is

probably due to oxide layers formed on both the sensor body and the adapter piece as well as the different contact interface steam pipe – sensor as compared to the ideal situation used at laboratory scale for calibration of the sensors. Hence, it can be concluded that, at least with the current methods and materials used, absolute steam flow measurement is not possible.

The absolute amount of steam flowing through a pipe is a quantity required for calculating the heat uptake of the individual pipe; see the schematic in Fig. A5.7. With knowledge of the intensive quantities T_{steam} and p_{steam} at the inlet and the outlet of the steam pipe and the steam mass flow, the total heat uptake by pipe \dot{Q} can be calculated. The steam pressure and temperature at the inlet can be assumed to be equal to values found in the inlet header, which are continuously monitored in power plants. The outlet pressure can be assumed to be equal to the pressure in the outlet header, and the steam outlet temperature in the steam pipe has to be measured by means of a thermocouple. The latter is readily done in most modern power plants. Using these values, the specific enthalpies h_{in} and h_{out} can be calculated by means of a steam table. The NISTFLOM sensors should ideally be mounted on the steam pipe directly after the inlet header in order to minimise the uncertainties concerning steam temperature. Since it was found that the absolute steam flow is not measurable with the current system, only relative values of the mass flow, and hence of the heat uptake can be obtained. The latter is sufficient for assessing deposit build-up and thermal stress of the pipe that can lead to spalling. By normalising the individual experimental total heat transfer coefficients (which can differ significantly per sensor), a relative signal can be generated. The latter treatment is shown in Fig. A5.8 for the NISTFLOM signals recorded at BPP on superheater P3 during the long-term measurement in WP4.

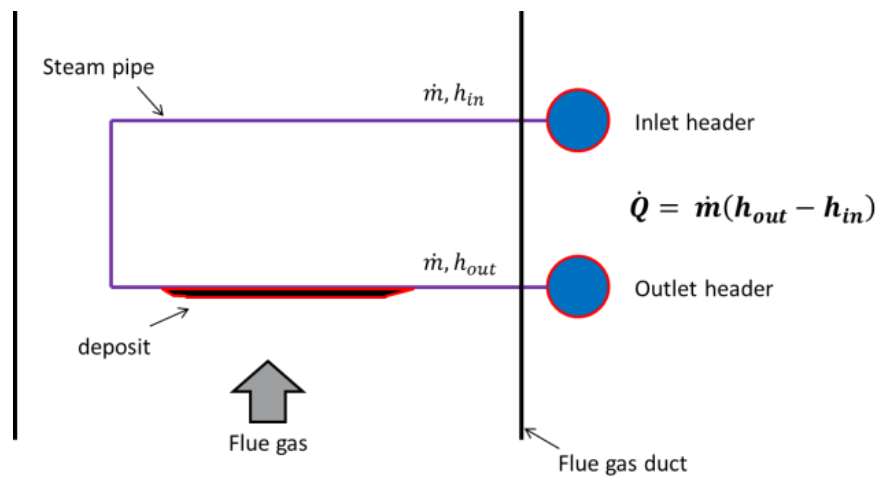


Fig. A5.7 Schematic of the heat uptake of a steam pipe in the convective section of a boiler

It can be seen that the normalised total heat transfer coefficients fall in the same order of magnitude, i.e. they correspond to the same magnitude of steam flow, which would be expected since ideally all steam pipes carry similar amounts of steam. The latter implies that a sensor calibration is only not possible, but also not necessary for assessing the information of interest, which reduces the maintenance burden of the system. Furthermore, it can be seen from the generated data that the flows through the pipes that are connected to different inlet and outlet headers resemble flows of communicating pipes, i.e. when the flow through one pipe reduces, the flow through the other pipe increases. The latter information is not accessible by other monitoring means in a power plant and can give valuable information about the thermal stress of the piping system.

While the NISTFLOM system generated data reliably over a course of roughly 8000 hours, it can be seen that there is a signal shift over the course of time. The latter can be due to internal fouling of the sensor by oil and/or dust carried with the cooling air or by ongoing corrosion of the interfaces between steam pipe-adapter-sensor body. The latter needs further investigation, but at the time of writing the sensors were still installed in the power plants, hence no evaluation was possible. However, when assessing the heat uptake of the pipes and the thermal stresses imposed, much shorter time scales are relevant, i.e. in the order of a few hours, and simple periodic re-normalisation of the signals might be sufficient for daily practice.

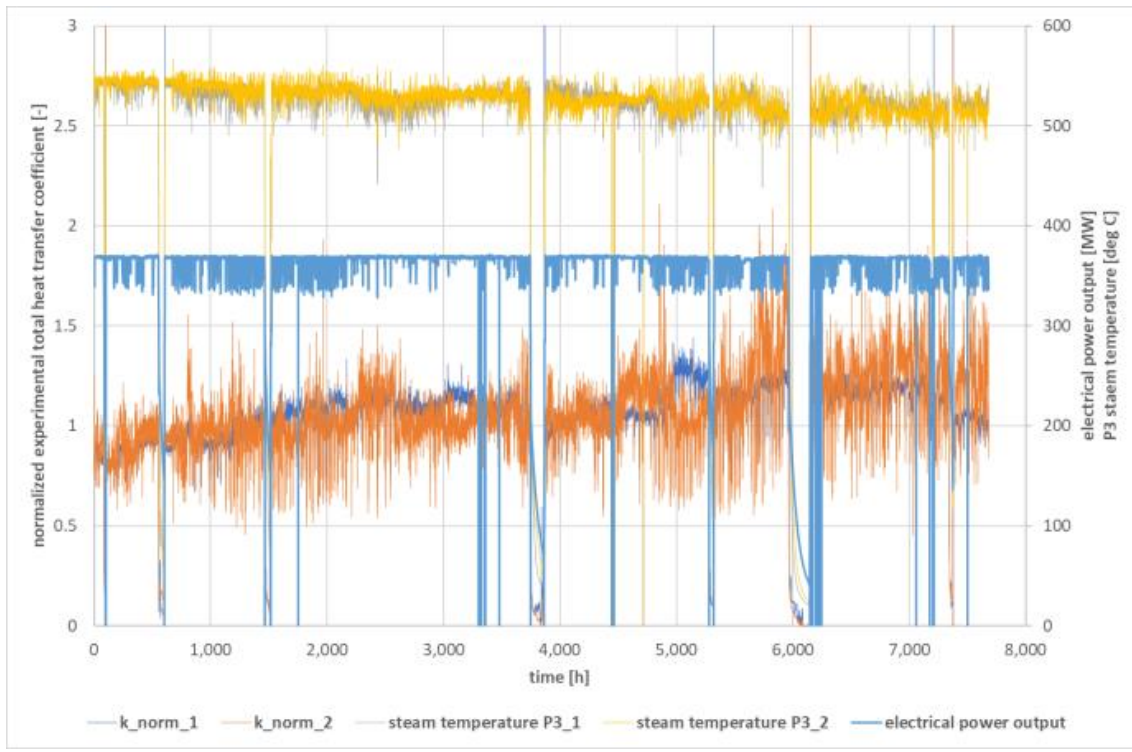


Fig. A5.8 Normalised total heat transfer coefficients measured with NISTFLOM at BPP

A similar plot of the recorded normalised experimental total heat transfer coefficients measured on the evaporator at OPP is shown in Fig. A5.9. Here too, stable operation of the sensors can be seen. The signal shift here is apparently less pronounced than for the measurements at BPP, which might be due to the lower steam temperatures in the membrane wall and subsequently less sensor fouling. A thorough inspection of the sensors could shed light on the cause of the signal shift after return of the sensors to TNO.

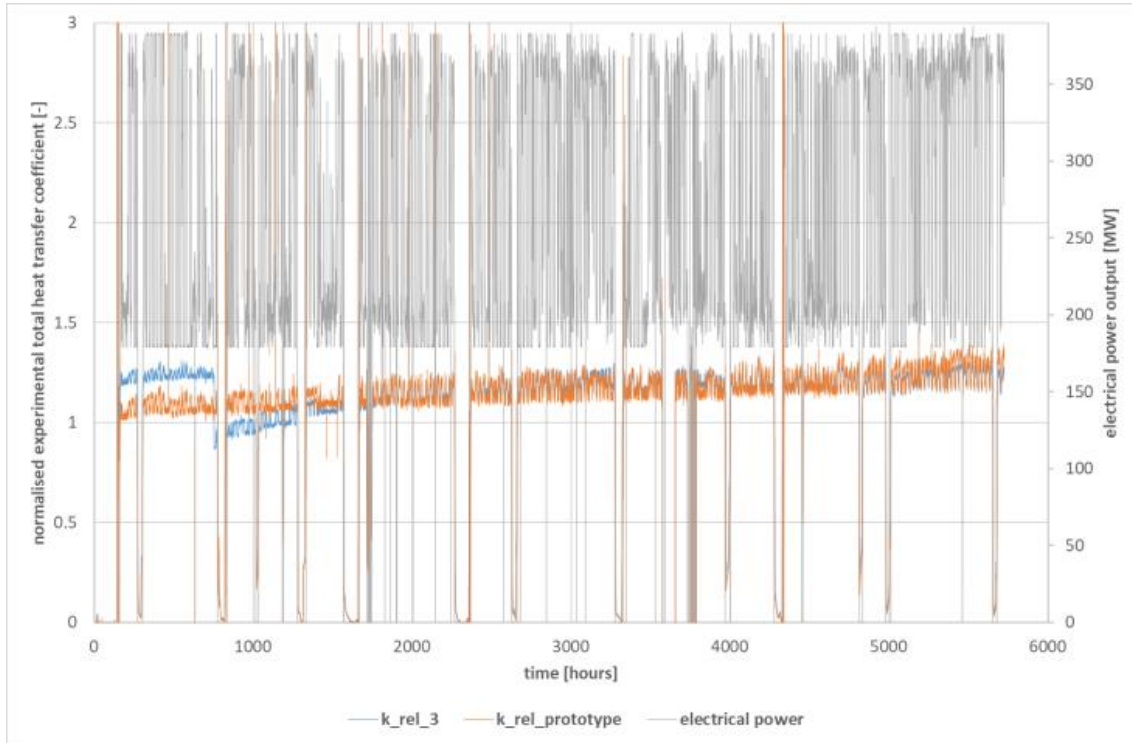


Fig. A5.9 Normalised total heat transfer coefficients measured with NISTFLOM on evaporator at OPP

The NISTFLOM sensors #1 and #2 installed on the superheater at OPP were mounted during a maintenance stop of the power plant. During installation, the cooling air flow was set to a level where sufficient cooling of the sensors was expected. However, after having received the measurement data from the sensors, it appeared that the cooling air flow was too little, or, and more likely, that the cooling air supply pipes of the sensors came into contact with the hot steam pipes entering the collection header

during re-insulating of the header bank, resulting in pre-heated cooling air. As a consequence, the temperature difference between the steam pipe and sensor was very small, sometimes close to zero and below. Bearing in mind that the total experimental heat transfer coefficient is defined by the heat flux through the sensor divided by the temperature difference between steam pipe and sensor, it is obvious that – to obtain meaningful data – the temperature difference must not take small values close to zero. However, this situation was observed after the long-term testing period during data analysis, hence no countermeasures could be taken at that stage. The raw heat flux data is unaffected by this circumstance and is shown in Fig. A5.10. Hence, it can be concluded that the sensors were working properly and only the sensor cooling was insufficient for further evaluation of the results.

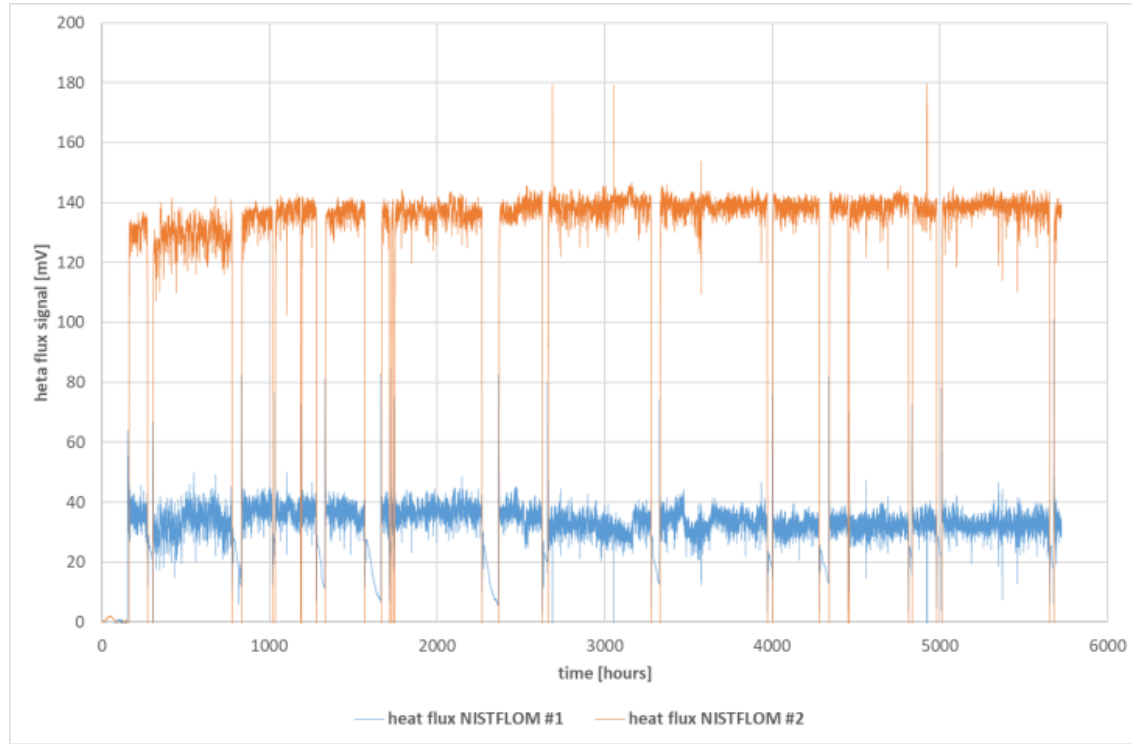


Fig. A5.10 Normalised total heat transfer coefficients measured with NISTFLOM on P3 superheater at OPP

A6- Development of intelligent software

Slagann module.

The Slagann module consist of two parts:

- the expert system (ES) which can estimate the combustion chamber outlet temperature of flue gases (1 D model),
- neural network (ANN) part which can estimate the slagging behaviour of fuels or fuel blends without laboratory experiments (except for the ANN training period).

The ES computes the outlet temperature from the combustion chamber for given geometry, burners arrangement, fuel quality and other important parameters and is a 1D model based on the empirical method. ES computes the outlet temperature by solving nonlinear equations [11].

The ANN part estimates two important slagging parameters: T_{beg} and k_z (determined experimentally in 20 kW IEN slagging reactor – see chapter 2.3.1) on the basis of proximate analysis of fuel and mineral analysis of ash. In the learning phase of ANN these parameters are taken from a database created during experiments. In the working phase of the ANN these parameters are estimated by the ANN and laboratory experiments are no longer needed.

Fig. A6.1 shows the main tasks of the described method.

During operation of the module the user determines the input parameters of the fuel (ash content, calorific value, ash mineral analysis) currently used in the boiler, other parameters of the fuel, geometry of the boiler and basic parameters describing the current combustion process such as boiler load, excess air, efficiency etc.

As presented in Fig. A6.1 the input values have to be known otherwise the model will not work. After the user provides the input data, k_z , T_{beg} and T_{out} are computed by the model. Then relative slagging intensity B_z is calculated (see A2). Depending on the value of B_z the risk (probability) of slagging in the combustion chamber is determined in four classes: low, medium, high and very high. After this, depending on the chosen class, the new coefficient ψ of fouling the combustion chamber walls is determined. As the last step, the new (if slagging occurs) outlet temperature T_{out} from the combustion chamber is computed.

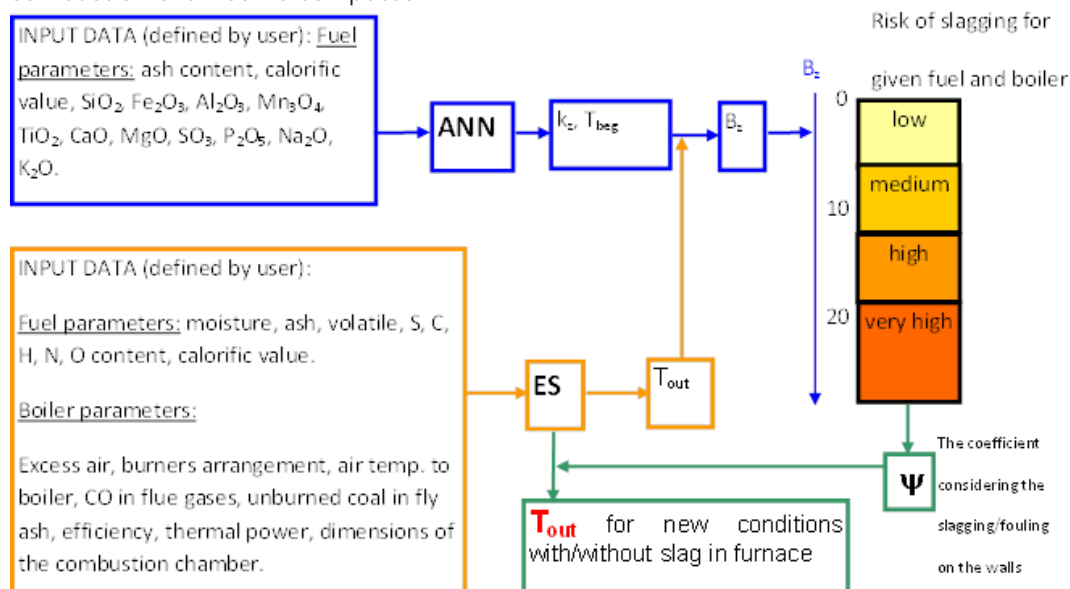


Fig. A6.1 Schematic chart of Slagann software operation

When developing the software in CERUBIS the main points of focus were:

- training the ANN with an enlarged database of slagging properties of fuels,
- developing a 3D ANN model of the boiler to better estimate the outlet temperature from the combustion chamber,
- changing the functionality of the user interface.

In the case of ANN, a PCA-MFNN hybrid network was used for estimation of k_z and T_{beg} . Principal component analysis (PCA) is a well-known and widely used statistical technique. In general, PCA finds an orthogonal set of directions in the input space and provides a way of finding the projections into these directions in an ordered fashion. The first principal component is the one that has the largest projection (the projection is the shadow of the data cluster in each direction). Since PCA orders the projections, the dimensionality can be reduced by truncating the projections to a given order. Sanger and Oja [13] demonstrated that PCA can be accomplished by a single layer linear neural network (Fig. A6.2) trained with a modified Hebbian learning rule.

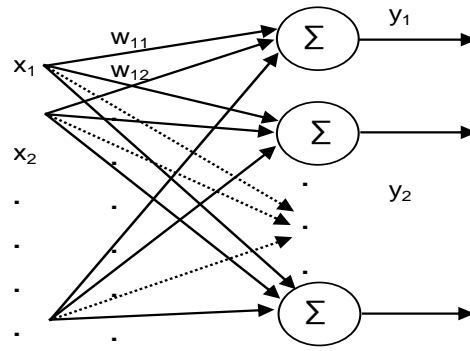


Fig. A6.2 PCA network to project the data from D to M dimensions (x - inputs, w -weights, y - outputs)

PCA-MFNN hybrid network was proposed with one hidden layer with statistical analysis of outputs which classifies which results are acceptable on the basis of averages and standard deviations of twenty trained-and-tested neural networks.

The main investigated elements of ANN were : number of principal components (PC) ranging from 3 to 8, number of hidden neurons (HN) ranging from 6 to 10 and multiplication of training patterns by random duplication of existing training data. Levenberg-Marquardt training algorithm was used to train the supervised part of the network – MFNN, whilst for unsupervised – **PCA, Oja's rule was used**. In MFNN tanh activation function was used both in hidden and output layer. 45 sets of data were chosen for training while 8 sets for testing.

Figures A6.3 to A6.6 present the final results of PCA-MFNN simulations. The graphs present training results, average testing results and the best test results. In a case of single MFNN, no satisfactory results were obtained. In that case the training process was unstable, very often not reaching the intended threshold. In a case of hybrid PCA-MFNN for 3-4 PC elements, similar behaviour was observed during training but testing results were more promising. Best results were obtained for PC ranging from 5 to 8. Further increase of PC does not decrease the test error and starts to increase training time. For some testing sets, no satisfactory results were obtained. This might be caused by e.g. not enough training data sets or inappropriate training data set selection for training. The presented test results are averages from 20 ANN. Results with overly high standard deviations were deemed too uncertain.

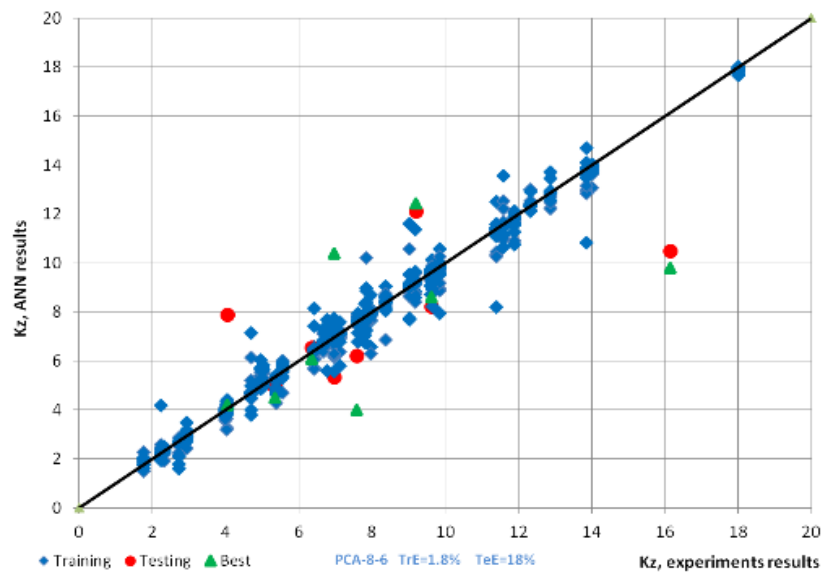


Fig. A6.3 PCA simulation results for k_z predicting for 8 PC elements and 6 hidden neurons

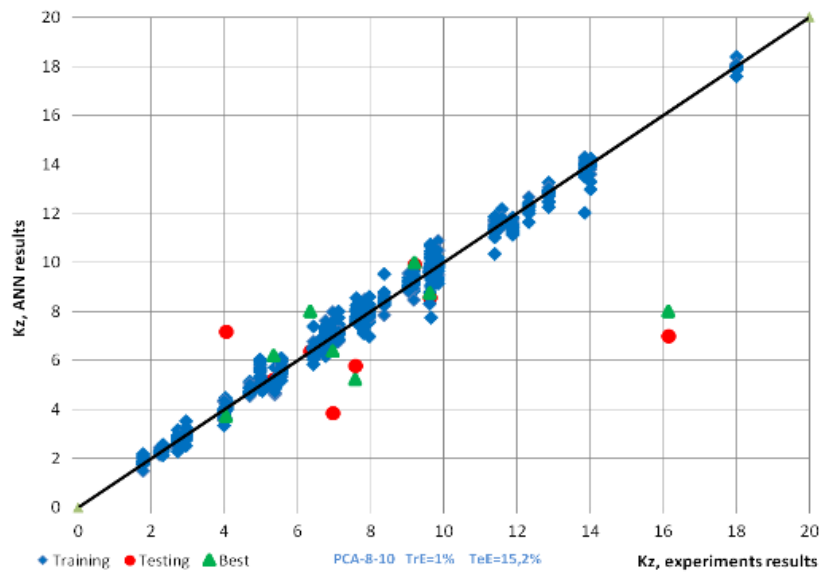


Fig. A6.4 PCA simulation results for kz predicting for 8 PC elements and 10 hidden neurons

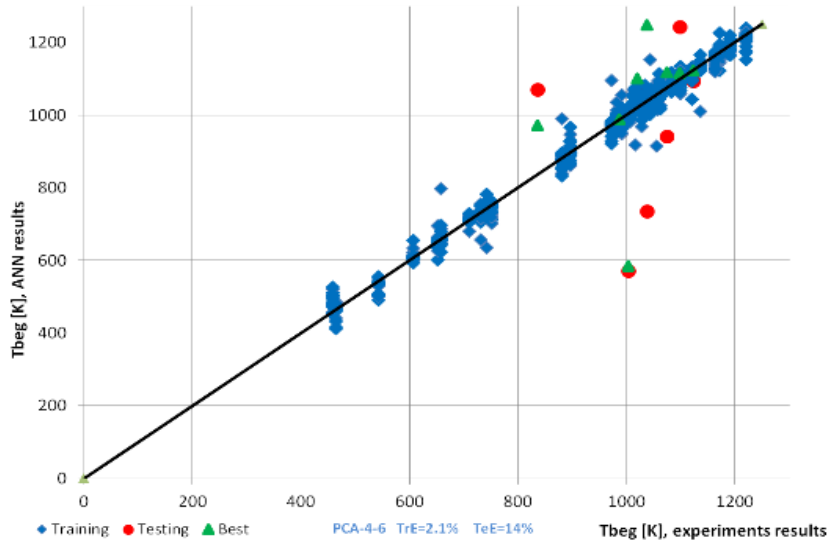


Fig. A6.5 PCA simulation results for Tbeg predicting for 8 PC elements and 6 hidden neurons

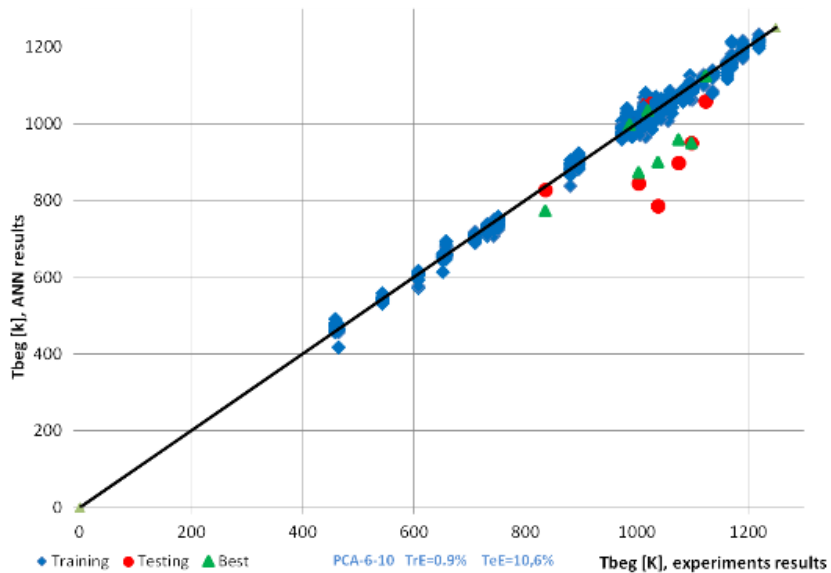


Fig. A6.6 PCA simulation results for Tbeg predicting for 8 PC elements and 10 hidden neurons

Fig. A6.7 presents the linear and average PCA-MFNN sensitivity analysis between inputs (more important ash components) and outputs (k_z and T_{beg}) of ANN

In general, there is no linear correlations of searched parameters with ash mineral analysis. Maximum values of linear correlation coefficient can be found for silica, potassium, aluminium and titanium in relation to T_{beg} which seems to be a more realistic parameter compared to k_z intensity. In the case of PCA-MFNN, sensitivity for T_{beg} and k_z covers each other and reaches a maximum for phosphorus and potassium. However, other parameters of ash are also important in PCA-MFNN performance.

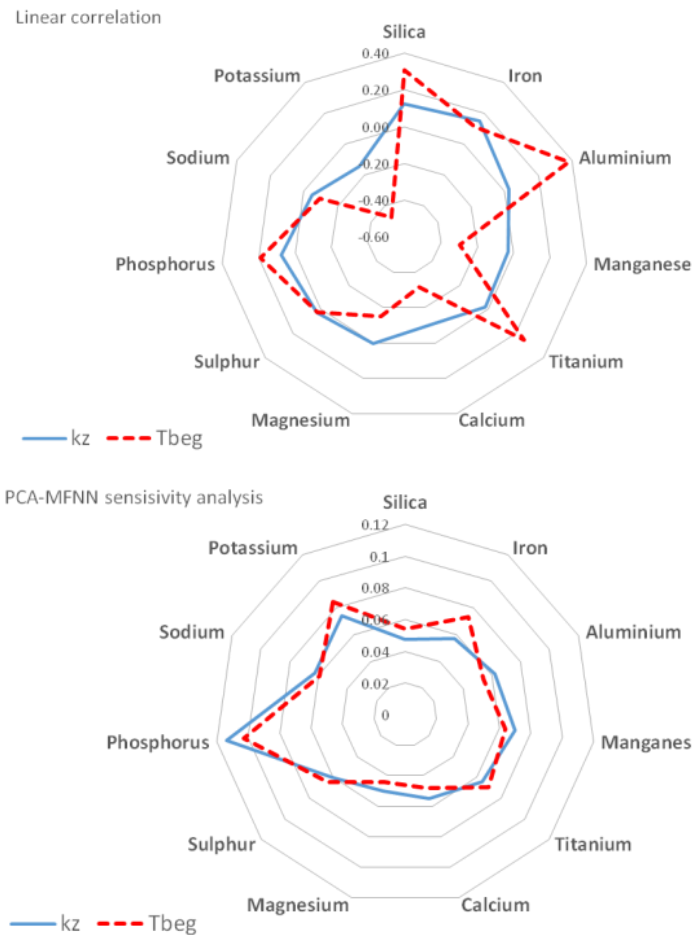


Fig. A6.7 Linear correlation and PCA-MFNN sensitivity analysis between inputs and outputs of ANN

For 3D ANN model of the boiler in order to estimate the outlet temperature of flue gases from the combustion chamber (dependent on slagging/fouling factors) training data from CFD calculations of both boilers was planned to be used. However, due to difficulties with CFD calculations of BPP boiler, only data from boiler no. 3 in OPP was used. During CFD calculations of several real cases, the CFD model was calibrated and verified. The outlet temperature of flue gases from the combustion chamber was determined by CFD, as presented in Tab. A6.1. In order to get more training data for ANN training, 24 cases were computed where load of the boiler, configurations of working mills, air flows etc. were changed in order to map possible inputs and outputs for the ANN using input data from boiler measurements carried out and described in chapter 2.3.3. Then, for 11 additional cases, the input data were determined manually (380 MW and 180 MW).

Tab. A6.1 CFD cases, cases 1-3 from CERUBIS main campaign, cases 4-24 from additional measurement, cases 25-35 set "manually" in order to increase training data

Case no	1	2	3	4	5	6	7	8	9	10	11	12	13	14	15	16	17	18
Power MWe	380	300	230	380	380	380	380	180	180	180	330	330	330	330	230	230	230	230
Mills in operation	1234	1245	245	1234	2345	2345	1345	1345	135	135	135	135	135	135	125	125	125	135
Total excess air	1.12	1.14	1.23	1.12	1.14	1.11	1.12	1.12	1.26	1.26	1.24	1.14	1.14	1.15	1.16	1.22	1.21	1.24
Burners belt excess air	0.88	0.86	0.91	0.88	0.91	0.84	0.89	0.93	0.96	1	0.98	0.87	0.91	0.92	0.89	0.9	0.9	0.93
Temperature on outlet of comb. chamber [K]	1365	1320	1230	1300	1395	1405	1370	1365	1220	1210	1235	1310	1320	1345	1290	1220	1205	1215

Case no	19	20	21	22	23	24	25	26	27	28	29	30	31	32	33	34	35
Power MWe	230	230	280	280	280	280	380	380	380	380	380	380	180	180	180	180	180
Mills in operation	135	135	235	235	234	234	2345	2345	2345	2345	1235	1235	1235	235	235	235	235
Total excess air	1.24	1.24	1.12	1.16	1.17	1.17	1.11	1.12	1.11	1.12	1.14	1.13	1.14	1.23	1.24	1.25	1.23
Burners belt excess air	0.93	0.95	0.84	0.87	0.88	0.91	0.87	0.88	0.84	0.87	0.86	0.89	0.86	0.98	0.97	0.94	0.99
Temperature on outlet of comb. chamber [K]	1222	1205	1240	1245	1230	1255	1385	1405	1390	1370	1390	1380	1375	1185	1190	1195	1190

Input to ANN were: power of boiler, coal feeder rate and all air flows (in sum, 25 inputs). The output as mentioned was always the outlet temperature of flue gases (just before first superheater). Of the 35 cases calculated by CFD, 29 were used for training and 6 for testing.

For error estimation, mean squared prediction error MSPE was used:

$$MSPE = \frac{\sum_{i=1}^n (dd_i - dt_i)^2}{n} * 100$$

where dd_i is normalised expected value (real value), dt_i is normalised estimated by ANN value, n number of samples.

Tab. A6.2 shows the results of ANN performance. Test were carried out in two regimes: firstly only using data from cases which were carried out in reality (24 cases) and then cases used both in reality and manually set cases (35 cases).

Tab. A6.2 MSPE for training and testing of ANN predicting outlet temperature from the combustion chamber, boiler no 3 OPP

MSPE/Case		380 MW cases	280-330 MW cases	180-230 MW cases
24 cases	MSPE train	4.05	5.25	7.2
	MSPE test	12.4	15.4	19
35 cases	MSPE train	3.54	4.87	5.45
	MSPE test	11.8	15	14.5

It can be seen that adding manually set cases decreases particular errors, especially in cases 180-230 MW. Good test results were obtained as well, MSPE reaching 10-20 % for 24-35 cases is reasonable. It has to be underlined that during real scale measurements it was not possible to measure the temperature before superheater, so the results presented here are a comparison of CFD and ANN data (there is an assumption that CFD credibility is good).

Fig. A6.8 presents a view of the Slagann graphical user interface after development in the CERUBIS project for BPP boiler and Fig A6.9 for OPP boiler. The software was created in Matlab environment. To summarise, reasonable predictions of index of slagging intensity (k_z) and beginning temperature of slagging (T_{beg}) were obtained for the PCA-MFNN hybrid network, with statistical analysis of output data. It was found that more than 4 PC elements and Oja's rule –instead of Sanger's rule – should be applied. There are still some prediction errors, especially for slagging intensity k_z , which are too high or results which have overly high standard deviations. Duplication of existing training data sets does not have a visible effect on ANN performance. The ANN 3D model for predicting outlet temperature of flue gases from the combustion chamber gives reasonable results. Increasing the number of training cases decreases the error.

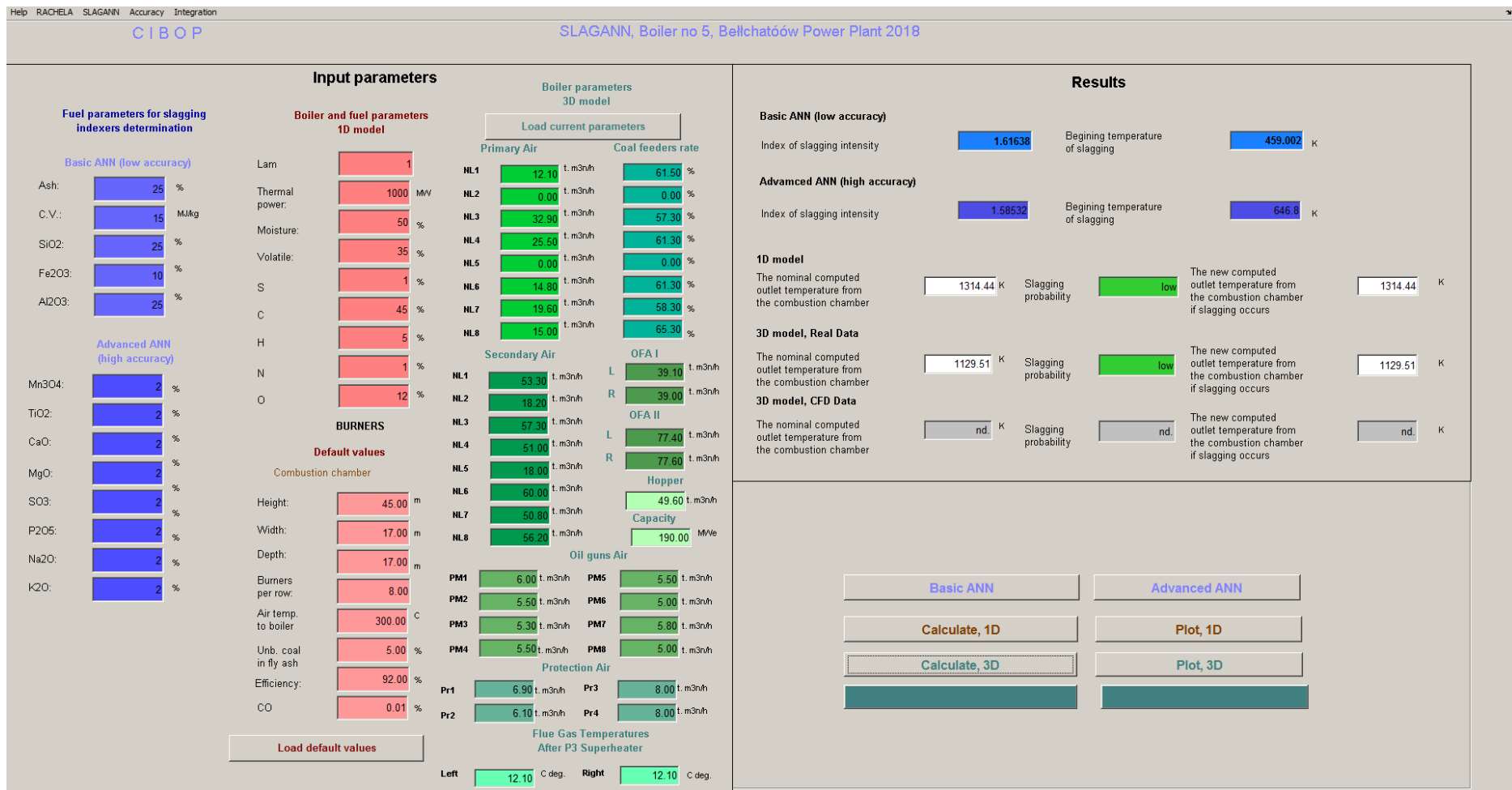


Fig. A6.8 View of Slagann user interface for the BPP boiler

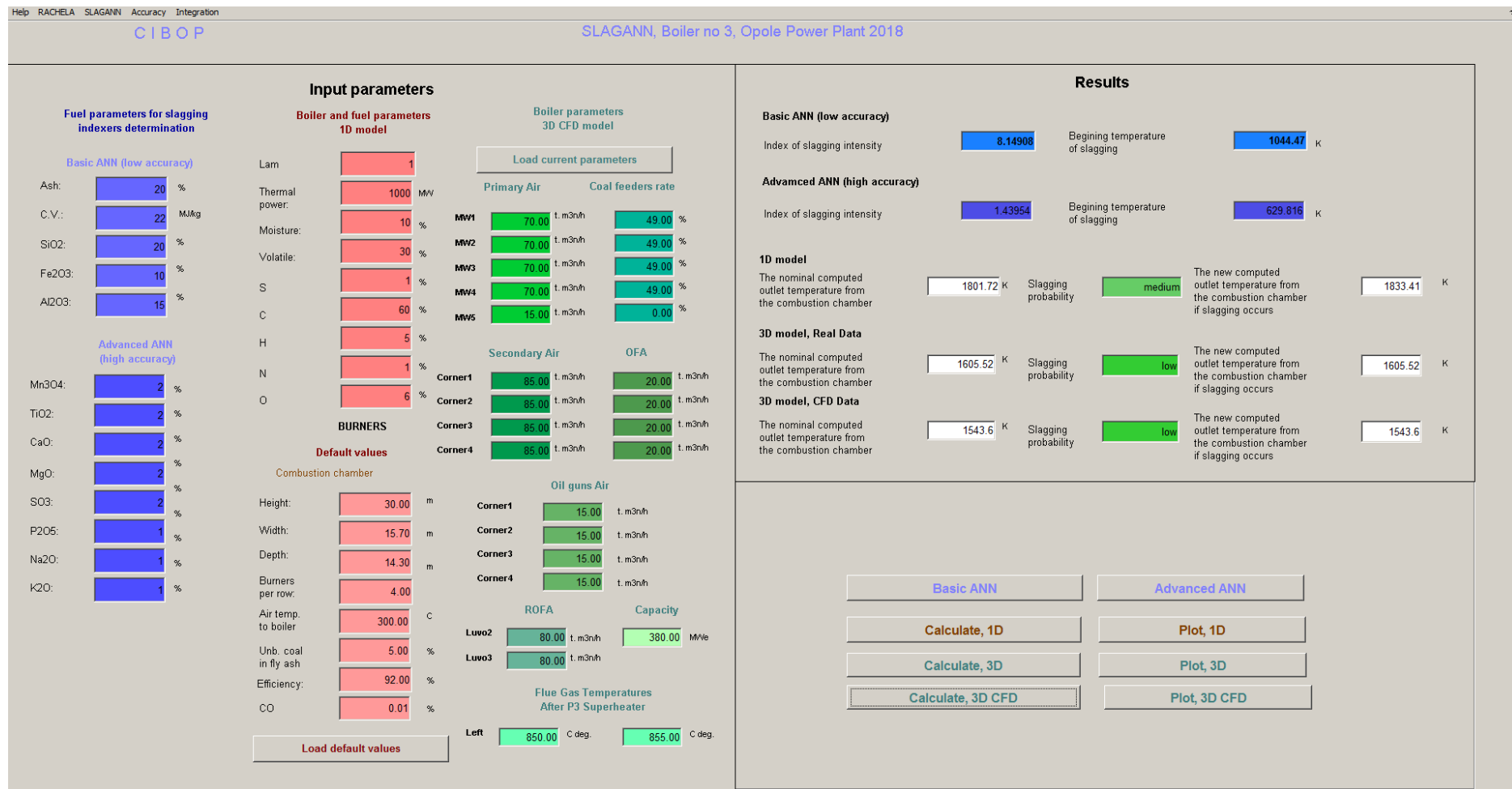


Fig. A6.9 View of Slagann user interface for the OPP boiler

Rachela module

The starting point for corrosion module Rachela was previous software: Dawid and Rachel.

Dawid software consisted of:

- ANNs which can estimate O₂ concentrations in the boundary layer of the evaporator wall on the basis of O₂ indications from several sensors on the given wall,
- ANNs which can estimate CO concentrations in the boundary layer of the evaporator wall on the basis of O₂ indications from several sensors on the given wall,
- ES which can estimate the risk of corrosion.

The software worked on the basis of continuous measurement of O₂ at several locations on each wall of the evaporator and on the artificial neural network (ANN) which determines the concentration of O₂ and CO in other areas of the walls where preliminary multi-cases measurements of O₂ and CO concentrations were carried out. Each particular ANN usually had 4-6 inputs (O₂ measurements on a particular wall) and 1 output (O₂ or CO on that wall at a given place) and usually 6-9 neurons in one hidden layer.

Tanh transfer function was used in the hidden layer and linear or tanh in the output layer. Typical Back Propagation algorithm was used to train the ANN. On the basis of ANN predictions of O₂ and CO, maps of O₂ concentration and corrosion risk were determined. Corrosion risk was determined on the basis of an expert system. Tab. A6.3 presents the thresholds in ES which determine the risk of corrosion together with assigned colours. After calculation, the software could visualise O₂ and corrosion risk maps on each wall.

Tab. A6.3 Previous criteria for corrosion risk estimation. O₂ and CO in %_{mol}

None	Very Small	Small	Average	High	Very High
O ₂ ≥ 5	4 ≤ O ₂ < 5 & 0.2 ≤ CO < 3	3 ≤ O ₂ < 4 & 0.2 ≤ CO < 3	3 ≤ O ₂ < 5 & CO ≥ 3	1 ≤ O ₂ < 2 & 0.5 ≤ CO < 1	O ₂ < 1 & CO ≥ 0.5
3 ≤ O ₂ < 5 & CO < 0.2	2 ≤ O ₂ < 3 & CO < 0.2	1 ≤ O ₂ < 2 & CO < 0.2	1 ≤ O ₂ < 2 & 0.2 ≤ CO < 0.5 O ₂ < 1 & CO < 0.2 2 ≤ O ₂ < 3 & CO ≥ 3 2 ≤ O ₂ < 3 & 0.2 ≤ CO < 3	O ₂ < 1 & 0.2 ≤ CO < 0.5 2 ≤ O ₂ < 3 & CO ≥ 3	1 ≤ O ₂ < 2 & CO ≥ 1

Rachela software consisted of:

- Several ANNs which can estimate NO_x, CO, LOI and average O₂ concentrations in the boundary layer for all walls (one value),
- GA (Genetic Algorithm) optimiser which optimise mainly the O₂ concentrations in the boundary layer of the evaporator (maximising) and NO_x emission (minimising) through air flows in the boiler.

In Rachela software the former neural network model of boiler consisted of several separated ANNs (FFMLP networks with 5-8 hidden neurons): one for NO_x, one for CO outlet boiler emissions, one for LOI and one for O_{2w} determination in the whole boundary layer of evaporator. Capacity of boiler, air flows and coal feed rates were used as inputs to these ANNs. After the learning process, the ANNs were used in GA to find primary and secondary air (including OFA) flows which would minimise the NO_x, CO, LOI and danger of high temperature corrosion, which was done mainly by maximising O_{2w} in the boundary layer of the combustion chamber. An assumption was made that coal feed rates, cooling air to oil burners and total air are not changed, as compared to input values. The objective function was determined as follows:

$$\Phi = \text{alfa} \cdot Y_{NO_x} + \text{beta} \cdot Y_{O2w} + (1 - \text{alfa} - \text{beta}) \cdot (Y_{CO} + Y_{C_p})$$

where *alfa* and *beta* are special coefficients (*alfa+beta≤1*), Y_{NO_x}, Y_{CO}, Y_{UBC} are predicted values of outlet boiler emissions and LOI, and Y_{O2w} inversion of average O₂ concentration in the boundary layer of the combustion chamber.

In the above formula there are two coefficients whose values should be stated before optimisation. These coefficients are decisive in determining which optimised value the boiler operator should put more stress on. A bigger *alfa* value means optimisation in the direction of NO_x optimisation, whilst a bigger *beta* value means better protection of waterwalls of the combustion chamber. Too high *alfa* will cause rapid CO and LOI increase. As a result of running Rachel, new air settings were determined for better protection of waterwalls, at the same time keeping NO_x at an acceptable level.

During development of the corrosion module in CERUBIS it was decided to continue the idea of Dawid and Rachela software by improving them and joining them in one graphical interface window. In the development process the main focus was put on:

- Showing more practical data in the main window, like averages of O₂ and CO for a given wall, visualisation of some boiler parameters, like power, configuration of working mills, emissions, O₂ at the outlet of the boiler etc.,
- Introduction of averages of O₂ and corrosion risk through a given period of time (from several hours up to one year),
- Introduction of wall thickness loss maps and the abovementioned averages on the basis of periodically made evaporator wall thickness measurements,
- Adding the measurements from partners' sensors,
- Preliminary diagnostic (level of creditability) of given O₂ measurements indicated by colours,
- Increasing the number of inputs to ANN (beside 3-6 O₂ sensor inputs more inputs like power, air flows etc.) in order to increase creditability,

- Development of other ANN to predict O₂ and CO in the boundary layer of the evaporator in case of O₂ sensor failure, based only on inputs from DCS of the boiler,
- Increase the visual quality of O₂ and corrosion risk maps,
- Improving the accuracy of the optimiser.

Figures A6.10 and A6.11 and Tabs. A6.4 and A6.5 show example results of training and testing of ANNs for low (27) and high (43) number of cases and two sets of inputs to the ANN for the right wall of the BPP boiler. The first set of inputs consists of six inputs – only indications of O₂ sensors for the given wall. The second set of inputs to the ANN consists of fifteen inputs: six as previous O₂ sensor indications, rest boiler parameters: power and eight coal feed rates as conveyor rotations. For ANN training and testing, some former, historical data from 2013 were also used (27 cases).

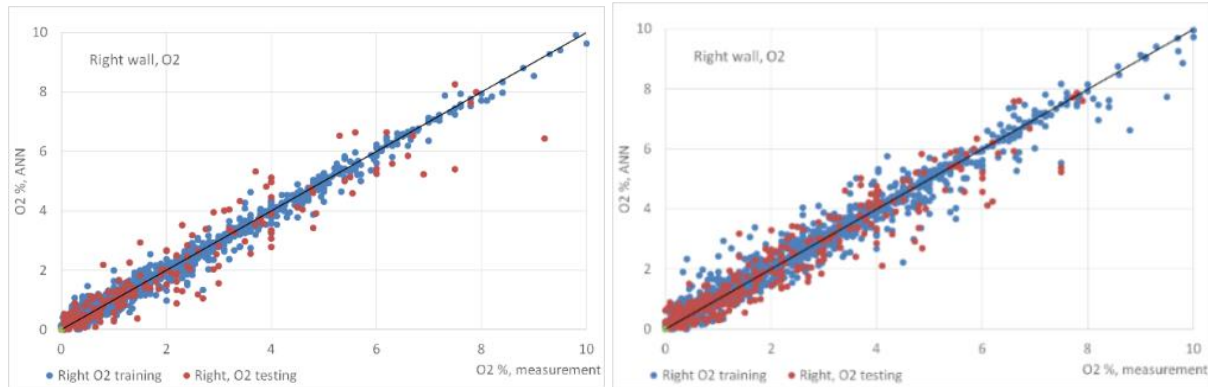


Fig. A6.10 Results of ANN performance in predicting O₂ in the boundary layer of the combustion chamber, right wall, boiler no. 5 in BPP. Left, for less cases and 6 inputs. Right, for 43 cases and 15 inputs. Solid line for the human eye.

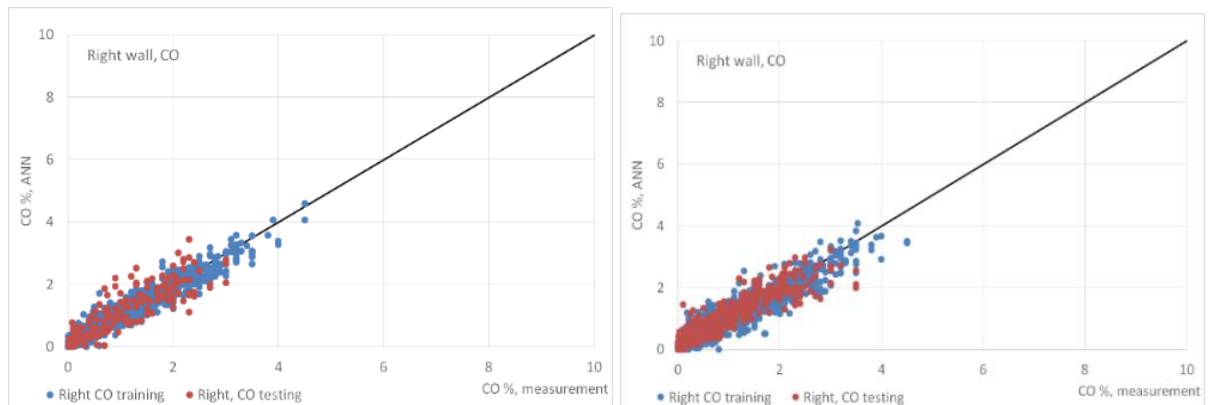


Fig. A6.11 Results of ANN performance in predicting CO in the boundary layer of the combustion chamber, right wall, boiler no. 5 in BPP. Left, for less cases and 6 inputs. Right, for 43 cases and 15 inputs. Solid line for the human eye.

Tab. A6.4 MSPE for training and testing of ANN predicting O₂ (left) and CO (right), 27 cases, 6 inputs, boiler no. 5 BPP

Error	Wall	Front, O ₂	Right, O ₂	Rear, O ₂	Left, O ₂	Front, CO	Right, CO	Rear, CO	Left, CO
MSPE training		1.95	1.29	1.37	2.35	3.36	3.08	3.08	8.19
MSPE test		16.20	10.46	7.87	12.40	16.03	8.87	13.47	16.86
MSPE training (of averages)		0.09	0.08	0.09	0.07	0.71	0.21	0.40	0.15
MSPE test (of averages)		0.12	0.34	0.48	0.11	0.33	0.31	1.08	1.48

Tab. A6.5 MSPE for training and testing of ANN predicting O₂ (left) and CO (right), 47 cases, 15 inputs, boiler no. 5 BPP

Error	Wall	Front, O ₂	Right, O ₂	Rear, O ₂	Left, O ₂	Front, CO	Right, CO	Rear, CO	Left, CO
MSPE training		1.84	2.19	2.13	2.72	6.52	6.99	5.50	9.07
MSPE test		7.88	9.66	6.00	6.55	8.90	8.00	8.11	10.30
MSPE training (of averages)		0.06	0.08	0.06	0.19	1.44	0.60	0.48	0.64
MSPE test (of averages)		0.39	0.36	0.22	0.31	1.42	0.52	2.61	6.92

With ANNs having 6 inputs and a low number of cases (Tab. A6.4) testing errors for O₂ and CO predictions were not high: 8-16%. The situation was even better if the average of O₂ or CO on a given wall for a given case was taken into account (which is relevant for optimisation, as described later). As regards O₂, errors were very small, almost in the region of training errors.

In the case of 15 inputs and a high number of cases (Tab. A6.5), 39 cases were used for training and 7 for testing. O₂ and CO prediction results were better. Also, other inputs to ANN were checked, such as for example eight total air flows to a particular coal burner (primary, secondary and cooling air) instead of eight coal feed rates, but the situation did not change markedly. Another trial was to add to indications of six O₂ sensors three air-to-fuel ratios (for coal burners level, combustion chamber and total), but in that case the results were even worse than for six inputs. Finally, it was decided that six O₂ sensor indications, boiler load and eight coal **feeders'** rates would be taken into account in the CIBOP application for BPP. The ANN performance obtained should be recognised as very good.

The situation was more difficult for boiler no. 3 in OPP. Older data, pre-2010, could not be used due to advanced modernisation of the boiler carried out in 2010. Only 24 measurement cases were carried out that were applicable for ANN training and testing in the CERUBIS project. Figure A6.12 and Tab. A6.6 present the results of ANN performance based on 24 available real data cases (20 used for training and 4 for testing). Slightly higher testing errors are observed for O₂ predictions than for CO, which is in general not expected. Similarly, as for BPP, in general, the errors are smaller for averages. Averages of O₂ are used in GA optimiser, whilst predictions of each single value of O₂ and CO are used to create maps and, moreover, to determine the final dynamic of wall thickness loss. Thus, it is important to predict values as accurately as possible, at least for O₂. However, it is also important to be aware that sometimes high errors do not mean bad predictions for the whole wall – in the case of 15-20 points per wall it is enough when 2-3 predictions are e.g. twice times higher/lower than the measured value and MSPE is already more than 15-20% higher.

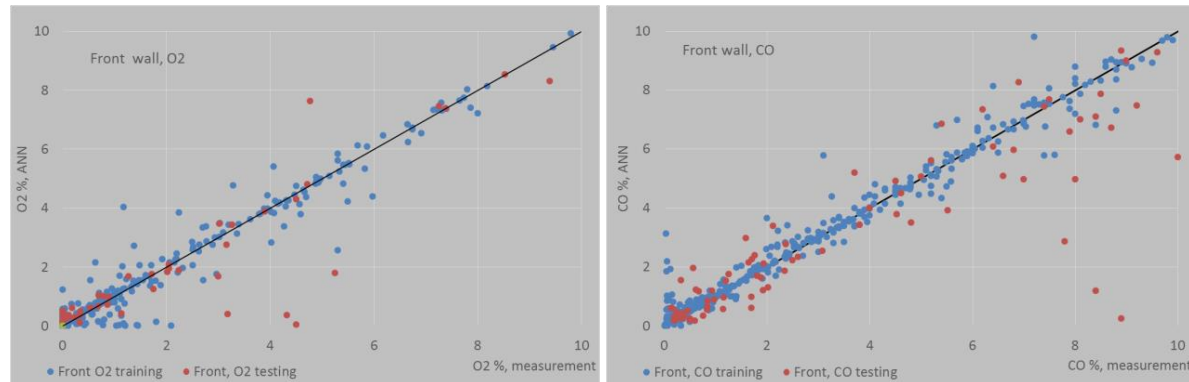


Fig. A6.12 Results of ANN performance in predicting concentration of O₂ (left) and CO (right) in the boundary layer of the combustion chamber, front wall, boiler no. 3 in OPP. 10 inputs, 24 cases. Solid line for the human eye.

Tab. A6.6 MSPE for training and testing of ANN predicting O₂ (left) and CO (right), 24 cases, 10 inputs (4xO₂ sensors indic., power, 5xprimary air), boiler no. 3 OPP

Error	Wall	Front, O ₂	Right, O ₂	Rear, O ₂	Left, O ₂	Front, CO	Right, CO	Rear, CO	Left, CO
MSPE training		4.39	1.87	4.04	6.27	2.85	6.04	4.27	7.89
MSPE test		15.07	10.17	10.91	6.76	8.31	10.95	7.59	9.83
MSPE training (of averages)		0.24	0.49	0.51	0.36	0.56	0.60	1.99	0.55
MSPE test (of averages)		0.62	1.81	0.71	0.82	0.56	0.81	1.94	1.64

In order to decrease errors even more, CFD cases were introduced for training. As with the SLAGGAN module, an additional 11 CFD cases were added for training and validation of ANN (in sum, 35 cases: 24 real and 11 CFD). Results are shown in Tab. A6.7 and Fig. A6.13. Errors then decrease further, in some cases even 2-3 times. It might be concluded that increasing the number of CFD cases in

ANN training, will further improve O₂ and CO predictions. However, the results obtained for 35 cases were considered satisfactory.

Tab. A6.7 MSPE for training and testing of ANN predicting O₂ (left) and CO (right), 35 cases, 16 inputs (4xO₂ sensors indic., power, 5xprimary air, 4xsecondary air, 2xROFA air), boiler no. 3 OPP

Error	Wall	Front, O ₂	Right, O ₂	Rear, O ₂	Left, O ₂	Front, CO	Right, CO	Rear, CO	Left, CO
MSPE training		2.95	2.30	2.18	1.81	2.62	3.24	2.95	3.38
MSPE test		6.35	4.63	8.91	4.10	3.72	3.28	6.31	3.83
MSPE training (of averages)		0.23	0.57	0.19	0.17	0.17	0.35	2.01	0.19
MSPE test (of averages)		0.31	1.33	1.34	0.10	0.04	0.24	2.43	0.30

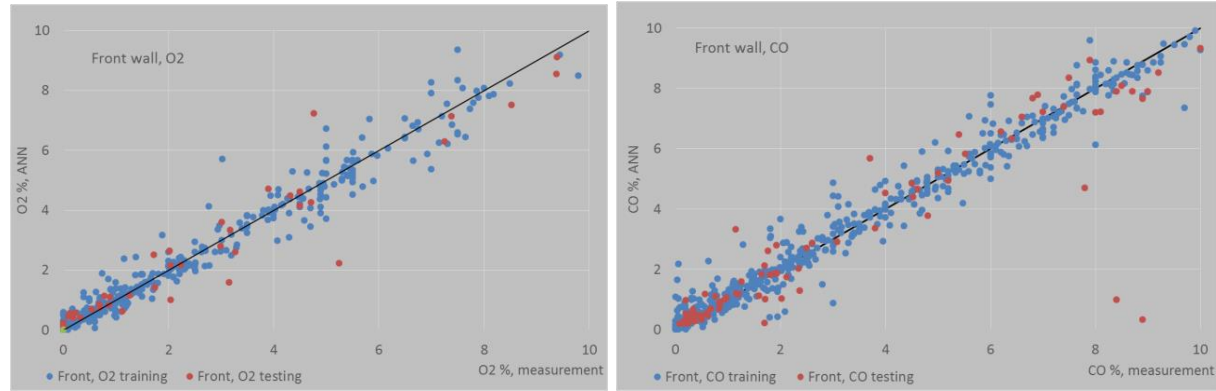


Fig. A6.13 Results of ANN performance in predicting concentration of O₂ (left) and CO (right) in the boundary layer of the combustion chamber, front wall, boiler no. 3 in OPP. 16 inputs, 35 cases. Solid line for the human eye.

ANN were also used for the diagnostic system. In case of O₂ sensor failure, O₂ and CO concentrations might be determined only on the basis of boiler parameters data: boiler load, 5 x primary air flows, 4 x secondary air flows, sum of OFA flows, sum of air to cooling oil guns flows, 2 x ROFA flows, sum of air flow to combustion chamber. Tab. A6.8 show the results of ANN performance in such case for every wall. In general, errors are not very high and these ANNs can be used to determine O₂, CO, corrosion risk and wall loss rate maps in case of failure of O₂ sensors or failure of communication with them. However, one can consider errors e.g. for the front wall to be too high for tests (to recall: the tests cover cases 9, 13, 19, 22). Figs. A6.14 and A6.15 highlight the behaviour of O₂ and CO concentration in the boundary layer of the front wall for each particular measurement point (adapter in the wall) in cases 9 and 19, both in real boiler operation and as ANN testing performance, for two MSPE levels (low and high).

Tab. A6.8 MSPE for training and testing of ANN predicting O₂ (left) and CO (right) without O₂ sensor indications, 35 cases, 15 inputs (power, 5xprimary air, 4xsecondary air, 2xROFA air, sum of oil guns cooling air, sum of OFA, sum of air to comb. chamber), boiler no. 3 OPP

Error	Wall	Front, O ₂	Right, O ₂	Rear, O ₂	Left, O ₂	Front, CO	Right, CO	Rear, CO	Left, CO
MSPE training		3.05	1.15	1.86	1.76	2.33	2.12	2.59	3.33
MSPE test		17.28	18.57	8.80	4.89	6.55	4.69	6.61	4.38
MSPE training (of averages)		0.30	0.84	0.22	0.13	0.16	0.35	1.78	0.20
MSPE test (of averages)		0.61	2.60	1.19	0.48	0.43	0.42	4.04	0.24

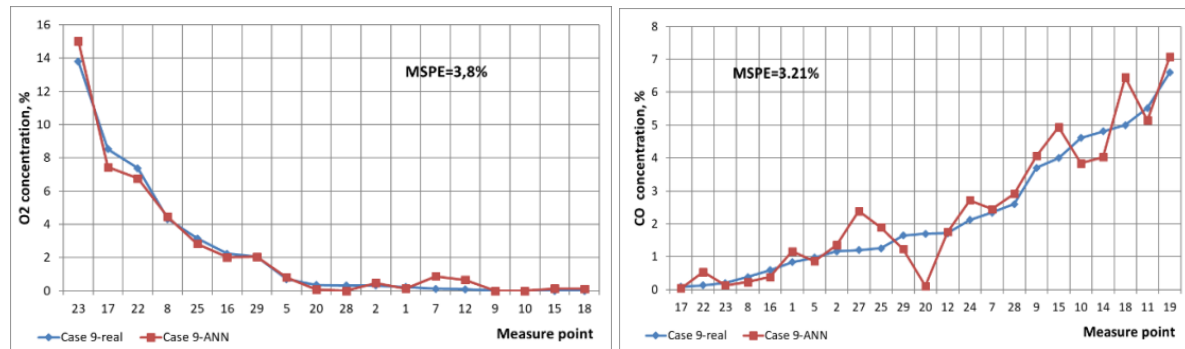


Fig. A6.14 Results of ANN test in predicting concentration of O₂ (left) and CO (right) in the boundary layer of front wall for case 9 – alternative ANN in diagnostic system of CIBOP (see Tab. A6.8). Boiler no. 3 in OPP

As one can see from Fig. A6.15, in spite of the MSPE reaching even more than 30% particular gas species concentrations in ANN predictions are not far from measured values, except for several points. Moreover, high fluctuations are features of high absolute values of O₂ & CO, which is not vital when determining high temperature corrosion risk, as only low O₂ values are important (corrosion risk is higher for low O₂). In the case of CO, as a matter of fact, high CO values are important but from the point of determination of corrosion risk) there is no difference if CO is 6, 8 or 10 % - for the corrosion risk is always very high for such levels of CO (more than 1%).

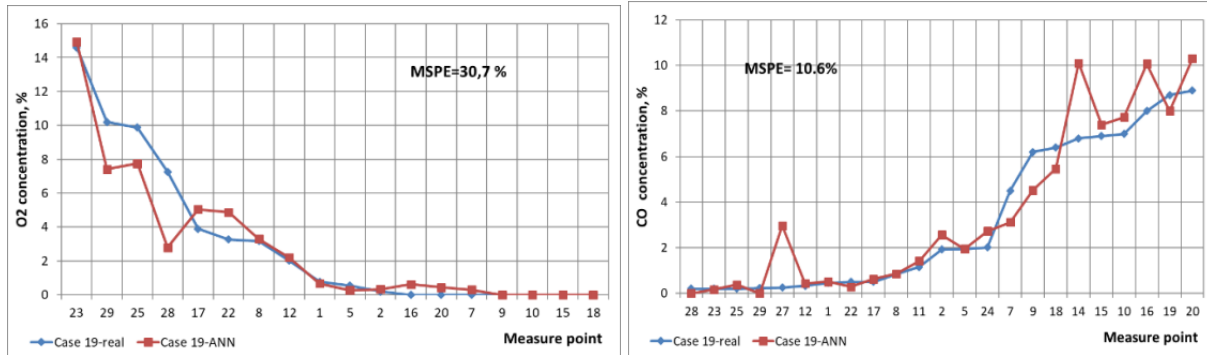


Fig. A6.15 Results of ANN test in predicting concentration of O₂ (left) and CO (right) in the boundary layer of front wall for case 19 – alternative ANN in diagnostic system of CIBOP (see Tab. A6.8). Boiler no. 3 in OPP

To recap, reasonable predictions of O₂ and CO concentrations in the boundary layer were found when more training data was added and more inputs to neural networks were involved in the case of boiler no. 3 in OPP and no. 5 in BPP. CFD multi-case calculations had improved the training process in spite of some overestimating of O₂ and understating of CO concentrations.

Regarding GA optimisation, several major issues were solved:

- in the objective function instead of one average of O₂ for the whole boundary layer, four averages for each wall were introduced,
- the number of optimised parameters were decreased,
- the training data were increased by additional measurement and CFD calculations.

Tables A6.9 and A6.10 contain inputs for ANNs, which determine averages of O₂ concentrations in the boundary layer (4 ANNs, 1 ANN per each wall), NO_x and CO emissions (2 ANNs), LOI (1 ANN, only in BPP) and new O₂ at the outlet from the boiler (1 ANN) for OPP and BPP, which are necessary for the GA optimiser. Tables also contain optimised parameters. In the case of BPP, twelve air flows are optimised (eight secondary air flows and four OFA flows). In the case of OPP, thirteen air flow are optimised (five primary air flows, four secondary air flows and four oil gun cooling air flows). The optimised parameters were chosen on the basis of optimising capabilities of boilers and technological possibilities/barriers. It must be underlined that, to simplify the GA optimisation, only one ANN per wall was used to determine the average of O₂ in the whole boundary layer of that wall. Averages for training and testing were determined on the basis of measurements from each point (adapter) for a given wall and case.

Tab A6.9 Number and kind of inputs to ANN and optimised parameters in GA optimiser, boiler no. 5 BPP

Parameter	Coal feed rates	Primary air flows	Secondary air flows	Oil guns air flows	Protection air flows	Bottom air flow	OFA air flows	Power	Cal. Value	Sum
Inputs for ANN	8	8	8	8	4	1	4	1	1	43
Optimised parameters			8				4			12

Tab. A6.10 Number and kind of inputs to ANN and optimised parameters in GA optimiser, boiler no. 3 OPP

Parameter	Coal feed rates	Primary air flows	Secondary air flows	Oil guns air flows	OFA air flows	ROFA air flows	Rotamix air flows	Power	Sum
Inputs for ANN	5	5	4	4	4	2	1	1	26
Optimised parameters		5	4	4					13

Figure A6.16 presents the MSPE for training and testing of the above-mentioned ANN for OPP. The left graph presents results when only real cases were used for training and testing while the right graph also includes CDF cases. In general, there are good ANN predictions, especially for NO_x and O₂ at the outlet from the combustion chamber. The highest MSPE testing error was obtained for the left wall. As one can see, adding more cases for training decreases training errors, but testing errors are only a little smaller or in the case of the front and right walls even a little higher. For final utilisation in CIBOP, ANNs with 30 training cases were used for OPP. For BPP (Fig. A6.17) 41 real cases were used for training and 6 for testing. The results obtained are very satisfactory, especially for predicting averages of O₂ in the boundary layer of the evaporator, and were finally used in CIBOP. Performance of the optimiser in real conditions is described in chapter 2.3.4.

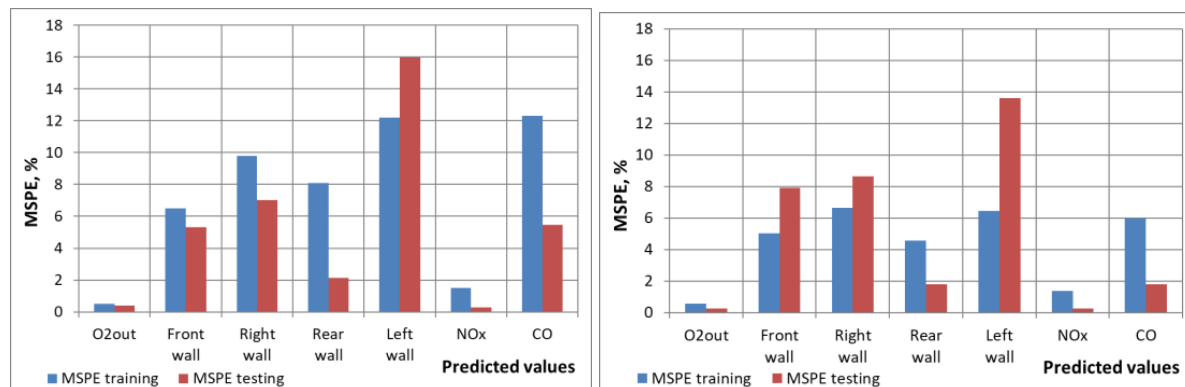


Fig. A6.16 Results of training and testing ANNs for GA optimiser for OPP. Left - 19 cases training, 5 testing. Right - 30 cases training, 5 testing. Front, right, rear and left wall denotes average concentrations of O₂ in the boundary region for the whole respective wall.

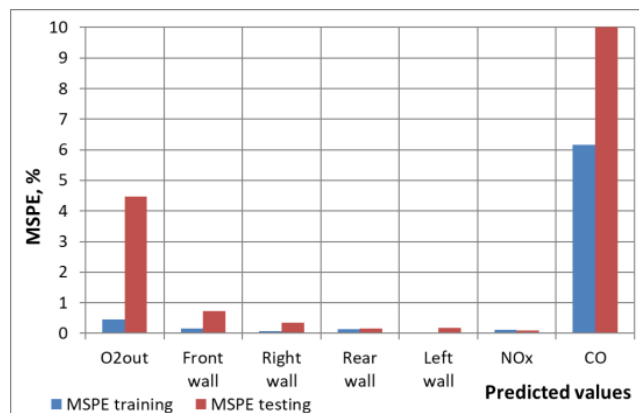


Fig. A6.17 Results of training and testing ANNs for GA optimiser for BPP, 41 cases training, 6 testing. Front, right, rear and left wall denotes average concentrations of O₂ in the boundary region for the whole respective wall.

Figure A6.18 presents the new main window of Dawid and Rachela software (determined as Rachela later in the text) for BPP and Fig. A6.19 for OPP. As one can see, a huge effort was put into changing the software view and its functionality. All of the above-mentioned objectives with regard to view, functionality etc. were achieved.

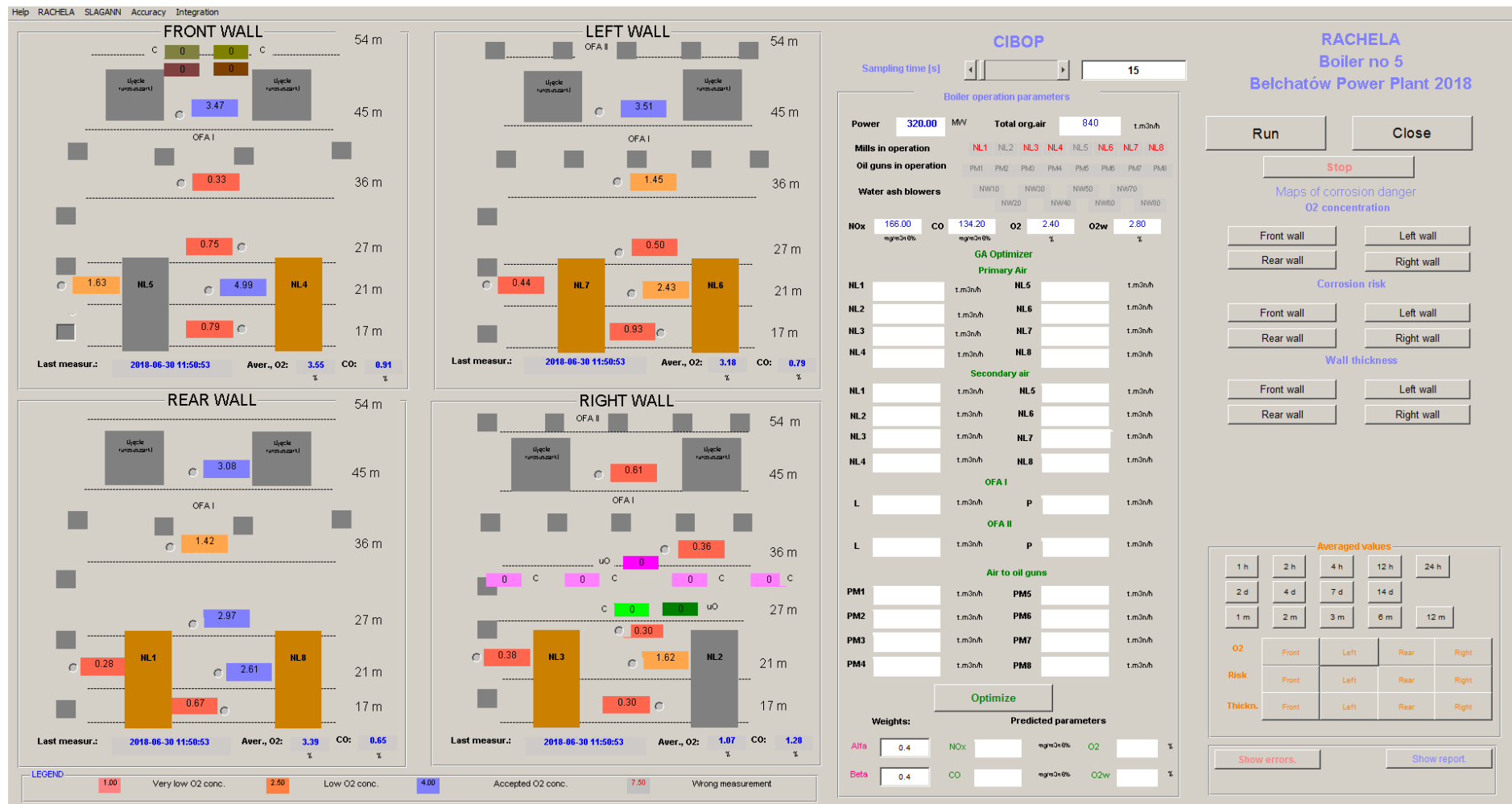


Fig. A.6.18 Rachela module main view in CIBOP developed for BPP

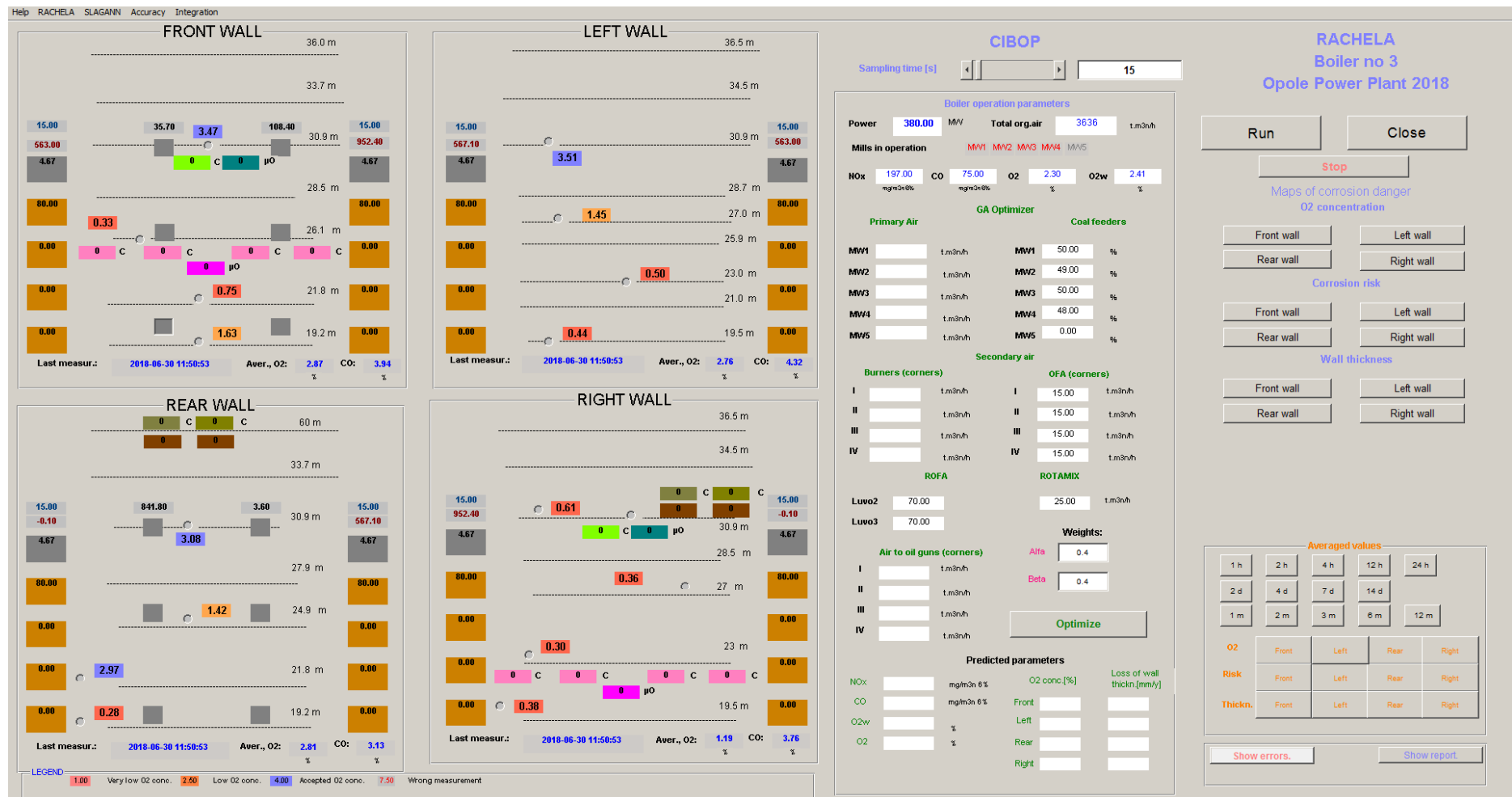


Fig. A6.19 Rachela main view in CIBOP developed for OPP

Measurement Accuracy Module.

There are two levels of diagnostics in the system. First, as described in chapter 2.3.2, one works in the local control system dedicated to a particular sensor (sensing system). If a failure has occurred, this is communicated to CIBOP and, instead of a value, error is displayed and saved to the database. The second diagnostics level is dedicated to values from a particular sensor that were measured and saved earlier. On the basis of historical data from the boiler or from the laboratory investigation, the software estimates the level of creditability of a particular sensor measurement in four levels: very good, acceptable, not acceptable and very wrong. These levels are not strict, they should be treated more like an estimation, **but 'very wrong' appears** for indications of a particular sensor, that sensor should be checked. Moreover, the level of creditability is determined not only for particular sensor measurement but also overall for the whole wall as a map. Thanks to such solution operator can estimate the places on walls with low and high creditability of measurements, what is especially important for online determination of dynamic of wall thickness loss. Moreover, with O₂ and CO measurements, since there are many sensors, if some sensors fail, it is still possible to determine O₂ and CO concentrations on walls by using alternative values determined by ANN, as was described earlier in this chapter.

Fig. A6.20 presents a view of the diagnostic module in graphical user interface for BPP boiler and Fig A6.21 for OPP boiler.

The integration module is a core of the CIBOP. The graphical user interface was designed in such a way that it is possible to work in that module with all sensors' indications, basic parameters of boiler performance, GA optimiser and several models of dynamic of wall thickness loss showed by online maps or as cumulated values from a specified historical period of time (from 1 h to 1 year). Moreover, predictions of future dynamic of wall thickness loss at given operation data of the boiler, i.e. boiler load, configuration of working mills and configuration of air flows is possible. This may be done on the basis of current boiler data or on the basis of data from GA optimiser. Results may be shown as maps or as average values for the whole wall. Views of integration modules are presented in Fig. A6.22 for BPP and Fig. A6.23 for OPP. A detailed description of this module is presented in [14].

Three models of rate of wall thickness loss are implemented in the Integration module of CIBOP. They were developed on the basis of ultrasonic measurements of the boiler evaporator (O₂ model), electric resistance measurement of evaporator wall (CMS model) and electric resistance measurement of corrosion probe (CP). All models can be treated as empirical models. The first model was developed by comparing O₂ concentrations in the boundary layer of the evaporator and real wall thickness loss. This model can be treated as the most realistic, because it is determined on the basis of real measurement of wall thickness loss. However, in the case of OPP the model was developed on the basis of historical data from the period 2010 to 2017. So, if the process of corrosion (and other phenomena) for future years is somehow similar to the data from 2010-2017, the model is working properly, if not, the other two models should be used. The other two models were both developed on the basis of electric resistance measurements, the first on the basis of resistance determined for a fragment of the real boiler wall, the second on the basis of resistance of the sensor located on the corrosion probe. A comparison of the various models was presented in chapter 2.3.4

The integration module presented here can be treated as boiler maintenance software (preliminary activity in task 3.5), since it (i) indicates the places with high corrosion risk, and (ii) can load current real maps of wall dynamic loss obtained from ultrasonic measurement and make various comparisons with historical or future data. Thus, the places in the evaporator which need special attention can be determined for each wall in advance of the next boiler outage.

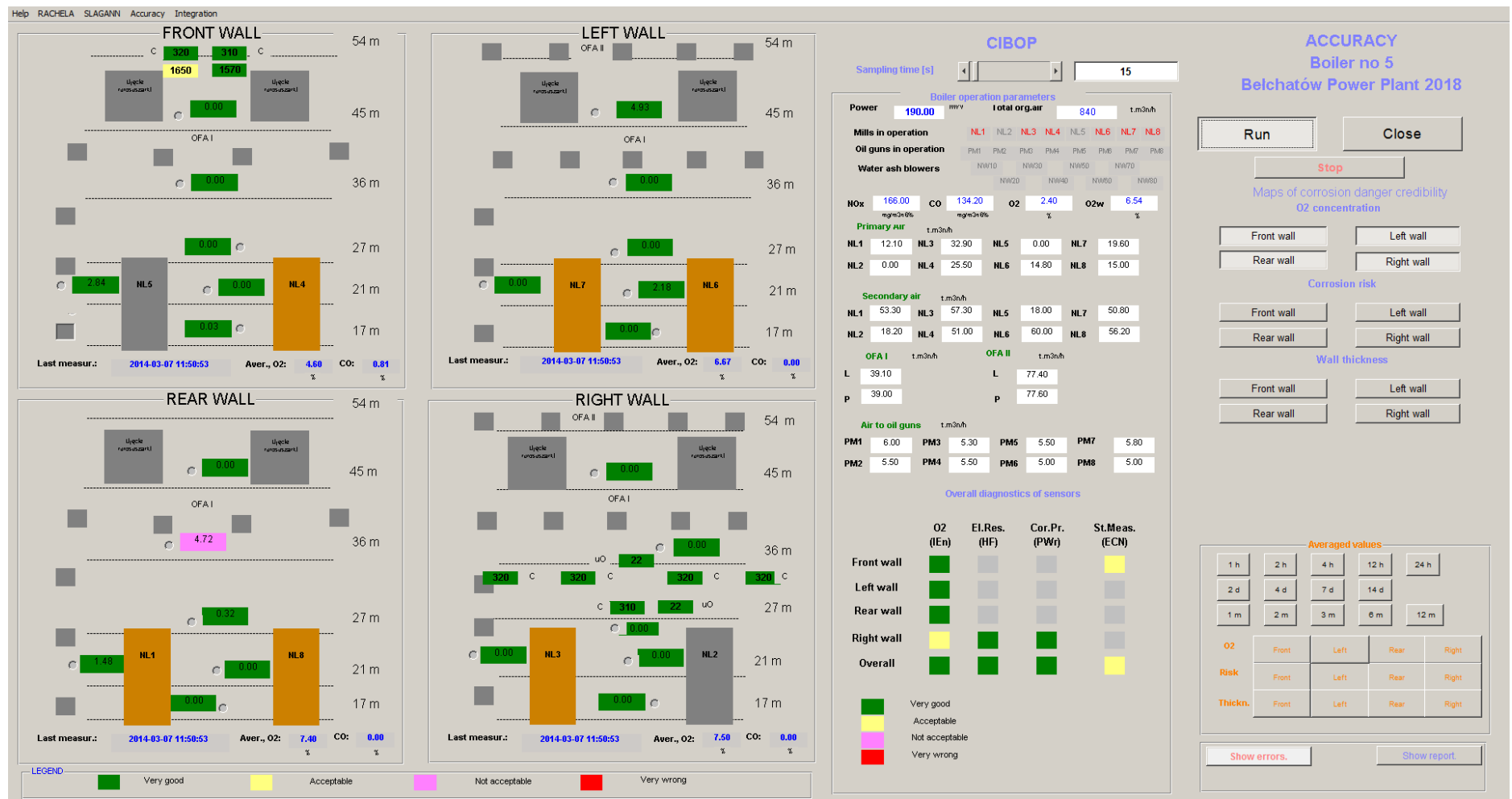


Fig. A6.20 Diagnostic module of CIBOP for OPP

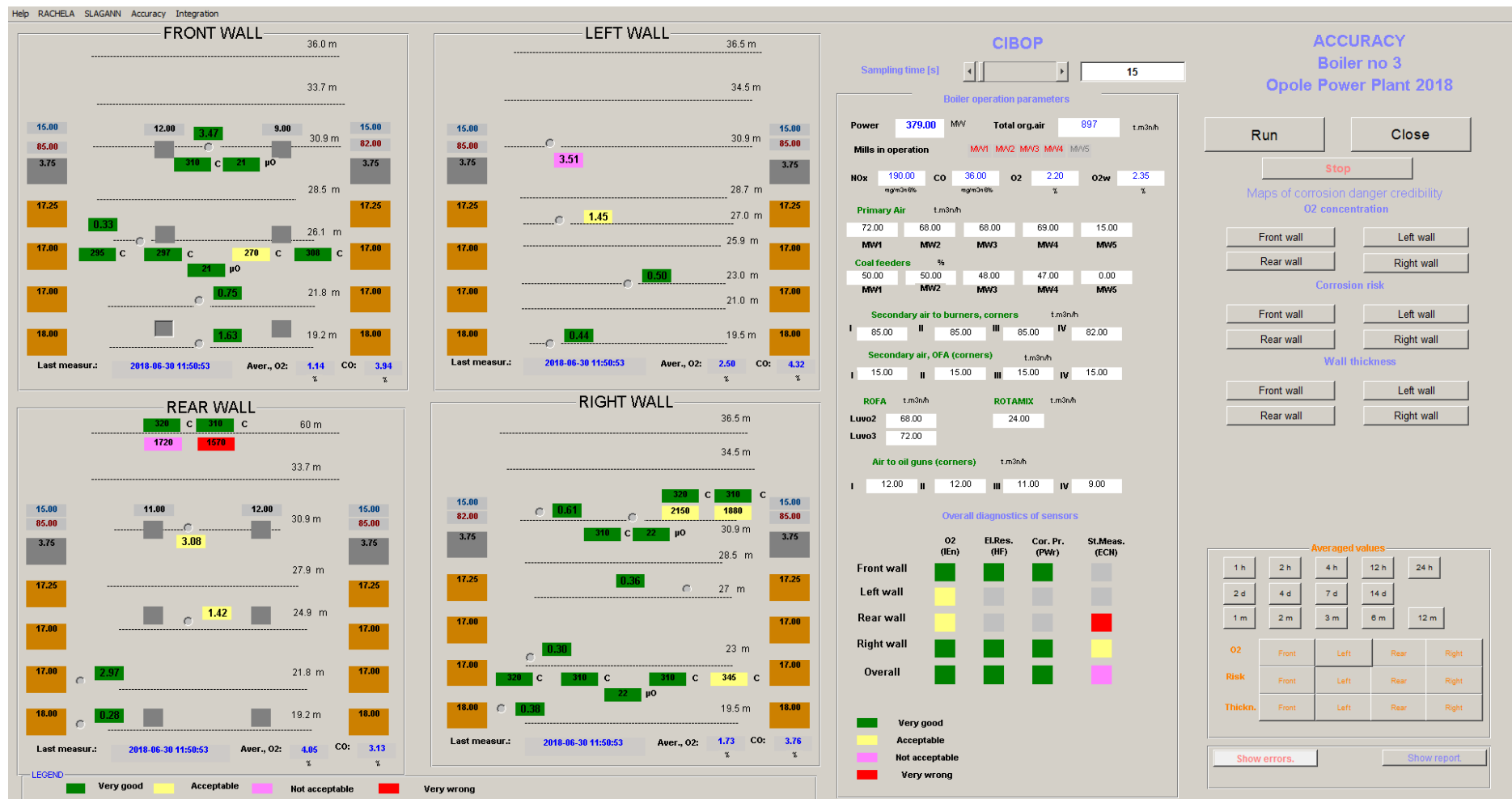


Fig. A6.21 Diagnostic module of CIBOP for BPP



Fig. A6.22 Integration module in CIBOP for BPP



A7 – Results of CIBOP optimisation of boiler no. 5 in BPP

Tab. A7.1 Initial cases (set by boiler DCS) for optimisation, BPP

Case number	Load	Number of working mills	Outlet emissions in mg/m ³ n, ref. 6% O ₂		Averages concentrations in boundary layer for all walls, %			Average corrosion rate for all walls, um/y	
			NO _x	CO	O ₂ , all	CO, all	CMS	Corr. probe	
Case 1	370	7	165	81	1.62	1.07	22	88	
Case 2	370	6	172	273	2.38	1.015	10	40	
Case 3	340	6	149	110	1.98	1.32	16	65	
Case 4	245	5	131	129	1.92	0.94	17	69	

Tab. A7.2 Initial and indicated by CIBOP air flows in two step optimisation for the case 1

Air flows in thousands m ³ n/h, excess air and coal feed rates in %									OFA	False air %	Case			
Mill	NL1	NL2	NL3	NL4	NL5	NL6	NL7	NL8	PCPAL	PCKOM	PCALK	POFA	DOSS	
Primary air	24	27	0	12.5	16	9.33	10.7	10.9	641.4	763.35	994.7	231	10.4	1
Secondary air	81	70	18	60.5	80	73.5	84.5	78.5						
Coal rates	65	60	0	45	59	51	57	54.5		λ	λ			
Excess air λ	0.63	0.62	∞	0.63	0.63	0.63	0.65	0.64		0.641	0.762368	0.993		
Mill	NL1	NL2	NL3	NL4	NL5	NL6	NL7	NL8	PCPAL	PCKOM	PCALK	POFA	DOSS	
Primary air	0	25	0	12.6	13	5.85	7.75	18	683.6	805.5	1026	221	8.4	1a
Secondary air	90	76	18	68.5	90	80.5	93	82						
Coal rates	61	57	0	44	57	48.5	55.5	56.5		λ	λ			
Excess air λ	0.56	0.67	∞	0.70	0.68	0.67	0.69	0.67		0.69	0.812776	1.036		
Mill	NL1	NL2	NL3	NL4	NL5	NL6	NL7	NL8	PCPAL	PCKOM	PCALK	POFA	DOSS	
Primary air	0	25	0	13	15	10.3	5.2	19.6	705.9	827.65	1034	207	6.0	1b
Secondary air	95	82	18	51.5	93	89.5	101	85						
Coal rates	59	55	0	41	55	51	53.5	55.5		λ	λ			
Excess air λ	0.60	0.73	∞	0.59	0.73	0.74	0.75	0.71		0.723	0.847929	1.06		

Tab. A7.3 Initial and indicated by CIBOP air flows in two step optimisation for the case 2

Air flows in thousands m ³ n/h, excess air and coal feed rates in %									OFA	False air %	Case			
Mill	NL1	NL2	NL3	NL4	NL5	NL6	NL7	NL8	PCPAL	PCKOM	PCALK	POFA	DOSS	
Primary air	0	30	0	0	33	0	26.8	14	666.7	787.5	1027	240	6.6	2
Secondary air	97	78	78	18	76	18	78.5	92.5						
Coal rates	67	64	65.5	0	67	0	63	64.5		λ	λ			
Excess air λ	0.57	0.66	0.46	∞	0.63	∞	0.65	0.64		0.676	0.798952	1.042		
Mill	NL1	NL2	NL3	NL4	NL5	NL6	NL7	NL8	PCPAL	PCKOM	PCALK	POFA	DOSS	
Primary air	0	29	0	0	32	0	24.5	13.6	700.7	821.5	1064	243	5.9	2a
Secondary air	100	90	84.5	18	88	18	82.5	98						
Coal rates	70	66	67.5	0	69	0	63	66		λ	λ			
Excess air λ	0.56	0.71	0.49	∞	0.69	∞	0.67	0.66		0.698	0.818846	1.061		
Mill	NL1	NL2	NL3	NL4	NL5	NL6	NL7	NL8	PCPAL	PCKOM	PCALK	POFA	DOSS	
Primary air	0	15	0	5.65	29	0	25.3	15.5	700.9	821.7	1058	236	5.6	2b
Secondary air	97	96	79.5	73	84	18	71.5	80						
Coal rates	61	56	59	49	58	0	50.5	53		λ	λ			
Excess air λ	0.62	0.76	0.52	0.62	0.75	∞	0.74	0.70		0.712	0.834993	1.075		

Tab. A7.4 Initial and indicated by CIBOP air flows in two-step optimisation for case 3

Air flows in thousands m3n/h, excess air and coal feed rates in %									Air to burners	Air to combust. chamber	Total org. air	OFA	False air %	Case	
Mill	NL1	NL2	NL3	NL4	NL5	NL6	NL7	NL8	PCPAL	PCKOM	PCALK	POFA	DOSS		
Primary air	0	0	0	15.5	5.2	0	27.3	23.1		606	726.8	973.3	246	6.8	3
Secondary air	75	18	78.5	67	97	18	73	75							
Coal rates	61	0	60.5	50	62	0	59.5	59.5	λ	λ	λ				
Excess air λ	0.47	∞	0.49	0.63	0.63	∞	0.64	0.63	0.666	0.798359	1.069				
Mill	NL1	NL2	NL3	NL4	NL5	NL6	NL7	NL8	PCPAL	PCKOM	PCALK	POFA	DOSS		
Primary air	0	0	0	17.1	5.2	0	25.2	24.5		630.9	751.65	979.2	228	3.9	3a
Secondary air	99	18	72	62	91	18	88.5	87							
Coal rates	57	0	57	46.5	59	0	56.5	56.5	λ	λ	λ				
Excess air λ	0.64	∞	0.47	0.63	0.61	∞	0.74	0.73	0.712	0.847861	1.105				
Mill	NL1	NL2	NL3	NL4	NL5	NL6	NL7	NL8	PCPAL	PCKOM	PCALK	POFA	DOSS		
Primary air	0	0	0	16.7	4.9	0	24.3	24.4		653.7	774.5	977	203	5.9	3b
Secondary air	94	18	71.5	81	95	18	90	96							
Coal rates	57	0	57	46.5	58	0	55	57	λ	λ	λ				
Excess air λ	0.60	∞	0.45	0.76	0.63	∞	0.75	0.76	0.727	0.861512	1.087				

Tab. A7.5 Initial and indicated by CIBOP air flows in two-step optimisation for case 4

Air flows in thousands m3n/h, excess air and coal feed rates in %									Air to burners	Air to combust. chamber	Total org. air	OFA	False air %	Case	
Mill	NL1	NL2	NL3	NL4	NL5	NL6	NL7	NL8	PCPAL	PCKOM	PCALK	POFA	DOSS		
Primary air	0	2.2	0	2.2	2.2	0	5.3	5.5		350.3	459.55	597.6	138	25.8	4
Secondary air	18	64	18	52	65	18	62.5	62.5							
Coal rates	0	55	0	45.5	56	0	53.5	54	λ	λ	λ				
Excess air λ	∞	0.46	∞	0.46	0.46	∞	0.49	0.48	0.518	0.679303	0.883				
Mill	NL1	NL2	NL3	NL4	NL5	NL6	NL7	NL8	PCPAL	PCKOM	PCALK	POFA	DOSS		
Primary air	0	2.2	0	2.22	2.2	0	2.17	16		391	500.25	607.3	107	18.2	4a
Secondary air	18	79	18	41	79	18	79	64.5							
Coal rates	0	52	0	42.5	53	0	51	50.5	λ	λ	λ				
Excess air λ	∞	0.59	∞	0.39	0.58	∞	0.60	0.60	0.605	0.774477	0.94				
Mill	NL1	NL2	NL3	NL4	NL5	NL6	NL7	NL8	PCPAL	PCKOM	PCALK	POFA	DOSS		
Primary air	0	2.1	0	5.65	2.3	0	2.05	10.4		402.3	511.55	598	86.5	22.0	4b
Secondary air	18	77	18	58.5	77	18	76.5	66.5							
Coal rates	0	51	0	41.5	50	0	49	49.5	λ	λ	λ				
Excess air λ	∞	0.56	∞	0.57	0.58	∞	0.59	0.57	0.617	0.78514	0.918				

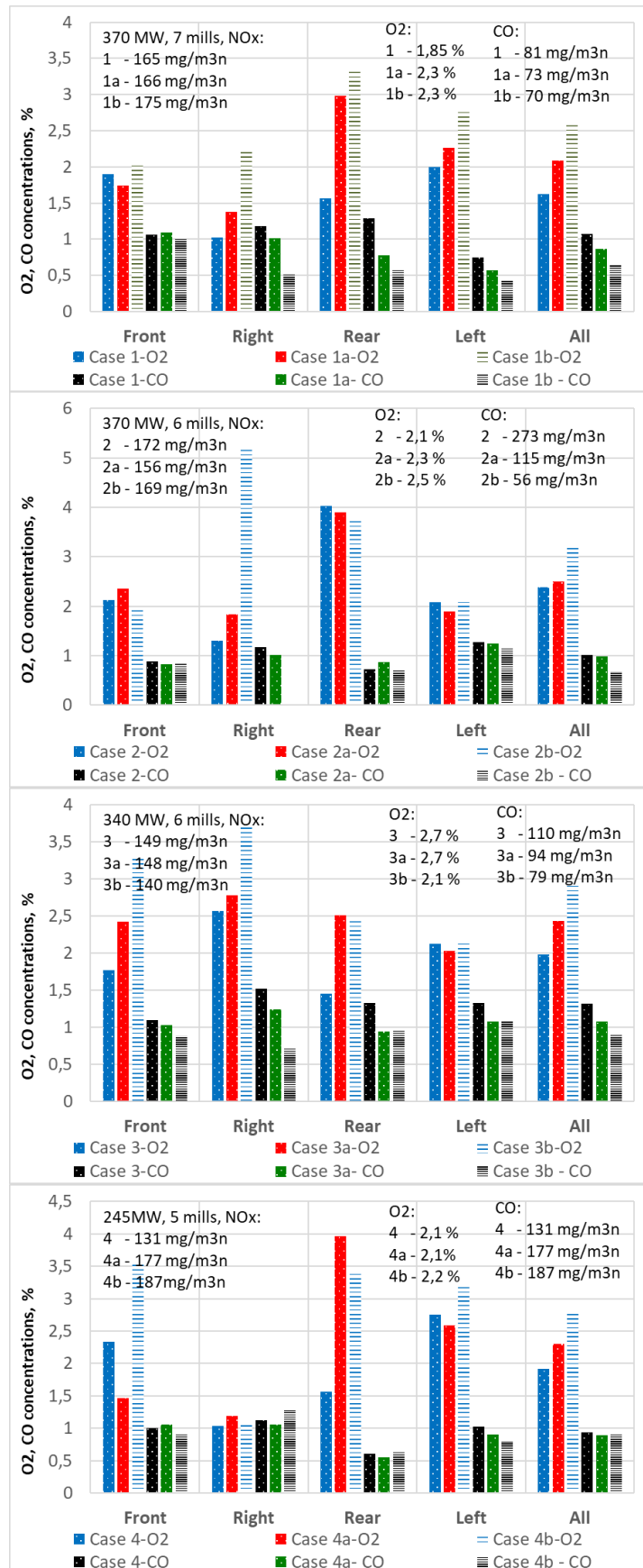


Fig. 7.1 Averaged over wall area concentrations of O₂ and CO for the four boiler operation cases. The graphs show – for each case – results from CIBOP of concentrations of O₂ and CO for unoptimised air settings and then for two optimisation cases denoted by *a* and *b*. NO_x and CO emissions and O₂ at the boiler outlet are also visible in graphs

Tab. A7.6 The rates of corrosion in um/y for CMS and corrosion probe model for all cases

Wall	Case 1		Case 1a		Case 1b	
	CMS	Corr.probe	CMS	Corr.probe	CMS	Corr.probe
	um/y	um/y	um/y	um/y	um/y	um/y
Front	17.6	70.1	20.2	80.2	15.2	60.5
Right	31.8	126.0	26.0	103.1	12.1	48.4
Rear	23.1	91.7	0.2	1.4	0.0	0.0
Left	16.0	63.7	11.8	47.2	3.6	14.7
All	22.1	87.9	14.6	58.0	6.3	25.5
Wall	Case 2		Case 2a		Case 2b	
	CMS	Corr.probe	CMS	Corr.probe	CMS	Corr.probe
	um/y	um/y	um/y	um/y	um/y	um/y
Front	14.1	56.1	10.4	41.4	16.6	66.2
Right	27.3	108.2	18.6	73.9	0.0	0.0
Rear	0.0	0.0	0.0	0.0	0.0	0.0
Left	14.7	58.6	17.6	70.1	14.7	58.6
All	9.9	39.5	8.0	32.2	3.0	25.0
Wall	Case 3		Case 3a		Case 3b	
	CMS	Corr.probe	CMS	Corr.probe	CMS	Corr.probe
	um/y	um/y	um/y	um/y	um/y	um/y
Front	19.7	78.3	9.2	37.0	0.0	0.0
Right	6.8	27.4	3.4	14.1	0.0	0.0
Rear	24.9	98.7	7.8	31.3	8.4	33.8
Left	14.1	56.1	15.5	61.8	13.6	54.2
All	16.4	65.1	9.0	36.0	1.5	6.5
Wall	Case 4		Case 4a		Case 4b	
	CMS	Corr.probe	CMS	Corr.probe	CMS	Corr.probe
	um/y	um/y	um/y	um/y	um/y	um/y
Front	10.7	42.7	24.5	97.4	0.0	0.0
Right	31.5	124.8	29.0	115.2	31.0	122.8
Rear	22.9	91.0	0.0	0.0	0.0	0.0
Left	3.9	16.0	6.5	26.2	0.0	0.0
All	17.2	68.6	11.1	44.5	3.2	13.0

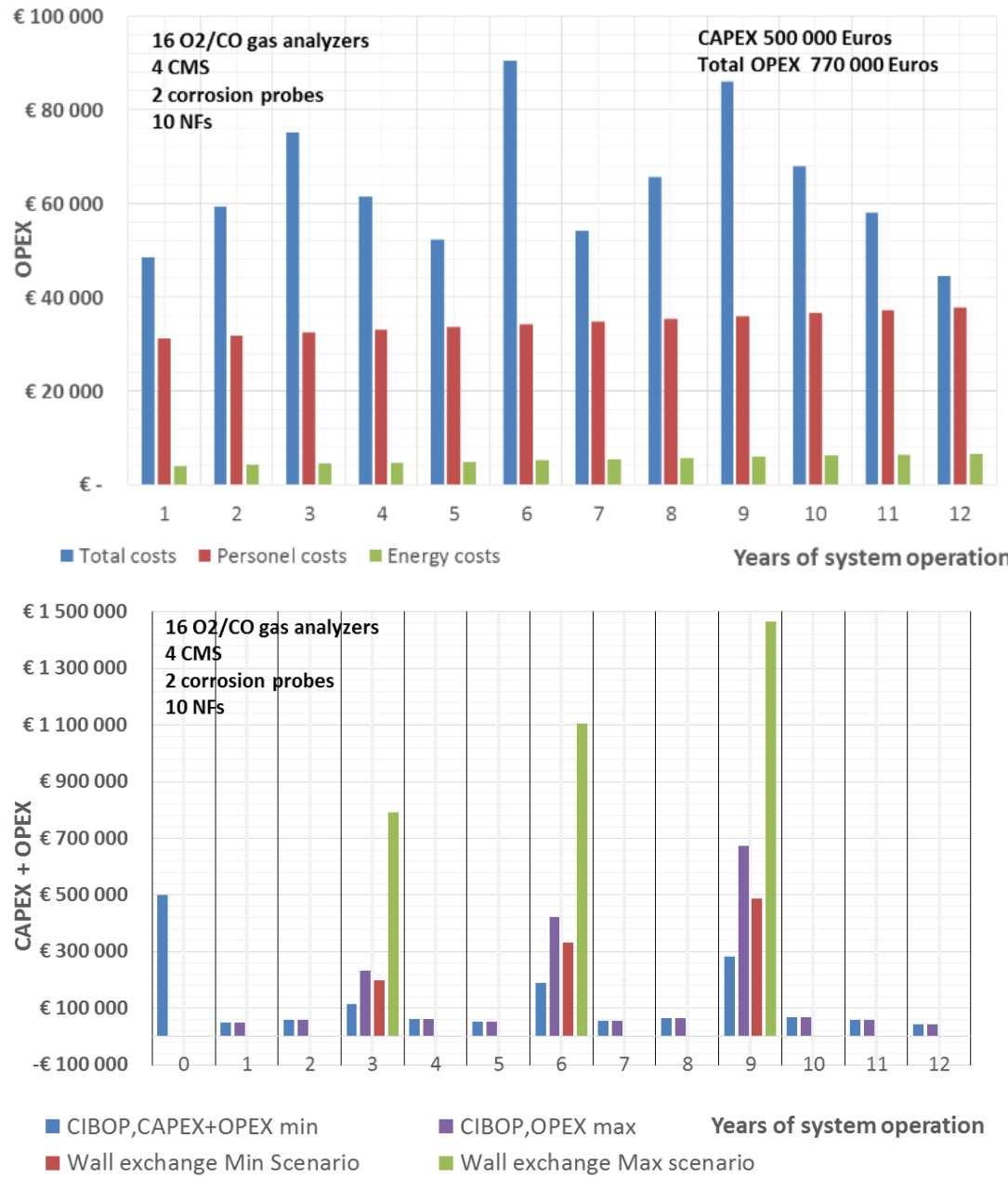


Fig. A8.1 Structure of OPEX costs for the advanced CIBOP scenario.

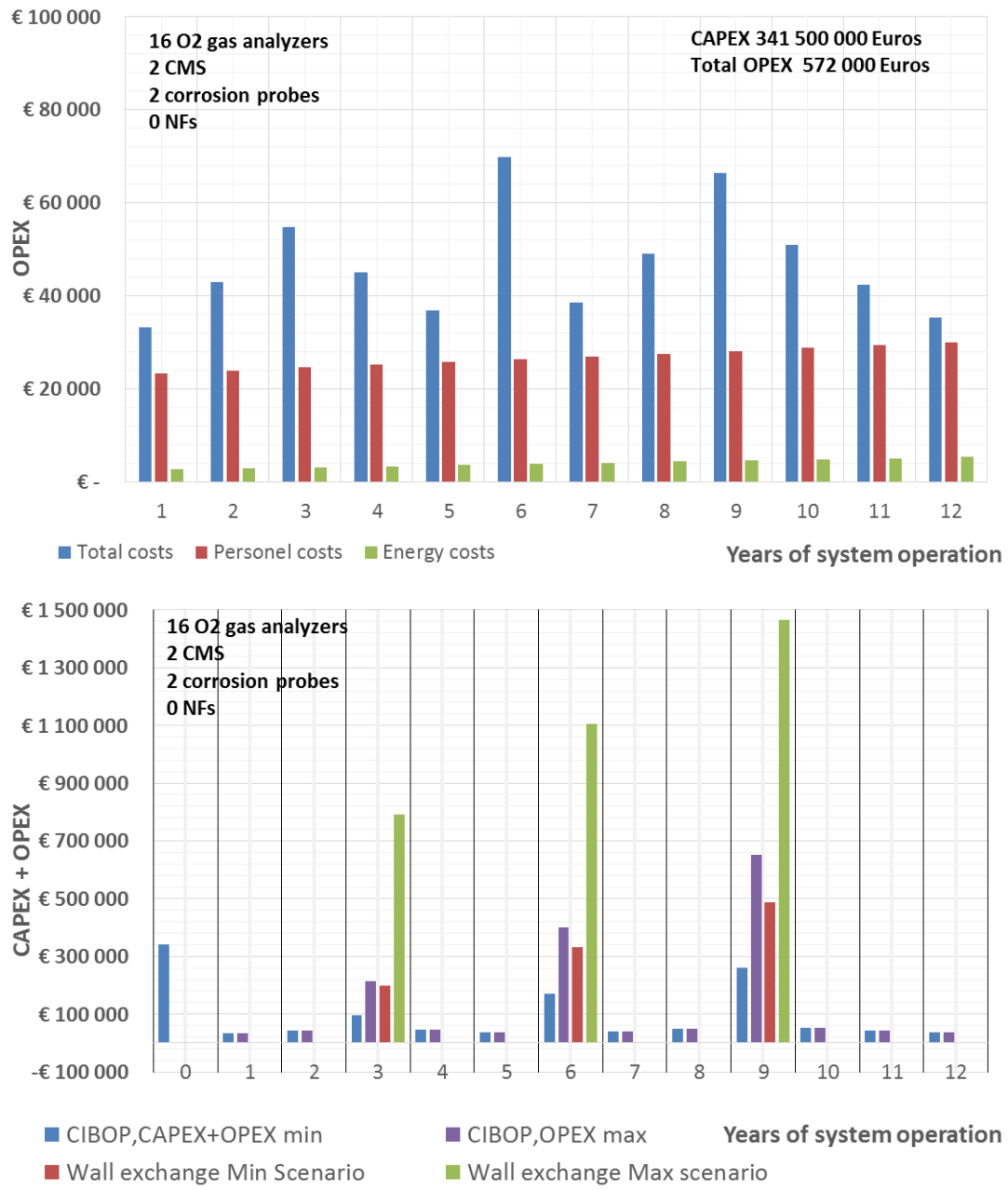


Fig. A8.2 Structure of OPEX costs for the basic CIBOP scenario.

Getting in touch with the EU

In person

All over the European Union there are hundreds of Europe Direct information centres. You can find the address of the centre nearest you at:

https://europa.eu/european-union/contact_en

On the phone or by email

Europe Direct is a service that answers your questions about the European Union. You can contact this service:

- by freephone: 00 800 6 7 8 9 10 11 (certain operators may charge for these calls),
- at the following standard number: +32 22999696 or
- by email via: https://europa.eu/european-union/contact_en

Finding information about the EU

Online

Information about the European Union in all the official languages of the EU is available on the Europa website at: https://europa.eu/european-union/index_en

EU publications

You can download or order free and priced EU publications at: <https://publications.europa.eu/en/publications>. Multiple copies of free publications may be obtained by contacting Europe Direct or your local information centre (see https://europa.eu/european-union/contact_en).

EU law and related documents

For access to legal information from the EU, including all EU law since 1952 in all the official language versions, go to EUR-Lex at: <https://eur-lex.europa.eu>

Open data from the EU

The EU Open Data Portal (<https://data.europa.eu/euodp/en/home>) provides access to datasets from the EU. Data can be downloaded and reused for free, for both commercial and non-commercial purposes.

Intensive corrosion and slagging of membrane walls of coal fired utility boilers is presently common problem related to low NOx emission combustion and resulting highly reducing atmospheres in a combustion chamber of the boiler.

The main result of the CERUBIS project is boiler diagnostic platform CIBOP enabling on-line monitoring and prediction of the corrosion risk and the corrosion rate for whole walls of the combustion chamber.

CIBOB integrates newly developed measurement devices dislocated in the boiler and an intelligent software processing data collected from these devices and boiler operational data.

CIBOB utilize four different sensing methods:

Measurement of O₂ and CO concentration near the walls of the combustion chamber,

Measurement of electrical resistance of selected part of evaporator walls.

A corrosion probe located in the boiler combustion chamber measuring the change of resistance of the mounted on its metal component.

Measurement of heat flux between the boiler steam pipe and the sensor.

A software using an artificial intelligence had been developed in order to determine a risk and a rate of corrosion for the entire walls of the combustion chamber on the basis of a limited number of sensors, what contributes to lowering the investment and operating costs of the system.

A methodology and the CIBOB itself had been confirmed in practice by implementation and

six-month operation on two different large utility boilers (bituminous coal and lignite fired), what allows for the use of CIBOP on any other coal fired boiler exposed to corrosion and slagging.

